FIELD TRIP GUIDEBOOK

for the 84th Annual Meeting of the
New York State Geological Association

Hamilton College
Clinton, New York
September 28th-30th 2012

About the cover: Hamilton College campus and surrounding area shown with hillshade derived from first return LiDAR data. This image shows same area with hillshade derived from LiDAR data processed using only bare-earth returns. LAS files courtesy of Oneida County Planning Office. Processing by Hamilton College Geosciences.

Field Trip Guidebook
for the
84th Annual Meeting of the
New York State Geological Association

Hosted by:
Hamilton College
Clinton, NY
September 28th-30th, 2012

Edited by: Todd W. Rayne

This guidebook was published by the New York State Geological Association.

Additional copies may be obtained from the Executive Secretary of the NYSGA.

Dr. Alan Benimoff

Executive Secretary, NYSGA

Dept of Engineering, Physics, and Science

College of Staten Island

Staten Island, NY 10314

ISSN: 1061-8724

Index

Saturday Trips & Workshops

Sunday Trips & Workshops

Geology of the Black River Valley and the western Adirondack Highlands.

Robert S. Darling
Geology Department
SUNY College at Cortland, Cortland, NY 13045
robert.darling@cortland.edu

INTRODUCTION

The Black River, in northern New York State, flows along a course that mostly follows the unconformity between Ordovician sedimentary rocks (to the west) and Proterozoic gneisses of the Adirondack Highlands (to the east; Figure 1). Consequently, the region has attracted sedimentologists, stratigraphers, paleontologists, mineralogists, and metamorphic & igneous petrologists. Our trip, however, will focus almost entirely on the Proterozoic meta-igneous and meta-sedimentary rocks.

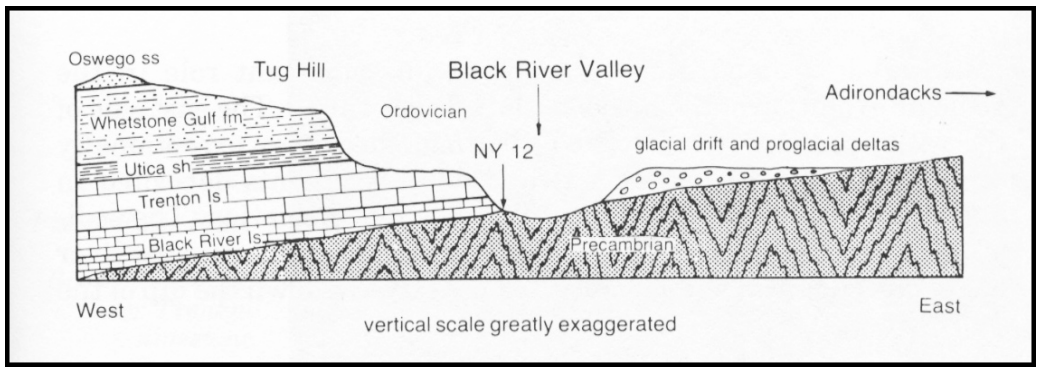

Figure 1. – Simplified west-east cross section across the Black River Valley showing relationship of Ordovician sedimentary rocks of the Tug Hill Plateau to Proterozoic metamorphic rocks of the Adirondack Highlands. From Van Diver (1985).

The Adirondack region of northern New York State is a roughly circular dome of high-grade metamorphic and igneous rocks that form a southeast extension of the Grenville Province in Canada (inset of Figure 2). The Adirondack Highlands comprise mostly meta-igneous rocks (anorthosites, charnockites, mangerites, gabbros, and granites) whereas the Adirondack Lowlands comprise mostly meta-sedimentary rocks (calc-silicates, marbles, metapelites). The Lowlands are separated from the Highlands by the Carthage-Colton

mylonite zone (CCMZ), which shows extensive down-to-the-northwest relative motion from the collapse of the Ottawan phase of the Grenville Orogenic cycle (Rivers, 2008). The CCMZ is a metamorphic facies boundary as well, with upper amphibolite facies metamorphic rocks in the Lowlands and granulite facies metamorphic rocks in the Highlands.

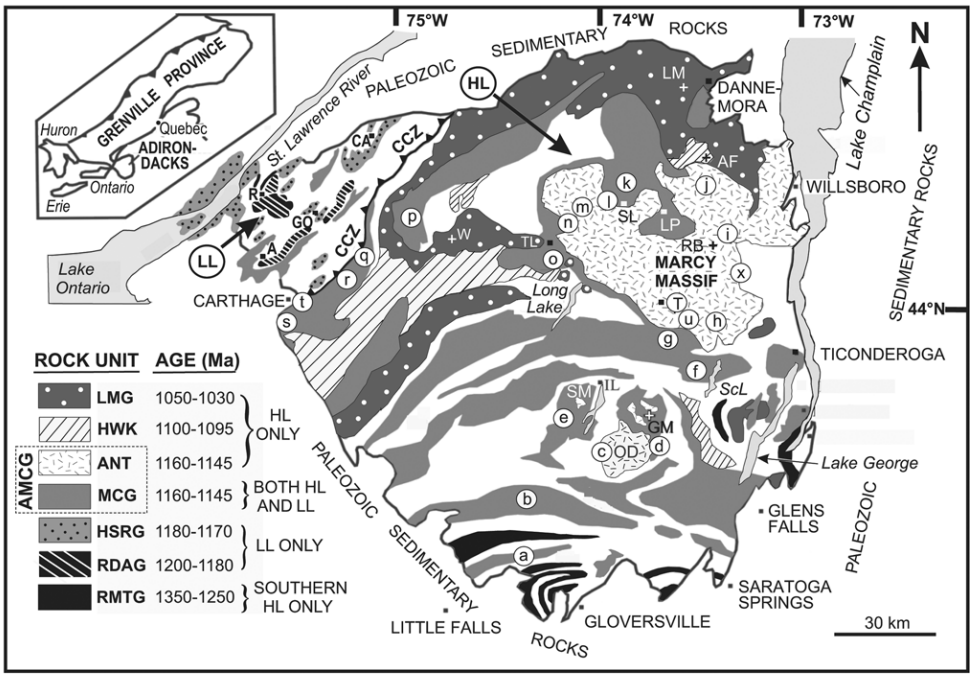

Figure 2. -- Generalized geologic and geochronological map of the Adirondacks from McLelland et al. (2004). Ages of meta-igneous rocks shown in legend. Refer to McLelland et al. (2004) for sample locations and unit descriptions.

As shown in Figure 2, Proterozoic rocks in the western Adirondacks are characterized by mostly charnockites and granites, with lesser amounts of amphibolite and meta-sedimentary rocks (metapelites and calcsilicates). Radiometric dating in the area has largely concentrated on the Lyon Mtn granite (McLelland et al., 2001, 2002b) and surrounding metapelites (Florence et al., 1995). The radiometric dates of zircon fall into two general categories, those associated with the Ottawan phase of the Grenville Orogeny (ca. 1050-1090 Ma) and those associated with earlier anorthosite-mangerite-charnockite-granite (AMCG) magmatism (1145-1160 Ma).

The metapelitic rocks have been the focus of two metamorphic studies (Florence et al., 1995; Darling et al., 2004) and pressure-temperature (PT) conditions of 700-770^{o}C, 4.0-6.4 kb near Port Leyden, NY, and 830-870^{o}C and 6.0-7.2 kb near Moose River, NY, have been determined, respectively. These PT conditions are well into the granulite-facies, but the lower than average pressures reported by Florence et al. (1995) suggest mid-crustal burial depths with an elevated geotherm. The metamorphic temperatures determined in the aforementioned studies are considerably higher than those projected by Bohlen et al. (1985) for the western Adirondacks.

On this trip, we will visit a number of unusual meta-igneous and meta-sedimentary rock types. The basic itinerary is as follows:

Stop 1.— Calc-silicate and sillimanite bearing gneisses on Rt. 12.
Stop 2.— Port Leyden nelsonite.
Stop 3.— Ordovician-age spheroidal weathering at the Knox unconformity.
---------- Lunch ----------
Stop 4.— Two-pyroxene amphibolite at Lyons Falls, NY
Stop 5.— Hydrothermal quartz + sillimanite veins and pegmatite at Lyonsdale, NY
Stop 6.— Prismatine locality at Moose River, NY
---------- Head back to Hamilton College ----------

More detailed rock descriptions and interpretations are included under each of the six stops.

REFERENCES CITED

Bohlen, S.R., Valley, J.W., and Essene, E.J., 1985, Metamorphism in the Adirondacks. I. Petrology, pressure, and temperature: Journal of Petrology, v. 26, pp. 971–992.

Buddington, A.F., 1939, Adirondack igneous rocks and their metamorphism: Geol. Soc. Amer. Mem. 7, 295 p.

Darling, R.S., and Florence, F.P., 1995, Apatite light rare earth chemistry of the Port Leyden nelsonite, Adirondack Highlands, NY: Implications for the origin of nelsonite in anorthosite suite rocks: Economic Geology, v. 90, p. 964-968.

Darling, R.S., Florence, F.P., Lester, G.W., Whitney, P.R., 2004. Petrogenesis of prismatine-bearing metapelitic gneiss along the Moose River, west-central Adirondacks, New York. In: Tollo, R.P., Corriveau, L., McLelland, J., Bartholomew, M.J. (Eds.), Proterozoic Tectonic Evolution of the Grenville Orogen in NorthAmerica, Geological Society of America Memoir 197, Boulder, CO, pp. 325–336.

Darling, R.S. and Crysler, J.L., 2011, An occurrence of microscopic sapphire (blue corundum) in the western Adirondacks: Geological Society of America, Abstracts with Programs, v. 44, no. 1, p. 130.

Dymek, R.F., and Owens, B.E, 2001, Petrogenesis of apatite-rich rocks (nelsonites and oxide-apatite gabbronorites) associated with massif anorthosites: Economic Geology v. 96, p. 797-815

Farrar, S.S., 1995, Mg-Al-B rich facies associated with the Moon Mountain metanorthosite sill, southeastern Adirondacks, NY: Geological Society of America Abstracts with Programs, v. 27, no. 1, p. 42–43.

Farrar, S.S., and Babcock, L.G., 1993, A sapphirine + kornerupine–bearing hornblende spinel periodotite associated with an Adirondack anorthosite sill: Geological Society of America Abstracts with Programs, v. 25, no. 6, p. A265.

Florence, F.P., Darling, R.S., and Orrell, S.E., 1995, Moderate pressure metamorphism and anatexis due to anorthosite intrusion, western Adirondack Highlands, New York: Contributions to Mineralogy and Petrology, v. 121, p. 424–436.

Florence, F.P. and Darling, 1997, Timing of intrusion, anatexis, and metamorphism in the Port Leyden area of the western Adirondacks: in Rayne, T.W., Bailey, D.G., and Tewksbury, B. J., (eds), Field Trip Guide for the 69th Annual Meeting of the New York State Geological Association, Trip A3, p. 37-50.

Grew, E.S., 1989, A second occurrence of kornerupine in Waldheim, Saxony, German Democratic Republic: Zeitschrift fur Geologische Wissenschaften, Berlin, v. 17. p. 67–76.

Grew, E.S., 1996, Borosilicates (exclusive of tourmaline) and boron in rockforming minerals in metamorphic environments, in Grew, E.S., and Anovitz, L.M., eds., Boron mineralogy, petrology and geochemistry: Washington, D.C., Mineralogical Society of America, Reviews in Mineralogy, v. 33, p. 387–480.

Grew, E.S., Cooper, M.A., and Hawthorne, F.C., 1996, Prismatine: Revalidation for boron-rich compositions in the kornerupine group: Mineralogical Magazine, v. 60, p. 483–491

Grew, E.S. and Carson, C., 2007, A treasure trove of minerals discovered in the Larsemann Hills: Australian Antarctic Magazine, no. 13, p. 18-19.

Hough, F.B., 1860, A history of Lewis County, in the state of New York, from the beginning of its settlement to the present time: Munsell & Rowland, Albany NY, 319 p.

Isachsen, Y.W., Landing, E., Lauber, J.M., Rickard, L.V., and Rogers, W.B., 1991, Geology of New York: A Simplified Account, New York State Museum, Educational Leaflet No. 28, 284 p.

Jacobs, G.K., and Kerrick, D.M., 1981, Devolatilization equilibria in H_2O-CO_2 and H_2O-CO_2-NaCl fluids; an experimental and thermodynamic evaluation at elevated pressures and temperatures American Mineralogist, v. 66, p. 1135-1153.

Kolker, Allan, 1980, Petrology, geochemistry and occurrence of iron-titanium oxide and apatite (nelsonite) rocks: MS Thesis, Univ. of Massachusetts, 156p.

Kolker, A., 1982, Mineralogy and geochemistry of Fe-Ti oxide and apatite (nelsonite) deposits and evaluation of the liquid immiscibility hypothesis: Economic Geology, v. 77, p. 1146-1158.

Korhonen, F.J., and Stout, J.H., 2005, Borosilicate- and phengite-bearing veins from the Grenville Province of Labrador: evidence for rapid uplift: Journal of Metamorphic Geology, v. 23, p. 297–311.

McLelland, J.M., Hamilton, M.A, Selleck, B.W., McLelland, Jo.M, and Walker, D., 2001, Zircon U-Pb geochronology of the Ottawan orogeny, Adirondack Highlands, New York; Regional and tectonic implications: Precambrian Research, v. 109, p. 39-72.

McLelland, J., Goldstein, A., Cunningham, B., Olson, C., and Orrell, S., 2002a, Structural evolution of a quartz-sillimanite vein and nodule complex in a late- to post-tectonic leucogranite, western Adirondack Highlands, New York: Journal of Structural Geology, v. 24, p. 1157–1170.

McLelland, J., Morrison, J., Selleck, B., Cunningham, B., Olson, C., and Schmidt, K., 2002b, Hydrothermal alteration of late- to post-tectonic Lyon Mt. Granitic Gneiss, Adirondack Highlands, New York: Origin of quartz sillimanite segregations, quartz-albite lithologies, and associated Kiruna type low-Ti Fe-oxide deposits: Journal of Metamorphic Geology, v. 20, p. 175–190.

McLelland, J.M., Bickford, M.E., Hill, B.M., Clechenko, C.C., Valley, J.W., and Hamilton, M.A., 2004, Direct dating of Adirondack massif anorthosite by U-Pb SHRIMP analysis of igneous zircon: implications for AMCG complexes: Geological Society of America Bulletin, v. 116, p. 1299-1317.

McLelland, J.M., Selleck, B.W., and Bickford, M.E., 2010, Review of the Proterozoic evolution of the Grenville Province, its Adirondack outlier, and the Mesoproterozoic inliers of the Appalachians, *in* Tollo, R.P., Bartholomew, M.J., Hibbard, J.P., and Karabinos, P.M., eds., From Rodinia to Pangea: Lithotectonic Record of the Appalachian region: Geological Society of America Memoir 206, p. 21-49.

Niocaill, C.N., van der Pluijm, B.A., and Van der Voo, R., 1997, Ordovician paleogeography and the evolution of the Iapetus ocean: Geology, v. 25; no. 2; p. 159–162.

Orrell, S., and McLelland, J., 1996, New single grain zircon and monazite U-Pb ages for Lyon Mt. granite gneiss, western Adirondack Highlands, and the end of the Ottawan orogeny. Geol. Soc. Am. Abs. Prog. 28, p. 88.

Philpotts, A.R., 1967, Origin of certain iron-titanium oxide and apatite rocks: Economic Geology, v. 62, p. 303-315.

Philpotts, A.R., 1981, A model for the generation of massif-type anorthosites: Canadian Mineralogist, v. 19, p. 233-253.

Rivers, T., 2008, Assembly and preservation of upper, middle, and lower orogenic crust in the Grenville Province – Implications for the evolution of large, hot, long duration orogens: Precambrian Research, v. 167, p. 237-259.

Schreyer, W., and Werding, G., 1997, High-pressure behaviour of selected boron minerals and the question of boron distribution between fluids and rocks: Lithos, v. 41, p. 251-266.

Selleck B.W., McLelland J.M., Hamilton M.A. 2004, Magmatic-hydrothermal leaching and origin of late- to post-tectonic quartz-rich rocks, Adirondack Highlands, New York, in Tollo R.P., et al. eds., Proterozoic tectonic evolution of the Grenville orogen in North America: Geological Society of America Memoir 197, p. 379–390.

Storm, L.C. and Spear, F.S., 2009, Application of the titanium-in-quartz thermometer to pelitic migmatites from the Adirondack Highlands, New York: Journal of Metamorphic Geol., v. 27, p. 479–494.

Valley, J.W., and Essene, E.J., 1977, Regional metamorphic wollastonite in the Adirondacks, Geological Society of America Abstracts with Programs, v. 9, p. 326-327.

Valley, J.W., and Essene, E.J., 1980, Calc-silicate reactions in Adirondack marbles: The role of fluids and solid solutions: Geological Society of America Bulletin, v. 91 p. 114-117, 720-815.

Valley, J.W., Essene, E.J., and Peacor, D.R., 1983, Fluorine-bearing garnets in Adirondack calc-silicates: American Mineralogist, v. 68, p. 444-448.

de Waard, D., 1967, The occurrence of garnet in granulite-facies terrane of the Adirondack Highlands and elsewhere, an amplification and a reply: Journal of petrology, v.8, p. 213-232.

Wark, D. and Watson, E.B., 2006, TitaniQ; a titanium–in–quartz geothermometer: Contributions to Mineralogy and Petrology, v. 152, p. 743–754.

Whitney, P.R., Fakundiny, R.F., and Isachsen, Y.W., 2002, Bedrock geology of the Fulton Chain-of-Lakes area, west-central Adirondack Mountains, New York: Albany, New York State Museum Map and Chart 44, 123 p. with map.

Young, D.A., 1995, Kornerupine group minerals in Grenville granulite facies paragneiss, Reading Prong, New Jersey: Canadian Mineralogist, v. 33, p. 1255–1262.

Van Diver, B.B., 1985, Roadside Geology of New York: Mountain Press, Missoula, MT, 411 p.

ROAD LOG

The road log for this field trip begins at the New York State Historical Marker describing the four preserved locks of the former Black River Canal on State Route 12, about 4 miles north of Boonville, NY. Boonville is located about 31 miles north of Utica, NY on State Route 12.

From the exit of the four locks pull-over, proceed north on Rt. 12.

Miles from last point	Cumulative mileage	Route description
0.0	0.0	At the exit for the four locks historical marker, continue on Rt. 12 north
1.2	1.2	Pull over to the exposures on the right side of the road.

STOP 1. -- Calc-silicate- and sillimanite-bearing gneisses.

(43°33'30.73"N; 75°19'47.92"W).

The large roadcut here comprises strongly foliated, northwest dipping, augite + K-feldspar + quartz + biotite gneiss. This rock occurs in a narrow but traceable band extending to the northeast under the Pleistocene deltaic sands and reappearing along the Moose River (Florence et al., 1995). The unconformity with Middle Ordovician sedimentary rocks is directly across the highway from this exposure, although it is not well exposed.

Other minerals occurring here include grandite garnet, titanite, wollastonite, calcite and scapolite. Florence and Darling (1997) report that the garnet is mostly grossular and the scapolite is mostly meionitic. The wollastonite contains thin rims of retrograde garnet similar to that described by Valley et al. (1983) from drill cores just 3 km northeast of this location. Interestingly, the garnet described by Valley et al. (1983) contains up to 0.76 wt. % stoichiometric fluorine. Wollastonite is also in contact with calcite and quartz.

As noted in some other Adirondack marbles, the presence of regional metamorphic wollastonite suggests a locally H_2O-rich fluid composition (Valley and Essene, 1977; 1980). At PT conditions in this region (700-750^oC, 4-6 kbar; Florence et al., 1995) a fluid composition of X_{H2O} = 0.8 to 0.9 is necessary to stabilize wollastonite, quartz and calcite (Jacobs and Kerrick, 1981). The margins of some quartz + pink K-feldspar veins are characterized by epidote + specular hematite suggesting a higher fluid O_2 fugacity than in the country rock interior. Very small and uncommon grains of amethyst have been observed in veins here, consistent with high O_2 fugacities.

A few meters to the north is a small exposure of leucocratic feldspar + quartz + sillimanite gneiss. Small amounts of biotite, magnetite and almandine garnet occur as well. The sillimanite does not occur in quartz veins like at Stop 5, but instead as small, sometimes radiating clusters. The rock's proximity to the calc-silicates suggests a metasedimentary origin. Also, note the convoluted reddish-pink color patterns in the gneiss. Note that the reddish-pink color is absent from rocks close to small fractures in the gneiss. This suggests that reducing fluids at one time penetrated these reddish-pink rocks, and either dissolved or replaced the earthy hematite inclusions that occupied fractures and cleavages in the K-feldspar. It is conceivable that the reddish-pink color of felsic gneiss here and elsewhere in proximity to the Knox unconformity throughout the Black River Valley is the result of Ordovician-age chemical weathering, an argument supported by spheroidal weathering at Stop 3.

Miles from last point	**Cumulative mileage**	**Route description**
1.9	3.1	Continue on Rt. 12 north to the village of Port Leyden. At traffic light, turn right onto E Main St.
0.1	3.2	After about 1 city block, turn left onto Lincoln St.
0.2	3.4	After passing by some houses, turn right onto North St. (dirt).
0.1	3.5	Proceed about 400 feet and park in the open field on the left.
		Look for a large rounded exposure of gneiss on the south side of the road near a power pole and walk over the top of it. Continue down and to the left about 40 meters until a water-filled mine shaft comes into view. Nelsonite specimens can be found south of the mine shaft, but watch for poison ivy!

STOP 2. -- Port Leyden nelsonite
(43°35'4.93"N; 75°20'27.46"W)

This is one of two occurrences of nelsonite in New York State (Darling and Florence, 1995). The other occurs near Cheney Pond, 110 km to the northeast, in the High Peaks region of the Adirondacks (Kolker, 1980; 1982). At Port Leyden, the nelsonite occurs as a dike about 3 to 4 meters wide and is traceable for about 30 meters to the north. The host rock is metapelitic gneiss comprising K-feldspar, quartz, garnet, biotite, sillimanite and spinel.

Nelsonites are igneous rocks comprising apatite and Fe-Ti oxides such as ilmenite, or magnetite and rutile. The Port Leyden nelsonite has 32-50% magnetite, 8-15% ilmenite, 30-45% apatite, and 5-11% pyrite (Darling and Florence, 1995). Chlorite and garnet occur as well, and zircon and monazite are observed in thin section. A characteristic feature is its overall fine-grain texture, a common attribute of nelsonites (A. Philpotts, personal communication). See Figure 3.

Nelsonites are normally associated with anorthosite-suite rocks (like at Cheney Pond) and there are two competing theories on their origin. They are believed to form by either magmatic immiscibility (Philpotts, 1967; 1981) or by cumulate processes (Dymek and Owens, 2001), but in both cases the source rocks are either anorthosites or oxide-apatite gabbro norites. Neither of these two rocks occurs within the vicinity of Port Leyden and so the parent rock of the Port Leyden nelsonite is unknown. It is possible that the parent rocks once existed in the Port Leyden area and were eroded away. This is plausible because Philpotts (1981) suggests that nelsonites actually intrude downward in the crust due to their high liquid density (~4.0 gms/cm^3). It is also possible that anorthosite-suite rocks currently located near Carthage, NY (~50 km to the north-northwest) could be a potential source rock as the Adirondack Lowlands once existed structurally on top of the Adirondack Highlands and slid in a NW direction along the CCMZ late in the history of the Grenville Orogeny (Rivers, 2008). This would require greater that 50 km of horizontal displacement along the CCMZ, however.

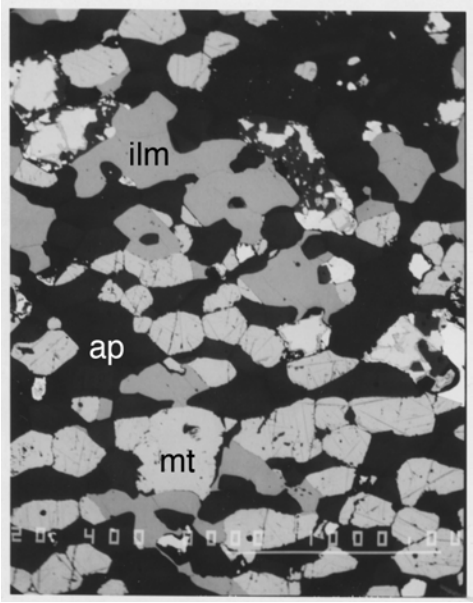

Figure 3. – Backscattered electron image of the Port Leyden nelsonite. Bar scale at bottom is 1 mm. Note distinctive fine-grained texture. ap = apatite; mt = magnetite; ilm = ilmenite. Brightest grains are pyrite (unlabeled).

Radiometric dates have not been published for the Port Leyden nelsonite but it is believed to coincide with intrusion of the AMCG suite, which McLelland et al. (2004) state occurred ca. 1155 Ma. This is interesting because the nelsonite dike cross-cuts the foliation in the metapelite, which would suggest that deformation and metamorphism of the host rocks predates the AMCG igneous event. This is not the case, however, because the nelsonite shows evidence of a weak foliation (mostly in form of oriented pyrite grains). It is interpreted that both the nelsonite and surrounding country rocks experienced regional metamorphism and deformation after the nelsonite intruded, but both deformation and metamorphism were much less pronounced in the nelsonite.

Small lenses (2 cm width) of nelsonite are locally observed in the surrounding metapelitic gneiss. One such lens occurring in rock excavated from the small hydroelectric plant on the Black River at the end of North St. was found to contain small (1 mm), highly fractured sapphires (Darling and Crysler, 2012). Their rich blue color is attributed to the presence of high amounts (up to 0.22 wt.%) of TiO_2, which is not surprising given the composition of the host lens. Although these sapphires are not gem quality, their presence here demonstrates that conditions necessary to form sapphire did exist in the Adirondacks and that gem grade material may exist elsewhere.

Miles from last point	Cumulative mileage	Route description

0.0	3.5	Turn around and head back along North St.
0.1	3.6	Continue straight (don't turn left onto Lincoln St.)
0.3	3.8	Turn right onto State Route 12, and continue for 12.0 miles
12.0	15.8	Turn right onto Cannan Rd.
0.2	16.0	Pull off to left side of road at the first sight of Roaring Brook.

STOP 3. -- Ordovician spheroidal weathering in Proterozoic gneiss
(43°44'32.78"N; 75°25'30.40"W)

Walk down to the exposures of pink feldspathic gneiss along Roaring Brook. Here fractured bedrock contains very good examples of spheroidal weathering preserving between the fractures sets (Figure 4). The spheroidal weathering is characterized by closely spaced (3-4 mm) bands of iron hydroxide, the bands extending a few centimeters into the gneiss (from the fracture sets). Microscopically, the bands are characterized by fine-grained iron-hydroxide, calcite, chlorite, and possibly serpentine. Locally, the bands are filled with medium-grained calcite, suggesting open fracture deposition.

Figure 4. – Vertical view onto surface of Ordovician–age, spheroidal weathering preserved in middle Proterozoic felsic gneiss just below the Knox unconformity at Roaring Brook (Stop 3). Hammer for scale.

From this location, walk upstream about 30 meters and observe the lowermost strata of the Pamelia Formation (Middle Ordovician) resting directly on top of Proterozoic gneiss.

This is the widely known Knox unconformity and is very well preserved in the stream bed. Spheroidal weathering also occurs directly below the nonconformable contact, but is observed only during low water levels (normally late summer). The spheroidal weathering directly below the nonconformity and ~30 meters downstream (location of Fig. 4) are the only locations where it has been observed. Both are located within one vertical meter of the nonconformity. Exposures of felsic gneiss farther downstream, which are a few meters below the projection of the unconformity, show little or no evidence of spheroidal weathering. The proximal relationship between the nonconformity and the spheroidal weathering is interpreted as evidence of Ordovician-age chemical weathering. Middle Ordovician time, therefore, was likely tropical or sub-tropical, which is consistent with paleomagnetic studies (Niocaill, et al., 1997).

Because the closely spaced bands of iron hydroxide (in the spheroidal weathered portion of the gneiss) contain chlorite, the rocks must have been buried to "chlorite-grade" depths following middle Ordovician deposition. This is interpreted to have occurred during the late Paleozoic Alleghanian Orogeny (Isachsen et al., 1991). Consequently, the chlorite cannot be associated with any retrograde metamorphism that occurred during exhumation of Proterozoic rocks following the Grenville Orogeny.

Miles from last point	Cumulative mileage	Route description
0.0	16.0	Turn around and head back toward State Rt. 12
0.2	16.2	Turn left onto State Rt. 12 and continue south to the Stewart's Shop in Lyons Falls (9.4 miles).
9.4	25.6	Turn left into Stewart's (restrooms and lunch stop).
0.0	25.6	LUNCH and RESTROOM STOP

Miles from last point	Cumulative mileage	Route description
0.0	25.7	Exit out of the east side of Stewart's and turn left (Cherry St.)
0.2	25.9	Turn right onto McAlpine St.
0.2	26.1	Turn right onto Center St and proceed through the village of Lyons Falls
0.3	26.4	Former Lyons Falls Pulp & Paper Co. on left; Gould Mansion on right. The road here is now Franklin St.
0.2	26.6	Turn left onto Laura St. immediately after Jim's Used Book Store, and cross the Black River.
0.2	26.8	Turn left onto Lyons Falls Rd. (County highway 39) and cross the Moose River. This is the site of the former "three-way bridge" of Lyons Falls
0.3	27.1	After crossing the Moose River, turn left into the dirt parking lot and walk down to the falls.

STOP 4. -- Two-pyroxene amphibolite at Lyons Falls
(43°37'7.02"N; 75°21'25.81"W)

Lyons Falls drops about 63 feet here and has been harnessed as a power source since the mid-1800's. The base of the falls served as an initial settlement for French explorers of the "Castorland Company," in June of 1794 (Hough, 1860).

Lyons Falls occurs here because of a ~100 meter wide band of highly resistant amphibolite gneiss that strikes SW-NE, normal to the course of the Black River. The amphibolite here is strongly lineated with discontinuous, thin, plagioclase-rich bands. Foliation is poorly developed. The unit has a sharp contact with quartz-feldspar gneiss to the south (observed at the foot of the upstream board dam) but the north contact is not exposed.

Petrologically, the unit is best described as a medium-grained, two-pyroxene amphibolite. Hornblende and plagioclase are the dominant mineral phases. A red-brown (presumably Ti-rich) biotite and opaque magnetite occurs as well (Figure 5). Unlike the central and eastern Adirondacks, the amphibolite at Lyons Falls contains no garnet, despite the fact they are compositionally similar.

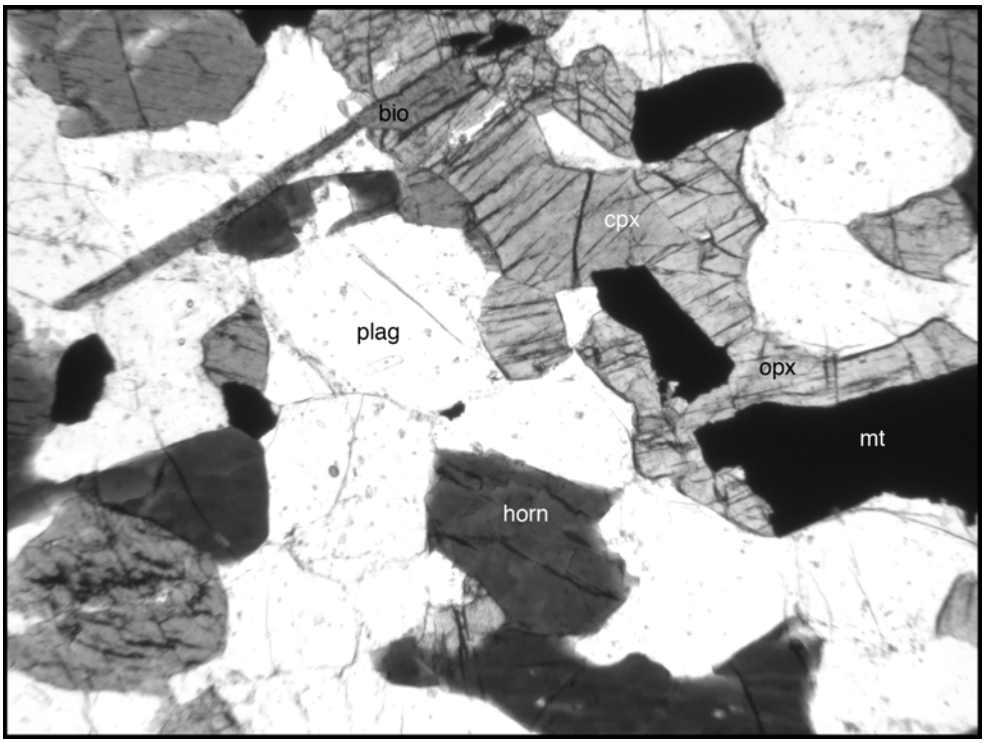

Figure 5. – Photomicrograph of amphibolite at Lyons Falls. Note granoblastic texture and medium grain size. Plag = plagioclase, horn = hornblende, cpx = clinopyroxene, opx = orthopyroxene, bio = biotite, mt = magnetite. Note absence of garnet (see text for discussion). Field of view = 2.5 millimeters width.

The absence of garnet in amphibolites from the western Adirondacks has been known for a long time (Buddington, 1939; de Waard, 1967 and references therein). Its absence is due to lower metamorphic pressures in this region of the Adirondacks as compared to the central and eastern Adirondack Highlands. Figure 6 shows that the amphibolite of Lyons Falls is located to the west of the garnet + clinopyroxene isograd. In mafic rock compositions, this isograd is based on the reaction:

orthopyroxene + anorthite = clinopyroxene + garnet + quartz (1),

where garnet is present on the higher pressure side of the reaction. The famous garnet amphibolites (e.g. Gore Mtn.), so common in the central and eastern Adirondacks could not form in the western Adirondacks simply because the rocks were not buried deep enough.

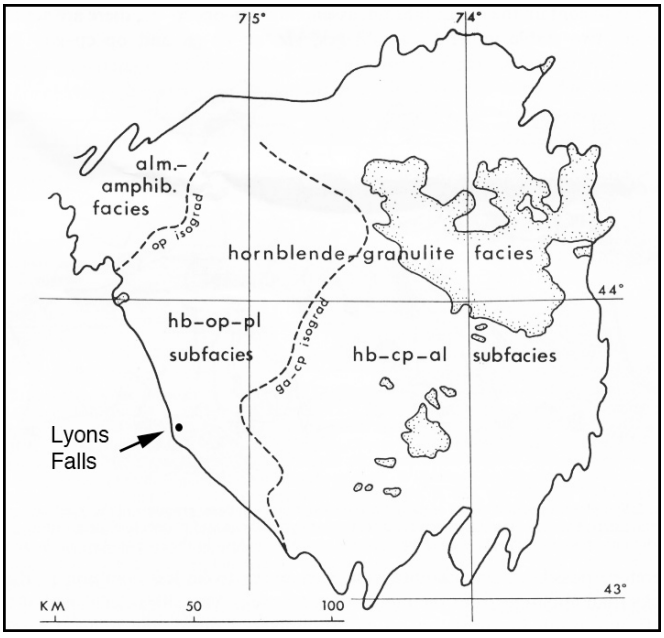

Figure 6. – Simplified metamorphic isograd map for the Adirondacks modified from de Waard (1967). Note the amphibolite at Lyons Falls is located west of the garnet + clinopyroxene isograd.

Also occurring at Lyons Falls are some meter-scale potholes carved into the amphibolite. These are best observed during low-water levels and closer to the water fall.

Miles from last point	Cumulative mileage	Route description
0.0	27.1	Turn around and head back across the Moose River toward Laura St.
0.3	27.4	Turn left (east) onto Laura St.
0.6	28.0	Bear left onto Lyonsdale Rd.
2.4	30.4	Once in Lyonsdale, turn left onto Lowdale Rd. at the Burroughs Mill and cross the Moose River again (caution, the bridges are narrow!)
0.2	30.6	After the second bridge, pull off in the sandy area to the right or left.
		First, walk out onto the last bridge crossed and look north (downstream). Then, walk down the path on the west side of the road for about 100 meters and walk out to exposures in the bed of the Moose River.

STOP 5. – Undeformed pegmatite and hydrothermal sillimanite + quartz veins in Lyon Mtn. granite. (43°37'10.63"N; 75°18'12.84"W)

This stop demonstrates important igneous and hydrothermal features of Lyon Mtn. granite along the Moose River. These exposures were studied extensively by McLelland et al. (2001, 2002a, 2002b) and Selleck et al. (2004). Their overall interpretation is that Lyon Mtn. granite experienced contemporaneous intrusion and hydrothermal alteration at about 1035 Ma. The hydrothermal activity leached large cations (K^+, Na^+) from the granite but left behind Al^{3+} and Si^{4+} to form quartz-sillimanite veins. Early vein sets were ductily deformed (due to magmatic flow or tectonic shear) and younger veins sets formed afterward.

These rocks were included in a large unit of mapped metapelites in Figure 1 of Florence et al. (1995) but the composition and textural features are more consistent with igneous rocks. Some of the country rocks into which the Lyon Mtn. granite intruded are indeed metapelites, and numerous exposures of sillimanite + garnet + hercynite + quartz + K-feldspar gneiss occur in the area.

Looking west from the bridge on the northern side of the Moose River, one can observe an undeformed pegmatite cutting hydrothermally altered Lyon Mtn. granite. The pegmatite is shown in Figure 7 and is compositionally zoned with an uncommon magnetite-rich core. McLelland et al. (2001) dated well-zoned igneous zircons from this pegmatite at 1034 ± 10 Ma. Because the pegmatite is undeformed, the 1034 Ma zircon age has been interpreted as the terminus of Ottawan deformation in the Adirondacks (Orrell and McLelland, 1996).

Figure 7. – Undeformed pegmatite just west of Lyonsdale bridge. Taken from Figure 4a of McLelland et al. (2001). See text for discussion.

The bedrock exposed farther downstream show excellent examples of quartz + sillimanite veins hosted by Lyon Mtn. granite (see Figure 8). These veins occur in two prominent orientations, N20E and N50E (McLelland et al., 2002a). At other locations in the area (e.g. Ager's Falls), the quartz-sillimanite veins are nodular in shape and strongly deformed (McLelland et al., 2002a,b).

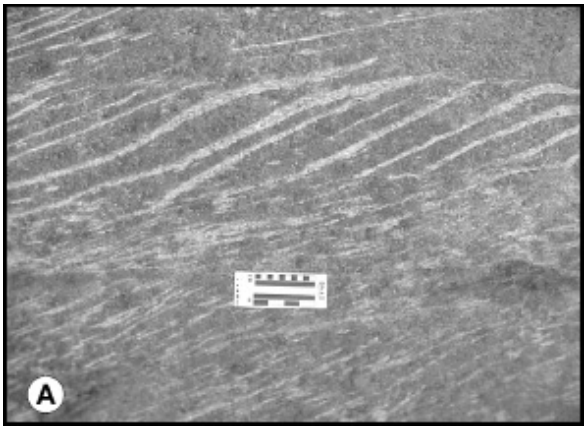

Figure 8. – Hydrothermal quartz + sillimanite veins in Lyon Mtn. granite at Stop 5. Taken from Figure 2a of Selleck et al. (2004).

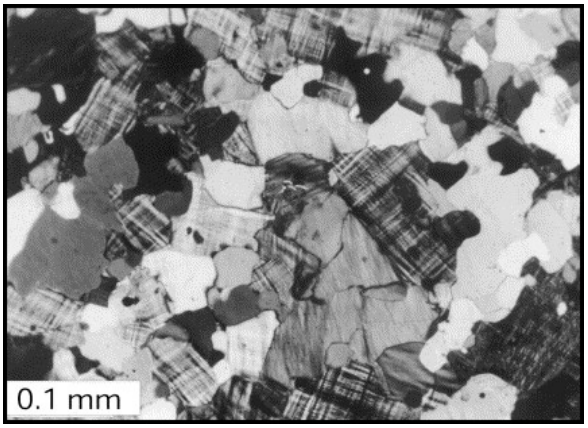

Figure 9. – Photomicrograph of Lyon Mtn. granite. Note little or no grain shape fabric of quartz and microcline. From Figure 11 of McLelland et al. (2002b).

Miles from last point	Cumulative mileage	Route description
0.0	30.6	Turn back and cross the Moose River again on the Lowdale Rd. Again, watch the bridges!
0.2	30.8	Turn left (east) onto Marmon Road.
0.3	31.1	Make a slight left onto Hunkins Rd.
1.1	32.2	Turn right (south) onto Fowlersville Rd.
0.3	32.5	Turn left onto Penney Settlement Rd.
0.5	33.0	Turn left onto North-South Rd.
2.0	35.0	Turn right onto Moose River Rd and head east.
6.9	41.9	1876 red school house on right.
0.2	42.1	Turn left into sandy parking area at first siting of the Moose River.

STOP 6. -- Moose River Prismatine locality
(43°36'36.38"N; 75°10'0.72"W)

Follow the all-terrain vehicle path downstream for about 200 meters. The path passes through the stone foundations of the former Moose River tannery and then follows rapids as the Moose River flows southwest. Here, the river cuts through northwest-dipping, calc-silicate gneisses and quartzites. Stay high on the river bank until the rapids disappear. The path will descend and cross a small, wet, muddy creek bed. Afterwards, the Moose River pools and turns north and the first outcrops on the west side of the river are the prismatine-bearing rocks. Please exercise caution while walking among the river boulders and talus at the base of the outcrops. Also, please DO NOT USE HAMMERS at this stop and refrain from collecting prismatine specimens unless you're planning to study them scientifically; a future geologist will be grateful someday.

Prismatine, the boron-rich endmember of the kornerupine solid solution (Grew et al., 1996; ideally $Mg_3Al_6Si_4BO_{21}(OH)$) occurs in metapelitic and quartzitic rocks along the Moose River. Kornerupine-group minerals are generally rare, having been described from nine localities in the Grenville Province (Grew, 1996; Darling et al., 2004; Korhonen and Stout, 2005) including two in the Adirondacks (Farrar and Babcock, 1993; Farrar, 1995; Darling et al., 2004).

Along the Moose River, prismatine occurs at two locations (separated by about 400 meters, Figure 10) within a unit of heterogeneous metasedimentary rocks (Figure 10, unit BL) mapped by Whitney et al. (2002). This unit comprises mostly quartzite and biotite-quartz-plagioclase gneiss with lesser amounts of calcsilicate rocks, and minor amphibolite,

quartzofeldspathic gneiss, and calcite marble (Whitney et al., 2002). These rocks are interlayered with other metasedimentary and meta-igneous rocks (Figure 10). These units occur in a complex, southeast-verging overturned synform bordered on the northwest by a tabular, northwest-dipping body of charnockitic gneiss (CG) several kilometers thick, and on the southeast by a domical body of batholithic proportions consisting of relatively leucocratic CG (Whitney et al, 2002). Although the granitic and charnockitic rocks have not been dated, they are lithologically and geochemically similar to felsic rocks of the ca. 1150 Ma anorthosite-mangerite-charnockite-granite (AMCG) suite found throughout much of the Adirondack Highlands (McLelland et al., 2001; Whitney et al., 2002).

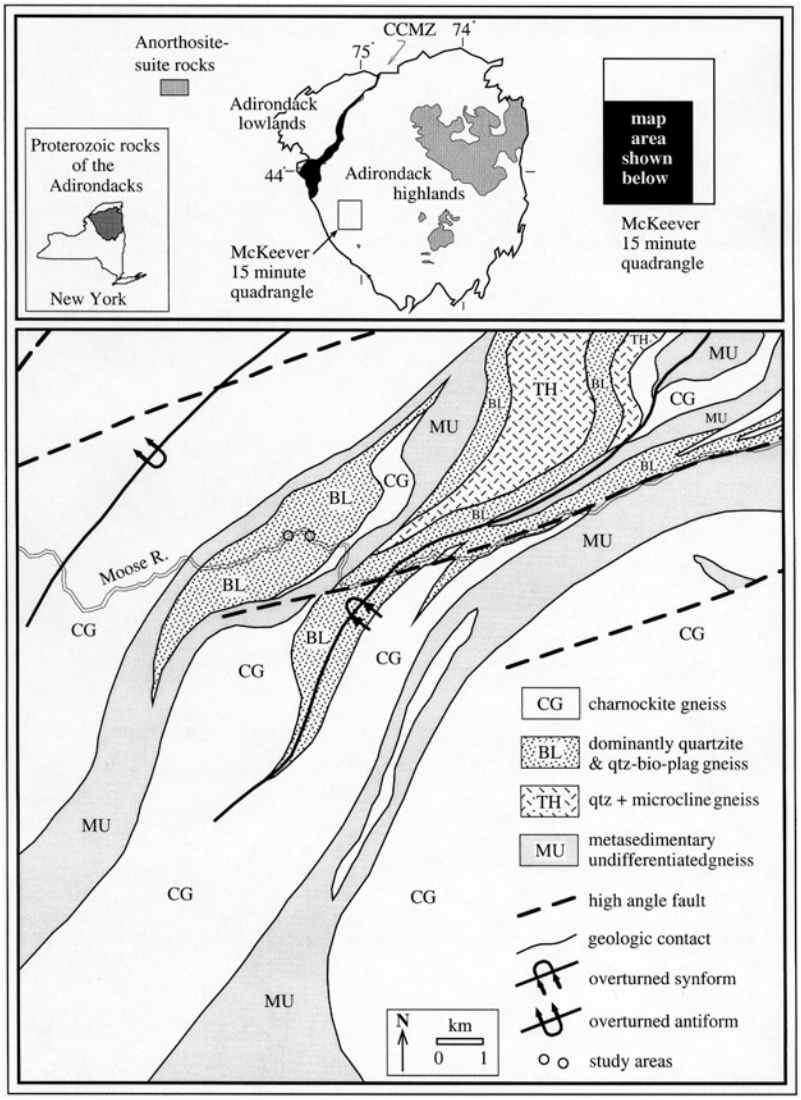

Fig. 10. - Map showing location of prismatine-bearing metapelites and quartzites (open circles on Moose River) and surrounding bedrock geology. Stop 6 is the easternmost open circle. Geologic map units, structures, and relations illustrated are from Whitney et al. (2002). *Taken from Darling et al. (2004).* Bio—biotite; CCMZ—Carthage-Colton mylonite zone; pl—plagioclase; qtz—quartz.

In addition to prismatine-bearing assemblages, the surrounding rocks contain metapelitic assemblages of a) cordierite + spinel + sillimanite + garnet + plagioclase + quartz + ilmenite + rutile +/- biotite, b) cordierite + orthopyroxene + biotite + K-feldspar + quartz, and c) orthopyroxene + plagioclase + K-feldspar + quartz +/- biotite, +/- garnet (Darling et al., 2004).

The feature of geologic interest at STOP 6 are the exceptionally well-developed prismatine crystals in coarse-grained, feldspathic lenses. Here, prismatine crystals form dark greenish-black, euhedral, elongated grains (up to 10 cm in length). Ed Grew (personal communication) indicates that only the prismatine crystals from the Larsemann Hills, Antarctica (Grew and Carson, 2007) are comparable in length to those at Moose River. The prismatine commonly displays radiating patterns in feldspathic lenses one to three cm thick (Figure 11A).

The prismatine crystals *appear* to have grown only within the plane of the foliation. However, upon closer examination, the prismatine grains are seen to be arranged randomly, but the longest and best-developed crystals formed parallel to the foliation plane. Because of this, Darling et al. (2004) inferred that nondeviatoric pressure conditions prevailed locally during prismatine formation. It should also be noted that a number of prismatine-bearing feldspathic lenses are located adjacent to fine-grained tourmaline + plagioclase + biotite–rich zones near the north end of the exposed rocks. In these locations, the prismatine-bearing feldspathic lenses texturally embay, cross-cut earlier foliation, and appear to form at the expense of the tourmaline-bearing zones (Figure 11B). The embayed country rocks, coarser grain size, and the random arrangement of the prismatine crystals led Darling et al. (2004) to interpret the feldspathic lenses and the prismatine found in them to be of anatectic origin.

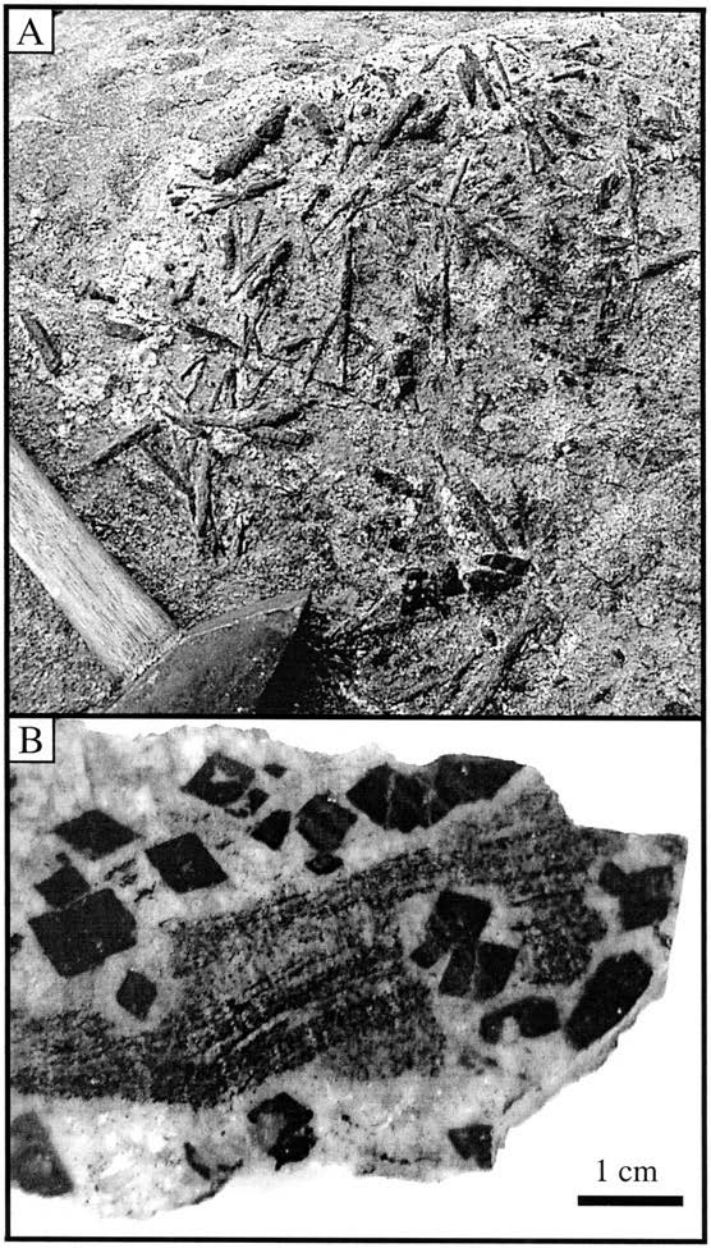

Fig. 11. - (A) Prismatine crystals (black) in coarse-grained feldspathic lens, taken parallel to plane of lens. Hammer for scale. (B) Euhedral prismatine (black) in coarse-grained feldspathic lens embaying fine-grained, foliated tourmaline + biotite + plagioclase–rich zones. *Taken from: Darling et al. (2004).*

Plagioclase, K-feldspar, minor quartz and rutile are the most common phases associated with prismatine, but biotite, cordierite, garnet and rarely sillimanite occur locally as well. The prismatine contains 0.73 to 0.79 formula units of B (out of 1.0) and has Mg / Mg + Fe between 0.70 and 0.73 (Table 3 of Darling et al., 2004). After determining the associated mineral compositions, Darling et al. (2004) proposed the following prismatine-forming reaction:

Tourmaline + sillimanite + biotite + cordierite → prismatine + rutile + melt (2).

Reaction 2 is similar to a number of proposed prismatine-forming reactions from other granulite terranes (Grew, 1996), including those in sapphirine-free rocks found in the Reading Prong, New Jersey (Young, 1995), and in Waldheim, Germany (Grew, 1989). In those cases, garnet rather than cordierite was a proposed reactant.

Metamorphic temperatures and pressures are difficult to estimate from prismatine-bearing mineral assemblages as little is known about the stability of boron-rich kornerupine at pressures less than 10 kb (Schreyer and Werding, 1997). However, the prismatine occurs in proximity to low-variance metapelitic assemblages in the surrounding rocks. Specifically, thermobarometry calculations from net transfer and exchange equilibria record temperatures and pressures of 850° ± 20°C and 6.6 ± 0.6 kilobars for orthopyroxene + garnet assemblages and 675° ± 50°C and 5.0 ± 0.6 kilobars for cordierite + garnet + sillimanite + quartz assemblages (Darling et al., 2004). The former assemblage is interpreted to have formed during partial melting whereas the latter assemblage is interpreted to have formed on the early retrograde metamorphic path (Darling et al., 2004). The ~850°C temperatures derived from the orthopyroxene + garnet assemblage are reasonable for partial melting conditions. Although the cordierite + garnet + sillimanite + quartz assemblage occurs at STOP 6, it and the orthopyroxene + garnet assemblage are better developed farther downstream at the second prismatine location (the westernmost open circle in Figure 10). These exposures can be reached by following the footpath on the south bank of the Moose River for a distance of about 400 meters.

Because many of the prismatine-bearing feldspathic lenses are saturated in both quartz and rutile, Storm and Spear (2009) intensely studied the prismatine-bearing lenses as part of a natural test of the titanium-in-quartz geothermometer of Wark and Watson (2006). Storm and Spear (2009) determined a wide range of metamorphic temperatures, specifically from 630 + 63 / -86 to 879 ± 8 °C, but most determinations fell between 700°C and 880°C (see Figure 8a of Storm and Spear, 2009). This is in good agreement with metamorphic temperatures determined by the aforementioned methods (Darling et al., 2004). Storm and Spear (2009) also provide convincing textural evidence that prismatine was locally replaced by leucosomatic quartz, most likely during melting of prismatine. Interestingly, it was the

leucosomatic quartz that yielded the highest Ti-in-quartz temperatures (800-880°C; Figure 8a of Storm and Spear, 2009).

The age of partial melting is unknown at this time but is likely associated with either intrusion of the AMCG suite at ~ 1160-1145 Ma, or burial associated with the Ottawan phase of the Grenville Orogenic cycle and the associated intrusion of Lyon Mtn. granite at ~ 1050-1030 Ma (McLelland et al., 2010).

ACKNOWLEDGEMENTS

I thank Drs. David Barclay and Gayle Gleason for reviewing an earlier version of this manuscript and for their helpful and constructive comments.

Miles from last point	Cumulative mileage	Route description
0.0	42.1	Turn around and head back (west) along the Moose River Rd.
4.7	46.8	Turn left (south) onto Moose River Rd going toward Boonville. Yes, it's another Moose River Rd.
8.1	54.9	Follow the Moose River Rd for about 8.1 miles until it intersects State Route 12 and head back toward Utica (about 30 additional miles).

Quaternary Geology of the Oneida Lake Basin

Eugene W. Domack,
Hamilton College, Clinton, NY
edomack@hamilton.edu

Madhav Krishna and Lewis A. Owen
University of Cincinnati, Cincinnati, OH

Dale P. Hess, Brock University
St. Catharines, Ontario, Canada

Todd W. Rayne and David A.Tewksbury
Hamilton College, Clinton, NY

The manuscript for this trip was not ready in time for reproduction for the guidebook. It is available from the lead author, Eugene Domack.

Pegmatites of New York State: The Batchellerville pegmatite

Abigail R. Seadler
American Geosciences Institute, Alexandria, VA 22302
arseadler@gmail.com

Marian Lupulescu
New York State Museum, Albany, NY 12230
mlupules@mail.nysed.gov

David G. Bailey
Hamilton College, Clinton, NY 13323
dbailey@hamilton.edu

INTRODUCTION

Despite their interesting petrographic features, geological associations, and mineral assemblages, there are only a few modern scientific studies on the pegmatite bodies of New York State (Tan 1966; Putman and Sullivan 1979). The pegmatites are found in two geological units: the Grenville-age (1300 - 1000 Ma) metamorphic rocks of the Adirondack Mountains (Figure 1) and the Taconic-age (~ 450 Ma) metamorphic rocks of southern New York. There are approximately 25 significant pegmatite bodies known in New York, and they can be placed into six different geologic / geographic groups:

A. The Bedford pegmatite district consisting of the amazonite- and the peristerite-bearing pegmatites at Valhalla in Westchester County, and the small pegmatite bodies in the Taconic-age metamorphic rocks of the Manhattan Prong (New York City) that are xenotime, or beryl- and chrysoberyl-bearing;
B. The Cranberry Creek (Mayfield), Batchellerville, Greenfield, Day (Overlook), and Corinth belt of pegmatites in the southern Adirondack Highlands;
C. The Crown Point, Rose Rock, Spar Bed Hill, Chestertown, and Fort Ann pegmatites in the central-eastern Adirondack Highlands;
D. The Scott Farm - Benson Mines pegmatite belt in the northwestern Adirondack Highlands;
E. The Lyons Falls and Stiles Farm pegmatites in the western Adirondacks; and
F. The McLear and other small pegmatite bodies in the Adirondack Lowlands.

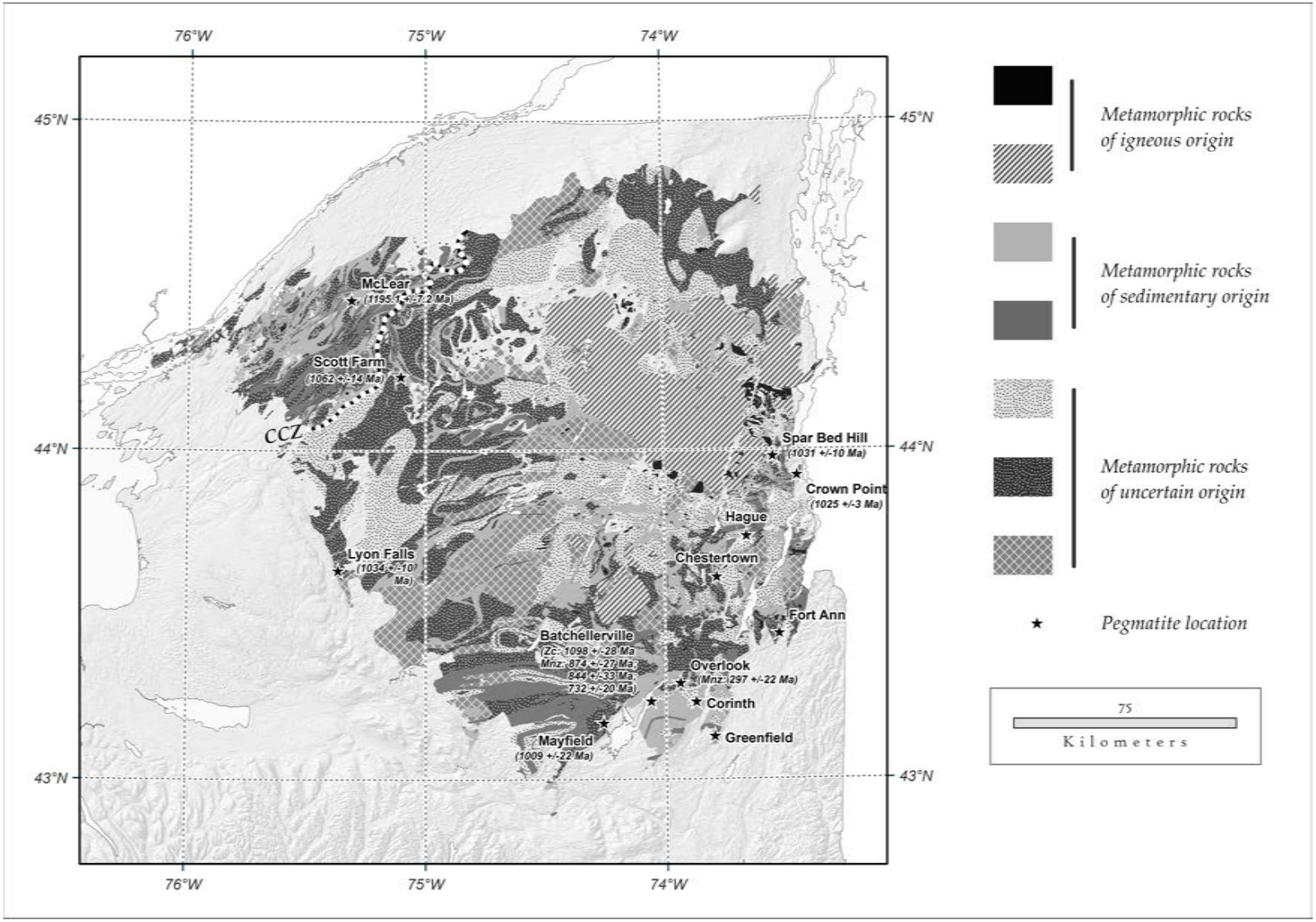

Figure 1. Locations and ages of major pegmatite bodies in the Adirondacks. (Zc – zircon age, Mnz – monazite age (Lupulescu et al. 2011). Map courtesy of Janet Manchester).

HISTORY

General

Interest in the pegmatites of New York started with the rush to find and mine high-quality feldspar in the second half of the nineteenth century. The second stage for pegmatite exploration began in 1950 when the USGS initiated a nationwide search for uranium resources. The first attempt to mine pegmatites in New York State began around 1878 at the Bedford pegmatite. Mining at Bedford lasted until 1949, and in 1962 and 1963 the dumps and most of the mine structures were leveled to build houses (Tan 1966).

The pegmatites in the east central Adirondacks were first mined for enamel, crushed stone, grit for chicken feed, and on a smaller scale, for quartz used in glass manufacturing. Mining began in the late nineteenth century and lasted until around 1926 (Tan 1966).

In the northwestern Adirondacks, the McLear pegmatite was discovered in 1907. Here, feldspar was found in high-quality masses 6 in to 3 feet in length with no iron staining, but with rare grains of pyrite as inclusions. The quarry was worked by the White Hill Mineral Company until 1937, and after that, by the Green Hill Mining Company. The feldspar that was mined was shipped to Trenton, New Jersey, and used in the ceramics industry. The mine was closed around 1938 (Tan 1966).

Batchellerville

The Batchellerville pegmatite is located in the south-central Adirondacks, in the northwestern corner of the Broadalbin 7.5" quadrangle, Saratoga County. The pegmatite was discovered on the Adelbert Gordon Farm, and in 1906 the Clapska Mining Company from Trenton, New Jersey began mining the feldspar. The pegmatite was worked continuously until 1921 and sporadically until about 1934 (Tan 1966). The main product was high-quality microcline for the ceramics industry (Tan 1966). A secondary product, very coarse muscovite, was typically sought after as a dielectric material. However, microgranular iron oxide inclusions and staining made most of it unsuitable for electrical applications (Tan 1966).

The nearby Cranberry Creek (Mayfield) pegmatite on the Richard Tyrell Farm was exploited at about the same time as the Batchellerville pegmatite by the Clapska Mining

Company, which later transferred it to the United States Feldspar Corporation (Tan 1966). The mining stopped here shortly before 1916. The Overlook (Day) body was worked until 1920. The Corinth prospect was mined first in 1899 by American Feldspar Company (Bastin 1910) and then transferred to the local Corinth Feldspar Company (Tan 1966).

Tan (1966) identified and named eight distinct pegmatite bodies that were mined at the Batchellerville property (Figure 2).

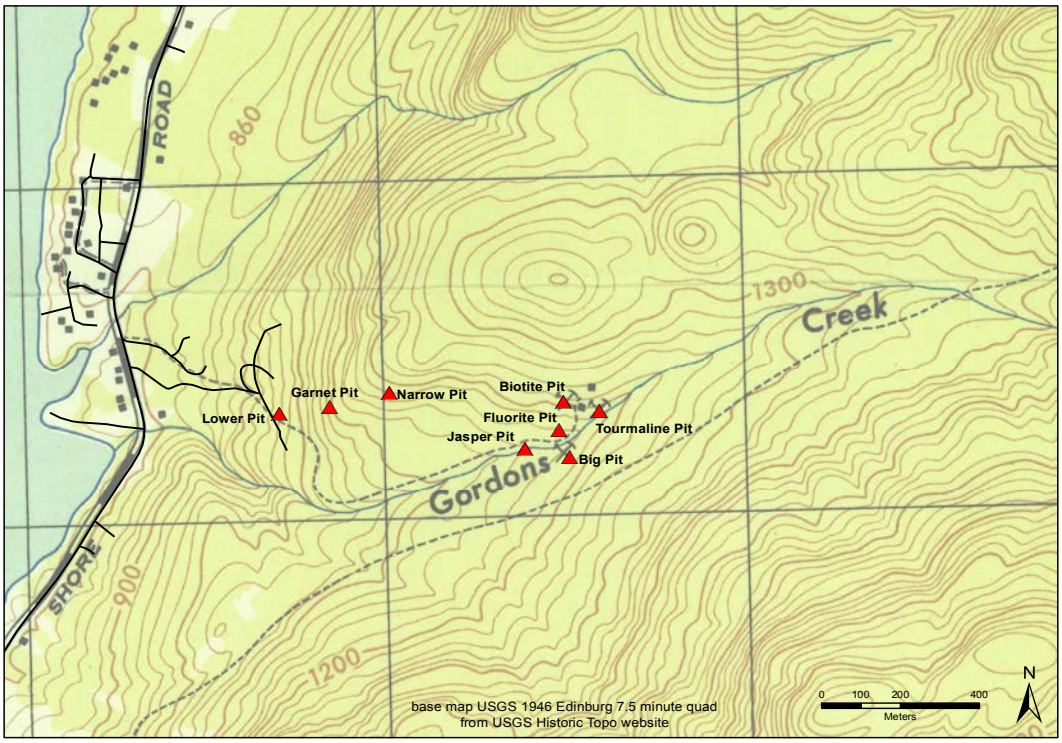

Figure 2: Map of the Batchellerville Pegmatite showing locations of eight distinct mine / exploration pits (modified after Tan (1966)).

The two largest excavations were at the Lower Pit and at the Big Pit, although both are still less than 150' in any dimension (Tan 1966). The pits appear to have worked a series of small tabular bodies with roughly E-W trends. The larger bodies exhibited mineralogical zonation, with quartz-rich cores and with Al-rich phases (muscovite, biotite, sillimanite, garnet, etc.) concentrated in the outer zones or along the contact with the surrounding biotite gneiss (Tan 1966).

GEOCHRONOLOGY

General

There are no modern or precise age data on the pegmatites emplaced in the Taconian-age rocks from the Manhattan Prong in southern New York (Bedford, Valhalla, and New York City). Most of the pegmatites from the Adirondacks were generated and emplaced during the late Elzeverian, Shawinigan, Ottawan, and Rigolet orogenies of the Grenville Orogenic Cycle (Figure 1)(Lupulescu et al. 2011). The oldest pegmatite ages reported are from the McLear pegmatite in the Adirondack Lowlands (1195 ± 7.2 Ma); the youngest pegmatite ages are on the Mayfield pegmatite in the southern Adirondack Highlands (1009 ± 22 Ma) (Lupulescu et al. 2011).

Batchellerville

Zircon Geochronology

One zircon crystal from the Batchellerville pegmatite was analyzed by LA-MC-ICPMS for an U-Th-Pb age. The crystal contained between 1562 and 5204 ppm uranium and a very high U/Th ratio (up to 189) and was almost completely metamict. Based on the concordant analysis within the analytical error of the upper concordia intercept, the crystallization age of this zircon was interpreted to be 1090 ± 28 Ma (Lupulescu et al. 2011).

Monazite geochronology

Monazite-(Ce) was found in the Batchellerville pegmatite as crystals up to 8 cm in length. One monazite crystal was analyzed by electron probe for chemical ages. The sample contains 18.1 Ce, 17.01 Th, 7.89 La, 7.12 Nd, and 1.69 Y (all in wt. % element). The crystal is fractured and contains tiny thorite crystals. Back-scattered electron images revealed a nearly homogeneous crystal with some patchy, lower atomic number areas. Twenty-four analyses on the crystal far from the fractures or inclusions yielded an average age of 874 ± 27 Ma; analyses closer to the fractures and from the darker, low-intensity backscatter areas yielded an average of 751 ± 71 Ma and 844 ± 33 Ma respectively (Lupulescu et al. 2011).

There are two ways to interpret the differences in the zircon and monazite ages (Lupulescu et al. 2011): 1) the zircon age is the intrusion age of the pegmatite and the monazite formed later, possibly as a result of the infiltration of crustal fluids during uplift, or,

2) the zircon age represents inheritance and the chemical age obtained on the monazite is the real age of the pegmatite. In the first scenario, the intrusion of the Batchellerville pegmatite would be associated with the early manifestation of the Ottawan phase of the Grenville orogeny; in the second, the pegmatite would have been entirely post-Grenville, an interpretation supported by the lack of any significant deformational features within the pegmatite itself (Lupulescu et al. 2011).

MINERALOGY

General

The pegmatites of New York have simple to complex, and variable, mineral assemblages (Table 1). The pegmatites from Valhalla and New York City, as well as those from the Adirondack Lowlands, do not show mineralogical zoning. Such zoning is a common feature of the Bedford pegmatites and those in the southern and eastern Adirondack Highlands. Post-emplacement metamorphic deformation features are commonly observed in the pegmatites from the Adirondack Lowlands and less commonly in the pegmatites from the Highlands. The pegmatites from southern New York lack even weak metamorphic features.

By world standards, the list of mineral species found in New York pegmatites is modest (Table 1) although museum quality specimens of columbite (the largest being a 5 lb crystal from the Baylis Quarry), beryl, chrysoberyl, amazonite, sillimanite, molybdenite, and schorl have been collected. At some locations, secondary minerals formed at the expense of primary igneous minerals; not all of these secondary minerals, including some of the uranium-bearing minerals, have yet been identified or well characterized.

Batchellerville

The Batchellerville pegmatite has a relatively complex mineral assemblage that varies widely from pit to pit (Table 2). Common pegmatite minerals such as quartz, feldspar and mica persist throughout the pegmatite; however, its unusually Al-rich assemblage and presence of rare-earth-bearing minerals sets the Batchellerville pegmatite apart from others in New York State.

Table 1. Minerals identified in selected New York pegmatites.

	Adirondacks										Southern NY	
MINERALS	**Bat**	**G**	**M**	**O**	**CP**	**HF**	**L**	**McL**	**SBH**	**SF**	**Bed**	**NY**
Albite	x		x		x			x	x	x		x
Almandine	x	x	x								x	x
Allanite-Ce					x				x			
Amphibole*					x							
Autunite											x	
Annite-Phlogopite*	x		x	x	x		x	x	x		x	x
Fluorapatite			x				x			x		
Beryl	x		x								x	x
Chabazite-Ca										x		
Chernikovite			x									
Columbite*		x									x	x
Chrysoberyl	x	x										
Danburite								x				
Diopside							x	x		x		
Dumortierite	x											x
Euxenite-Y	x			x								
Fergusonite-Y												
Ferro-actinolite										x		
Fluorite	x									x		
Fluoro-edenite								x				
Fluoriantremolite								x				
Heulandite-Ca										x		
Magnetite	x		x									
Microcline	x		x	x	x		x	x	x	x	x	x
Monazite-Ce	x			x								
Muscovite	x		x	x	x							x
Polycrase-Y				x								
Pyrrhotite									x			
Quartz	x	x	x	x	x	x	x	x	x	x	x	
Schorl	x	x	x	x		x			x		x	
Sillimanite	x	x										
Stilbite-Ca										x		
Stellerite										x		
Titanite							x	x				
Torbernite											x	
Uraninite	x							x	x			
Vanmeersscheite											x	
Xenotime-Y			x									x
Zircon	x				x	x	x				x	

Bat – Batchellerville; CP – Crown Point; G – Greenfield; HF – Hall's Falls; L – Lewis; M – Mayfield; McL – McLear; Bed - Bedford; O – Overlook; SBH – Spar Bed Hill; SF – Scott Farm; NY- NY City pegmatites.
(*)= Species not identified. Bold = Museum quality specimens.

Characteristic of all pegmatites, mineral sizes at Batchellerville vary from a few millimeters to tens of centimeters in length. Minerals occur in coarse- to fine-grained aggregates of anhedral to subhedral crystals.

Quartz, feldspar and mica are the most abundant mineral phases in the Batchellerville pegmatite. Quartz and feldspar commonly occur as the characteristic "graphic granite" texture most often associated with pegmatites (Figure 3). Quartz occurs in a variety of colors including clear, "milky" white, rose, and smoky varieties. Some rose quartz exhibits an internal play of color, and the smoky quartz ranges from light gray to black in color (Seadler 2011). Perthitic microcline and albite occur at the Batchellerville pegmatite in pink, white, and green-gray varieties (Seadler 2011). Though located in all of the pits, quartz, feldspar and mica appear most abundantly in the Lower Pit of the Batchellerville pegmatite. A dark brown annite-phlogopite is the most common mica associated with the pegmatite, followed by muscovite. Each of these micas occurs in massive aggregates and small- to moderate-sized books (up to 30 cm in diameter).

Figure 3. "Graphic Granite", intergrown smoky quartz and feldspar from the Lower Pit (Seadler 2011).

Aluminum-rich minerals, typically uncommon in the pegmatites of New York State, are abundant in the Batchellerville pegmatite. Beryl, chrysoberyl, sillimanite, dumortierite, almandine, and Al-rich tourmaline (var. schorl) are all found in hand sample, although not in

all pits. In fact, Batchellerville is one of the best localities for chrysoberyl in New York State (Lupulescu 2007).

The chrysoberyl at the Batchellerville pegmatite is found only in the Garnet Pit, and occurs as pale green to yellow crystals in aggregate with quartz and feldspar (Seadler 2011). Green to blue gemmy beryl can be found in the Lower Pit, and large beryl samples (up to 25 cm wide and 50 cm long) have been recovered from the Big Pit (Figure 4). Sillimanite is common in the Garnet pit as radiating to bladed, gray/blue to yellow/black crystals up to 3 cm (Seadler 2011). Small (up to 3 mm in length), blue-gray to purple dumortierite crystals, though uncommon, can be found in the Lower and Garnet pits of the Batchellerville pegmatite. They typically occur in the finer-grained graphic intergrowths of quartz and feldspar (Seadler 2011).

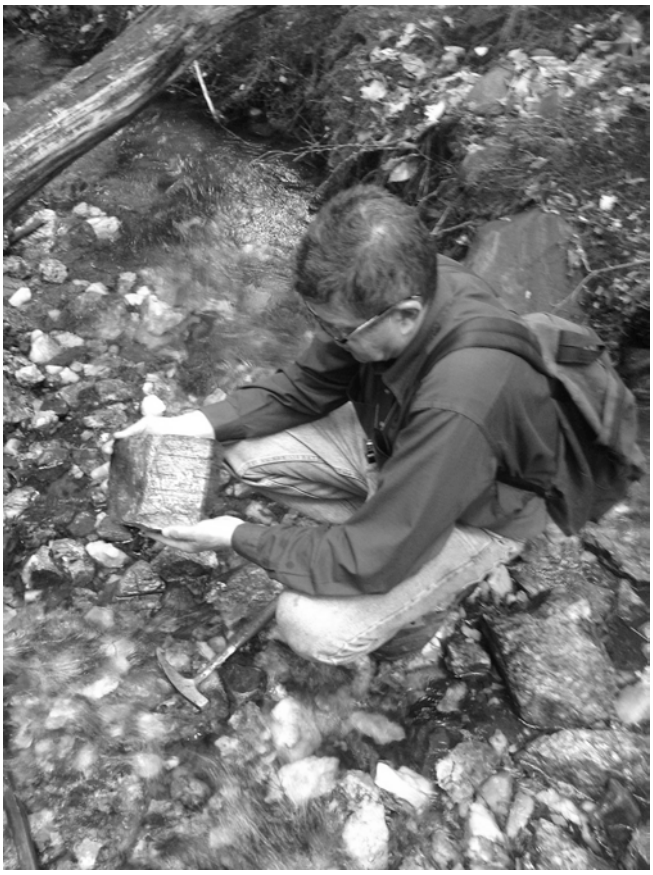

Figure 4. Large beryl crystal (14 cm across) collected by authors in June 2012.

Except for beryl, these Al-rich mineral phases are most common in the Garnet Pit of the Batchellerville pegmatite. Beryl and, to a lesser extent, dumortierite and schorl, can all be found in the Lower Pit; and, beryl and schorl can be found in the Big and Fluorite Pits.

Poorly formed, red-brown almandine crystals (up to 1 cm) are also found in the Garnet Pit (Tan 1966).

Many other minerals have been identified at the Batchellerville pegmatite (Tables 1 and 2). Most, however, are only visible in thin section or with the SEM/EDS. These minerals include allanite-(Ce), chlorite, columbite-(Fe), euxenite-(Y), fluorapatite, fluorite, magnetite, monazite-(Ce), phenakite, pyrite, rutile, uraninite, and zircon. Some Th-U-Y-bearing minerals mentioned by Seadler (2011) have yet to be identified.

Table 2. Minerals identified in three major pits of the Batchellerville pegmatite. Compiled from Tan (1966), Lupulescu (2007), Seadler (2011).

MINERALS	Lower Pit	Big Pit / Fluorite Pit	Garnet Pit
Albite (Ab_{70-95})	C	C	C
Allanite-(Ce)	U		
Almandine			C
Annite-Phlogopite	C	C	A
Beryl	U	C	
Chlorite	U	U	U
Chrysoberyl			C
Columbite-(Fe)			U
Dumortierite	U		U
Euxenite-(Y)		U	
Fluorapatite	U		
Fluorite		U	
Hematite		A	U
Magnetite			U
Microcline	C	A	A
Monazite-Ce	U		
Muscovite	A	C	U
Phenakite			?
Pyrite		U	
Quartz	A	A	A
Rutile*	C	U	C
Schorl	U	U	C
Sillimanite			C
Uraninite	U		U
Zircon			U

(A=Abundant, C=Common, U=Uncommon, *= as exsolved needles in biotite and muscovite)

CLASSIFICATION & ORIGIN

There have been multiple attempts to create a suitable pegmatite classification scheme. Landes (1933) classified pegmatites based on the silica content of their derivative magmas and cites Harker (1909), Lacroix (1922), and Fersman's (1931) prior classifications while trying to explain his own. More recent attempts include the classification systems developed by Černý (1991), Wise (1999), Zagorsky, Makagon & Shmakin (1999), Pezzotta (2001), Ercit (2004), Černý and Ercit (2005) and Simmons (2007). All of these classification systems confirm one thing: classifying pegmatites is extremely difficult. The complex origins of pegmatites, their ambiguous definition, and the disagreement amongst professionals even about the classification of their assumed parent melts – granites – all contribute to the confusion (London 2008).

Historically, pegmatite classification relied on simple mineralogical and field criteria; however, as technology and overall understanding of geologic processes have advanced, current classification schemes have gone beyond these criteria, focusing on the chemical composition and tectonic settings of pegmatites.

Following the classification system of Černý (1991) there are two broad categories of pegmatites: simple and complex. The vast majority of pegmatites are simple, composed primarily of quartz, feldspar, and mica. Complex pegmatites, however, attract the most attention due to their exotic mineral assemblages and enrichment in unusual elements (e.g. Li, Be, B, U, etc.). Within this framework, the most widely used pegmatite classification scheme was set forth by Černý (1991). His classification subdivided pegmatites based on emplacement depth, metamorphic grade of the host rocks, and minor element content of the pegmatite itself (Table 3). From deep to shallow, Černý's categories or "classes" are: 1) abyssal (4-9kb), 2) muscovite (5-8kb), 3) rare-element (2-4kb) and 4) miarolitic (1-2kb).

Černý (1991) further subdivides the rare-element and miarolitic classes of pegmatites into two families on the basis of minor element chemistry: the NYF and LCT families. Initially, these acronyms simply represented the geochemical signatures relating to the relative concentrations of niobium-yttrium-fluorine and lithium-cesium-tantalum found within a specific pegmatite deposit.

Table 3. Pegmatite classification scheme based on depth of emplacement (Černý 1991).

THE FOUR CLASSES OF GRANITIC PEGMATITE CERNY, 1991						
CLASS	**Family**	**Typical Minor Elements**	**Metamorphic Environment**	**Relation to Granite**	**Structural Features**	**Examples**
Abyssal	–	U, Th, Zr, Nb, Ti, Y, REE, Mo Poor (to moderate) mineralization	(Upper amphibolite to) low- to high-P granulite facies ~4-9kb ~700-800C	None (segregations of anatectic leucosome)	Conformable to mobilized cross-cutting veins	Rae and Hearne Princes, Sask. (Tremblay, 1978); Aldan and Anabar Shields, Siberia (Bushev and Koplus, 1980); Eastern Baltic Shield (Kalita, 1965)
Muscovite	–	Li, Be, Y, REE, Ti, U, Th, Nb>Ta Poor (to moderate) mineralization, micas and ceramic minerals	High-P, Barrovian amphibolite facies (kyanite-sillimanite) ~5-8kb ~650-580C	None (anatectic bodies) to marginal and exterior	Quasi-conformable to cross-cutting	White Sea region, USSR (Gorlov, 1975); Appalachian Province (Jahns *et al.*, 1952); Rajahstan, India (Shmakin, 1976)
Rare-Element	**LCT**	Li, Rb, Cs, Be, Ga, Nb< > Ta, Sn, Hf, B, P, F Poor to abundant mineralization, gemstock industrial minerals	Low-P, Abukuma amphibolite to upper greenschist facies (andalusite-sillimanite) ~2-4kb ~650-500C	(Interior to marginal to) exterior	Quasi-conformable to cross-cutting	Yellowknife field, NWT (Meintzer, 1987); Black Hills, South Dakota (Shearer *et al*, 1987); Cat Lake-Winnipeg River Field, Manitoba (Cerny *et al.*, 1981)
	NYF	Y, REE, Ti, U, Th, Zr, Nb>Ta, F Poor to abundant mineralization, ceramic minerals	Variable	Interior to marginal	Interior pods, conformable to cross-cutting exterior bodies	Llano Co., Texas (Landes, 1932); South Platte district, Colorado (Simmons *et al.*, 1987); Western Keivy, Kola, USSR (Beus, 1960)
Miarolitic	**NYF**	Be, Y, REE, Ti, U, Th, Zr, Nb>Ta, F Poor mineralization gemstock	Shallow to sub-volcanic ~1-2 kb	Interior to marginal	Interior pods and cross-cutting dikes	Pikes Peak, Co (Foord, 1982); Sawtooth batholith, Idaho (Boggs, 1986); Korosten pluton, Ukraine (Lazarenko *et al.*, 1973)

However, these criteria do not always apply, as some LCT pegmatites can be extremely rich in niobium, and some NYF pegmatites can have Li-bearing minerals. Therefore, whether or not a pegmatite can actually be classified as an NYF- or an LCT-type pegmatite also depends on the detailed mineralogy of the specific body. Furthermore, highly evolved NYF-type pegmatites can sometimes resemble LCT pegmatites, and under-evolved LCT pegmatites can sometimes resemble NYF pegmatites.

Chemically and mineralogically, New York pegmatites span the range of nearly all of Černý's (1991) pegmatite classes, with the exception of the shallow "Miarolitic" and "REE – LCT" classes, of which there are no clear examples.

Many of the pegmatites from the southern Adirondack Highlands (e.g. Batchellerville, Mayfield, and Greenfield) and from New York City contain Al-rich silicates with or without Be and B such as sillimanite, beryl, chrysoberyl, dumortierite, and tourmaline as well as monazite-(Ce) and uraninite. In addition, they do not show any spatial or temporal relationship with any granitic intrusions (Lupulescu et al. 2011). On the basis of their mineral assemblages, in particular the presence of allanite-(Ce), polycrase-(Y), columbite, titanite, zircon, fluorite, microcline, and albite, many of the Adirondack pegmatites (e.g. the Scott's Farm, Crown Point, Roe Spar Bed, Day (Overlook) Bedford and some of the New York City pegmatites are most closely related to Černý's (1991) REE class NYF-type.

The Batchellerville and Mayfield pegmatites are clusters of small pegmatitic bodies hosted by gneisses. Based upon their geological setting, lack of associated granitic bodies, and their mineralogies, they seem to belong to Černý's (1991) Muscovite and/or Abyssal class of pegmatite. They appear to have formed from in situ partial melts of the local country rock rather than as late-stage magmatic derivatives of larger granitic intrusions. The lack of any significant deformation features within the Batchellerville pegmatite itself indicates that crustal anatexis and the intrusion of these bodies occurred in an extensional setting after the Ottawan orogeny collapse.

REFERENCES CITED

Černý, P., 1991, Rare-element granite pegmatites. I. Anatomy and internal evolution of pegmatite deposits: Geoscience Canada, v. 18, p. 49-67.

Černý, P. and Ercit, T.S., 2005, The classification of granitic pegmatites revisited: The Canadian Mineralogist, v. 43, # 6, p. 2005-2026.

Ercit, T.S., 2004, Global database of pegmatite localities: Journal of Pegmatology, v. 1, # 1, 2 p.

Fersman, A.E., 1931, Ueber die geochmisch-genetische Klassification der Granit-pegmatite: Tschermaks Mineralogische und Petrographische Mitteilumgen, v. 41, p. 64-83.

Harker, A., 1909, Natural history of igneous rocks: New York, 327 p.

Lacroix, A., 1922, Minéralogie de Madagascar: Paris, 310 p.

Landes, K.K., 1933, Origin and Classification of Pegmatites: American Mineralogist, v.18, p. 33-56.

London, D., 2008, Pegmatites: The Canadian Mineralogist, Special Publication 10, 347 p.

Lupulescu, M., Chiarenzelli, J., Pullen, A. and Price, J., 2011, Using pegmatite geochronology to constrain temporal events in the Adirondack Mountains: Geosphere, v. 7, p. 23-39.

Lupulescu, M., 2007, Minerals from New York State pegmatites: Rocks & Minerals, v. 82, # 6, p. 494-500.

Pezzotta, F., 2001, Madagascar's rich pegmatite districts: A general classification: extraLapis English No. 1, Madagascar, p. 34-25.

Putman, G.W. and Sullivan, J.W., 1979, Granitic pegmatites as estimators of crustal pressures - A test in the eastern Adirondacks, New York: Geology, v. 7, p. 549–553.

Seadler, A., 2011, Pegmatite origins and classification: A look at the Batchellerville pegmatite, Batchellerville, NY: Unpublished B.A. Thesis, Hamilton College, Clinton, NY, 120 p.

Simmons, S., 2007, A look at pegmatite classifications: http://www.minsocam.org/msa/special/pig/PIG_articles/Elba%20Abstracts%2018%20Simmons.pdf

Tan, L-P., 1966, Major pegmatite deposits of New York State: New York State Museum and Science Service Bulletin #408, 138 p.

Wise, M., 1999, Characterization and classification of NYF-type pegmatites: Canadian Mineralogist, v. 37, # 3, p. 802-803.

Zagorsky, V., Makagon, V. and Shmakin, B., 1999, The systematics of granitic pegmatites: Canadian Mineralogist, v. 37, # 3, p. 800-802.

ROAD LOG

The field trip will depart from Hamilton College at 7:30 AM and return around 5 PM. The Road Log starts at the intersection of NY State Thruway Exit 27 (Amsterdam) ramp and NY-30N.

Miles from Last Point	Cumulative Mileage	Description
0.0	0.0	Intersection NY-30 N and Thruway Exit 27 ramp. Head NORTH on NY-30 N.
1.0	1.0	Bear left. Stay on NY-30 N.
7.9	8.9	At traffic circle, continue straight on NY-30 N.
0.4	9.3	Go straight; take Co Rd 155 (Do NOT take NY-30 N)
1.1	10.4	In Broadalbin. Continue onto Co Rd 110/117 (N Main St)
0.9	11.3	Bear right, continue on Co Rd 110
1.1	12.4	Bear left, continue on Co Rd 110
6.5	18.9	Continue straight onto Co Rd 7 (S Shore Rd)
4.7	23.6	Slight right to stay on Co Rd 7 (S Shore Rd)
2.4	32.8	Get permission to park.

STOP #1: Access Road to Batchellerville Pegmatite Pits

**NOTE: The Batchellerville pegmatite is on private property; trespassing is not allowed! Permission is required before entering the property for any reason. We are extremely fortunate that the landowner has allowed us to access the site for this field trip. Please do not jeopardize the possibility of future trips for scientific research by trespassing and/or any large-scale mineral collecting activities.

Stop 1a). The "Lower Pit" (Lat: 43.23917, Long: -74.06146)
Stop 1b). The "Big Pit" (Lat: 43.23816, Long: -74.05219)
Stop 1c). The "Garnet Pit" (Lat: 43.23953, Long: -74.05979)

Workshop A4: Technology in the field: GPS, iPads and Gigapans

Jonathan Cobb
Waypoint Technology Group, 17 Computer Dr. E, Albany, NY 12205,
jcobb@waypointtech.com

David Tewksbury
Dept. of Geosciences, Hamilton College, Clinton, NY 13323 dtewksbu@hamilton.edu

Barbara Tewksbury
Dept. of Geosciences, Hamilton College, Clinton, NY 13323 btewksbu@hamilton.edu

This workshop provided college/university-level faculty and researchers with hands-on experience with best practices in field GPS, including recent developments in GPS technology that make it possible to accurately determine positions in challenging environments, using iPads effectively in the field for research and teaching, and taking Gigapan panoramas for research, teaching, and visualization in Google Earth.

GPS

Jonathan Cobb of Waypoint Technology Group (www.waypointtech.com) reviewed the current state of GNSS (Global Navigation Satellite System), which includes the United States NAVSTAR satellite constellation and the Russian GLONASS satellite constellation. Currently these are the only two complete constellations providing global coverage. Some current GPS receivers can receive signals from both sets of satellites improving location positioning. Trimble hardware and software provides an integrated system using the GNSS and land based reference stations to determine 3D positions on the Earth's surface or atmosphere. For the field researcher, GPS receivers and how the data are processed can provide positions from tens of meters to centimeter accuracy. Best practices of configuring and using receivers as well as post processing techniques were covered.

iPADS

Barb Tewksbury demonstrated the use of several iPad apps that can be used in the field for both research and teaching, and participants had a chance to try out these apps, discuss their pros and cons, and brainstorm ways of using the iPad with students in the field. The apps included a variety of Brunton compass apps, note-taking apps, and field GIS apps.

GIGAPANS

Dave Tewksbury covered the setup and use of Gigapan camera systems (http://www.gigapan.com/) to capture high-resolution field imagery. The Gigapan camera system, developed from the Mars Rover Camera technology, uses a robotic camera head to move a digital camera in a set pattern capturing small sections to cover a large scene. These individual images are composited together by the Gigapan Stitcher software to create a single, large, high-resolution image of the scene. This image can be "zoomed-into" without pixelation. Although most Giagapans focus on expansive scenes from panorama to outcrop scale, macro to micro Gigapans (www.gigapan.com/gigapans/100119)
are also possible. If GPS location data was recorded for the camera position, the image can be georeferenced and ported to Google Earth where it can be viewed by simply sharing a KML/KMZ file. The Gigapan website allows users to share Gigapan images with the ability to pan and zoom into the image. An iPad app allows access to Gigapan images via the iPad. High quality prints can be made on a large format printer.

A Census of Devonian Life in Central New York State: Fossil Collecting for Teachers and Students

Constance M. Soja
Department of Geology, Colgate University, Hamilton, NY 13346
csoja@colgate.edu

Cynthia R. Domack
Department of Geosciences, Hamilton College, Clinton, NY 13323
cdomack@hamilton.edu

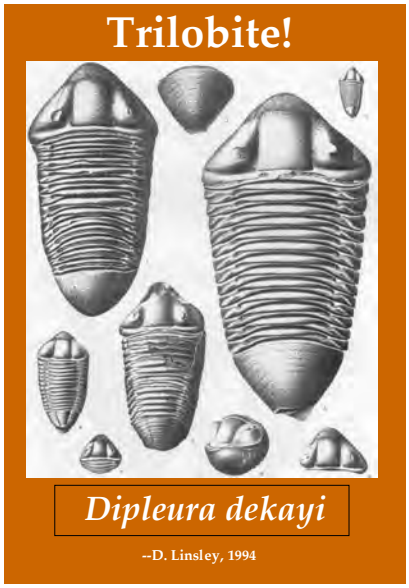

84th Annual Meeting
New York State Geological Association (NYSGA)
September 28 - 30, 2012
Hosted by Geosciences Department,
Hamilton College
Clinton, NY 13323

Richly fossiliferous rocks of Middle Devonian age (375 million years old) are exposed near Hamilton, NY, and represent some of the most complete fossil-bearing sequences that formed during this time period anywhere in the world. The shale we will examine was deposited at a time when the Acadian Mountains (precursor of the younger Appalachian Mountains) were forming in eastern New York state (present day Catskills Mountains area) as a result of collision between a microcontinent and eastern North America. Uplift and mountain building resulted in extensive erosion and transport of sediment towards Hamilton where these materials accumulated. As the fossils below indicate, the shallow epi-continental (epeiric) sea that once covered central New York State had abundant, teeming life.

Photographs by C.M. Soja of Middle Devonian fossils from central New York State
in the R.M. Linsley Collections, Department of Geology, Colgate University, Hamilton, NY

Our goal during the field exercise is to accumulate as much information as possible to complete a detailed "census" and paleoecological analysis of the fossils. Upon arrival at the field site, participants will draw specialist roles from a hat and work in small groups collecting fossils. Time will be allotted for specialists to work together compiling data before our group discussion. We will brainstorm questions that paleontologists can ask and answer about the fossils preserved at the field site. Participants will depart the field site appreciating the diversity of life that existed in central New York State during the Devonian and the environmental conditions that were conducive to exquisite fossil preservation.

Field Trip Schedule

12:00 noon—group departs Hamilton College for fossil site near Lebanon Reservoir
(32 miles + one quick restroom stop = 1 hour)

1:00 pm—bus arrives at fossil locality

1:00-1:15 pm—welcome and orientation

1:15-2:15 pm—group collects fossils in specialist teams

2:15-3:00 pm—each team compiles fossil data

3:00-3:45 pm—group discusses data and makes interpretations

3:45-4:00 pm—Q&A, participants pack up samples

4:00 pm—group departs Geer Road (+ one quick restroom stop)

5:00 pm—group arrives at Hamilton College

A fossil guide (Some Common Invertebrate Macrofossils of the Hamilton Group of Central New York modified by C. M. Soja) will be provided to each participant.

Environmental and Geotechnical Drilling

Mr. William Morrow, P.G. and Mr. Sean Pepling
bmorrow@pwinc.com / spepling@pwinc.com
Parratt-Wolff, Inc.
5879 Fisher Road
East Syracuse, New York 13057

Environmental and Geotechnical drilling projects provide subsurface data critical in the evaluation of a site. Whether the purpose of the investigation is to assess for the presence of soil and ground water contamination or for the design and construction of structures, proper subsurface investigations must be performed. Drilling provides one of the most fundamental ways in which subsurface information is obtained for evaluation by a geologist or engineer. In the text that follows, a brief overview of environmental and geotechnical drilling is provided. Also included are typical methods for describing soil and rock samples.

DRILLING METHODS

Prior to choosing a particular drilling method, consideration should be given to a number of variables including:

- Type of formation to be drilled (unconsolidated or consolidated material),
- Borehole depth,
- Borehole diameter,
- Quality of samples desired,
- Cross Contamination potential, and
- Whether a well will be installed in the borehole.

Once these variables have been considered one of the following four drilling methods are commonly used to make the boring.

Cable Tool Method

In the cable tool method, the borehole is advanced by lifting and dropping a heavy string of drilling tools (Figure 1). The tools are suspended on a steel cable and terminate in a chisel shaped bit. The impact of the bit breaks up the formation, which must then be removed from the borehole. Typically, the soil or rock cuttings are suspended in water in the borehole and are removed with a large bailer. In unconsolidated formations, temporary casing is advanced during drilling to keep the borehole from collapsing. The temporary casing also minimizes potential cross-contamination between materials in environmental investigations. Formation samples can either be collected from the bailer or with a variety of different soil samplers.

Fluid Rotary Method

Fluid rotary drilling involves rotation of a drill rod and bit. The most common type of bit is a tri-cone roller bit, designed to cut through soil and rock. A drilling fluid is circulated through the drill rod and bit and up the annular space between the rod and borehole (see Figure 2). The drilling fluid is used to lubricate the bit, carry cuttings to the surface and maintain hole stability. Additives, such as bentonite, are often mixed with water to increase the weight and viscosity of drilling fluid. Bentonite fluid drilling is often referred to as "mud rotary". Fluid rotary is a rapid way of advancing a large diameter borehole. However, soil samples recovered from the drilling fluid are marginal for accuracy due to loss of fine-grained materials. In addition, fluid remaining in the formation after drilling may lower borehole permeability and potentially alter ground-water chemistry.

Air Rotary Method

Air rotary drilling is similar to fluid rotary except that air compressed is used to cool the bit and carry cuttings to the surface. Air rotary drilling is generally limited to consolidated formations because air alone will not maintain an open hole in unconsolidated material. Air rotary is a very effective rock drilling methods. When combined with a downhole hammer drill bit, boreholes can be drilled very rapidly in bedrock. Another advantage of air rotary drilling is that water produced from the rock is carried to the surface allowing evaluation of the relative productivity of various strata. However, soil or rock sampling is limited to evaluating the drill cuttings as they are conveyed out of the borehole by the air.

Hollow Stem Auger Method

Hollow stem auger drilling is the most commonly used method in both environmental and geotechnical investigations. Figure 3 provides an illustration of the typical components in a hollow stem auger. This method is fast, relatively inexpensive and provides excellent sampling capabilities. With hollow stem augers, the hole is advance by rotating and pressing the auger into the soil. As the auger is advanced into the soil, cuttings are conveyed upwards on the auger flights. This methods is limited to unconsolidated materials and to depths generally less than 100 feet. The hollow stem auger method allows the collection of representative soil samples ahead of the lead auger. The hollow stem augers also permit the installation of monitoring wells.

MONITORING WELL INSTALLATION

Monitoring wells are installed for a variety of purposes but generally to allow discrete sampling of ground water. These purposes must be defined prior to installation so that a well can be properly designed and constructed from the right materials. The objectives for installing monitoring wells may include:

- Determining ground-water elevations, flow directions and velocities,
- Sampling and monitoring for the presence of contaminates, and
- Assessing aquifer characteristics (e.g., hydraulic conductivity).

Most monitoring wells are completed in the first permeable, water-bearing zone encountered. Care must be taken to assure that the well is completed at a depth sufficient to allow for seasonal water-table fluctuations. Monitoring well construction materials include: riser pipe and screen materials, annular materials and protective covers. The selection of well construction materials depends on the method of drilling, type of contamination expected, and the natural water quality.

Riser pipe and screen materials are specified by diameter, type of material and thickness of pipe. Well screens require an additional specification of slot size. Riser pipe and screen materials are commonly constructed from polyvinyl chloride (PVC); although Teflon, carbon steel, stainless steel, and galvanized steel are also available. The annular space between the borehole and the screen is usually backfilled with sand to an elevation 2 to 3 feet above the top of the screen. Bentonite is then placed on top of the sand pack and expands by absorbing water. This provides a seal between the screened interval and the rest of the annular space and formation. Cement grout is placed on top of the bentonite to ground the surface. The grout stabilizes the well and limits the potential of surface runoff reaching the screened interval. Gout, as applied to environmental or engineering projects, is typically a mixture of cement, bentonite and water.

A steel protective casing is often placed around the monitoring well. The protective casing has a locking cover and is set into a concrete pad. Small-diameter manholes are also available for situations requiring ground surface completions (i.e. wells located in roadways or parking lots). The purpose of the protective cover or manhole is to prevent vandalism that may result in groundwater contamination. An example of a monitoring well completion diagram is included as Figure 4. ASTM Standard Practice Design and Installation of Groundwater Monitoring Well in Aquifers (D5092-90) provides additional detailed information on the installation of monitoring wells.

SOIL AND ROCK SAMPLING METHODS

Although preliminary sample information can be obtained from soil or rock cuttings, far more accurate soil and rock samples can be obtained by collecting discrete soil samples or rock coring.

Soil Sampling

Discrete soil sampling consists of pressing or driving a sampler into the soil. The samplers can collect either disturbed or undisturbed soil samples. An example of a disturbed sample is one that is driven into place (i.e. split spoon sample, Geoprobe® sample, etc.). An undisturbed sample is one recovered in such a way that the physical structure and soil properties are relatively unchanged during sampling. These samples are typically obtained

by pressing a thin-walled tube (such as a Shelby tube) through the desired interval. These galvanized steel tubes are typically 3 inches outside diameter with a sample length of about 30 inches. The retrieved tube is then sealed for shipment to a physical testing laboratory. Detailed information about undisturbed sampling may be found in the ASTM Standard Practice for Thin-Walled Tube Sampling of Soils (D1587-83).

A disturbed sample is collected by driving a sampler into the soil with either a free falling hammer or hydraulic hammer. These samples are usually either as split spoon sampler or a tube sampler. The split spoon sampler is driven through the desired interval by dropping a 140-pound hammer 30 inches. The number of blows required to drive the sampler for 6-inch increments are recorded and used to compare the penetration resistance between samples. The split spoon sampler normally measures 2 inches or 3 inches outside diameter with a minimum sample length of 18 inches. At the surface, the sampler is opened, allowing for soil classification and containerization for subsequent evaluation. Tube samplers, such as those made by Geoprobe, are lined with plastic sleeves and driven into the soil with a hydraulic percussion hammer. After removal from the borehole, the sleeve is removed and the sample classified and contained. Additional information about split spoon sampling may be found in the ASTM Method for Penetration Test and Split Barrel Sampling of Soils (D1586-84).

Rock Coring

Rock coring is used to collect discrete rock samples. The rock is cored with a tubular diamond-studded bit attached to a core barrel. As the diamond bit cuts a rock, a cylindrical-shaped rock sample is bushed into an inner barrel. Removal of the rock core from the subsurface is normally accomplished by lowering a wireline with a coupling into the drill rods, latching onto and pulling out the inner barrel. The recovered rock core is then removed from the inner barrel for examination or testing. The inner barrel is reinserted and the diamond bit advanced to the end of the next sampling interval. Water is constantly pumped down the rods during sampling to cool the core bit and flush cuttings to the ground surface. Diamond core barrels come in a variety of diameters and lengths. In environmental and geotechnical drilling, typically 2.0" or 2.5" diameter rock cores are collected (NX or HX size respectively) in 5.0-foot penetration runs.

Sample Description

Soil penetration tests and rock coring provide the geologist or engineer samples that can be used to make a variety of interpretations. The first step, however, is to describe and classify the recovered soil or rock sample.

Soil Description

Soils may be described and classified using a variety of methods. The most common method is the Unified Soil Classification System (USCS). This method identifies soil types on the basis of grain size and liquid limits. The soil is then categorized using a series of descriptive terms, followed by a two-letter symbol. In the USCS system, all soils are broken down into two broad categories – fine-grained soils (silt and clay) and coarse-grained soils (sand and gravel). The order of description for fine-grained soil is:

- Consistency (determined from blow counts)
- Moisture Content
- Color
- Modifying Soil
- Major Soil
- Other soil components
- Observations

An example of a fine-grained soil described according to the USCS classification system is "Moist red-brown silty CLAY, trace rounded quartz gravel (CL)". The order of description for coarse-grained soils is:

- Moisture
- Color
- Modifying soil
- Angularity
- Graduation
- Major Soil
- Other soil components

- Observations

An example of a coarse-grained soil is "Dry brown clayey fine to coarse SAND, little subangular fine gravel (SW-SC)". ASTM Practice for Description and Identification of Soils, (visual-manual procedure) (D2488) in an excellent reference for describing and classifying soils.

Rock Description

The components typically used to describe a rock core are color, thickness of bedding, rock type, weathering state, hardness, and joint or fracture spacing. Additional components, such as texture are used to further describe a rock as needed. An example of a rock description could be "Brown, thin bedded, fine-grained SANDSTONE, highly weathered, soft, close fractured". The definition of each of the components is given in Figure 5. Another important component worth noting in a core run is its structural integrity. This component can be approximated by calculating the rock quality designation (RQD). The RQD is determined by adding the total lengths of all pieces exceeding 4 inches and dividing by the total length of the coring run, to obtain a percentage (see Figure 6). The percentages between different core runs can be compared to quickly assess the rock quality between samples.

WELL LOG PREPARATION

Well logs provide documentation of drilling activities conducted during environmental and geotechnical investigations. The importance of properly completed well logs cannot be overemphasized. The information well logs contain is used by the geologist or engineer to make decisions which are critical to the successful completion of a project. It is the responsibility of the individual overseeing the drilling activities to prepare well logs that are accurate, consistent and legible. Most well logs include the following information:

- Project name and location,
- Boring/Well number,
- Date(s) drilling started and finished,
- Boring location and elevation,
- Page number and total number of pages for each boring,

- Depth of each sample taken,
- Depth at which obstacles were encountered while advancing the borehole (boulders, etc.).
- Length of drive for soil samples and length of sample recovered.
- Number of blows required to drive sampler when standard penetration test is used,
- Length of each run for rock core and footage of core recovered,
- RQD values for each run,
- Changes in drilling rate and fluid loss when coring rock,
- Full description of soil and/or rock samples, as discussed in Section 3.0,
- Reason for boring abandonment when specified depth is not reached,
- Unusual conditions encountered in advancing the boring and in sampling,
- Complete description of well materials used and depths (if applicable), and
- Depth to water while drilling, prior to removal of any casing and 24 hours after all down-hole tools have been removed.

An example of a boring log used by Parratt-Wolff, Inc. is shown in Figure 7.

CONCLUSION

The methods and procedures described provide a general overview of environmental and geotechnical drilling and sampling. These methods and procedures are used to provide critical subsurface data on many projects. The references that follow are just a partial list of the many publications currently available about Environmental and Geotechnical drilling.

REFERENCES

Aller, L. – et al, 1989. Handbook of suggested practices for the design and installation of groundwater monitoring wells; National Water Well Association, Dublin, Ohio, 398p.

American Society for Testing Materials (ASTM), 1993. Proceedings from Groundwater Monitoring and Sampling Technology Short Course: Design, Installation, Development and Sampling of Groundwater Monitoring Wells; American Society for Testing Materials, Philadelphia, Pennsylvania 244p.

American Society for Testing Materials (ASTM), 1995. Practices for design and installation of groundwater monitoring well in aquifers: D5092; 1997 Annual Book of American Society for Testing Materials Standards, Philadelphia, Pennsylvania, Vol. 04.09 pp.77-87.

American Society for Testing Materials (ASTM), 1994. Practice for thin-walled tube sampling of soils: D1587; 1997 Annual Book of American Society for Testing Materials standards, Philadelphia, Pennsylvania, Vol. 04.08 pp. 142-144

American Society for Testing Materials (ASTM), 1992. Practice for description and identification of soils (visual/manual procedure: D2488; 1997 Annual Book of American Society for Testing Materials standards, Philadelphia, Pennsylvania, Vol. 04.08 pp. 228-238.

Driscoll, F.G., 1986. Ground water and wells, 2nd edition; Johnson Division, St. Paul, Minnesota, 1089 pp.

Company Profile

Parratt-Wolff, Inc. (PWI) was founded in 1969 to provide soil and rock drilling to the Northeast. Since then, PWI has grown to a company of three offices, 50 employees and 29 major pieces of field equipment. Our service area includes all states from New Hampshire to Florida. Each year, PWI makes thousands of borings in both soil and rock. We keep a test boring log on nearly every hole drilled, giving us a comprehensive geologic data base. If you are in the Syracuse area and would like to tour PWI's facility or would like to discuss subsurface conditions in your project area, give us a call.

William H. Morrow or Sean Pepling
Parratt-Wolff, Inc.
5879 Fisher Road
East Syracuse, NY 13057
bmorrow@pwinc.com / spepling@pwinc.com
(315) 437-1429

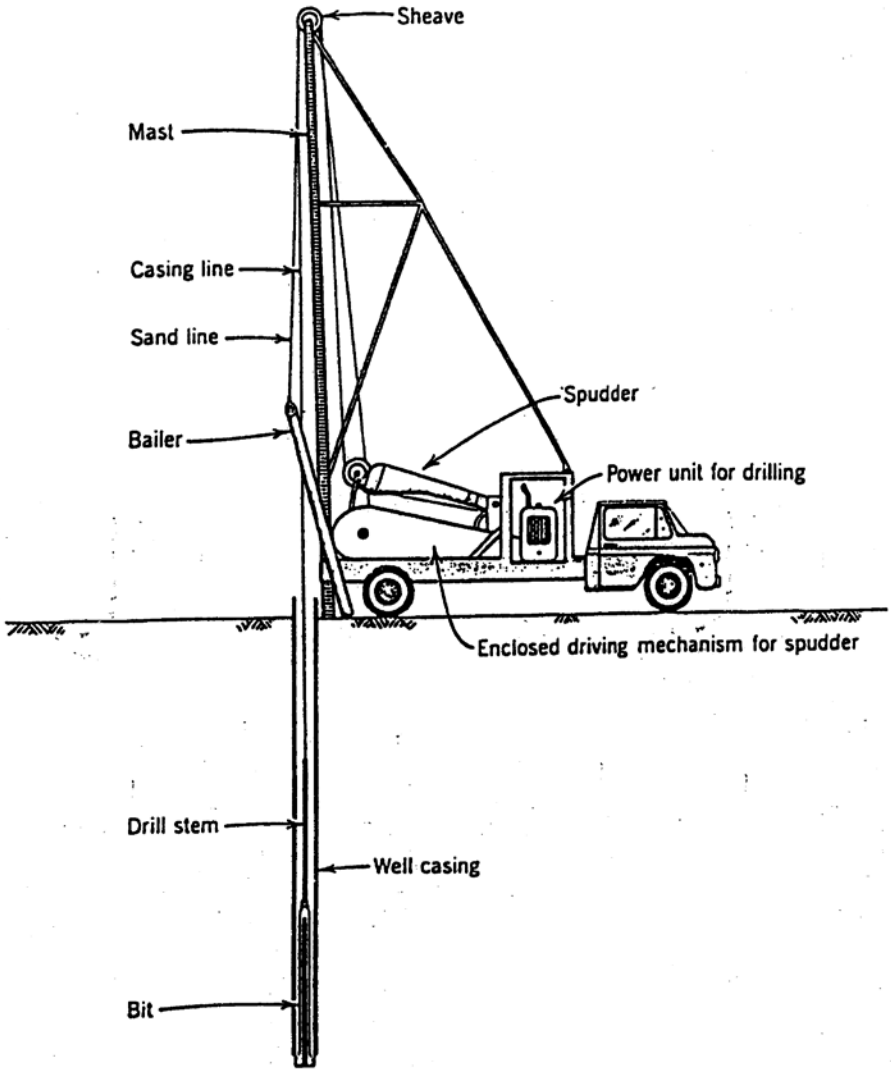

Figure 1. Cable tool method for making boreholes. The casing is advanced as the borehole is drilled in unconsolidated formations (Aller et al, 1989).

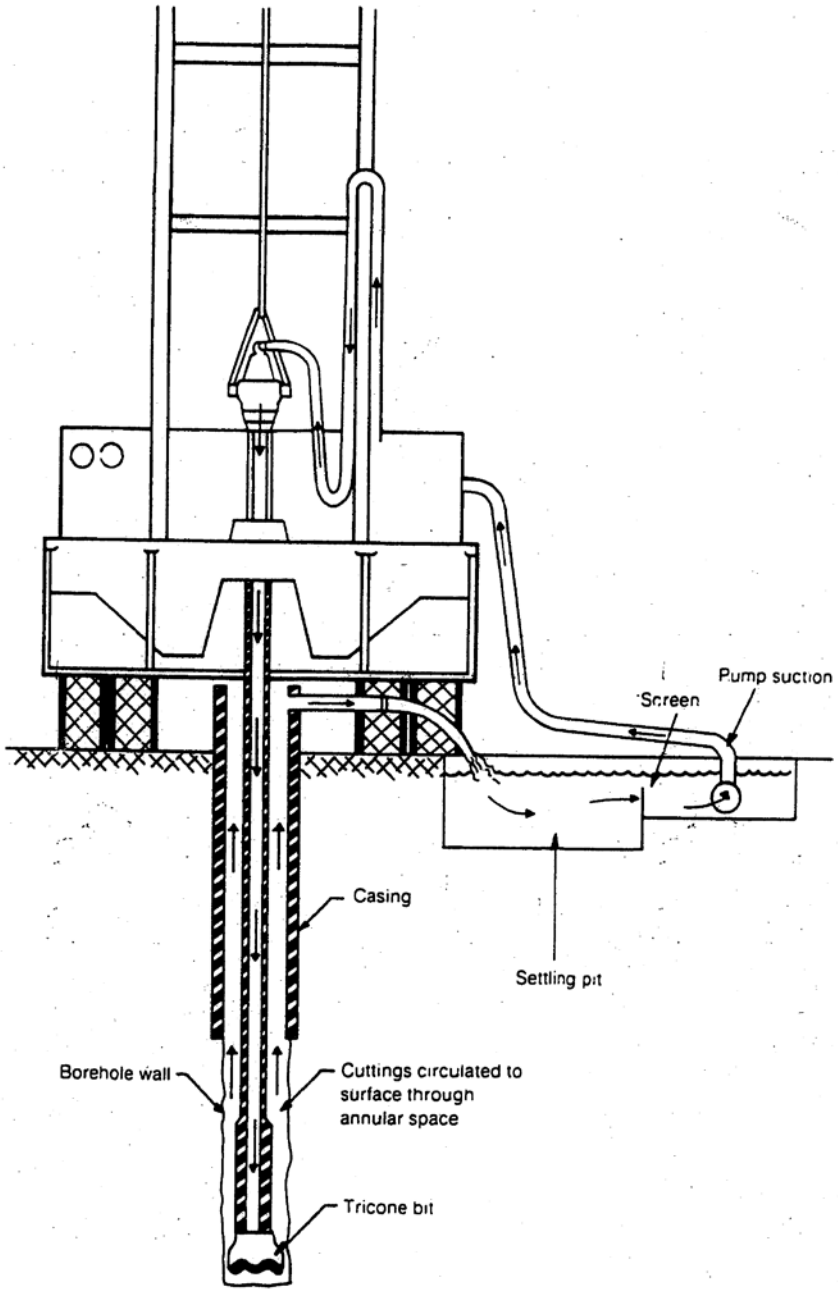

Figure 2. Diagram of direct fluid rotary circulation system (From Aller et al, 1989).

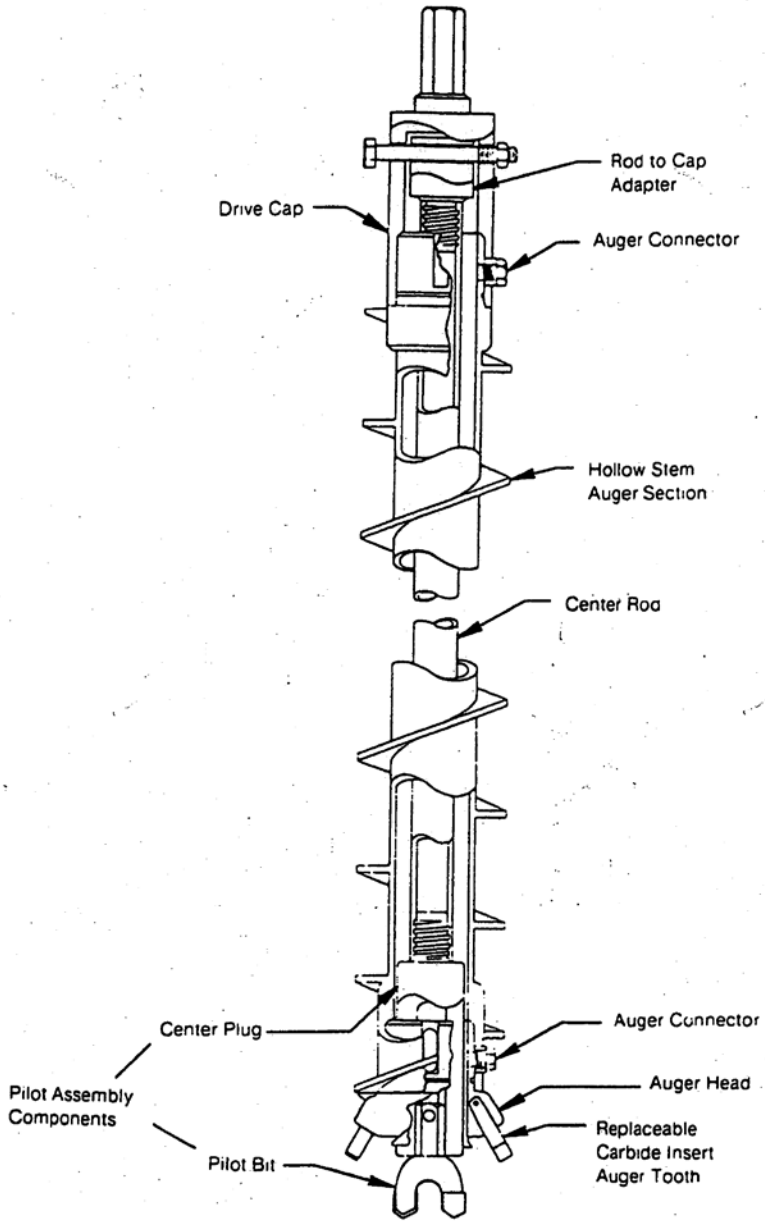

Figure 3. Typical components of the down-hole tools used with the hollow-stem auger drilling method (Aller et al, 1989).

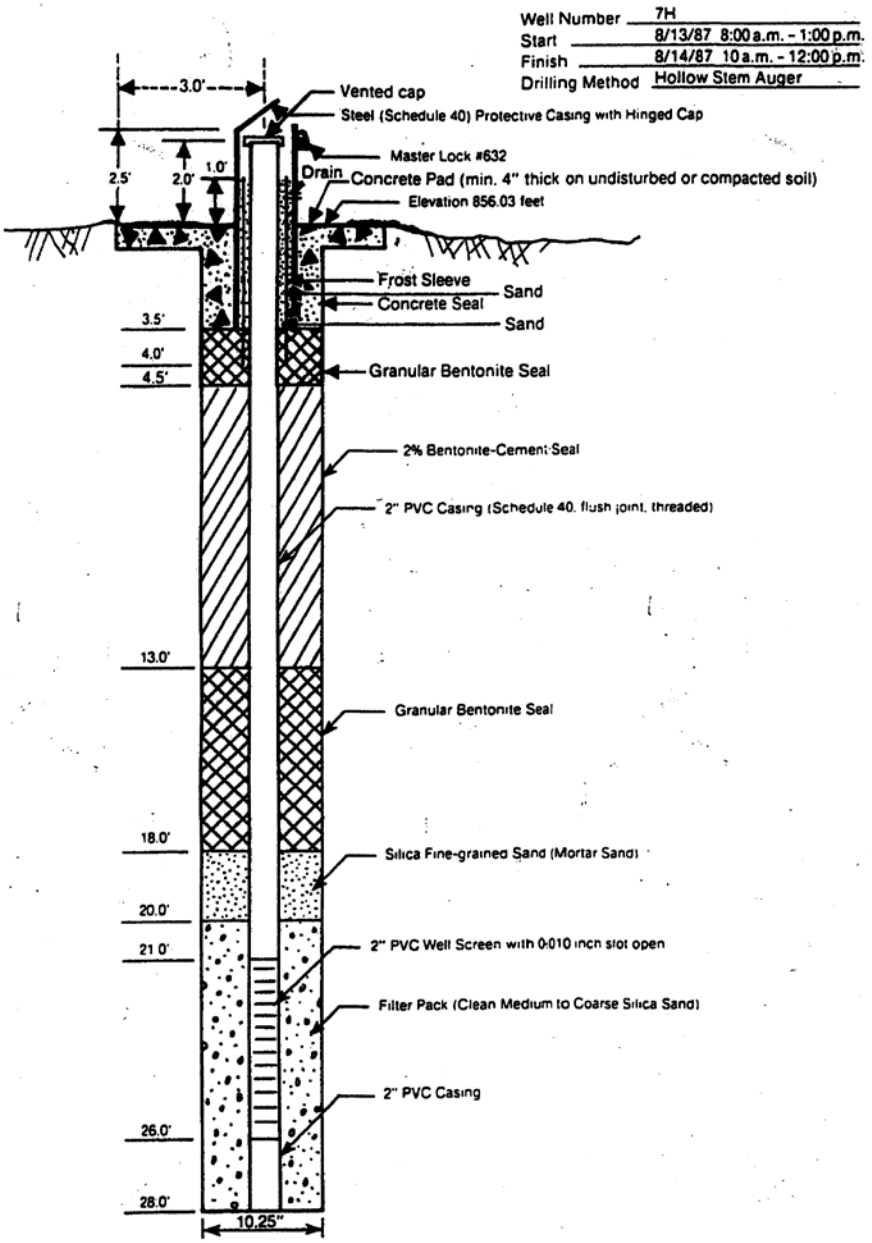

Figure 4. Typical monitoring well completion diagram showing the materials and dimensions of each component (Aller et al, 1989).

ROCK CORE DESCRIPTION

The following components are commonly used by our drillers to describe collected rock cores:

depth of core run;
run number (R-1, R-2, etc.);
recovery (in feet);
rate of penetration - recorded as "minutes per foot" of penetration (ex: MPF = 6); and
generalized rock description (i.e. Red/brown sandstone).

If the rock is logged by a Parratt-Wolff, Inc. geologist, the rock core descriptions will also commonly include:

recovery (in percent);
rock quality designation (RQD); and
detailed rock description.

The RQD or "Rock Quality Designation" is the combined length of all core pieces whose individual lengths are greater than four inches, divided by the length of the core run. RQD is typically only used when describing NX cores or larger.

EXAMPLE OF DETAILED ROCK DESCRIPTION:

"Brown, thin bedded, fine-grained sandstone, highly weathered, soft, close fractured".

The components used to describe the rock core in detail are color, thickness of bedding, rock type, weathering state, hardness, and joint or fracture spacing. Additional components, such as texture, are used to further describe the rock as needed. The following tables include the definitions of these different rock descriptive terms.

Component	Term	Defining Characteristic
Bedding Thickness	Laminated	< 0.1 in.
	Very Thin Bedded	0.1 - 1.0 in.
	Thin Bedded	1.0 - 4.0 in.
	Medium Bedded	4.0 - 12.0 in.
	Thick Bedded	12.0 - 36.0 in.
	Massive	> 36 in.
Hardness	Soft	Scratched with fingernail
	Medium Hard	Scratched with a knife
	Hard	Difficult to scratch with a knife
	Very Hard	Can not be scratched with a knife
Joint or Fracture Spacing	Very Close	< 1.0 in.
	Close	1.0 - 2.0 in.
	Moderately Close	2.0 - 12.0 in.
	Wide	12.0 - 36.0 in.
	Very Wide	> 36.0 in.
Weathering State	Fresh	No visible sign of decomposition or discoloration
	Slightly Weathered	Slight discoloration inward from open fractures
	Moderately Weathered	Discoloration throughout fracture. Weaker minerals such as feldspar are decomposed.
	Highly Weathered	Most minerals are somewhat decomposed. Specimens can be crumbled by hand with effort and easily scraped by a knife.
	Extremely Weathered	Rock is decomposed to extent that it looks like soil, but original fabric or structure are preserved.

Figure 5 Components & Definitions Used to Describe Rock Core Samples

☒**P.O. Box 56, 5879 Fisher Road, East Syracuse, NY 13057 Telephone 315-437-1429 or 800-782-7260 Fax 315-437-1770**
☐**P.O. Box 1029, 501 Millstone Drive, Hillsborough, NC 27278 Telephone 919-644-2814 or 800-627-7920 Fax 919-644-2817**

Calculations:
Core recovery = total length of all recovered pieces.
RQD = the sum of all pieces greater than 4" in length, divided by the length of the run.

Example:

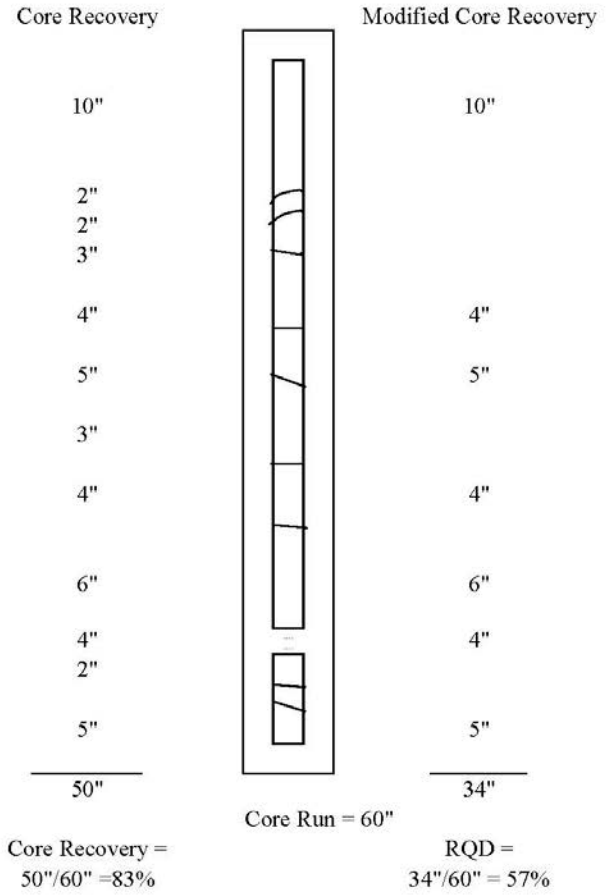

Figure 6 Method for calculating RQD - Rock Quality Designation.

TEST BORING LOG

parratt wolff inc

PROJECT XYZ Facility

HOLE NO. B-1

LOCATION Syracuse, New York

JOB NUMBER: 9700

GROUNDWATER DEPTH
WHILE DRILLING 12.0'

DATE STARTED 8/10/97
DATE COMPLETED 8/10/97

BEFORE CASING
REMOVED 22.0'

N - NO. OF BLOWS TO DRIVE SAMPLER 12" W/140# HAMMER FALLING 30" - ASTM D-1586 STANDARD PENETRATION TEST

AFTER CASING
REMOVED 19.0'

C - NO. OF BLOWS TO DRIVE CASING 12" W/ # HAMMER FALLING "/ OR PERCENT CORE RECOVERY

CASING TYPE HOLLOW STEM AUGER, NQ WIRELINE

SHEET 1 OF 1

Subsurface Elevation: 100.0'

DEPTH	SAMPLE DEPTH	SAMPLE NO.	C	SAMPLE DRIVE RECORD PER 6"		N	DESCRIPTION OF MATERIAL	STRATA CHANGE DEPTH
	0.0'-	1		11	15		Dry brown clayey fine to coarse SAND with	
	2.0'			17	5	32	little fine gravel (SW-SC)	
5.0								7.0'
	7.0'-	2		1	2		Firm moist red-brown silty CLAY with trace	
	9.0'			4	6	6	gravel (CL)	
10.0								
15.0								15.0'
	15.0'-	3		10	25		Hard moist brown silty SAND with some fine	
	17.0'			30	30	55	subrounded gravel (SM)	
20.0							Top of Weathered Rock	20.0'
	20.0'-	R-1	Rec	NX CORE			Brown thin bedded fine grained SANDSTONE,	
	25.0'		5.0'				highly weathered, soft, close fractured	
			100%					
25.0			RQD=68%					
	25.0'-	R-2	Rec				Gray thick bedded CRYSTALINE LIMESTONE,	
	30.0'		4.0'				slightly weathered, medium hard, wide	
			80%				fractured	
30.0			RQD=90%				Bottom of Boring	30.0'

Figure 7
Typical Test Boring Log

☐ P.O. Box 56, 5879 Fisher Road, East Syracuse, NY 13057 Telephone 315-437-1429 or 800-782-7260 FAX 315-437-1770
☐ P.O. Box 1029, 501 Millstone Drive, Hillsborough, NC 27278 Telephone 919-644-2814 or 800-627-7920 FAX 919-644-2817

Silicic Appalachian Magmatism During the Ordovician and Devonian: Perspectives from the Foreland Basin, and the Hinterland

Charles Ver Straeten
New York State Museum and Geological Survey, 3140 Cultural Education Center, Albany, NY 12230 cverstra@mail.nysed.gov

Gordon Baird
Department of Geosciences, SUNY Fredonia, Fredonia, NY 14063 Baird@fredonia.edu

Paul Karabinos
Geosciences, Williams College, Williamstown, MA 01267
Paul.M.Karabinos@williams.edu

Scott Samson
Earth Sciences Department, Syracuse University, Syracuse, NY 13244-1070
sdsamson@syr.edu

Carlton E. Brett
Department of Geology, University of Cincinnati, Cincinnati, OH 45221-0013
carlton.brett@uc.edu

INTRODUCTION

At times, viscous, silica-rich molten rock in the upper portion of a magma chamber is forced upward and out of the chamber, through conduits to the surface, where volcaniclastic materials are explosively erupted through the mouth of a volcano and high into the atmosphere. Once buoyantly aloft, the extruded pumice, ash, crystals and rock fragments become sediments, and settle out close to far from the volcano, blanketing any and all

environments downwind. These airborne volcanic sediments may sometimes be transported thousands of kilometers from the source volcano by wind.

The history of explosive silicic magmatism on Earth is recorded in the plutonic and volcanic igneous rocks of their source areas, in volcanic and magmatic arcs; and in sediments, modern and ancient, downwind of their eruptive centers. Reconstruction of the history of silicic paleovolcanism, especially when the igneous source areas have been deeply eroded over deep geologic time (e.g., the Appalachian mountains), may be best determined through data from both hinterland (orogenic belt) igneous and foreland sedimentary rocks.

The purpose of this article and fieldtrip is, perhaps for the first time, to bring together a diverse team of geologists and their perspectives on regional silica-rich magmatic activity during the Ordovician and Devonian Periods – from both foreland sedimentary and hinterland igneous/tectonic records.

Following an overview of volcanic tephra processes from the magma chamber to final burial in sedimentary deposits (by Ver Straeten), Paul Karabinos will present a tectonic overview of the Appalachian hinterland during the low to mid Paleozoic, and compare data on volcanism of that time from the hinterland and foreland. Scott Samson then examines the materials in foreland basin volcanic layers that yield geochronologic, isotopic and geochemical data, which in turn yield an overview of the composition, source characteristics and petrogenetic origins of Ordovician magmas in eastern North America. Baird presents a detailed analysis and discussion of the sedimentologic, preservational, and diagenetic histories of Late Ordovician airfall volcanic layers in the Mohawk Valley. Finally, Ver Straeten lays out the time-stratigraphic occurrence of foreland basin tephra layers in the Devonian of the eastern U.S., and then provides an example comparing foreland basin and hinterland data from the Lower Devonian, with implications for possible igneous sources. In turn, the field trip will stop at four localities, to examine Ordovician and Devonian airfall volcanic "tephra" layers in sedimentary rocks, and feature similar discussions.

Various terms are utilized for the volcaniclastic products of explosive volcanism (e.g., tephra, ash, tuff, bentonite, K-bentonite, and others), as seen in this paper. The term "K-bentonite" is often applied to these Paleozoic volcanic layers. However, such beds may be not only K-bentonites, as seen at Stops 1 and 2. There they occur in three to four different states; as clay-rich K-bentonites, as phenocryst-rich tuffs, and as clay-poor calcite-cemented

layers in which the original glass was apparently altered to zeolite minerals instead of clays. Rather than use multiple terms that actually describe their multifarious diagenetic and sedimentologic histories, it is perhaps best to recognize their shared volcanic origin – and call them "tephras", the term chiefly utilized by modern and recent volcanologists for the products of explosive volcanism.

Technically, tephra consists of various components: volcanic glass fragments (= "volcanic ash"), pumice clasts, and crystals formed in the magma ("phenocrysts"), plus or minus country rock fragments. This is commonly termed "volcanic ash", but as just noted, ash actually represents only the fine volcanic glass component of volcaniclastic materials. "Tuff" is commonly used for coarser-grained volcaniclastic deposits. "Bentonite" is clay-rich altered tephra, in which the glassy ash is altered to smectitic clays; in "K-bentonites" or "metabentonites", clays are further altered to potassium-rich, mixed layer illite-smectite clays.

I. VOLCANIC TEPHRA EVENT PROCESSES (Chuck Ver Straeten)

Volcanic Tephra Processes

The fate of airfall volcanic tephra in sedimentary environments, the result of a single volcanic eruption, involves a vast array of igneous and sedimentary processes. From the degassing of volatiles in a magma chamber and formation of pyroclastic materials, through their explosive eruption, transport and deposition, to varied post-depositional pathways of burial and reworking that occur in sedimentary environments, preservation of a single eruptive event layer depends on so many variables. And is generally a rather unlikely occurrence. The purpose of this section is to provide a medial-level overview of processes involved from the magma chamber to final burial of airfall tephra sediments in sedimentary environments.

Eruption Processes (based on Schmincke 2004, p. 155-157)

Explosive volcanic eruptions result from complex interactions and processes that begin in the upper part of a magma chamber (Figure 1). When a magma becomes oversaturated in

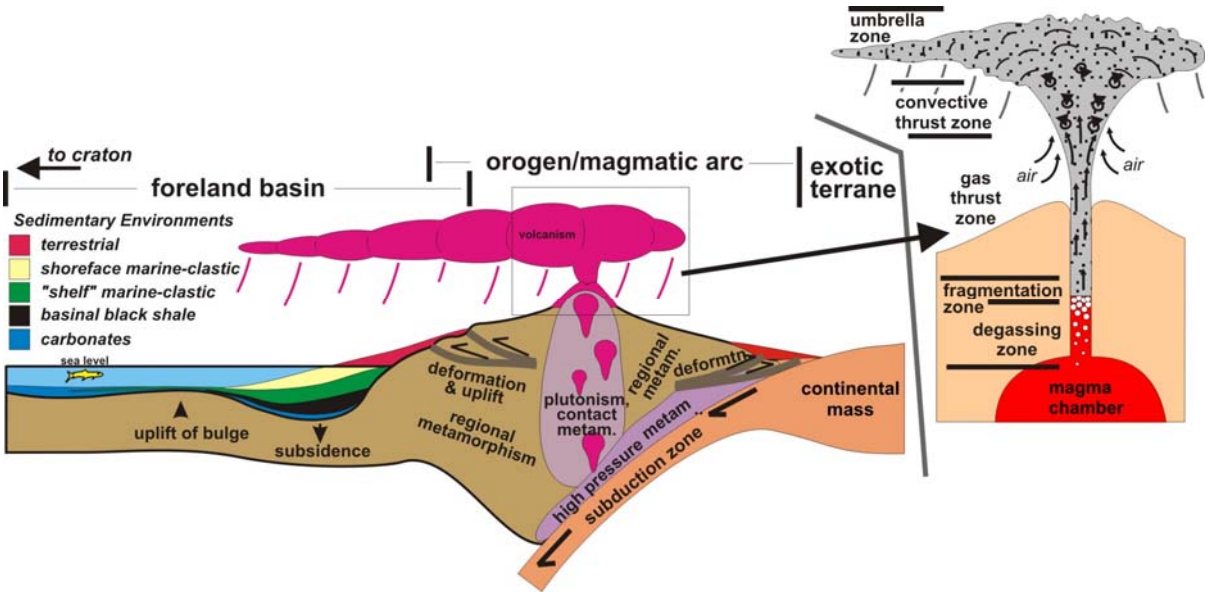

Figure 1. Settings of volcanic tephra processes. Generalized cross-section of subduction zone, orogenic belt/magmatic arc, and adjacent foreland. Inset provides close-up perspective of internal processes from magma chamber to stratosphere during explosive silicic eruption.

volatile components, gases separate out and form bubbles, which undergo expansion ("degassing zone"). This, and/or other factors, leads to expulsion of magma through conduits.

Degassing and bubble expansion continues in the rapidly rising magma. When the volume of gas bubbles approaches 65%, the magma begins to fragment ("fragmentation zone"), which leads to the formation of pyroclasts via: 1) brittle fracture of the magma from explosive "rarefaction" waves; 2) gas bubble bursting with rapid decompression of the magma; and 3) fragmentation of tephra particles in rapid flow conditions within the volcanic conduit.

Rapid gas expansion within the fragmentation zone generates a strong accelerating jet of gas and pyroclastic fragments ("tephra", i.e., volcanic glass fragments commonly termed "ash", pumice, and crystals, plus or minus country rock fragments) through the upper part of the conduit. The mix of gases and tephra is forcefully ejected at the mouth of the volcano and shot upward into an overlying "eruption column".

Driven by momentum, the relatively dense mix of pyroclasts and gas is jetted into the atmosphere through the lower part of an eruption column ("gas thrust zone"). As the column continues to rise, cold air is generally incorporated into the column along its margins; the column's density decreases as larger pyroclasts fall out, and the introduced air heats up. As a result, buoyant convective processes drive upward motion through the overlying "convective

thrust zone" (upper portion of eruption column). Positive buoyancy may drive the eruption column to 30 or more kilometers into the atmosphere. At a level where the eruption column reaches neutral buoyancy, gases and pyroclastic material (tephra) spread out ("umbrella zone").

Fallout and Sedimentation Processes

Once ejected into the atmosphere, the transport, distribution and settling of airborne volcanic tephra is controlled by numerous, interacting factors. Wind is perhaps the most commonly invoked process involved. In the absence of wind, the tephra is dispersed in a bulls-eye pattern. In the presence of winds, the degree of lateral transport of pyroclastic material depends on the direction and speed of wind flow, which may simultaneously vary at different levels in the atmosphere.

Other key processes and properties controlling atmospheric transport of airborne pyroclastic material include plume height, eruption rate, tephra size distribution, duration of the eruption, and erupted volume (Mastin et al. 2009), along with wind advection, turbulent diffusion, and gravitational settling of particles and particle aggregates which is largely associated with particle diameter, density and shape; non-wind meteorological conditions can also be important (Folch and Costa 2010). Some additional key references include Fisher and Schminke (1991), Wiesner et al. (1995), Schminke (2004), and Rose and Durant (2011).

Settling through the low density medium of atmospheric gases, particles and particle aggregates settle largely following Stokes Law. Settling of airfall tephra through water has long been interpreted as strictly related to density- and shape-related factors acting upon individual grains (again, following Stokes Law). However, recent laboratory and field studies indicate that settling of tephra particles through waters is more complex (Carey 1997; Manville and Wilson 2004). Experimental analyses indicate that at the air-water interface, the settling velocity of airfall tephra undergoes a sharp decrease, resulting in high tephra concentration at the top of the water column. This dense mix of tephra particles and water leads to rapid downward transport of tephra through waters via diffuse vertical gravity currents. These flows are analogous to more horizontal density-driven turbidite flows along the sea floor (which may also happen when tephra-laden vertical density currents impinge on the sea floor).

Post-depositional Processes

Pyroclastic materials settle onto the surface of any and all depositional environments within reach of the tephra plume (Figure 1). This may include a broad variety of terrestrial and sub-aqueous (marine, lacustrine and fluvial) environments. In each of these environments, various physical, biological and chemical processes may lead to a variety of post-depositional fates. These include preservation of the fallout tephra material as deposited or with reworking of ash from the same event, resulting in preservation of only the same eruptive event deposit. Alternatively, the interaction of varied environmental processes may lead to amalgamation and/or mixing of tephra from a single event with older or younger tephra or background sediments, or total mixing of tephra materials with background sediments, sometimes to the point where the record of a volcanic contribution is lost.

In terrestrial settings, primary airfall material is commonly highly reworked and redeposited through erosion. This may occur via hydrologic runoff following rainfalls or snowmelt, landslides or mass flows on steeper slopes, redistribution by eolian processes, mixing within the sediment column via plant rooting and animal burrowing, or pedogenic (soil-forming) processes, among others. Fluvial systems redistribute both primary and reworked ash deposits, transporting the material sometimes great distances downstream, and during flood conditions out onto flood plains. Processes acting on tephra in lacustrine systems in large degree mimic those of shallower marine systems (see below), with some variations. Some key references include Mullineaux (1996); Nakayama and Yoshikawa, (1997); Riggs et al. (1997); Kataoka (2005), Kataoka et al. (2009).

In marine environments, primary airfall material is also subject to numerous processes, which may lead down various pathways of reworking and redeposition, with or without mixing of airfall tephra with background sediments. Alternatively, burial may result in preservation of the primary airfall tephra layer. Once settled onto the sea floor, a broad range of environment-related physical, biological and chemical conditions and processes may act upon, and alter the original airfall event deposit (Figure 2a). Sometimes these processes completely mix the tephra sediments with background sediments, essentially erasing and destroying the record of volcanism. These various conditions and processes may occur on the scale of day-to-day activity (e.g., tides, waves, currents, biological burrowing), as uncommon

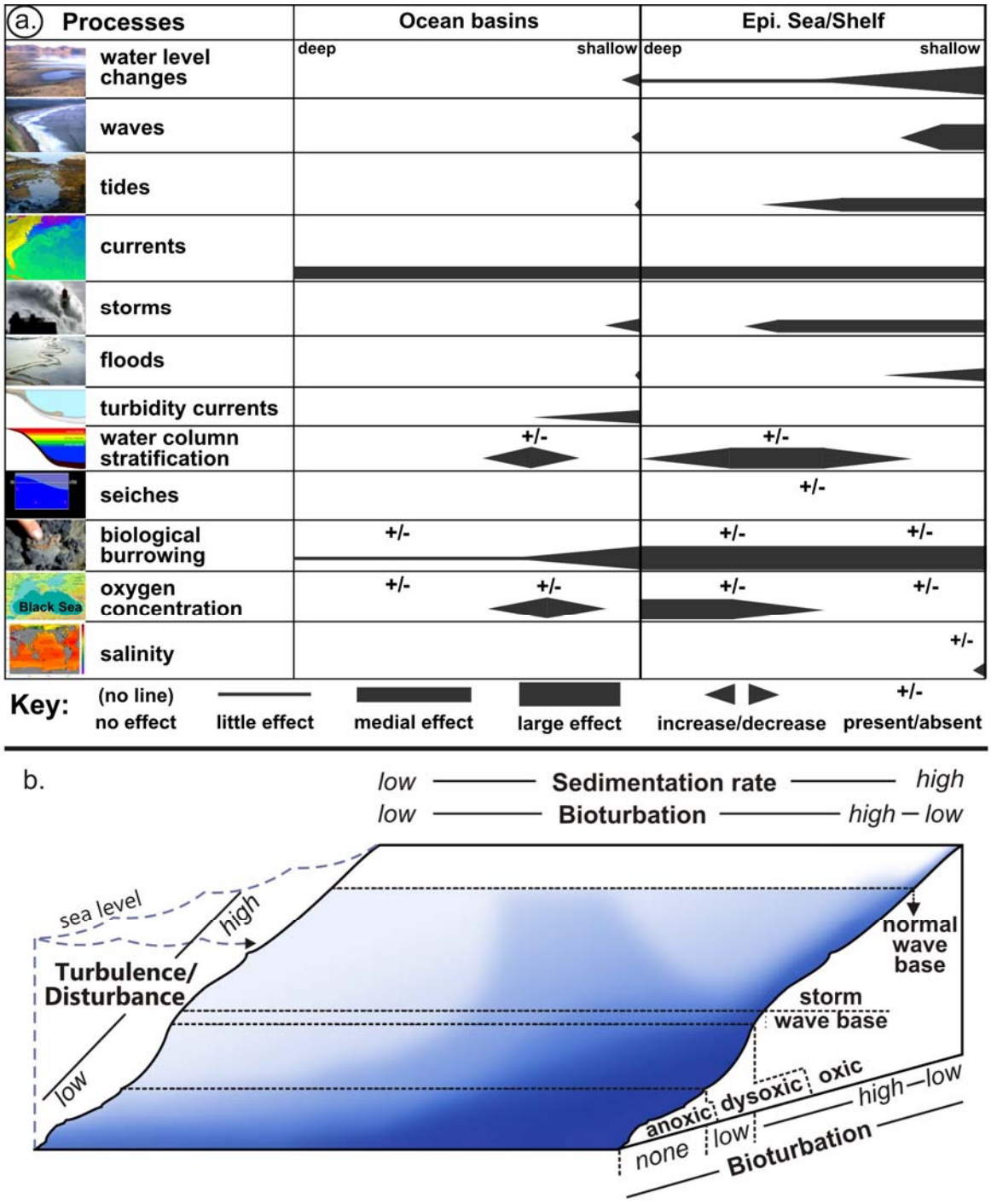

Figure 2. The preservation of tephra layers in marine environments. a) Overview of the generalized distribution of select physical, biological and chemical processes that may affect the preservation of airfall tephra layers in marine settings. Columns for ocean basins, and shelf/epicontinental sea/foreland basin settings; deeper water to left, shallower to right in each column. Thicker lines indicate stronger effects; absence of lines indicate no effect. b) Conceptual model of potential for tephra bed preservation in an epicontinental sea, accounting for sedimentation rate of background sediments, hydrodynamic disturbance, and oxygenation; bioturbation controlled by both oxygen content and sedimentation rate. Darker shades delineate areas of greater tephra bed preservation potential; lighter shades represent decreased chances of preservation.

to rare events (e.g., storms, tsunamis, gravity-driven mass flow events) or over long times spans (e.g., sea level changes, climate- or uplift-related sedimentation rate changes, water chemistry/oxygenation).

Figure 2b portrays a conceptual model of preservation potential of an airfall tephra layer in continental shelf/epicontinental sea/foreland basin settings. Darker areas represent areas of greater potential preservation of tephras. Controls are largely associated with the degree of physical or biological disturbance of sediments at and close below the sea floor, sedimentation rate, and decreasing oxygenation, typically into more basinal environments. Effects of physical processes such as day-today wave action and tides decrease with depth; in this model, bioturbation decreases with depth related to oxygen availability; but it also can decline due to high sedimentation rate. Burial, one of the most significant factors in the preservation of airfall tephra layers, especially primary (unreworked) airfall layers, is associated with increased sedimentation rates (to the right).

As can be seen in Figure 2b, the preservation potential of primary tephra beds increases in this model with greater depth, increased sedimentation rates, and decreased physical and biological disturbance (lower right); and with very high sedimentation rates at any depth, especially when combined with potentially common, episodic burial events. For more discussion of the model, see Ver Straeten (2004a).

In addition to the discussion by Baird in this paper, and publications on tephra preservation by Ver Straeten (2004a, 2007a, 2008), Benedict (2004), and Ver Straeten et al. (2005), there is an extensive and growing literature on the fate of airfall tephra deposits in Paleozoic to recent marine (and relatively similar lacustrine) settings, utilizing various detailed sedimentologic and petrologic methods, and geochemical analyses of the volcanic glass ("ash") and/or phenocrysts contained within a single tephra layer (e.g., Huang et al. 1973; Sparks et al. 1983; Carter et al. 1995; Huff et al. 1999; Koniger and Stollhofen 2001; Reidel et al. 2001; Scasso 2001; Puspoki et al. 2005, 2008; and Allen and Freundt 2006).

In an extreme example of the post-depositional fate of an airfall tephra from a single eruption, Reidel et al. (2001) examined an airfall tephra deposit from a small lake deposit in Washington State. They found that the primary airfall portion of the layer was only two centimeters thick, at its base. Up to 17 additional meters of reworked tephra from the same eruption was redeposited in lake sediments from the surrounding watershed. Furthermore,

they estimated that the reworked tephra was eroded, transported and redeposited in the small lake within one year of the original eruption.

Finally, volcanic glass ("ash") is thermodynamically unstable at surface and near-surface conditions on Earth. Over geologically short to long time spans, glass undergoes devitrification, and may be altered along several different pathways. Under various conditions, volcanic glass may alter to smectitic clays, zeolites, feldspar, or to silica minerals (e.g., amorphous silica, precursors of opal CT, or quartz), and undergo further alteration. Alternatively, tephra may become cemented early in diagenesis and be preserved. Some key references on the diagenetic alteration of volcanic glass include Marshall (1961), Hein and Scholl (1978), Fisk et al. (1998), and Jeans et al. (2000).

In summary, studies of ancient to modern airfall silicic tephra beds indicate a complex depositional history to most layers. In terrestrial and subaqueous environments, many physical, biological and chemical processes may act on primary airfall volcanic sediments; this may lead to rapid burial and preservation, amalgamation with other airfall events, partial mixing of tephra with background sediments, or complete mixing with background sediments, the latter masking the record of explosive volcanic activity in sedimentary strata.

II. INTEGRATING DATA FROM THE FORELAND BASIN AND HINTERLAND OF THE NORTHERN APPALACHIANS (Paul Karabinos)

As someone who works on metamorphosed and deformed rocks in the hinterland of the northern Appalachians, I am envious of geologists who study rocks in the foreland basin. Through careful field observations, they can determine the ages, thicknesses, and depositional environments of stratigraphic units. Correlation of units throughout the basin makes it possible to reconstruct spatial and temporal variations in thickness and facies of the sedimentary rocks, and thereby constrain the timing of subsidence in the basin. It is also possible to make inferences concerning uplift and tectonic history in the hinterland. In contrast, those of us who work in the deformed Appalachians struggle to determine the ages and estimate the thicknesses of units. When we are fortunate enough to find formational contacts, we typically struggle to identify them correctly as faults, unconformities, or

conformable stratigraphic contacts. Differences in interpretation of a critical contact commonly result in heated debates. Without reliable age data, correlations between units are tenuous. However, it is the record of deformation and metamorphism in the hinterland that provides us with direct evidence of tectonic activity, even if it is difficult to decipher.

Integrating information from the foreland basin and hinterland has tremendous potential for advancing our understanding of both parts of the orogen. Evidence from the rock record in the foreland basin is commonly well constrained and detailed; it gives a clear picture of the depositional history in the basin. However, the foreland basin record does not provide direct evidence of the plate tectonic activity or geometry in the hinterland. It is a reliable time-integrated record of sediment transfer from the hinterland to the foreland that is controlled by relative elevation between the basin and the tectonically active hinterland, along with climate and drainage patterns. Thus, the foreland basin record is reliable but it does not fully explain what caused the variations in sedimentation rate. On the other hand, our knowledge of the stratigraphy, depositional setting, and tectonic affinity of rocks in the hinterland are commonly incomplete. To make up for this deficiency, however, field mapping combined with structural, metamorphic, geochemical, geophysical, geochronological, and paleomagnetic studies from the hinterland provide direct evidence for subduction, accretion of arcs and microcontinents, rifting, tectonic exhumation, and crustal thickening in the northern Appalachians. In other words, studies of the foreland basin and hinterland have complementary strengths and weaknesses.

Advances in the precise U-Pb dating of zircon have made it possible to integrate more fully data from the foreland basin and the hinterland. The recognition and precise dating of K-bentonites in the foreland basin (Tucker and McKerrow 1995; Tucker et al. 1998), combined with an expanded database of the age and tectonic significance of volcanic and plutonic rocks in the hinterland (Tucker and Robinson 1990; Karabinos et al. 1998; Bradley et al. 2000), allow us to identify some specific tectonic events that were coeval with the formation of air-fall tephras in the foreland basin. Because the dated K-bentonite layers constrain the ages of important changes in the evolution of the foreland basin, it is possible to test models of how tectonism in the hinterland affects foreland basin evolution (e.g., Ver Straeten 2010).

Long before plate tectonic theory was first applied to the Appalachians (e.g., Dewey 1969), and even before absolute radiometric ages were available, three major orogenies were recognized based on fossil dating of deformed rocks below angular unconformities: the Ordovician Taconic, the Devonian Acadian, and the Pennsylvanian to Permian Alleghenian orogenies. During the 1970s and 1980s, it was common for geologists working in western New England to ascribe deformation to either the Taconic or Acadian orogenies, both of which were considered to have consisted of several phases. This simplified view of early Paleozoic tectonism held that the Taconic orogeny resulted from the collision of Laurentia with the 'Taconic' arc (e.g., Rowley and Kidd 1981; Stanley and Ratcliffe 1985) and that the Acadian orogeny marked the collision of a microcontinent separated from Gondwana called Avalon (e.g., Rast and Skehan 1993). The Alleghenian orogeny was believed to have only affected rocks in southeastern New England.

Detailed work in New England and in the Canadian Appalachians, especially Newfoundland and New Brunswick where arcs of both Laurentian and Gondwanan affinities are better preserved, has resulted in a much more detailed and complex history of arc and microcontinent accretion, reversals in subduction polarity, and intermittent back-arc rifting (e.g., van Staal et al. 1998, Zagorevski et al. 2007). For example, we now know that Alleghenian deformation affected rocks as far west as the Bronson Hill arc in western Massachusetts (Robinson et al. 1992; Figure 3). Our expanding geochronological database in the northern Appalachians suggests that the Laurentian margin was continuously active from approximately 470 to 270 Ma. Perhaps too much effort has been expended trying to assign dated features to either the Taconic or Acadian orogeny. We should instead focus our efforts on reconstructing the rich history of tectonic events and document the evolving plate tectonic geometry during this interval. For example, a stratigrapher might use the increased influx of sediment to the foreland basin to propose a Late Ordovician to Early Silurian age for the Taconic orogeny (e.g., Rodgers 1970), whereas I would argue that from a plate tectonic perspective the Taconic orogeny, i.e. the collision of Laurentia with the Notre Dame-Shelburne Falls arc, was over before or soon after the start of the Late Ordovician (Karabinos et al. 1998, van Staal et al. 2007). As discussed below, the increase in Late Ordovician sediment flux may record changes to the continental margin following arc collision, slab

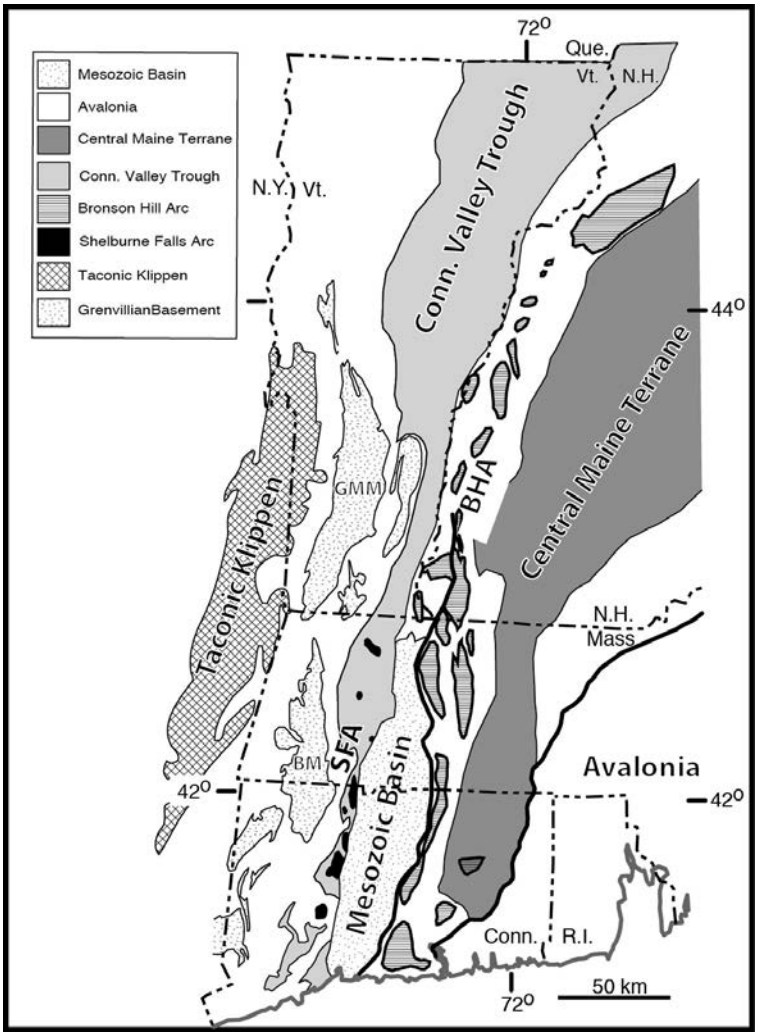

Figure 3. Tectonic map of New England. BHA- Bronson Hill arc. BM- Berkshire massif, GMM- Green Mountain massif, SFA- Shelburne Falls arc.

break-off, subduction reversal, and formation of the Bronson Hill arc along the Laurentian margin.

The formation of air-fall tephras in a foreland basin requires explosive volcanism. Island arcs (e.g., the Aleutian Islands) and magmatic arcs (e.g., the Cascade Range) are obvious settings for explosive volcanism. But hot spots beneath continents (e.g., Yellowstone) and rifting beneath continents (e.g., Valles Caldera) can also produce explosive eruptions. The transient nature of tectonically active continental margins would seem to favor arc-related eruptions as a more likely source of air-fall tephras, but other possibilities must also be considered.

If we make the reasonable assumption that the age of K-bentonites in the foreland basin can be correlated with explosive arc magmatism proximal to the active Laurentian margin, can we use tephras to date periods of increased tectonic activity (e.g., Ver Straeten 2010)? If oceanic lithosphere is subducted beneath a continental margin (e.g., Andean margin) and plate convergence rates are high, it is possible to have explosive eruptions during crustal deformation. Alternatively, if subduction polarity dips in the opposite direction, away from the continental margin and under an island arc or an impinging microcontinent (e.g., Indonesian-Australian collision), explosive eruptions should precede collision and crustal deformation, but cease soon after collision commences. This is because the subduction of oceanic lithosphere necessary to trigger melting in the overlying mantle wedge, which eventually leads to explosive eruptions, ceases soon after collision begins. Thus, it is important to not only correlate K-bentonite ages with volcanic activity in the hinterland, but also to discriminate between magmatic arcs that formed above subducting oceanic lithosphere along the continental margin from colliding arcs that overrode the continental margin.

Ordovician K-bentonites

Early Ordovician (Floian) K-bentonites have been reported by Thompson et al. (2012) from the Argentine Precordillera, a microcontinent that may have rifted from the southeastern margin of Laurentia, which later collided with Gondwana (Thomas and Astini 2003). It is unclear, however, if these older K-bentonites in the Precordillera record explosive volcanism directly related to the Appalachians. Middle Ordovician (Dapingian and Darriwilian) K-bentonites are found in North America and in the United Kingdom (Huff et al. 2010). The oldest Middle Ordovician K-bentonites in North America partly overlap with arc magmas from the Shelburne Falls arc in western New England (486 to 470 Ma, Karabinos et al. 1998), but are younger than most of the dated rocks from the Shelburne Falls arc and all of the dated rocks from the Notre Dame arc in Newfoundland (489-477 Ma, van Staal et al. 2007).

The lack of older K-bentonites corresponding to older arc magmatism in the Shelburne Falls and Notre Dame arcs may be due to the lack of a deep basin at the time of eruption to preserve the air-fall tephra, or later erosion of Early Ordovician basin deposits.

Numerous Late Ordovician K-bentonite deposits are preserved in North America (Huff et al. 2010) and many dated layers overlap in age with volcanic rocks dated in the Bronson Hill arc by Tucker and Robinson (1990), ca. 454-440 Ma. Karabinos et al. (1998) argued that the Bronson Hill arc was a peri-Laurentian arc that formed after collision of Laurentia with the Shelburne Falls arc, slab break-off, and a reversal in subduction polarity to accommodate west-dipping oceanic lithosphere under the Laurentian margin. Another interpretation is that the Bronson Hill arc is a continuation of the Popelogan-Victoria arc, which formed on a sliver of Ganderia, before it collided with Laurentia in the Late Ordovician (e.g., Zagorevski et al. 2007). In any case, coeval arc-related plutons have been dated in western Connecticut that intruded rocks of unambiguous Laurentian affinity, which had been deformed during the Taconic orogeny prior to intrusion (Sevigny and Hanson 1995), so it is almost certain that a west-dipping subduction zone existed under the Laurentian margin after collision of Laurentia and the Shelburne Falls arc. Thus, it is possible that Middle Ordovician K-bentonites in the Appalachian foreland basin were derived from two separate arc systems: one along the Laurentian margin and the other along the Ganderian margin. Collision during the Late Ordovician and Early Silurian would have presumably shut off the supply of explosive eruptions.

The increase in sediment flux from Late Ordovician into Early Silurian must reflect an increase in elevation of the hinterland relative to a subsiding foreland basin. Loading of the continental margin by the Shelburne Falls arc may account for basin subsidence, but loading occurred some 10 to 15 m.y. before the observed increase in sedimentation. Some other factor must be invoked to explain the time lag between the onset of collision and the increase in sediment influx. It is possible that crustal shortening caused by the collision of Laurentia and the Shelburne Falls arc, was augmented by buoyant uplift of the hinterland following slab break-off of dense oceanic lithosphere. The combined effect of crustal thickening and buoyant uplift may be responsible for the required increase in hinterland elevation relative to the foreland to initiate the formation of a clastic wedge. Slab break-off must have occurred prior to subduction reversal and formation of arc-related rocks along the Laurentian margin beginning at approximately 455 Ma. This late increase in hinterland elevation may have created the critical taper needed to trigger the late advance of Taconic thrust sheets in the Caradoc (e.g., Rowley and Kidd 1981; Bradley 1983). Continued crustal shortening and

erosion in the hinterland and subsidence of the foreland basin during the Late Ordovician and Early Silurian may reflect either Andean-style deformation of the Laurentian margin above a west-dipping subduction zone, collision of Laurentia with Ganderia, or both.

Devonian K-bentonites

Ver Straeten (2010) showed that the foreland basin record could be used to enhance our understanding of the Acadian orogeny, and he included air-fall tephras in his analysis. There are approximately 100 K-bentonite deposits in the Devonian foreland basin. Within the Devonian sequence, numerous tephra beds form five clusters that appear to record pulses of concentrated explosive eruptions (Ver Straeten 2010) at approximately 418 Ma (Bald Hill cluster), 409 Ma (Sprout Brook cluster), 391 Ma (Tioga MCZ cluster), 390 Ma (Tioga A-G cluster), and 381 Ma (Belpre cluster).

The oldest cluster, Bald Hill, is similar in age to the Standing Pond Volcanic Member of the Waits River Formation (423 $\pm$ 4 Ma, Aleinikoff and Karabinos 1990) and a felsic sill in the Barnard Volcanic Member of the Missisquoi Formation (419 $\pm$ 1 Ma, Aleinikoff and Karabinos 1990) in Vermont. Both of these units are likely related to Late Silurian rifting and the inception of the Connecticut Valley trough. The Bald Hill cluster is also similar in age to detrital zircons recovered from the Waits River Formation (418-415 Ma; McWilliams et al. 2010).

The Connecticut Valley trough (which is the 'other' Devonian foreland basin) received large volumes of sediment until at least 405 Ma. It contains two dated tuff layers. One tuff is 407 $\pm$ 3 Ma, and in the Meetinghouse Slate Member of the Gile Mountain Formation in eastern Vermont (Rankin and Tucker 2009). The other tuff is 405 $\pm$ 4 Ma, and in the Goshen Formation in western Massachusetts (Karabinos and Aleinikoff 2011). McWilliams et al. (2010) reported detrital volcanic zircons extracted from a quartzite bed in the Gile Mountain Formation in Royalton, Vermont, that are 409 $\pm$ 5 Ma and indistinguishable in age from the tuffs. The Littleton Formation in New Hampshire also contains a 407 $\pm$ 2 Ma tuff layer (Bradley et al. 2000). These tuffs and detrital zircons are very similar in age to the Sprout Brook cluster in the foreland basin. The rocks in the Connecticut Valley trough and the Littleton Formation, however, were deformed during the Acadian orogeny shortly after deposition. A likely source for the air-fall tephras in the foreland basin and the Connecticut

Valley trough and Littleton Formation is in Maine, where the coeval Traveler and Kineo Formations form a thick succession of rhyolite (Rankin and Hon 1987; Rankin and Tucker 1995; Bradley et al. 2000).

The Acadian orogeny records the collision of Laurentia with Avalon. Bradley et al. (2000) showed convincingly that it began in the Late Silurian in the easternmost part of Maine, and that deformation migrated westward during the Early and Middle Devonian.

The three youngest air-fall tephra clusters in the foreland basin, 391 to 381 Ma, are coeval with intense Acadian deformation and metamorphism in the hinterland. Numerous $^{40}Ar/^{39}Ar$ cooling ages in this 390 to 380 Ma age range occur throughout central New England and record cooling through the closure temperatures of hornblende, biotite, and muscovite of mid-crustal rocks, and suggest that at least 10 to 15 kilometers of crust has been eroded since then. Thus, it is unlikely that any evidence for explosive eruptions would remain. If the eruptive sources of these clusters are preserved, they must be located near the suture zone between the eastern edge of Avalon and the western margin of Meguma, which collided during the Late Devonian (van Staal et al. 2009).

III. DECIPHERING THE ORIGIN, MAGMATIC EVOLUTION, AND TECTONIC SETTING OF PALEOZOIC VOLCANOES BY EXAMINING K-BENTONITES (Scott Samson)

Introduction

Widespread volcanic ash beds, or their altered equivalents (K-bentonites), are geologically useful because of their combined extensive geographic distribution and geologically instantaneous deposition. These event beds provide a tie-line, or a stratigraphic reference, which can be used to correlate the host rocks that envelop the ash bed. This, in turn, contributes to the understanding of ancient facies relationships among widespread locations. This is of particular importance in areas with little or no biostratigraphic control or for regions where there is inadequate overlap of time-diagnostic fossils (e.g., conodont bearing facies versus graptolite-bearing facies). K-bentonite correlation has thus become an

extremely important aspect of stratigraphy in many areas around the globe. In New York there are numerous K-bentonites in key Ordovician and Devonian strata.

Perhaps one of the best known aspects of K-bentonites is their ability, under ideal circumstances, to provide material that is amenable to high-precision radiometric dating. Volcanic ash beds, and their highly altered (i.e. bentonite) equivalents, have proven absolutely invaluable in the calibration of the Geologic Time Scale. Combining age determinations with long-distance correlation, i.e. tephrochronology, has thus become a critical aspect of a wide variety of geological studies. What is not particularly well known about K-bentonites is their frequent ability to provide extremely important isotopic and geochemical information. This, in turn, has the potential to shed considerable light on such diverse topics as ancient magma chamber evolution, constraining potential versus impossible source regions of the K-bentonites, the tectono-magmatic setting of the volcanoes producing the ash, the degree of crustal evolution of the source regions, and finally possible constraints on paleogeography. This is an impressive list by any standard, but given that K-bentonites appear to be essentially glorified mud it is (or should be) hard to imagine the above claims are realistic! The key to accomplishing the above items is in the surviving phenocryst (and xenocryst) assemblage as discussed below.

Phenocryst Assemblage in K-bentonites

The phenocrysts in highly altered ash beds (K-bentonites, tonsteins etc.) are critical because the original volcanic glass has either largely, or entirely, been chemically modified. Most tephrochronological studies of Recent tephra are based on the unique chemical composition of the volcanic glass. However, in the Ordovician and Devonian bentonites in New York the glass has been entirely altered to clay minerals (typically illite and smectite). Thus it is the remaining chemically resistant phenocrysts that are found in many, but by no means all, K-bentonites that still preserve invaluable information about original magmatic conditions. Typically the surviving phenocrysts include quartz, zircon, and apatite. Biotite can also be found in some K-bentonites, but it is not a particularly resistant mineral and thus is often chemically altered, in some cases completely, leaving only pseudomorphs of biotite. The useful characteristics of the phenocrysts most likely to survive are given, followed by some specific examples.

Quartz

Quartz is both a physically and chemically extremely resistant mineral and thus it is not surprising that it can occur as pristine phenocrysts in altered tephra. Because it is nearly pure SiO_2 there is limited utility to determining either its major or trace element chemical composition. However, quartz phenocrysts often contain glass inclusions that in most cases represent trapped quenched melt (i.e. melt inclusions). These inclusions are thus microscopic samples of the original magma as it existed prior to the volcanic eruption producing the tephra. We now know, for example, that many of the Ordovician K-bentonites in New York are actually high K rhyolites thanks to the major element composition of the glass inclusions contained in quartz phenocrysts (Delano et al. 1994). That information, in turn, sheds some light on the source characteristics of the original magma as not all tectonic settings are conducive to generating magma with such high SiO_2 and K_2O contents.

Apatite

Apatite phenocrysts have proven to be one of the most useful aspects of bentonites in terms of unraveling details about the likely source material of the parent magma, potential links of the ash beds to exposed volcanic/plutonic terrain, and to details of magma evolution during a series of eruptions. This is possible because apatite contains high enough levels of rare earth elements and strontium to allow for the determination of the Nd and Sr isotopic composition of the phenocrysts, and hence the magma that the apatite crystallized from. This is so important because by knowing the initial $^{143}Nd/^{144}Nd$ and $^{87}Sr/^{86}Sr$ ratios of the parent magma considerable information is obtained about the conditions in which that magma originated. Furthermore, in contrast to quartz, apatite incorporates a considerable number of elements into its lattice. Thus, determining the trace and minor element composition of apatite can shed further light on magmatic conditions as well as help provide a potential "geochemical fingerprint" to assess if exposed igneous regions of identical age might be the possible source location of the ancient volcanoes. Specific examples given below will help demonstrate these concepts.

Zircon

Like quartz, zircon is an extremely resistant mineral both physically and chemically and thus survives in tephra even under the most extreme diagenetic conditions. The utility of zircon phenocrysts is obvious: high precision U-Pb radiometric dates may be determined using the phenocrysts. While U-Pb dating of zircon phenocrysts may not provide much insight into magmatic characteristics, determining the presence and age of zircon xenocrysts can provide considerable information. Many of the North American Paleozoic bentonites do contain zircon xenocrysts, which adds to our information arsenal. Another utility of zircon is that the initial $^{176}Hf/^{177}Hf$ isotopic ratio can be determined for zircon phenocrysts. This information is similar to that obtained from the Nd isotopic data of apatite phenocrysts as it also provides critical information about magmatic source characteristics.

Xenocrysts

As with any igneous rock, there is the possibility of the presence of xenocrysts in bentonites. Some of the xenocrystic minerals that have been found in Ordovician bentonites besides zircon include garnet (Delano et al. 1990), hornblende and pyroxene (Samson 1996). Xenocrysts are important in that they provide a direct window into the characteristics of the magma source material.

Critical geochemical data for Ordovician volcanism in Appalachians

Most of what is known about the composition, source characteristics and petrogenetic origins of the Taconic K-bentonites in eastern North America comes from chemical and isotopic analyses of the 'crystal cargo' (i.e. phenocrysts and xenocrysts) of the bentonites. These data can be compared to those collected from more conventional igneous rocks to establish a larger view of Taconic magmatism. In general terms, the available geochemical data suggest that much of the Ordovician magmatism was the result of melting pre-existing continental crust. Speaking specifically about bentonites, that tephra was generated from volcanoes that were built on Proterozoic continental crust. A major source of the magmas feeding those Taconian volcanoes is inferred to be that ancient crust itself (based on data published in Samson et al. 1995; Samson 1996); this appears to be true for many other regions of exposed Ordovician igneous rocks.

Isotope Geochemistry of Ordovician Volcanic Rock/Continental Crustal Interaction

Initial isotope ratios (primarily $^{87}Sr/^{86}Sr$ and $^{143}Nd/^{144}Nd$) have been determined on many of the exposed igneous and metaigneous Ordovician rocks of the Appalachians. This has also been accomplished for Taconian K-bentonites using apatite phenocrysts. Here I focus on the bentonite data, but note that the same conclusions would be reached for any volcanic rock.

The initial $^{87}Sr/^{86}Sr$ ranges from 0.70564 to 0.70905, with most samples having values close to 0.708. The initial Nd isotopic data, using †epsilon (ε_{Nd}) Nd notation, ranges from -0.9 to -5.4. These isotopic data are consistent with 'evolved' magmas (magmas that extensively interacted with continental crust), as opposed to 'juvenile' magmas, or ones that are primarily formed by melting of the mantle. For example, modern island-arc volcanic rocks have $^{87}Sr/^{86}Sr \approx 0.704$ and $\varepsilon_{Nd} \approx +5$ to +9. Mid-ocean ridge volcanic rocks have even lower Sr ratios (< 0.703) and higher ε_{Nd} values ($\geq +9$). Old continental crust has the opposite characteristics (high $^{87}Sr/^{86}Sr$ and very negative ε_{Nd}). Taconic magmatism appears to be a hybrid, and thus it is inferred that magma may originally have been mantle-derived but it became heavily contaminated by old continental crustal material.

Further evidence that continental crust must play a very important role in Ordovician magmatism is the presence of Proterozoic zircon xenocrysts in many Appalachian Ordovician igneous rocks, including the Taconic K-bentonites. A rarer, but spectacular example of xenocrysts inherited from underlying continental crust is Mesoproterozoic hornblende in some Ordovician K-bentonites of the Mohawk Valley. $^{40}Ar/^{39}Ar$ ages of 950 – 900 Ma for individual hornblende crystals suggest an interaction of Ordovician magma with Grenville basement during rapid ascent of the magma in the volcanic plumbing system (Samson 1996).

The importance of the above data lie not only in the demonstration that the Paleozoic volcanoes are built on a continental substrate, but that very important constraints are placed on potential links between the tephra and any source candidates. Any Ordovician igneous terrane that might be viewed as a potential source, such as the Bronson Hill terrane, Shelburne Falls terrane, or Stokes Domain in the northern Appalachians, or the Chopawamsic terrane and its equivalents in the southern Appalachians, must contain igneous rocks with appropriate Nd and Sr isotopic composition, must have Ordovician rocks with

Precambrian zircon xenocrysts, and must have evidence for being built on Grenville crust with a thermal history indicating cooling below ~ 500 °C around 950 Ma. This is a very powerful test on any proposition of linking foreland and hinterland units.

For additional reading on the topics examined in this section, see Samson et al. (1988 1989), Emerson et al. (2004), Carey et al. (2009), Sell and Samson (2011a,b).

$^{\dagger}\varepsilon_{Nd} = 10{,}000 \times [^{143}Nd/^{144}Nd_{sample} - {}^{143}Nd/^{144}Nd_{Bulk\ Earth}]/[{}^{143}Nd/^{144}Nd_{Bulk\ Earth}]$

IV. MOHAWK VALLEY ORDOVICIAN TEPHRAS (Gordon Baird and Carlton Brett)

Introduction

Upper Ordovician deposits, comprising the Trenton Group, Dolgeville Formation, and Utica Shale have been the subject of a variety of classic paleontological, sedimentological, tectonic, and chronostratigraphic studies that span nearly two centuries of investigation. The sum gain of this work presently reveals the dynamic interaction of forearc convergence effects with platform margin-to-basin sedimentary processes. Altered volcanogenic layers ("K-bentonites" of most authors), are numerous in this succession and have figured prominently in attempts to correlate across time-variable (diachronous) facies tracts in this region (see Cisne et al. 1982; Delano et al. 1994; Goldman et al. 1994; Mitchell et al. 1994; Samson et al. 1995). Herein, we continue work by Baird and Brett (2002) and Berkley and Baird (2002) to characterize tephras in the sedimentary record from a sedimentological and diagenetic perspective. Our earlier work focused on tephra features that were useful for physical bed correlation between outcrops. In this paper, we are more interested in the intrinsic properties of these beds that relate to their sedimentological origin and diagenetic alteration. Accordingly, the first two field trip stops are directed to the study of Upper Ordovician tephra layers that accumulated in an oxygen-deficient basin setting represented by the Utica Shale. Multiple tephra beds will be seen at both localities.

Geologic Setting

The Ordovician tephra record in the Appalachian region is understood to reflect the presence of arc development and associated southeastward oceanic subduction within the

Neo-Iapetus Ocean along the southeast margin of the continent of Laurentia (proto-North America). Consumption of the oceanic lithosphere led to arc collisions with the southeast edge of Laurentia, subduction of portions of the proto-North American continental margin, and emplacement of accretionary prism complexes (Taconic allochthons) onto the Laurentian craton (Kolata et al. 1996). These events, culminating in the Upper Ordovician Taconian Orogeny, were associated with pulses of overthrusting that produced orogenic mountains, southeast of the present day Appalachians. Flexural thrust-loading, associated with this collisional phase, led to the development of a large peripheral foreland basin northwest of the mountain system, which was then filled with terrigenous sediment, mainly derived from the collisional uplifts (Cisne et al. 1982; Quinlan and Beaumont 1984; Lehmann et al 1995).

As collisional deformation advanced cratonward, the foreland basin both expanded and deepened. A cratonic shelf, recorded by richly fossiliferous shelf carbonate deposits (Trenton Group), west of the foreland basin, underwent progressive westward subsidence and drowning as a result of stepwise down-to-the-east movement along fault systems as the basin expanded (Bradley and Kidd 1991). Hence, the middle and upper parts of the Trenton Limestone pass eastward (downslope) into minimally fossiliferous slope facies (Dolgeville Formation) before grading into dysoxic basinal facies (Cisne et al. 1982; Mitchell et al. 1994; Lehmann et al. 1995; Brett and Baird 2002; Jacobi et al. 2002).

The organic-rich Utica Shale, accumulated in variably oxygen-deficient, deeper portions of the basin. The lower part of the Utica succession (Flat Creek Shale Member) is variably calcareous, and it does yield a modest benthic fauna as we will see at Stop 2. An interval of numerous ribbon limestone layers (Dolgeville Formation) overlies the Flat Creek Shale in the field trip area. This unit, visible in the high cliffs at Canajoharie Creek (Stop 2), represents a turbiditic limestone facies that correlates westward into the upper Trenton Group carbonate shoal facies (Brett and Baird 2002). Above this unit is the Indian Castle Shale Member, a black, fissile to platy shale that is stratigraphically condensed in western Mohawk Valley sections. In the Poland-Middleville-Little Falls-Dolgeville area, it disconformably overlies the Dolgeville Formation; Indian Castle Shale strata, including important tephra layers, progressively onlap westward onto this contact across this region (Baird and Brett 2001; Baird and Brett 2002). This contact (Thruway Unconformity) is spectacularly displayed along the NYS Thruway (I-90), 1.0-1.6 mile west of the Little Falls exit.

Ordovician Ash Beds: Physical Description

Volcanogenic layers

The eastern North American Upper Ordovician section has been long known for the occurrences of sedimentary layers of apparent volcanogenic origin. At least 60 diagenetically altered, airfall volcanic beds are estimated to be present within this succession (Kolata et al. 1996). Herein, we apply the more generalized term "volcanic tephra" for such beds. However, within the Mohawk Valley region, numerous similar layers are present higher in the Trenton Group, Dolgeville Formation, and Utica Shale (Cisne et al. 1982; Delano et al. 1990, 1994). These latter deposits, serving as the focus of the present study, occur within the lower and middle parts of the Upper Ordovician global Katian Series (Bergström et al. 2008). Aside from their utility in isotopic dating, volcanogenic phenocrysts in these beds also yield distinctive geochemical signatures ("chemical fingerprints") useful, in tandem with graptolite and conodont biostratigraphy, for correlation of strata (Goldman et al. 1994; Mitchell et al. 1994; Samson et al. 1995).

Tephras In Outcrop

Approximately 30 altered tephra layers are present within the overall central Mohawk Valley, Upper Ordovician basinal facies succession, although only about 12 to 15 of these can be correlated between sections (Delano et al. 1990, 1994; Baird and Brett 2002). (1994), Baird and Brett (2001), and Baird and Brett (2002). These beds are most often expressed as bands of unctuous gray-greenish-to-china white clay that stands in dramatic contrast to enclosing limestone facies (Trenton Group or Dolgeville formation) or hard, black Utica Shale deposits (Flat Creek Shale Member, Indian Castle Shale Member successions: Figures 4, 5). Most of these beds display thicknesses in the 0.5 – 4.0 cm-range, but some, particularly the Paradise tephra bed in the basal Indian Castle Shale, exceed 14 cm. Bases of these ash layers are almost always very sharp, but the upper parts of the tephra layers usually grade conformably upward into succeeding lithologies. Weathered tephras typically form reentrants in sections (Figure 6a), often characterized by bands of plant growth on the outcrop face as can be seen along I-90 west of the Little Falls exit. Even very thin tephras are often marked

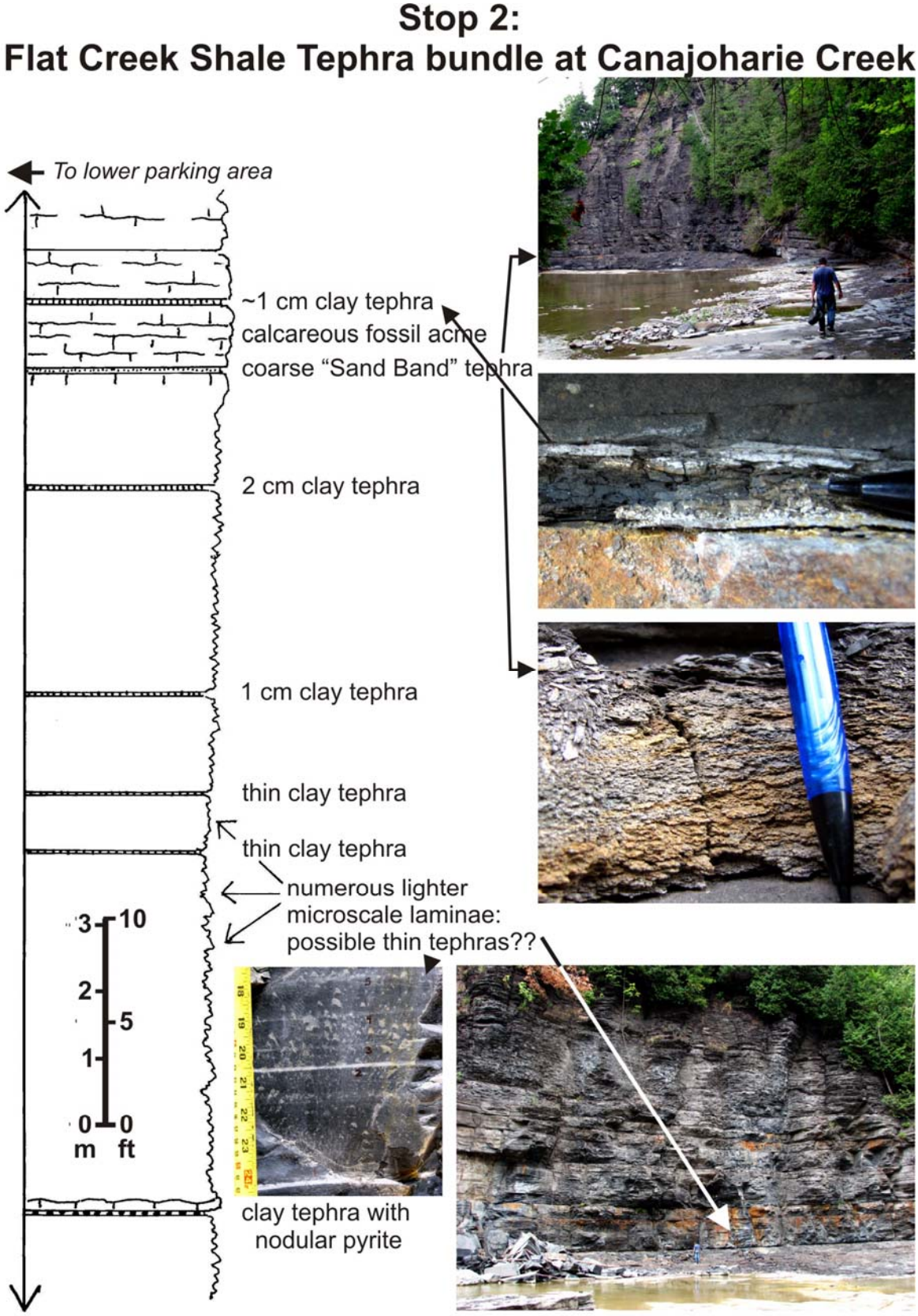

Figure 4. Schematic section of a portion of the Flat Creek Shale section in the classic Canajoharie Creek

gorge south of Canajoharie, NY (Stop 2). The top of the section shown is immediately downstream from the Wintergreen Park ingress trail from the lower parking area within the park. Two intervals of interest include a lower interval of concentrated pyrite-bearing, thin tephra layers that bleed orange on the canyon wall as they weather as well as numerous thinner beds and laminae of possible tephra origin (see inset images). Upstream, closer to the parking lot entrance, are several thicker tephra layers, including the very coarse, gritty "sand band" bed, which occurs below a fossil-rich interval (see inset images; Figure 4a,b).

by rusty, Fe-hydroxide stains in shale sections or between limestone layers. Disseminated pyrite in the clay bands degrades to rusty Fe-hydroxides on weathered surfaces, imparting an orange cast to these layers. This effect is striking in sections along I-90, west of the Little Falls exit, and along Canajoharie Creek (Stop 2). As noted above, many tephras are regionally widespread, but some vary in thickness, often within outcrops, due to low-angle tectonic slippage effects (Zambito et al. 2005; Zambito and Baird 2006). A few tephra layers are partly to entirely carbonate cemented; these concretionized occurrences can be studied on polished surfaces and in thin sections (Berkley and Baird 2002). Several thick tephra beds rest upon selectively indurated underlying layers, particularly, within the Indian Castle Shale. These "ash seats" represent dark muds that have been diagenetically altered by the overlying tuffaceous accumulation.

Mixed-layer Illite-Smectite Tephra Occurrences

Typical, "soft", clay-rich tephra beds show up as pale gray-greenish to beige-tan bands of sticky clay, which can be easily scooped out when the layers are thick. Even when such beds are sampled in the minimally weathered state, as from the bottom of a creek plunge pool, the samples have a greasy, soapy feel when handled. When these samples are rewetted, they often slake and swell to a shapeless, mud mass. This clay is the product of diagenetic alteration of unstable volcanic glass, which is initially converted to smectite. Later, following development of deeper, thermal-burial conditions, such as that associated with burial of the eastern New York Ordovician succession, the smectite was converted to a mixed-layer, illite-smectite phase (Perry and Hower 1970; Epstein et al. 1977; Delano et al. 1990).

Petrography and trace element geochemistry suggest a generally felsic to intermediate, calc-alkaline composition of the volcanic component that is consistent with the probability of an upwind arc source (Berkley and Baird 2002). Rare Earth Element (REE) analysis of these ashes shows that the clay-dominated layers, as well as calcareous ash beds, are enriched in

Stop 1
Otsquago Creek at "Pretzel Farm"

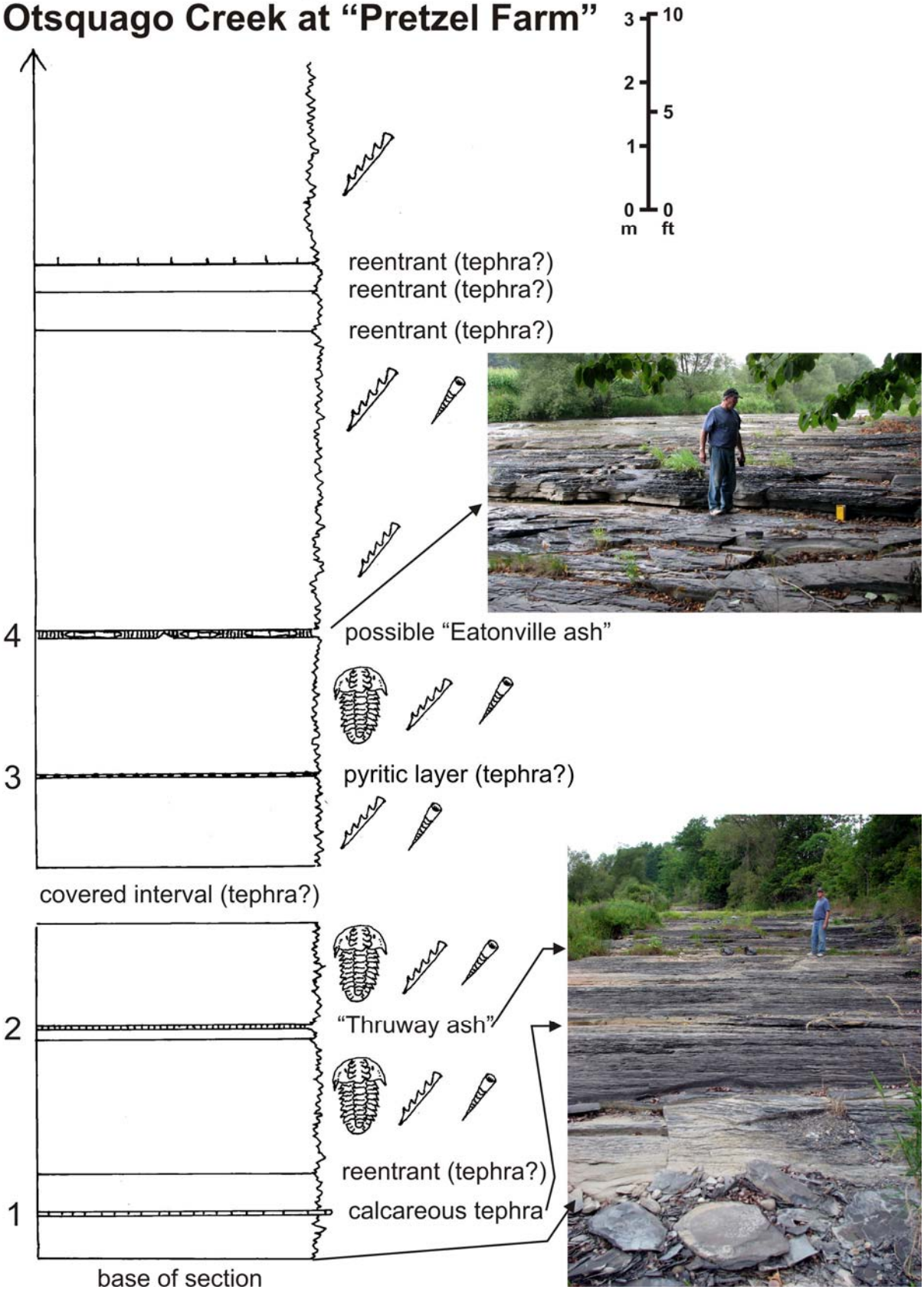

Figure 5. Stop 1 schematic section in the lower part of the Upper Ordovician Indian Castle black shale along Otsquago Creek east of Hallsville, NY ("Pretzel Farm" locality). This section is notable for several easily accessible and distinctive tephra layers. It is also an important locality for distinctive Utica Shale fossils including graptolites, flattened and current-aligned orthoconic cephalopods, as well as, the trilobite Triarthrus, which is especially common in the lower part of this section. Key tephra layers include: a 1.2 cm-thick, tabular, calcareous tephra bed displaying a rich, weakly graded concentration of phenocryst minerals as well as carbonate pseudomorphed small pumice clasts that are preserved in bas-relief along the base of the bed (lower inset image) and a thicker tephra layer displaying both carbonate and clay phases (Figure 4c,d).

light REE with moderate to pronounced Europium anomalies indicative of a felsic-to-intermediate igneous signature (Berkley and Baird 2002). Additional convincing evidence of pyroclastic origin is the variable presence of volcanogenic phenocrysts obtained from disaggregation of clay fractions. Moreover, both Utica Shale and Middle Devonian Onondaga Limestone clay tephras have yielded pumice fragments that have been geochemically analyzed (see Fenton et al. 1995). Unweathered samples of thicker, stiffer tephras often display upward-fining, graded interiors with the coarsest fraction either at or immediately above the base of the tephra layer (Figure 6a,b). The Sherman Falls tephra bed (lower part of Flat Creek Shale), the lower Wolf Hollow tephra bed (lower part of Flat Creek Shale), the Paradise tephra bed (basal part of Indian Castle Shale), and the Countrymen tephra bed (lower part of Indian Castle Shale) are thicker clay tephra units that show this internal grading texture.

Many clay-dominated tephra beds display thin planes of secondary carbonate at their bases and sometimes at higher levels within the bed (Zambito et al. 2005; Zambito and Baird 2006). These display internal slickensides indicative of tectonic shearing. Some tephras when followed along the outcrop, will expand and pinch out due to low-angle bed-slippage. Ongoing work with Jay Zambito (West Virginia University) is directed to measuring and plotting these slippage azimuths to determine their probable time of formation relative to major orogenies and ash illitization.

Calcite cemented tephras

A number of tephras in the Utica Shale succession are partly to entirely calcite cemented (Figure 6c,d,f). Where a tephra has been completely cemented, it can be easily mistaken in sections for a typical micritic limestone layer or a siltstone bed. However, close examination of such layers show that they differ from normal bedding in all facies types. Where this cemented concretionary phase is developed, the tephra is preserved as a pale, sometimes

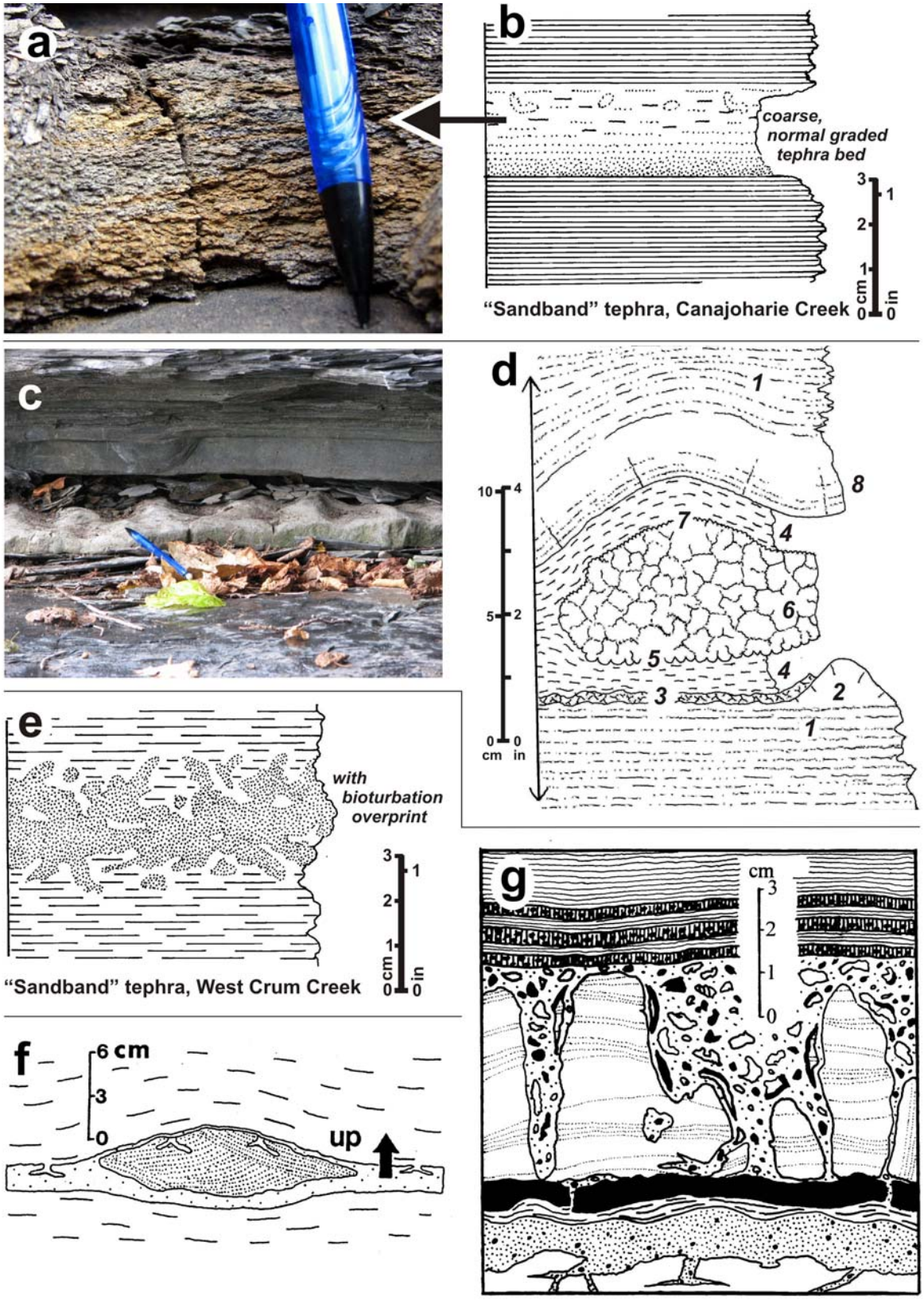
a
b
coarse,
normal graded
tephra bed
3
1
2
1
cm
0
in
0
"Sandband" tephra, Canajoharie Creek
c
d
1
8
7
4
6
5
4
3
2
1
10
4
5
2
0
0
cm
in
e
with
bioturbation
overprint
3
1
2
1
cm
0
in
0
"Sandband" tephra, West Crum Creek
f
6 cm
3
0
up
g
cm
3
2
1
0

Figure 6. Distinctive Ordovician tephra layers. a) Very coarse tephra bed ("sand band" K-bentonite) exposed at Canajoharie Creek (STOP 2); b) Schematic cross-sectional view of the sand band layer (a) showing weakly developed sedimentary grading and sharp basal, bed contact; c) Partially cemented tephra (possible Eatonville Ash bed (sensu Baird and Brett 2002) in the lower Indian Castle Shale at Otsquago Creek (STOP 1). Note pale colored, concretionary bed protruding from the outcrop reentrant. The top of this bed displays parallel ridges that may represent ripple marks; d) Schematic vertical cross-section of this same tephra bed. Note the prominent development of a laterally discontinuous concretionary bed that is surrounded by a clay tephra phase. Lettered features include: 1) enclosing black shale; 2) enigmatic concretionary? knob projecting upward into the ash bed interval from below; 3) basal zone of sparry cemented tephra phase; 4) soft, recessive, clay phase; 5) base of cemented interval displaying distinctive, pustulate, "bubbly" basal surface; 6) pale, sparry, coarsely crystalline, mosaic texture of carbonate nodule; 7) linear, parallel, ridge crests along top of nodular layer resembling "ripples"; 8) carbonate indurated shale bed displaying possible upward grading of tephra layer into overlying shale; e) Schematic, cross-sectional view of completely bioturbated sand band tephra layer as seen in equivalent, upslope, dysoxic facies at West Crum Creek west of St. Johnsville, New York; f) Cross-sectional schematic of limestone concretion within a gray clay tephra bed observed within the uppermost part of the Dolgeville Formation interval along Auries Creek upstream from (west of) the NY Route 30 A overpass bridge, south of Fultonville, NY (Baird and Brett 2002). Note development of cross-lamination indicative of lateral tephra transport by currents. Note also that this carbonate cementation preserved this sedimentary texture prior to later diagenetic alteration of the surrounding texture to clay. See text discussion (from Baird and Berkley (2002); g) Schematic cross-section of lag debris concentration associated with the Dolgeville Formation – Indian Castle Shale contact along Rathbun Brook southeast of Poland, NY. The topmost Dolgeville limestone bed in this section was subjected to intense corrosion as well as abrasion during the formation of this regional disconformity; as carbonate dissolved, insoluble material, including residual terrigenous mud, phosphatic debris, pyroclastic grains, and organic matter settled into solution fissures in a sediment-starved, dysoxic, slope setting. Tephra in this image has been variably admixed with non-ash constituents in a strongly condensed, multi-event deposit.

nearly whitish or pinkish limestone that often displays a distinctive, coarsely crystalline "mosaic" texture (Berkley and Baird 2002: Figure 6d). A given widespread tephra layer, such as the Countryman Bed, may be completely cemented in one section, non-cemented in a second, and partly cemented in a third. Partial cementation of ash is splendidly illustrated in the lower Indian Castle Member section along Otsquago Creek (Stop 1: Figures 5, 6c,d). This bed, possibly the Eatonville tephra bed (*sensu* Baird and Brett 2002; Berkley and Baird 2002), is a clay layer at one end of the exposure that passes laterally into a pale, nodular limestone layer with a distinctive coarse, internal texture of mosaic-like intergrown crystals (Figure 6c,d). Along its exterior, are protruding "popcorn-like" pustules that protrude into the surrounding clay tephra (Figure 6c,d). The pustulate concretionary surface may reflect the alteration of at least some of the volcanic ash/glass to zeolite minerals instead of smectite clays.

A second cemented tephra at Stop 1 best illustrates another aspect of the carbonate cementation process. Berkley and Baird (2002) describe remarkably well preserved glass shard textures from at least five tephras that indicate that the cementation process was early diagenetic and distinctly preceded the alteration of glass to clay. These shard textures

represent glass vesicle walls replaced by smectite. Moreover, visible exteriors of apparent sand-size pumice grains, apparently preserved as pseudomorphed carbonate casts, have been recently discovered along the underside of a thin carbonate tephra layer in the lower part of the Indian Castle Shale along Otsquago Creek (see Stop 1; Figure 5). This same bed is marked by an abundance of quartz and mica phenocrysts along its base.

Inferred Tephra Sedimentology

Multi-event- and transported tephra deposits

Overview. Several thick and very widespread Ordovician tephras, most notably the Deicke and Millbrig beds in North America, have been attributed to massive eruptive episodes involving the expulsion of thousands of cubic kilometers of tuffaceous products, which display an extraordinarily broad distribution (Kolata et al. 1996). A larger number of thinner, less widely distributed tephras, comparable to tephras examined here, would have recorded great eruptions on a smaller scale or at greater distances. Although many tephras in the marine Ordovician succession display an internal upward-fining sediment texture, and many contain diverse volcanogenic phenocryst minerals, relict pumice textures, and a geochemical ash signature, a single air-fall event interpretation for all of these beds is premature (Berkley and Baird 2002). Moreover, what geological record would be expected in offshore marine settings for "big" single eruptions, such as Tambora, Krakatau, or Vesuvius, observed in historic time? Might these correspond to airfall dustings to the sea surface that are effectively erased by ocean current dispersal, bottom current transport, and bioturbation by infaunal organisms?

Tephra accumulation as background sedimentation. A specific volcanic eruption occurring today is an event emanating from a point source on a real-time frame of days to weeks for completion. Most such events should produce a discrete tephra layer, though it may be thin and prone to dilution owing to reworking by currents. Most such eruptions generate only a trace of tephra across areas hundreds or thousands of miles from the source. If a 0.5 - 1.0 cm-thick layer of tuff accumulates on the seafloor as a single event, burrowing organisms are likely to mix and blur part or all of this layer with underlying muds during a succeeding interval of hundreds of years or more. Moreover, thousands of eruptions along a very distant,

upwind arc system theoretically should produce a blended ash component within slowly deposited and bioturbated marine muds on the temporal scale of geologic time. The degradative alteration of volcanic glass and feldspathic constituents in marine settings would further obscure the record of normal, real-time, volcanic events in shaly successions. The potential sedimentary record of such eruptions will be discussed at Stop 2.

Sediment traction by currents. Examination of carbonate-cemented Indian Castle tephras led to the discovery of current-generated cross-laminations in some of these beds (Figure 6f). Early diagenetic, partial to complete cementation of tephra layers preserved, not only relict, microscopic, tuffaceous textures, but also macroscopic bed-scale sedimentary structures. At Auries Creek, south of Fultonville, a thin clay tephra bed in the upper part of the Dolgeville Formation grades laterally into carbonate nodules that preserve cross-stratification generated by current traction (Figure 6f). Lateral termination of this current texture at the perimeter of this early diagenetic concretion reveals the degree of information loss as the original ash degraded to clay.

This indicates that shows that, at least, some of this tuffaceous material was moved by current traction along the sea bed. Given that the Indian Castle interval is a classic basinal black shale deposit, the cross-lamination is most likely linked to turbidity flow transport or the action of unspecified bottom currents. In the light of this discovery, it is particularly significant that these same beds, as well as almost all other tephra layers in the greater Dolgeville Formation and Utica Shale succession have knife-sharp lower contacts. This suggests that some tephras may have accumulated on scour surfaces floored by firm bottom muds.

Marine ash concentrations as lag deposits and/or time-rich facies. Several tephra beds in the greater Utica Shale succession are characterized by coarse, friable, “sandy” concentrations of volcanogenic clasts in nearly grain-supported texture throughout the tephra layer. Although these beds display variable amounts of associated soft, clay fraction, volcanogenic phenocrysts (quartz, apatite, micas, and zircons), comprise up to 25-30 % of the bed volume. Beds of this type are distinctly less common than the typical clay tephra bed, and they appear to record bigger eruptive events or ones distinctly closer to the source area.

However, we also document the occurrence of thin beds of bioturbated, coarse, volcanogenic phenocryst-rich, “sandy”, dark shale or calcareous mudrock, distinctly lacking

any, expandable clay fraction and containing admixed fossil debris. We interpret some of these clay-bearing and non-clay-bearing beds as representing time-rich tephra-rich lag concentrations associated with long-term sedimentary condensation and/or episodes of shorter-term bottom erosion (Baird et al. 1994; Baird and Brett 2001; Fenton et al. 1995; Berkley and Baird 2002).

The informally designated "sand band tephra" (Baird et al. 1994) particularly illustrates this condition (Figures 4, 5a,b,e). This layer, which occurs in the upper-middle part of the Flat Creek Shale, will be seen at Canajoharie Creek (Stop 2). It can be traced in sections from Florida Township, southeast of Amsterdam, westward to the vicinity of St. Johnsville. This bed ranges in thickness from 1.0 – 3.5 cm, and it displays a sharp base on underlying black shale deposits (Figure 6a,b). It is characteristically soft due to the clay component, except where it is cemented by concretionary carbonate. Viewed closely, the sand band displays a weakly graded accumulation of volcanogenic phenocrysts and exploded quartz fragments known as phenoclasts (Figure 6b). Distinctive grains including euhedral beta quartz crystals up to 1.0 mm in diameter and larger, sharp-edged, quartz phenoclast fragments up to 2.0 mm in the longest dimension. A thimble-full of distilled coarse grains can be easily isolated from the surrounding clay with the application of ultrasound. This layer can be sampled from the bed of Canajoharie Creek a short distance from our ingress route from the Wintergreen Park lower parking area at Stop 2.

To the west of St. Johnsville, the sand band grades laterally into a thin, pyroclastic shale bed distinctly lacking soft associated clay (Figure 6e). This phase, extensively bioturbated and characterized by admixed small fossils, can be seen along West Crum Creek (Figure 6e) and in a west-facing bank section along the reservoir lake on East Canada Creek above Ingham Mills. Still further west (upslope), this bed is tentatively correlated to an even thinner lag blanket of mixed pyroclastic and phosphatic debris in sections near Little Falls, on the up-thrown side of the Little Falls fault zone.

Tephra Distribution In Foreland Basin Context

The Indian Castle Shale is most condensed where it onlaps diachronously westward onto the regional, Thruway Unconformity surface, characterized by a widespread lag concentration of phosphatic debris, corroded carbonate clasts, and variable amounts of

pyroclastic debris that accumulated under strongly dysoxic conditions (Figures 6g, 7). This unconformity surface is interpreted to represent an eastwardly sloping submarine ramp that marked the sediment-starved western slope of the foreland basin (Baird and Brett 2002). Tephra layers are observed to terminate westward onto this surface as the hiatus increases in time-magnitude (Figure 7). It is significant that several tephra layers (Paradise, Fishers, Eatonville, and Countryman beds) appear to thicken slightly westward towards their respective termini at the toe of the ramped erosion surface, rather than toward the east in the direction of the inferred orogen. Perhaps this eastward thinning is simply an artifact of differential tectonic compression and shearing of tephra deposits in eastern localities. However, another possibility is that tephra was differentially concentrated due to secondary reworking (downslope transport) from the adjacent ramp slope (see below).

We also observe an upward decline in the number of ashes and average thickness of tephra layers within the Utica shale succession across the Mohawk Valley region. Though there is a tendency for tephra beds to be bundled into groups of closely-spaced K-bentonite layers, both tephra bundles and isolated tephras trail off as one ascends through the Utica, such that tephras become very widely-spaced and thin in the upper parts of the Indian Castle Shale as progradational turbiditic facies of the Frankfort and Schenectady formations are approached (Baird and Brett 2002). It is particularly significant that these observations, based on outcrop work in the 1992 - 2001 period, predated examination of numerous long drill core sections by Baird, including three that extend from Grenville basement upward into the Schenectady succession (see: Baird and Brett 2006, 2008). This additional subsurface record corroborates the above observation that tephras become less common and thinner within the middle and upper portions of the Indian Castle succession. Inferential upward loss of tephra layers appears to have commenced within the upper part of the *Climacograptus spiniferus* graptolite biozone with near complete loss of observable tephras in overlying turbiditic facies (uppermost *C. spiniferus* and *Geniculograptus pygmaeus* biozones (see Goldman et al. 1994; Mitchell et al. 1994).

One explanation would be that Taconian arc activity could have slowed down or ceased following a transition from forearc subduction processes into the phase of high Taconic overthrusting. Cessation of the subduction process would have resulted in a significant reduction of, or the end of, volcanism along the proximal arc system, leading to a trailing off

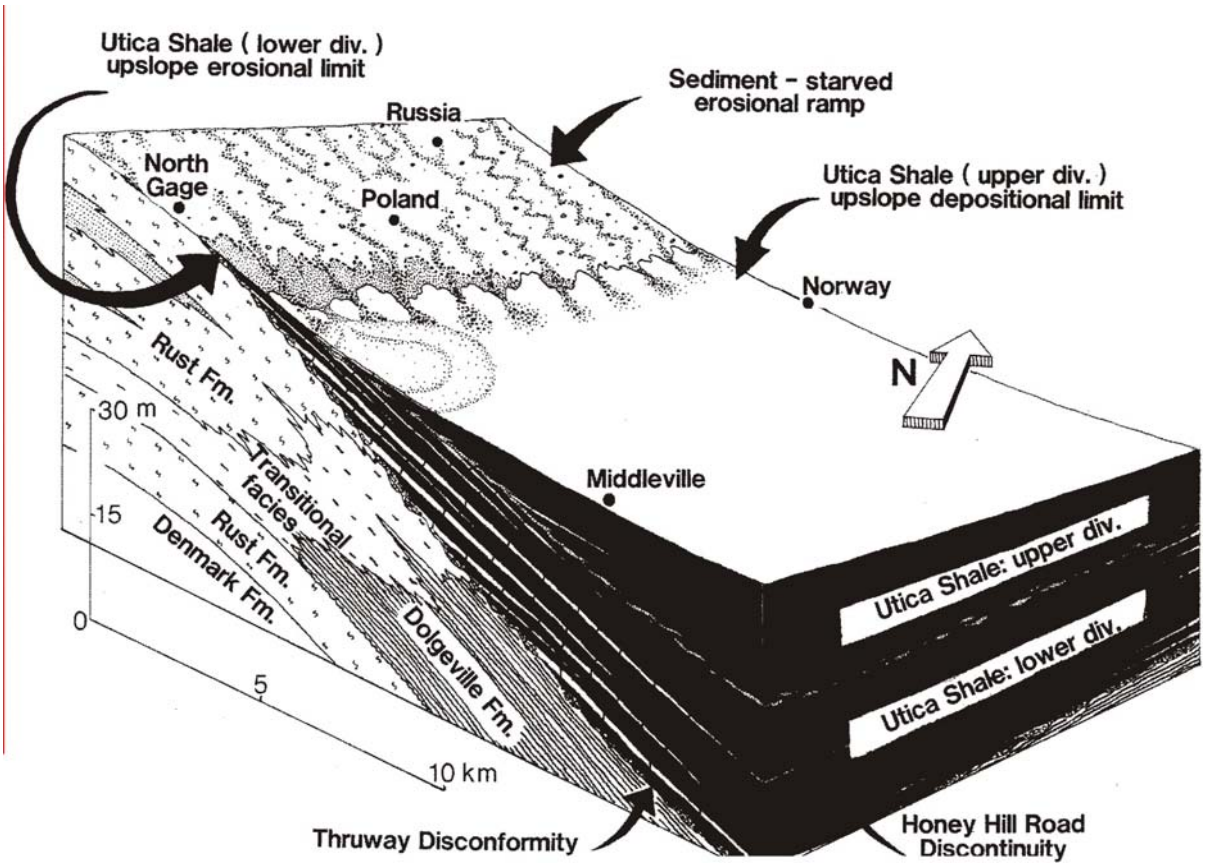

Figure 7. Process model showing onlap of condensed black Utica mud deposits onto a sediment-starved, east-facing basin margin slope during deposition of the upper part of the Indian Castle Shale. This erosional ramp corresponded to the subsiding west side of the expanding foreland basin; progressive burial of this surface produced a widespread corrosional-erosional disconformity in the westernmost Mohawk Valley region and across adjacent central New York State. Note the westward onlap of several lower Indian Castle tephras onto the older Thruway Unconformity surface (Baird and Brett (2002).

of aerial tephra supplies to the foreland basin sea. However, foreland basin sedimentary dynamics may have exerted an even greater effect. The most closely-spaced and thickest tephra layers are focused, in stratigraphically condensed, time-rich Indian Castle sections above the Thruway Unconformity in western Mohawk Valley sections (Little Falls-Middleville area; Figure 7). In this detrital mud-starved setting, tuffaceous sediment would have become more concentrated, particularly with the tractional effects of bottom currents. Moreover, several dilute tephra-rich calcareous siltstone beds in the basal 1.0-2.0 meters of the Indian Castle Shale, in sections west of the Little Falls Fault, suggest that tuffaceous material deposited on the eastward-, and southward-sloping, onlap ramp, may have been

swept down that ramp and deposited as turbiditic layers within onlapping Utica black mud deposits (Figures 6g, 7). Hence, black shale deposits, comprising the basal part of the Indian Castle Shale above the Thruway Unconformity, should be particularly potassium-rich, owing both to sediment condensation and to downslope tuff transport from the nearby submarine onlap slope.

V. THE DEVONIAN TEPHRA RECORD, AND COMPARING FORELAND AND HINTERLAND RECORDS OF EXPLOSIVE VOLCANISM (Chuck Ver Straeten)

Devonian tephra beds, New York and the eastern U.S.

The convergence of multiple terranes with eastern Laurentia between the latest Silurian to early Mississippian resulted in orogenesis and magmatic arc magmatism and extrusive to explosive volcanism (Acadian orogeny; = Acadian and Neo-acadian orogenies of van Staal 2007 and van Staal et al. 2009). The orogeny developed over multiple tectonically-active to -quiescent phases (Ettensohn 1985, 2008; Ver Straeten 2010), a result of the multiple collisions and oblique convergence, seen in an overall northeast to southwest development of the orogen and sedimentation in the adjacent Acadian foreland basin system. Explosive eruption of silicic tephra in the orogen, and its subsequent transport, deposition and burial history, followed patterns outlined in the "Volcanic Tephra Processes" section earlier in this paper.

The record of explosive silicic volcanism during the Acadian Orogeny is, at least in part, recorded by airfall volcanic tephras preserved sedimentary rocks in New York and across the eastern U.S. Forty years ago, only a few such beds were known. Currently, approximately 100 volcanic airfall tephras are reported from Devonian strata in the Appalachian, Michigan, Illinois and Iowa basins (Table 1).

Many of the documented Devonian tephra beds occur within one of five clusters of relatively closely spaced beds (Table 1, Figure 8). Others, however, occur as a single isolated to a few closely spaced beds, sometimes within thick strata with no other apparent volcanogenic layers. The five clusters generally consist of 8 to 15 beds each, although in areas proximal to the apparent volcanic source, Dennison and Textoris (1988) report as many

TABLE 1. DEVONIAN AIRFALL TEPHRAS, APPALACHIAN BASIN/EASTERN U.S.

Major Devonian airfall tephra clusters:

Bald Hill K-bentonites cluster. Lower Devonian, mid Lochkovian, 417.6±1.0 Ma (Tucker et al. 1998). Up to 15 K-bentonites in cluster; NY, PA, MD, VA, WV; in NY, within Kalkberg and New Scotland Fms.; elsewhere within Corriganville and Mandata Fms. Smith et al. 1988, 2003; Shaw et al. 1991; Hanson 1995, Ver Straeten 2004a; Benedict 2004.

Sprout Brook K-bentonites cluster: Lower Devonian, lower Emsian (?), 408±1.9 Ma, (Tucker et al. 1998). Up to 15 K-bentonites in cluster; eastern NY, possibly VA and WV; In NY, in lower part of Esopus Fm.; elsewhere in basin, if present, at base of Beaverdam Mbr., Needmore Fm., Virginia. Ver Straeten 1996, 2004a&b, 2010; Benedict 2004; Ver Straeten et al. 2005.

Tioga Middle Coarse Zone cluster (recognized in Ver Straeten 2004a as separate from Tioga A-G K-bentonites cluster): lower Eifelian, 391.4±1.8 Ma, (Tucker et al. 1998); up to 32 tuffs and K-bentonites in cluster; restricted to southern part of Appalachian Basin, in parts of VA, WV outcrop belt; occurs within upper part of Needmore Fm., or "Tioga Zone". Dennison and Textoris 1970, 1978, 1987; Dennison 1983; Ver Straeten 2004a, 2007a.

Tioga A-G K-bentonites cluster (recognized by Ver Straeten 2004a as separate from Tioga Middle Coarse Zone cluster). Middle Devonian, lower Eifelian, 390±0.5 Ma, (Roden et al. 1990). Up to 9 K-bentonites in cluster; NY, PA, MD, VA, WV, OH. In NY within Onondaga Fm.; in other states within Onondaga Fm. (eastern PA), Selinsgrove Mbr., Needmore Fm. (PA, MD, VA, WV), Columbus Fm. (OH), and/or lower part of Marcellus Shale locally (PA, MD, VA, WV). Conkin and Conkin 1979, 1984; Smith and Way 1983; Way et al. 1986; Brett and Ver Straeten 1994; Ver Straeten 2004a, 2007a; Benedict 2004.

Belpre K-bentonites Cluster. Upper Devonian, Frasnian, 381.1 +/- 1.3 Ma (Tucker et al. 1998). Up to 8 K-bentonites in cluster; in Rhinestreet Fm. in western NY, and equivalent strata in TN to PA. Collins 1979; Over 2007.

Other Devonian airfall tephras:

Sub-Schoharie Fm. K-bentonite. Lower Devonian, mid Emsian. Single bed; found only in east-central NY, at Esopus-Schoharie Fms. contact; not recognized elsewhere in basin; bed rests on unconformity (shale firmground), and contains glauconite and phosphate. Hanson 1995; Ver Straeten 2004a.

Sub-Onondaga Fm. K-bentonite. Lower Devonian, upper Emsian. Single bed; found exclusively in east-central New York, at Schoharie-Onondaga Fms. contact; not recognized elsewhere in basin; bed rests on an unconformity, and contains glauconite and phosphate. Ver Straeten 2004a.

Other Onondaga Fm. K-bentonites. Middle Devonian, lower Eifelian; up to 8 separate beds scattered through Fm., not within the Tioga Middle Coarse Zone or Tioga A-G K-bentonite clusters; through NY, PA, MD, VA, WV, OH; in New York within the Onondaga Fm.; elsewhere within Onondaga Fm. (eastern PA), Selinsgrove Mbr. of the Needmore Fm. (PA, MD, VA, WV) and Columbus Fm. (OH); key references; Conkin and Conkin 1979, 1984; Ver Straeten 1996, 2004a.

Mid-Union Springs Fm. K-bentonite. Middle Devonian, mid Eifelian. Single bed; found in NY, PA, MD, VA, WV, OH; in NY in the middle of the Union Springs Fm.; elsewhere within the Marcellus Fm. (PA, VA, WV), Millboro Fm. (VA, WV) or Delaware Fm. (OH). Ver Straeten 2004a.

Sub-Cherry Valley K-bentonite. Middle Devonian, upper Eifelian; single bed; only recognized locally in NY. Not in VA, as reported by Ver Straeten 2004a. In NY, occurs immediately below the Cherry Valley Mbr. of the Oatka Creek Fm. Hanson 1995; Ver Straeten 2004a.

Additional Occurrences

Kashong-Windom mbrs. contact, Moscow Fm., mid Givetian, western NY. Wilcott and Over 2005.
Lower Geneseo Fm., upper Givetian, western NY. Over, Baird notes.
Lower & upper Pipe Creek Fm., upper Frasnian, western NY, possibly OH. Over et al. 1998. (2 beds?).
Center Hill K-bentonite, upper Hanover Fm., western NY; also reported in TN, possibly MI, IA. Over 2002.
Lower Dunkirk Fm., Tioga Dam, PA. D.J. Over notes.
Uppermost Olentangy Fm., OH. Over and Rhodes 2000.

Other Possible Devonian Airfall Tephra Beds

Lowest Otsego Mbr., Mount Marion Fm., lower Givetian, eastern NY. Ver Straeten 2004a.
Basal Butternut Mbr., Skaneateles Fm., Givetian, central NY. Ver Straeten notes, 1996.
"Probable bentonites", Wanakah Mbr., Ludlowville Fm., mid Givetian, western NY. Batt 1996.
Possible K-bentonites, Tully Fm., central NY, upper Givetian. Baird notes, and Ver Straeten notes, 1996.

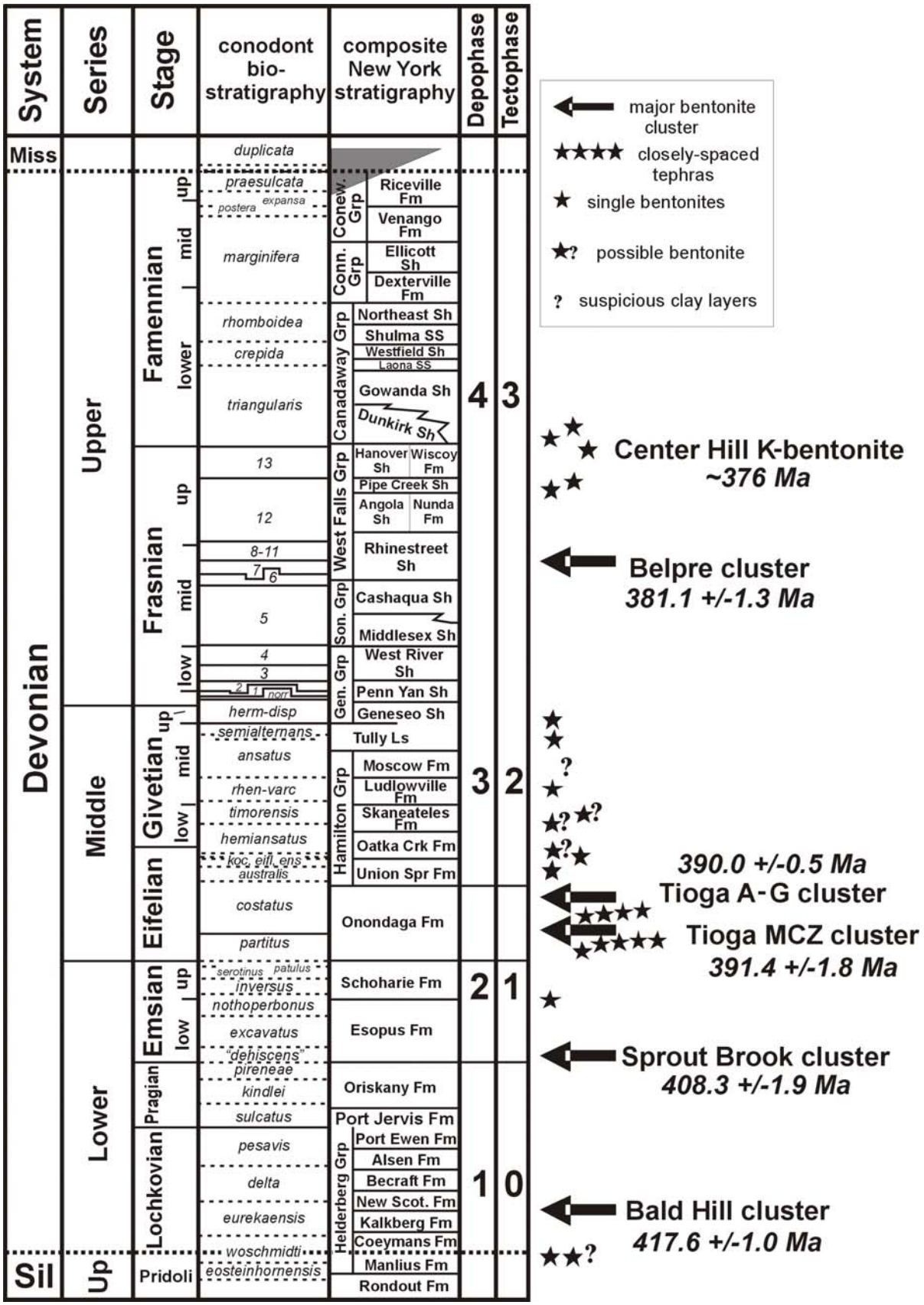
System
Series
Stage
conodont bio-stratigraphy
composite New York stratigraphy
Depophase
Tectophase
major bentonite cluster
closely-spaced tephras
single bentonites
possible bentonite
suspicious clay layers
Devonian
Miss
Sil
Upper
Middle
Lower
Up
Famennian
Frasnian
Givetian
Eifelian
Emsian
Pragian
Lochkovian
Pridoli
up
mid
low
duplicata
praesulcata
postera
expansa
marginifera
rhomboidea
crepida
triangularis
13
12
8-11
7
6
5
4
3
2
1
norr
herm-disp
semialternans
ansatus
rhen-varc
timorensis
hemiansatus
koc. eifl. ens
australis
costatus
partitus
serotinus
patulus
inversus
nothoperbonus
excavatus
"dehiscens"
pireneae
kindlei
sulcatus
pesavis
delta
eurekaensis
woschmidti
eosteinhornensis
Conew. Grp
Riceville Fm
Venango Fm
Conn. Grp
Ellicott Sh
Dexterville Fm
Canadaway Grp
Northeast Sh
Shulma SS
Westfield Sh
Laona SS
Gowanda Sh
Dunkirk Sh
West Falls Grp
Hanover Sh
Wiscoy Fm
Pipe Creek Sh
Angola Sh
Nunda Fm
Rhinestreet Sh
Son. Grp
Cashaqua Sh
Middlesex Sh
Gen. Grp
West River Sh
Penn Yan Sh
Geneseo Sh
Tully Ls
Hamilton Grp
Moscow Fm
Ludlowville Fm
Skaneateles Fm
Oatka Crk Fm
Union Spr Fm
Onondaga Fm
Schoharie Fm
Esopus Fm
Oriskany Fm
Port Jervis Fm
Helderberg Grp
Port Ewen Fm
Alsen Fm
Becraft Fm
New Scot. Fm
Kalkberg Fm
Coeymans Fm
Manlius Fm
Rondout Fm
4
3
2
1
0
Center Hill K-bentonite
~376 Ma
Belpre cluster
381.1 +/-1.3 Ma
390.0 +/-0.5 Ma
Tioga A-G cluster
Tioga MCZ cluster
391.4 +/-1.8 Ma
Sprout Brook cluster
408.3 +/-1.9 Ma
Bald Hill cluster
417.6 +/-1.0 Ma

Table 1. Reported Devonian Airfall Tephra Beds, Eastern U.S. Based on compilation of data from various sources, summarized in Ver Straeten et al. (2007) and Ver Straeten (2010). Modified from Ver Straeten (2010).

Figure 8. Stratigraphic occurrence of reported airfall volcanic tephra beds in the Devonian, eastern U.S. Major clusters marked by arrows; stars mark individual beds; stars with question marks denote possible additional beds. Occurrences plotted against generalized New York stratigraphy and biostratigraphy. Detailed information provided in Table 1. Modified after Ver Straeten (2010).

as 44 beds in the Middle Devonian Tioga Middle Coarse Zone. These tephra-rich intervals appear to indicate times of greater volcanism in the Acadian magmatic/orogenic belt (see discussion below, and in Ver Straeten 2004a).

In New York the major clusters occur, from older to younger, in the Lower Devonian Kalkberg and New Scotland formations (Bald Hill Tephras; Figures 8, 9a,b); the lower part of the Lower Devonian Esopus Formation (Sprout Brook Tephras; Figures 8, 9c-f'); apparently in the middle of Middle Devonian Onondaga equivalent strata in the Needmore Formation in Virginia and West Virginian only (Tioga Middle Coarse Zone; see note below); and in the upper Onondaga Formation (Tioga A-G Tephras; Figures 8, 10a,b,d-g); and in the Upper Devonian Rhinestreet Formation (Belpre Tephras). The Bald Hill, Tioga A-G, and Belpre tephras are found in equivalent strata around the Appalachian basin, and sometimes into the cratonic basins. In contrast, the Sprout Brook tephras and apparently the Tioga Middle Coarse Zone have a more restricted distribution (New York, and Virginia-West Virginia, respectively).

Most of the Devonian airfall tephras are preserved as altered, clay-rich K-bentonites. In the southern Appalachian basin (VA, WV) beds of the Tioga Middle Coarse Zone occur as crystal-rich sandy "tuffs", often largely comprised of biotite phenocrysts. Even in western New York, freshly exposed beds in the Tioga A-G cluster may be tuffaceous, with common to abundant fine biotites in a lithified matrix.

Geochronologic age dates for the Devonian tephras presented here are from Tucker et al. (1998). It should be noted, however, that at least some of the dates have been recalculated by different authors (e.g., Williams et al. 2000; Kaufmann 2006). Interestingly, the Geologic Time Scale of 2008 (Ogg et al. 2008) sometimes payed little attention to dated tephra numbers when assigning ages to boundaries between Devonian stages (e.g., the clearly mid Eifelian-age Tioga tephras clusters, at 390 and 391 Ma, fall within Ogg et al.'s 2008 range of ages given for the succeeding Givetian Stage).

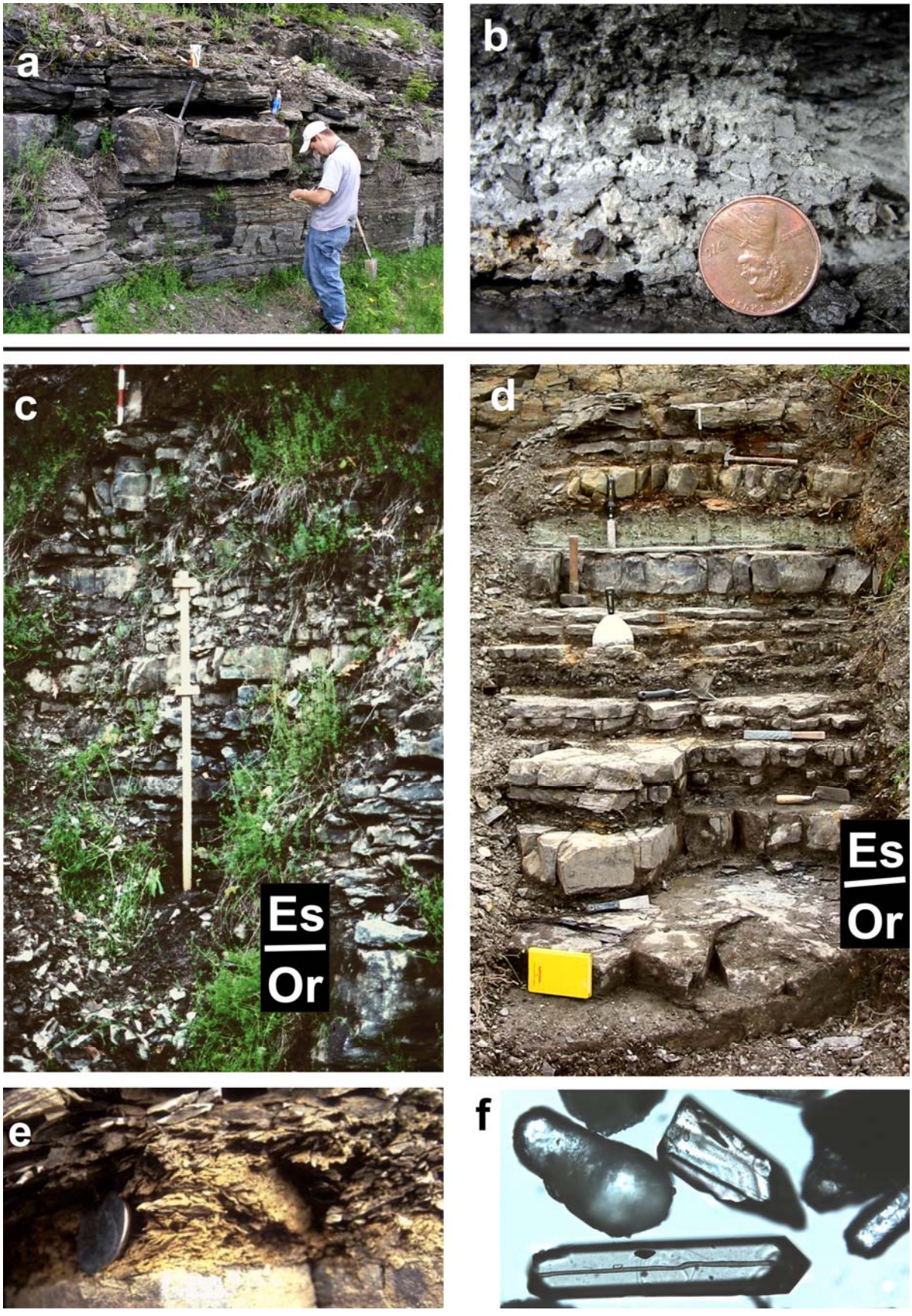
a
b
c
Es
Or
d
Es
Or
e
f

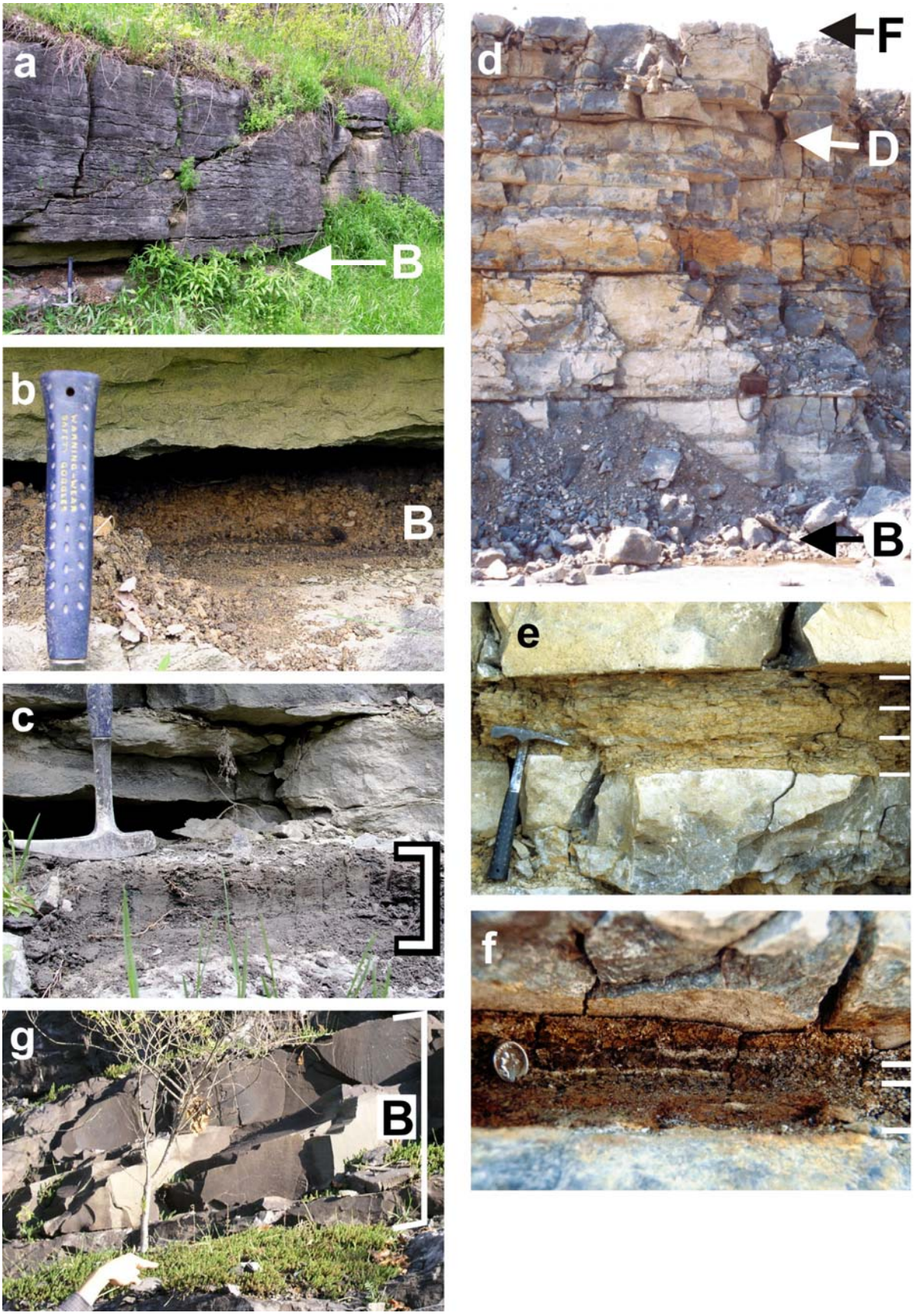
a
B
b
B
c
d
F
D
B
e
f
g
B

Figure 9. Lower Devonian Tephras, Cherry Valley and other localities, eastern New York. a) Outcrop view of Rickard's original clay-rich tephra, in prominent crevice above head level. From the Bald Hill Tephra Cluster, Kalkberg Formation, Cherry Valley. b) close-up of Rickard's K-bentonite; original volcanic glass ("ash") altered to clays. Penny for scale. c) Outcrop view of lower part of the Esopus Formation, Cherry Valley. Fifteen clay beds of the Sprout Brook Tephra cluster are interbedded with shales, cherts and siliceous siltstones. Jake staff at center is 1.5 meters tall. d) Outcrop of Sprout Brook cluster 19 miles to the east-southeast, along I-88 near Cobleskill. Field book marks Oriskany-Esopus formational contact. e) Close-up of thin Sprout Brook tephra bed, along NY Rte. 23a, southwest of Catskill. Quarter for scale. f) Zircons and apatites from lower part of 12 cm-thick Sprout Brook tephra bed, 2.7 m above Oriskany Fm. at Cherry Valley. Note zoning in zircon fragment (upper center); apatites to left and right. Lower zircon is approximately 800 microns in length.

Figure 10. Middle Devonian Tephras, Onondaga Limestone, Cherry Valley and other localities. . a) Seneca Member of Onondaga Limestone at Stop 4 of this trip. Prominent crevice of Tioga B Tephra visible at base. Hammer for scale in lower left, at base of outcrop. b) Close-up view of Tioga B at Stop 4, showing 12 cm-thick K-bentonite clay bed. Deep recession due to bioerosion (decades of geologists collecting samples). c) Impure tephra at unconformable base of Onondaga Limestone, in bracketed interval. North side of Rte. 20, ca. two miles west of Stop 4. The clay-rich bed contains a mix of volcanic phenocrysts, detrital sand, and authigenic glauconite and phosphate grains, indicative of a complex history of tephra accumulation and mixing with background sediments over time. Hammer for scale. d) Complete development of Seneca Member, with Tioga tephra beds A through F. At quarry west of Honeoye Falls, Monroe County, western New York. For details, see Ver Straeten et al. (1994). Camera bag at lower prominent crevice for scale. e. Tioga B tephra bed in quarry west of Stafford, Genesee County, western New York. White bars on right delineate three distinct layers within Tioga B, a pattern seen in multiple exposures. At the Honeoye Falls Quarry (Figure 10d), Gordon Baird found two smothered fossil assemblages within the Tioga B, apparently at these same positions – these lines of evidence indicate a complex depositional history to the Tioga B tephra. f) Fresh exposure of the Tioga D tephra bed, also at Honeoye Falls quarry. White bars on right denote positions of three light gray bands of concentrated volcanic phenocrysts, each overlain by brown clays (=fine volcanic glass), again indicative of a complex depositional history prior to burial of the tephra layer. Dime for scale. g. Anomalously thick outcrop of Tioga B Tephra on south side of Interstate 80, Stroudsburg, PA (between brackets). The Tioga B at this locality is uncharacteristically thick, coarser and well-lithified. As in New York, it also features internal fossil-rich layers, sharp grain-size changes vertically, and other features that again show a complex depositional history over a broad swath of the Appalachian basin. Wrist and hand for scale in lower left.

A significant issue that is currently unresolved involves interpreted correlations of the two Tioga tephra clusters. Ver Straeten (2004a, 2007b) correlated the Tioga A-G cluster from New York and Pennsylvania with the upper of two mid Eifelian (lower Middle Devonian) tephra clusters along the Virginia-West Virginia border area, in contrast to earlier work by Dennison (e.g., Dennison and Textoris 1970, 1978, 1987; Dennison 1983), Subsequent fieldwork by Ver Straeten through Maryland and northern outcrops in Virginia and West Virginia, and discussion with T. Carr (West Virginia University) in 2011 raise questions about the correlation. Further fieldwork, possibly with geochemical fingerprinting of phenocrysts, is needed to resolve the issue.

The post-depositional history and preservation of Devonian tephra beds in the eastern U.S. has been previously examined by Ver Straeten (2004a, 2008), Benedict (2004), and Ver Straeten et al. (2005; see also Figure 10c,e-g). A strong understanding of the depositional

history of the tephra beds is important, to attempt to filter out potential preservational biases in the record of explosive silicic volcanism in sedimentary successions, as outlined in the later part of the previous section. Do some conditions in sedimentary environments preferentially preserve, or alternatively destroy and alter the sedimentary record of paleovolcanism? These issues need to be examined and reasonably resolved prior to attempting to use the sedimentary airfall tephra record as a proxy for paleovolcanism. For further discussion and application to explosive Devonian volcanism during the Acadian orogeny, see Ver Straeten (2004a, 2008, 2010).

Crossing the boundary: An example comparing foreland and hinterland records of silicic magmatism

If the overall time distribution of Devonian airfall tephras in New York and the eastern U.S. is not a product of preservational biases (as discussed in the "Volcanic Tephra Processes" section above), and they do reflect a coarse record of paleovolcanism, then the major clusters should reflect times of more significant silicic magmatism in the hinterland. Therefore, one would suspect greater volcanism in the Acadian magmatic arc in the Lower Devonian at around 417 Ma (Bald Hill cluster) and 408 Ma (Sprout Brook cluster); in the Middle Devonian at around 391 Ma (Tioga Middle Coarse Zone) to 390 Ma (Tioga A-G cluster); and around 381 Ma (Belpre cluster; dates from Tucker et al. 1998, except Tioga A-G from Roden et al. 2000). The additional scattered tephra beds through the stratigraphic column may imply lower levels of background volcanism, at least at times if not continuously.

In recent years, an increasing number of plutonic and volcanic igneous rocks have been geochronologically dated in the hinterland (New England and adjacent maritime Canada), to compliment dates on the foreland basin tephras. Error bars on a relatively large number of dated lower Emsian-age igneous rocks in the hinterland overlap with the error bars on Tucker et al.'s (1998) age for the Lower Devonian Sprout Brook tephras, in the lower part of the Esopus Formation of New York (Table 2). No silicic igneous rocks of the same age are known to the author at this time south of New England.

As noted above, the Sprout Brook Tephras have a very restricted distribution across the foreland, apparently only developed in eastern New York (Ver Straeten 2004b). In the

TABLE 2. LOWER EMSIAN IGNEOUS ROCKS, ACADIAN OROGEN AND FORELAND (WITH ERROR BARS THAT OVERLAP WITH AGE OF THE SPROUT BROOK K-BENTONITES)

Igneous rock type	Unit	Composition	Locality	Age (Ma)	References
Volcanic	Sprout Brook K-bentonites	K-bentonites, from high silica rhyolites	NY; VA?	408.3 +/- 1.9	Ver Straeten and Brett 1995; Hanson 1995; Ver Straeten 2004 a,b; Date from Tucker et al. 1998
	Traveler Fm.	rhyolite	ME	407.3 +/-0.5; 406.7 +/-1.4	Rankin 1968; Rankin & Hon 1987; dates for lower and upper Traveler Fm. from Rankin & Tucker 1995.
	Kineo Fm.	rhyolite	ME	406.3 +/-3.8	Boucot & Heath 1969: date from Bradley et al. 2000
	York River Fm.	bimodal	Que (Gaspe Pen.)	(lower Emsian)	Poole & Rogers 1972; Doyon & Valiquette 1987
	Val d'Amour Formation	rhyolite (+more?)	New Brunswick	407.4 ± 0.8	Wilson 2004
	Littleton Fm.	(tuff layer)	NH	407 +/-2	Tucker and Rankin, in Bradley et al. 2000.
	Littleton Fm.	bimodal	NH	(lower Emsian)	Billings 1937, 1956; A.J. Boucot, pers. commun. 1993.
Plutonic	Bald Mtn. pluton	granodiorite	ME	408	Bradley et al. 2000
	Ebeemee pluton	granite	ME	407.8 +/-2.4; 405.7 +/-2.6	Bradley et al. 2000
	Berry Brook pluton	gabbro, diorite	ME	410	Ludman and Idleman 1998
	Harrington pluton	granite	ME	406.9 +/- 1	Bradley et al. 2000
	Haskell Hill pluton	granite	ME	408.0 +5/-4	Tucker et al. 2001
	Katahdin pluton	quartz monzanite	ME	406.9+/-0.4	Rankin and Tucker 1995
	Mattamiscontis pluton	granite	ME	406.9 +/-3.6	Bradley et al. 2000
	Moxie Pluton, eastern part	gabbro	ME	406.3 +/-3.8	Bradley et al. 2000
	Redington pluton	granite	ME	407.6 +/-4.7	Solar et al. 1998
	Russell Mtn pluton	granodiorite	ME	406.0 +/-1.3	Bradley et al. 2000
	Sebec Lake pluton	granodiorite	ME	407.8 +/-2.5	Bradley et al. 2000
	Shirley-Blanchard pluton	granodiorites	ME	406.9 +/-1.4	Bradley et al. 2000
	Skiff Lake pluton, Pokiok batholith	granite	NB	409.0 +/-2	Bevier and Whalen 1990
	S. Roxbury pluton	granite	ME	408.2 +/-2.5	Solar et al. 1998
	Swift River pluton	leucogranite	ME	407.9 +/- 1.9	Solar et al. 1998
	Wamsutta pluton	quartz diorite	NH	408.2 +/- 2.0	Eusden et al. 2000
	Spaulding pluton	tonalite	NH	408 +/-2	Robinson and Tucker 1996
	Prescott pluton	gabbro	MA	407 +3/-2	Tucker and Robinson 1990

Table 2. Lower Emsian (Lower Devonian) igneous rocks, Acadian orogen and foreland. Error bars of all units overlap with error bars of Tucker et al.'s (1998) date for the Sprout Brook K-bentonites in eastern New York. From Ver Straeten (2010).\

absence of distinct K-bentonite beds from the equivalent position to the southwest in Pennsylvania, Maryland, Virginia, and West Virginia, bulk samples of shales were collected

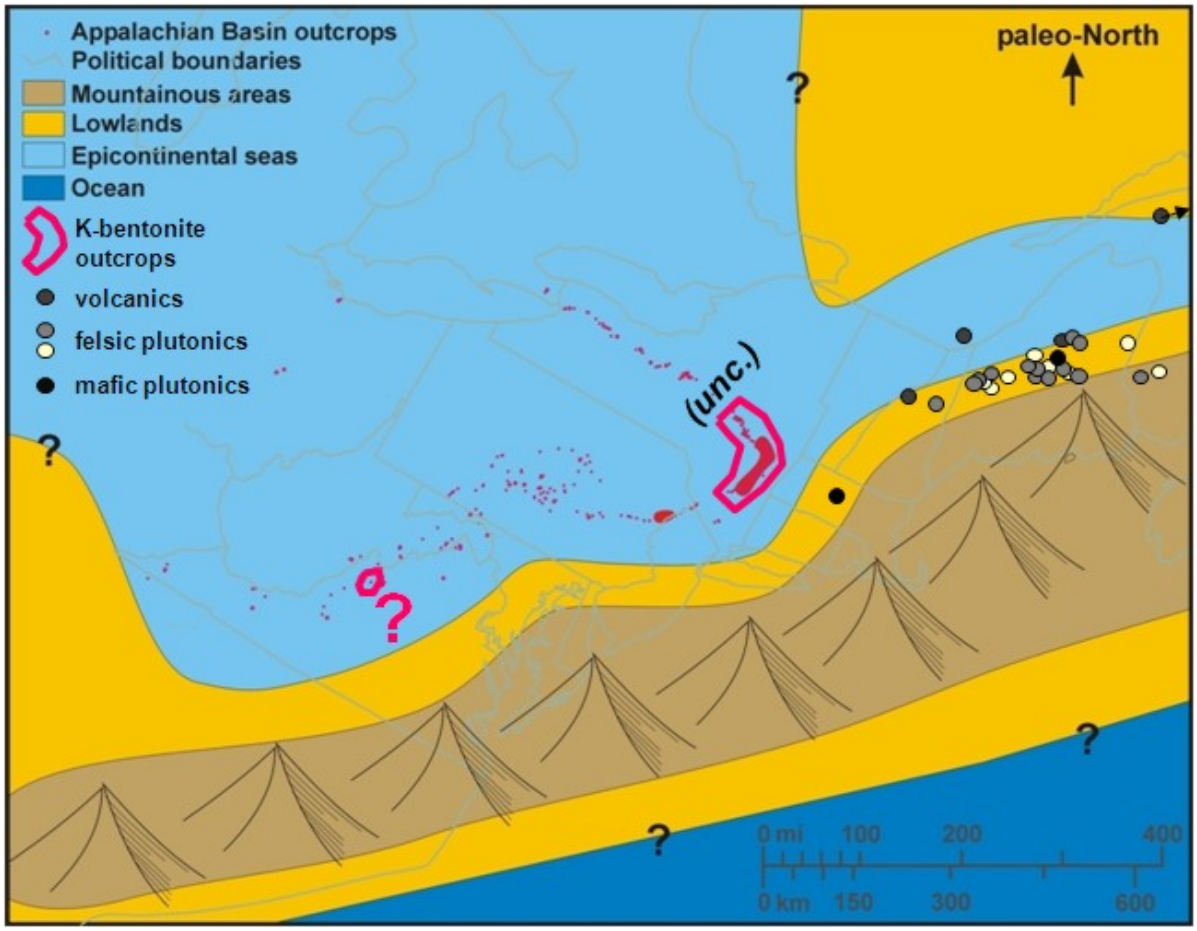

Figure 11. Lower Emsian igneous rocks, Acadian orogen and foreland. Map of distribution and type of lower Emsian–age igneous rocks within margin of errors of Tucker et al.'s (1998) age for the Sprout Brook tephra cluster in eastern New York. For details see Table 2. Positions of the front edge of the orogen and marine strata in Maine and adjacent areas are after Bradley et al. (2000). From Ver Straeten (2010).

and processed. Only one or two samples yielded apparent unabraded zircons of possible volcanogenic origin (Ver Straeten 2004b).

At least two significant non-volcanic factors could account for the restricted distribution of lower Emsian tephras across the Appalachian Basin. A first hypothesis is that tectonic-related subsidence at the onset of a new phase of Acadian uplift began earlier in the northeast part of the basin. If this is so, it is possible that the Sprout Brook Tephras were preferentially preserved in deeper water facies in eastern New York, while other portions of the basin remained longer in shallow water facies (Oriskany Sandstone), and tephra sediments became mixed with background sediments. No high resolution biostratigraphic data (e.g., conodonts, goniatites, dacryoconarids) is available to test this. However, Ver Straeten (2007b, 2009) was

able to correlate all three third order (apparently global) sea level cycles that comprise the Esopus Formation from eastern New York to southwest Virginia – including the lower cycle, which features the Sprout Brook Tephras in New York. Therefore, some record of volcanism should also be preserved southwest of New York.

A second hypothesis is that enhanced preservation of the Sprout Brook beds in eastern New York could be related to higher sedimentation rates in the northeast portion of the basin. This would result in more rapid burial, leaving less time for physical and biological mixing of airfall pyroclastic sediments with background sediments at the sea floor, essentially erasing the record of volcanism – as potentially may have occurred more distal portions of the basin. However, the paucity of unabraded zircons in the shale samples from the central Appalachians makes the possibility of obliteration by mixing unlikely.

A third major hypothesis is that the restricted distribution of the Sprout Brook Tephras is related to a high concentration of lower Emsian-age silicic magmatism (at roughly 408 Ma) in New England and nearby Maritime Canada (Table 2, Figure 11). The bulk of these occur in Maine; they include the co-magmatic Katahdin Granite and Travel Rhyolite, the largest of five lower Emsian volcanic centers of the Piscataquis Volcanic Belt of north-central to western Maine (Rankin 1968). The preserved volume of ash flow tuffs of the Traveler Rhyolite is "conservatively" estimated to be 800 km^3, a "significant world occurrence of ash flow tuff" (Rankin and Hon 1987). This volume, preserved over the northeast corner of the Katahdin Pluton, is comparable with major Cenozoic tuffs in the western U.S., including the Lava Creek Tuff in the Yellowstone Caldera (more discussion in Ver Straeten 2004b). Furthermore, the approximately 3.2 kilometer-thick ash-flow tuffs of the preserved portion of the Traveler Rhyolite was deposited over an interval on the order of 1 million years (base at 407.3 ± 0.5; top at 406.7 ± 1.4 Ma; Rankin and Tucker 1995; Bradley and Tucker 2002).

The abundance of Sprout Brook age-equivalent volcanic and plutonic rocks in New England and adjacent areas in Canada, especially the great volume in the Piscataquis Volcanic Belt in Maine, suggests that the restricted distribution of New York's Sprout Brook Tephras could reflect explosive volcanic sources to the northeast (Figure 11). Considering the paleogeographic rotation of the eastern Laurentian margin at that time, and prevailing trade winds north of 30 degrees south (blowing to the west-northwest), eastern New York may have lain on the southern fringe of the prevailing pathway of airborne tephra sourced

from Maine, approximately 400 to 500 km to the northeast. More distal areas of the Appalachian basin, further to the southwest, may have been beyond the margin of transport for explosive silicic pyroclastics from the Piscataquis Volcanic Belt and other northern New England sources.

SUMMARY

The Appalachian record of silicic magmatism and explosive volcanism is contained in the magmatic and volcanic rocks of the Appalachian hinterland, and in the sedimentary record of volcanic layers in the adjacent foreland, and sometimes the more distal cratonic basins beyond it. It is through a fusion of these diverse and varied data sets/perspectives from both hinterland and foreland basin records that we can approach a greater understanding of the history, character and timing of silicic magmatism and explosive volcanism in the Appalachians, through the early to mid Paleozoic.

This paper and field trip represent a first attempt at such a broader synthesis. Some key points include:

- By any name (tephra, K-bentonite, tuff), airfall volcanic layers in sedimentary rocks have a complex history, from the initiation of an eruption in a magma chamber to final burial, and diagenetic alteration.
- "Tephra" beds in sedimentary successions provide a relatively high resolution, if incomplete, record of volcanism through time. Biases of tephra event preservation in sedimentary environments must, however, be accounted for. Only rarely does a single layer represent a single eruption event; and many events are not preserved. Does the preserved tephra record provide a coarse outline of volcanism through time? If so, for example, there should be increased volcanism during the Devonian Period at around 417, 407, 390, and 381 Ma; and upper Lower Devonian tephras in eastern New York (Sprout Brook Tephra cluster) should be sourced in northern New England +/- adjacent maritime Canada.
- Geochemical tools such radiometric dating, isotopic analysis, and other geochemical data provide a range of perspectives on ancient silicic magmatism and explosive volcanism. These include age, composition, source characteristics and petrogenetic origins. For

example, strontium and neodymium isotopic analyses from apatites in Ordovician K-bentonites from the Taconic foreland, and from igneous and metaigneous rocks in the Taconic hinterland, indicate that magmatic sources were "evolved" – that the magmas extensively interacted with continental crust prior to crystallization below the surface, or to their eruption. And that the crust involved was Grenville (i.e., Laurentian).

- Late Ordovician airfall tephras in the Mohawk Valley have a complex sedimentologic, preservational and diagenetic history. Condensation processes play an important part in the post-depositional history of many layers. Volcanic glass ("ash") in some beds altered to smectite-rich clay beds, and subsequently to potassium-rich mixed layer illite-smectite clays; however, in some beds glass was altered to zeolite minerals, and/or were cemented early. Reworking and condensation on the sea floor at times led to the formation of relatively coarse-grained tuff layers. Foreland basin flexure, during the onset of new tectonic pulses, may also affect the preservation of tephra beds, which may vary laterally from proximal to distal areas across the foreland.
- Finally, foreland and hinterland data of silicic magmatism and explosive volcanism in the Ordovician and Devonian Appalachian region both have strengths and weaknesses. The integration of information from the foreland basin and hinterland, utilizing high-resolution geochronologic age dates, has tremendous potential for advancing our understanding of not only magmatic history, but also broader tectonic processes and events involving both parts of the orogen. This could possibly include significant questions such as the possibility and timing of slab break-off events, reversals in subduction polarity, and the timing of migration of the deformation front into the foreland.

REFERENCES

Aleinikoff, J. N., and Karabinos, P., 1990, Zircon U-Pb data for the Moretown and Barnard Members of the Missisquoi Formation and a dike cutting the Standing Pond Volcanics, southeastern Vermont, *in* Slack, J. F., Summary results of the Glens Falls CUSMAP Project, New York, Vermont, New Hampshire, Volume 1887, U.S. Geological Survey Bulletin, Chapter D, 10 p.

Allen, S.R., and Freundt, A., 2006, Resedimentation of cold pumiceous ignimbrite into water: Facies transformations simulated in flume experiments: Sedimentology, v. 53, p. 717-734.

Baird, G.C. and Brett, C.E. 2001, Genesis of black shale-roofed discontinuities associated with the Ordovician Utica Shale in New York State: a review of existing and new concepts: Geological Society of America, Abstracts with Program, v. 33, p. A-102.

Baird, G.C. and Brett, C.E. 2002, Indian Castle Shale: late synorogenic siliciclastic succession in an evolving Middle/Late Ordovician foreland basin, eastern New York State, *in* Mitchell, C.E. and R. Jacobi, Taconic Convergence: Orogen, Foreland Basin, and Craton, Physics and Chemistry of the Earth, Vol. 27, p. 203-230.
Baird, G.C. & Brett, C.E. 2006, The Early Upper Ordovician Taconian Foreland Basin Sedimentary Succession: Integrated Outcrop and Drill Core Perspectives in the Mohawk Valley Region, Eastern New York: Geological Society of America, Abstracts with Programs, v. 38, p. 20.
Baird, G.C. and Brett, C.E. 2008, The Mohawk Valley drill core bonanza: New insights relating to the post-Sauk succession as seen through core and outcrop perspectives, Geological Society of America, Abstracts with Programs, v. 40, p. 63.
Baird, G. C.; Brett, C. E.; and Hannigan, R. E. 1994, Middle-Late Ordovician K-bentonite stratinomy, Mohawk Valley, New York: evidence for sedimentary condensation within ash beds: Geological Society of America, Abstracts with Program, v. 26, p. 432.
Baird G.C., Brett, C.E. and D. Lehmann, 1992, The Trenton-Utica problem revisited: New observations and ideas regarding Middle-Late Ordovician stratigraphy and depositional events in central New York, *in* April, R. H., Field Trip Guidebook, New York State Geological Association, 64th Annual Meeting, Colgate University, p. 1-40.
Batt, R.J., 1996, Faunal and lithological evidence for small-scale cyclicity in the Wanakah Shale (Middle Devonian) of western New York: Palaios, v. 11, p. 230–243.
Benedict, L., 2004, Complexity of Devonian K-bentonites in the Appalachian foreland basin: Geochemical and physical evidence supporting multi-layered K-bentonite horizons**[** M.S. thesis]: State University of New York at Albany, 258 p.
Bergström, S.M., Xu Chen, Gutierrez-Marco, J.C., and Dronov, A., 2008, New Ordovician Chronostratigraphic Chart: Lethaia, DOI10.1111/j.1502-3931.2008.00136.x.
Berkley, J.L. and Baird, G.C. 2002, Calcareous K-bentonite deposits in the Utica Shale and Trenton Group (Middle Ordovician), of the Mohawk Valley, New York State, *in* Mitchell, C.E. and Jacobi, R., Taconic Convergence: Orogen, Foreland Basin and Craton: Physics and Chemistry of the Earth, v. 27, p. 265-278.
Bevier, M.L., and Whalen, J.B., 1990, U-Pb geochronology of Silurian granites, Miramichi terrane, New Brunswick, *in* Radiogenic Age and Isotopic Studies, Report 3: Ottawa, Geological Survey of Canada Paper 89-2, p. 93–100.
Billings, M. P., 1937, Regional metamorphism of the Littleton-Moosilauke area, New Hampshire: Geological Society of America Bulletin, v. 46, p. 463–566.
Billings, M. P., 1956, The geology of New Hampshire. Part II: bedrock geology: Concord, New Hampshire State Planning and Development Commission 203 p.
Boucot, A.J., and Heath, E.W., 1969, Geology of the Moose River and Roach River Synclinoria, Northwestern Maine: Maine Geological Survey Bulletin 21, 117 p.
Bradley, D.C., 1983, Tectonics of the Acadian Orogeny in New England and adjacent Canada: Journal of Geology, v. 91, p. 381-400.
Bradley, D.C. and Kidd, W.S., 1991, flexural extension of the upper continental crust in collisional foredeeps. Geological Society of America Bulletin, vol. 103, p. 1416-1438.
Bradley, D.C., and Tucker, R.D., 2002, Emsian synorogenic paleogeography of the Maine Appalachians: Journal of Geology, v. 110, p. 483-492.
Bradley, D.C., Tucker, R.D., Lux, D.R., Harris, A.G., and McGregor, D.C. 2000, Migration of the Acadian orogen and foreland basin across the Northern Appalachians of Maine and adjacent areas: U.S. Geological Survey, Professional Paper 1624, 49 p.
Brett, C.E. and Baird, C.G. 2002, Revised stratigraphy of the Trenton Group in its type area, central New York State: sedimentology and tectonics of a Middle Ordovician shelf-to-basin succession, *in* Mitchell, C.E. and Jacobi, R., Taconic Convergence: Orogen, Foreland Basin, and Craton: Physics and Chemistry of the Earth, v. 27, p. 231-263.
Brett, C.E., and Ver Straeten, C.A., 1994, Stratigraphy and facies relationships of the Eifelian Onondaga Limestone (Middle Devonian) in western and west central New York State, *in* Brett, C.E., and Scatterday, J., eds., 66th Annual Meeting Guidebook: New York State Geological Association, p. 221–269.
Carey, A., 1997, Influence of convective sedimentation on the formation of widespread tephra fall layers in the deep sea: Geology, v. 25, p. 839-842.
Carey, A., Samson, S.D., and Sell, B. 2009, Utility and limitations of apatite phenocryst chemistry for continent-scale correlation of Ordovician K-bentonites: Journal of Geology, v. 117, p. 1-14.

Carter, L., Nelson, C.S., Neil, H.L., and Froggatt, P.C., 1995, Correlation, dispersal, and preservation of the Kawakawa Tephra and other late Quaternary tephra layers in the southwest Pacific Ocean; New Zealand Journal of Geology and Geophysics, v. 38, p. 29-46.
Cisne, J. L., Karig, D. E., Rabe, B.D. and Hay, B. J., 1982, Topography and tectonics of the Taconic outer trench slope as revealed through gradient analysis of fossil assemblages, Lethaia, vol. 15, p. 229-246.
Collins, H.R., 1979, Devonian Bentonites in Eastern Ohio: American Association of Petroleum Geologists Bulletin, v. 63, p. 655–660.
Collinson, C., 1968, Devonian of the north-central region, United States, *in* Oswald, D.H., ed., International Symposium on the Devonian System: Calgary, Alberta Society of Petroleum Geologists, v. 1, p. 933–971.
Conkin, J.E., and Conkin, B.M., 1979, Devonian pyroclastics in Eastern North America, their stratigraphic relationships and correlation: *in* Conkin, J.E., and Conkin, B.E., Devonian-Mississippian Boundary In Southern Indiana and Northwestern Kentucky, Field Trip 7, Ninth International Congress of Carboniferous Stratigraphy and Geology, University of Louisville, p. 74-141.
Conkin, J.E., and Conkin, B.M., 1984, Paleozoic metabentonites of North America: part 1.-Devonian metabentonites in the eastern United States and southern Ontario: their identities, stratigraphic positions, and correlation: University Of Louisville Studies In Paleontology And Stratigraphy, No. 16, 136 p.
Delano, J.W., Schirnick, C., Bock, B., Kidd, W.S.F., Heizler, M.T., Putnam, G.W., De Long, S.E., and Ohr, M., 1990, Petrology And Geochemistry Of Ordovician K-Bentonites In New York State: Constraints on the nature of a volcanic arc: Journal of Geology, v. 98, p. 157-170.
Delano, J.W., Tice, S.J., Mitchell, C.E., and Goldman, D., 1994, Rhyolitic glass in Ordovician K-bentonites: A new stratigraphic tool: Geology, v. 22, p. 115-118.
Dennison, J.M., 1983, Internal stratigraphy of Devonian Tioga ash beds in Appalachian Valley and Ridge province: Geological Society of America Abstracts with Programs, v. 15, p. 557.
Dennison, J.M., and Textoris, C.A., 1970, Devonian Tioga Tuff in Northeastern United States: Bulletin Volcanologique, v. 34, p. 289-294.
Dennison, J.M. and Textoris, C.A., 1978, Tioga bentonite time-marker associated with Devonian shales in Appalachian basin, *in* Schott, B.L., Overbey, W.K., Jr., Hunt, A.E., and Komar, C.A., Proceedings Of The First Eastern Gas Shales Symposium, U.S. Department of Energy, Publication MERC/SP-77-5, p. 166-182.
Dennison, J.M, and Textoris, D.A., 1987, Paleowind and depositional tectonics interpreted from Tioga Ash Bed: Appalachian Basin Industrial Associates Program, vol. 12, p. 107-132.
Dennison, J.M, and Textoris, D.A., 1988, Devonian Tioga ash beds: The Nineteenth Annual Appalachian Petroleum Geology Symposium: Geology of Appalachian Basin Devonian Clastics: West Virginia Geological and Economic Survey, Circular. C-42, p. 15-16.
Dewey, J. F., 1969, Evolution of the Appalachian/ Caledonian orogen: Nature, v. 222, p. 124-129.
Doyon, M., and Valiquette, G., 1987, Devonian and Tertiary volcanism in the Lemieux Dome, central Gaspe, Quebec: Geological Association of Canada and Mineralogical Association of Canada Joint Annual Meeting, Program with Abstracts, v. 12, p. 38.
Emerson, N. R., Simo, J. A. T., Byers, C. W., and Fournelle, J. 2004, Correlation of (Ordovician, Mohawkian) K-bentonites in the upper Mississippi valley using apatite chemistry: implications for stratigraphic interpretation of the mixed carbonate-siliciclastic Decorah Formation: Palaeogeography, Palaeoclimatology, Palaeoecology, v. 210, p. 215-233.
Epstein, A. G., Epstein, J. B., and Harris, L. D., 1977, Conodont color alteration – An index to organic metamorphism, U. S. Geological Survey Professional Paper 995, 27 p.
Ettensohn, F.R., 1985, The Catskill Delta Complex and the Acadian Orogeny: A model: *in* Woodrow D.L., and Sevon, W.D., eds., The Catskill Delta, Geological Society of America Special Paper 201, p. 39-49.
Ettensohn, F.R., 2008, The Appalachian foreland basin in the eastern United States, in Miall, A., The Sedimentary basins of the United States and Canada: Sedimentary Basins of the World, Amsterdam, Elsevier, p. 105–179.
Eusden, J.D., Jr., Guzofski, C.A., Robinson, A.C., and Tucker, R.D., 2000, Timing of the Acadian orogeny in northern New Hampshire: The Journal of Geology, v. 108, p. 219–232.
Fenton, C.R, Teichmann, F., Cole, R.B., Ver Straeten, C.A., Basu, A.R. and G.C. Baird, 1995. Pumice fragments in Appalachian Basin bentonites: a petrographic and REE geochemical study. Geological Society of America, Abstracts with Program, v. 27, p. 43.
Fisher, RV and Schmincke, H.-U., 1991, Pyroclastic Rocks: New York, Springer-Verlag, 472 pp.

Fisk, M.F., Giovannoni, S.J., and Thorseth, I.H., 1998, Alteration of oceanic volcanic glass: Textural evidence of microbial activity: Science, v. 281, p. 978-980.
Folch, A., and Costa, A. 2010, FALL3D-6.2 – User Guide. http://193.206.115.76/download/fall3d/manual-fall3d-6.2.pdf.
Goldman, D., Mitchell, Bergström, S. M., Delano, J. W. and Tice, S., 1994, K-bentonites and graptolite biostratigraphy in the Middle Ordovician of New York State and Quebec: a new chronostratigraphic model, Palaios, vol. 9, p. 124-143.
Hanson, B., 1995, A geochemical study of rhyolitic melt inclusions in igneous phenocrysts from Lower Devonian bentonites [Ph.D. dissertation]: State University of New York - Albany, 470 p.
Hein, J. R., and Scholl, D. W., 1978. Diagenesis and distribution of late Cenozoic volcanic sediments in the southern Bering Sea. Geological Society of America Bulletin, v. 89, p. 197-210.
Huang, T.C., Watkins, N.D., Shaw, D.M., and Kennett, J.P., 1973, Atmospherically transported volcanic dust in South Pacific deep-sea sedimetnary cores at distances over 3,000 km from the eruptive source: Earth and Planetary Science Letters, v. 20, p. 119-124.
Huff, W. D., Bergstrom, S. M., and Kolata, D. R. 2010, Ordovician explosive volcanism: Geological Society of America, Special Paper no. 466, p. 13-28.
Huff, W.D., Muftuoglu, E., Kolata, D.R., and Bergstrom, S.M., 1999, K-bentonite bed preservation and its event stratigraphic significance: Acta Universitatis Carolinae – Geologica, v. 43, p. 491-493.
Jacobi, R. D. and Mitchell, C. E. 2002, Geodynamical interpretation of a major unconformity in the Taconic Foredeep: slide scar or onlap unconformity?: *in* Mitchell, C. E. and Jacobi, R., Taconic Convergence: Orogen, Foreland Basin and Craton: Physics and Chemistry of the Earth, vol. 27, p. 169-202.
Jeans, C.V., Wray, D.S., Merriman, R.J., Fisher, M.J., 2000, Volcanogenic clays in Jurassic and Cretaceous strata of England and the North Sea Basin: Clay Minerals, v. 35, p. 25-55.
Karabinos, P., and Aleinikoff, J. N. 2011, An Emsian age for the Goshen Formation in the Connecticut Valley-Gaspe Trough in Massachusetts: Geological Society of America, Abstracts with Programs, v. 43, p. 160-160.
Karabinos, P., Samson, S. D., Hepburn, J. C., and Stoll, H. M., 1998, Taconian Orogeny in the New England Appalachians; collision between Laurentia and the Shelburne Falls Arc: Geology, v. 26, p. 215-218.
Kataoka, K.S. 2005, Distal fluvio-lacustrine volcaniclastic resedimentation in response to an explosive silicic eruption: The Pliocene Mushono tephra bed, central Japan: Geological Society of America Bulletin, v. 117, p. 3-17.
Kataoka, K.S., Manville, V., Nakjo, T., and Urabe, A. 2009, Impacts of explosive volcanism on distal alluvial sedimentation: Examples from the Pliocene-Holocene volcaniclastic successions of Japan: Sedimentary Geology, v. 220, p. 306-317.
Kaufmann, B., 2006, Calibrating the Devonian time scale: A synthesis of U-Pb ID-TIMS ages and conodont stratigraphy: Earth-Science Reviews, v. 76, p. 175–190,
Kolata, D. R., Huff, W. D. and Bergström, S. M., 1996, Ordovician K-bentonites of eastern North America, Geological Society of America Special Paper 313, 84 p.
Koniger, S., and Stollhofen, H. 2001, Environmental and tectonic controls on preservation potential of distal fallout ashes in fluvio-lacustrine settings: the Carboniferous-Permian Saar – Nahe Basin, southwest Germany, *in* White, J.D.L., and Riggs, N.R., Volcaniclastic Sedimentation in Lacustrine Settings, Special Publication No. 30, International Association of Sedimentologists, p. 263-284.
Lehmann, D.M., Brett, C.E., Cole, R. and G.C. Baird, 1995. Distal sedimentation in a peripheral foreland basin: Ordovician black shales and associated flysch of the western Taconic Foreland, New York State and Ontario: Geological Society of America Bulletin, v. 107, p. 708-724.
Ludman, A., and Idleman, B., 1998, The Berry Brook gabbro; NW-most Siluro-Devonian mafic magmatism in the Coastal lithotectonic belt, Maine: Geological Society of America Abstracts with Programs, v. 30, no. 1, p. 58.
Manville, V., and Wilson, C.J.N., 2004, Vertical density currents: a review of their potential role in the deposition and interpretation of deep-sea ash layers: Journal of the Geological Society**,** v. 161, p. 947-958.
Marshall, R.R., 1961, Devitrification of natural glass: Geological Society of America Bulletin, v. 72, pp. 1493-1520.
A7- Mastin, L., Guffanti, M., Servranckx, R., Webley, P., Barsotti, S., Dean, K., Durant, A., Ewert, J., Neri, A., Rose, W., Schneider, D., Siebert, L., Stunder, B., Swanson, G., Tupper, A., Volentik, A., Waythomas, C. 2009, A multidisciplinary effort to assign realistic source parameters to models of volcanic ash-cloud transport and dispersion during eruptions: Journal of Volcanology and Geothermal Research, v. 186, p. 10-21.

McWilliams, C. K., Walsh, G. J., and Wintsch, R. P. 2010, Silurian-Devonian age and tectonic setting of the Connecticut Valley-Gaspe Trough in Vermont based on U-Pb SHRIMP analyses of detrital zircons: American Journal of Science, v. 310, p. 325-363.

Mitchell, C. E., Goldman, D., Delano, J. W., Samson, S. D. and Bergström, S. M., 1994, Temporal and spatial distribution of biozones and facies relative to geochemically correlated K-bentonites in the Middle Ordovician Taconic foredeep, Geology, vol. 22, p. 715-718.

Mullineaux, D.R., 1996, Pre-1980 tephra-fall deposits erupted from Mount St. Helens, Washington: USGS Professional Paper 1563, http://vulcan.wr.usgs.gov/Volcanoes/MSH/Publications/PP1563/framework.html.

Nakayama, K. and Yoshikawa, S., Depositional processes of primary to reworked volcaniclastic on an alluvial plain: An example from the Lower Pliocene Ohta tephra bed of the Tokai Group, central Japan: Sedimentary Geology, v. 107, p. 211-229.

Ogg, J.G., Ogg, G., and Gradstein, F.M., 2008, The Concise Geologic Time Scale: Cambridge, Cambridge University Press, 184 p.

Over, D.J. 2002, The Frasnian-Famennian Boundary in the Appalachian Basin, Michigan Basin, Illinois Basin, and southern continental margin, central and eastern United States: Palaeogeography, Palaeoclimatology, Palaeoecology, 181, p. 153-170.

Over, D.J. 2007, Conodont biostratigraphy of the Chattanooga Shale, Middle and Upper Devonian, southern Appalachian Basin, eastern United States: Journal of Paleontology, v. 81, p. 1194–1217.

Over, D.J., and Rhodes, M.K. 2000, Conodonts from the Upper Olentangy Shale (Upper Devonian, central Ohio) and stratigraphy across the Frasnian-Famennian boundary: Journal of Paleontology, v. 74, p. 101– 112.

Over, D.J., Reynolds, S.A., Rhodes, M.K., and Wichtowski, J.L., 1998, Conodonts, ash horizons, Kellwasser Intervals, high-energy events, and the Frasnian-Famennian boundary in the deep shelf and basin facies of the Appalachian Basin: Geological Society of America Abstracts with Programs, v. 30, no. 2, p. 66.

Perry, E. and Hower, J., 1970, Burial diagenesis in gulf coast pelitic sediments: Clay and Clay minerals, v. 18, p. 165-177.

Poole, W.H., and Rodgers, J., 1972, Appalachian geotectonic elements of the Atlantic provinces and southern Quebec, *in* Glass, D.J., 24th International Geological Congress, Guidebook to Excursion A-63-C63, Montreal 200 p.

Puspoki, Z., Kozak, M., Kovacs-Palffy, P., Foldvari, M., McIntosh, R., and Vincze, L. 2005, Eustatic and tectonic/volcanic control in sedimentary bentonite formation—a case study of Miocene bentonite deposits from the Pannonian Basin: Clays and Clay Minerals, v. 53, p. 71–91.

Puspoki, Z., Kozak, M., Kovacs-Palffy, P., Szepesi, J., McIntosh, R., Konya, P., Vincze, L., and Gyula, G. 2008, Geochemical records of a bentonitic acid-tuff succession related to a transgressive systems tract—indication of changes in the volcanic sedimentation rate: Clays and Clay Minerals, v. 56, p. 24–38.

Quinlan, G. M. and Beaumont, C., 1984, Appalachian thrusting, lithospheric flexure and Paleozoic stratigraphy of the eastern interior of North America, Canadian Journal of Earth Sciences, vol. 21, p. 973-996.

Rankin, D.W., 1968, Volcanism related to tectonism in the Piscataquis Volcanic Belt, an island arc of Early Devonian age in north-central Maine, *in* Zen, E., White, W.S., Hadley, J.B., and Thompson, J.B., Jr., Studies of Appalachian Geology: Northern and Maritime: New York, John Wiley and Sons, Interscience Publishers, p. 355-370.

Rankin, D. W., and Hon, R. 1987, Traveler Rhyolite and overlying Trout Valley Formation and the Katahdin Pluton: a record of basin sedimentation and Acadian magmatism, north-central Maine, *in* Roy, D. C., Centennial field guide, Northeastern Section: Geological Society of America, v. 5, p. 293–301.

Rankin, D. W., and Tucker, R. D. 1995. U-Pb age of the Katahdin-Traveler igneous suite, Maine, local age of the Acadian Orogeny, and thickness of Taconian crust: Geological Society of America, Abstracts with Program, v. 27, p. A-225.

Rankin, D. W., and Tucker, R. D. 2009, Bronson Hill and Connecticut Valley sequences in the Stone Mountain area, Northeast Kingdom, Vermont: Annual Meeting - New England Intercollegiate Geological Conference, v. 101, p. 187-198.

Rast, N., and Skehan, J. W., 1993, Mid-Paleozoic orogenesis in the North Atlantic; the Acadian orogeny: Geological Society of America, Special Paper no. 275, p. 1-25.

Riedel, J. L., Pringle, P. T., and Schuster, R. L. 2001, Deposition of Mount Mazama tephra in a landslide dammed lake on the upper Skagit River, Washington, USA, *in* White, J. D. L., and Riggs, N. R., Volcaniclastic Sedimentation in Lacustrine Settings: International Association of Sedimentologists, Special Publication 30, p. 285–298.

Rickard, L.V., 1962, Late Cayugan (Upper Silurian) and Helderbergian (Lower Devonian) stratigraphy in New York: New York State Museum, Bulletin No. 386, 157 p.
Riggs, N.R., Hurlbert, J.C., Schroeder, T.J., and Ward, S.A., 1997, The interaction of volcanism and sedimentation in the proximal areas of a mid-Teriary volcanic dome field, central Arizona, U.S.A.: Journal of Sedimentary Research, v. 67, p. 142-153.
Robinson, P., and Tucker, R., 1996, The "Acadian" in central New England: New problems based on U-Pb ages of igneous zircon and metamorphic monazite and sphene: Geological Society of America, Abstracts with Programs, v. 28, no. 3, p. 94.
Robinson, P., Tucker, R. D., Gromet, L. P., Ashendon, D. D., Williams, M. L., Reed, R. C., and Peterson, V. L., 1992, The Pelham Dome, central Massachusetts; stratigraphy, geochronology, and Acadian and Pennsylvanian structure and metamorphism: Contribution - Geology Department, University of Massachusetts, v. 66, Vol. 1, p. 132-169.
Roden, M.K., Parrish, R.R., and Miller, D.S., 1990, The absolute age of the Eifelian Tioga Ash Bed, Pennsylvania: Journal of Geology, vol. 98, p. 282-285.
Rodgers, J., 1970, The tectonics of the Appalachians, New York, NY, United States, Wiley-Interscience, 271 p.
Rose,W.I., and Durant, A.J. 2011, Fate of volcanic ash: Aggregation and fallout: Geology, v. 39, p. 895-896.
Rowley, D. B., and Kidd, W. S. F., 1981, Stratigraphic relationships and detrital composition of the Medial Ordovician flysch of western New England: Implications for the tectonic evolution of the Taconic orogeny: Journal of Geology, v. 89, p. 199-218.
Samson, S.D., 1996, $^{40}Ar/^{39}Ar$ and Nd-Sr isotopic characteristics of mid-Ordovician North American K-Bentonites: A test of early Paleozoic Laurentia-Gondwana interactions: Tectonics, v. 15, p. 1084-1092.
Samson, S.D., Kyle, P.R., and Alexander Jr., E.C., 1988, Correlation of North American Ordovician bentonites by using apatite chemistry: Geology, v. 16, p. 444-447.
Samson, S.D., Matthews, S., Mitchell, C.E., and Goldman, D., 1995, Tephrochronology of highly altered ash beds: The use of trace element and strontium isotope geochemistry of apatite phenocrysts to correlate K-bentonites: Geochimica et Cosmochimica Acta, v. 59, no. 12, p. 2527-2536.
Samson, S.D., Patchett, P.J., Roddick, J.C., and Parrish, R.R., 1989, Origin and tectonic setting of Ordovician bentonites in North America: Isotopic and age constraints: Geological Society of America Bulletin, v. 101, p. 1175-1181.
Scasso, R.A. 2001, High-frequency explosive volcanic eruptions in a Late Jurassic volcanic arc: The Ameghino Formation, Antarctic Peninsula: Journal of Sedimentary Research, v. 71, p. 101-106.
Schminke, H.-U., 2004, Volcanism: Berlin, Springer-Verlag, 324 p.
Sell, B.K. and Samson, S.D. 2011a, Apatite phenocryst compositions demonstrate a miscorrelation between the Millbrig and Kinnekulle K-bentonites of North America and Scandinavia: Geology, v. 39, p. 303–306.
Sell, B.K and Samson, S.D. 2011b, A tephrochronologic method based on apatite trace-element chemistry: Quaternary Research, v. 76, p. 157-166.
Sevigny, J. H., and Hanson, G. N., 1995, Late-Taconian and pre-Acadian history of the New England Appalachians of southwestern Connecticut: Geological Society of America Bulletin, v. 107, p. 487-498.
Shaw, G.J., Chen, Y-A., and Scott, J., 1991, Multiple K-bentonite layers in the Lower Devonian Kalkberg Formation - Cobleskill, N.Y.: Geological Society of America, Abstracts With Program, v. 23, no. 1, p. A-126.
Smith, R.C., and Way, J.H., 1983, The Tioga ash beds at Selinsgrove Junction: *in* Silurian Depositional History And Alleghenian Deformation In The Pennsylvania Valley And Ridge, 48th Annual Field Conference of Pennsylvania Geologists, p. 74-88.
Smith, R.C., II, Berkheiser, S.W., Jr., and Way, J.H., 1988, The Bald Hill Bentonite beds: A Lower Devonian pyroclastic-bearing unit in the northern Appalachians: Northeastern Geology, vol. 10, p. 216-230.
Smith, R.C., II, Berkheiser, S.W., Jr., and Way, J.H. 2003, Bald Hill Bentonites A, B, and C – history and data since 1988, *in* Way, J.H., and others, Geology On The Edge: Selected Geology of Bedford, Blair, Cambria, and Somerset Counties: Guidebook, 68th Annual Field Conference of Pennsylvania Geologists, p. 73-77.
Solar, G.S., Pressley, R., Brown, M., and Tucker, R.D., 1998, Granite ascent in convergent orogenic belts; testing a model: Geology, v. 26, p. 711–714.
Sparks, R. S. J., Brazier, S., Huang, T. C., and Muerdter, D, 1983, Sedimentology of the Minoan deep-sea tephra layer in the Aegean and eastern Mediterranean: Maritime Geology v. 54, p. 131–167.
Stanley, R. S., and Ratcliffe, N. M., 1985, Tectonic synthesis of the Taconian orogeny in western New England: Geological Society of America Bulletin, v. 96, p. 1227-1250.
Thomas, W. A., and Astini, R. A. 2003, Ordovician accretion of the Argentine Precordillera terrane to Gondwana; a review: Journal of South American Earth Sciences, v. 16, p. 67-79.

Thompson, C. K., Kah, L. C., Astini, R., Bowring, S. A., and Buchwaldt, R. 2012, Bentonite geochronology, marine geochemistry, and the Great Ordovician Biodiversification Event (GOBE): Palaeogeography, Palaeoclimatology, Palaeoecology, v. 321-322, p. 88-101.

Tucker, R.D., Bradley, D.C., Ver Straeten, C.A., Harris, A.G., Ebert, J.R., and McCutcheon, S.R., 1998, New U-Pb ages and the duration and division of Devonian time: Earth and Planetary Science Letters, v. 158, p. 175-186.

Tucker, R. D., and McKerrow, W. S., 1995, Early Paleozoic chronology; a review in light of new U-Pb zircon ages from Newfoundland and Britain, *in* Brandon, A.D., and Goles, G.G., A special issue in memory of Richard St John Lambert, Canadian Journal of Earth Sciences, v. 32, p. 368-379.

Tucker, R.D., Osberg, P.H., and Berry, H.N., III 2001, The geology of a part of Acadia and the nature of the Acadian orogeny across central and eastern Maine: American Journal of Science, v. 301, p. 205–260.

Tucker, R.D., and Robinson, P., 1990, Age and setting of the Bronson Hill magmatic arc; a re-evaluation based on U-Pb zircon ages in southern New England: Geological Society of America Bulletin, v. 102, p. 1404–1419.

van Staal, C.R. 2007, Pre-Carboniferous tectonic evolution and metallogeny of the Canadian Appalachians, *in* Goodfellow, W.D., ed., Mineral Resources of Canada: A Synthesis of Major Deposit Types, District Metallogeny, the Evolution of Geological Provinces, and Exploration Methods: Ottawa, Geological Association of Canada, Mineral Deposits Division, Special Publication 5, p. 793–818.

van Staal, C. R., Dewey, J. F., Mac, N. C., and McKerrow, W. S., 1998, The Cambrian-Silurian tectonic evolution of the Northern Appalachians and British Caledonides; history of a complex, west and southwest Pacific-type segment of Iapetus, *in* Blundell, D.J. and Scott, A.C., Lyell; the past is the key to the present,: London, United Kingdom, Geological Society of London, Special Publication no. 143, p. 199-242.

van Staal, C. R., Whalen, J. B., McNicoll, V. J., Pehrsson, S., Lissenberg, C. J., Zagorevski, A., van Breemen, O., and Jenner, G. A. 2007, The Notre Dame Arc and the Taconic Orogeny in Newfoundland, in Prodehl, C., and Mooney, W.D., Exploring the Earth's Crust—History and Results of Controlled-Source Seismology: Geological Society of America, Memoir no. 200, p. 511-552.

van Staal, C.R., Whalen, J.B., Valverde-Vaquero, P., Zagorevski, A., and Rogers , N. 2009, Pre-Carboniferous, episodic accretion-related, orogenesis along the Laurentian margin of the northern Appalachians, *in* Murphy , J.B., Keppie, J.D., and Hynes, A.J., Ancient Orogens and Modern Analogues: Geological Society of London Special Publication 327, p. 271–316.

Ver Straeten, C.A., 1996, Stratigraphic synthesis and tectonic and sequence stratigraphic framework, upper Lower and Middle Devonian, Northern and Central Appalachian Basin: Unpublished Ph.D. thesis, University of Rochester, 800 p.

Ver Straeten, C.A. 2004a, K-bentonites, volcanic ash preservation, and implications for Lower to Middle Devonian volcanism in the Acadian Orogen, eastern North America: Geological Society of America Bulletin, v. 116, p. 474–489.

Ver Straeten, C.A. 2004b, Sprout Brook K-bentonites: new interval of Devonian (Early Emsian?) K-bentonites in eastern North America: Northeastern Geology and Environmental Sciences, v. 26, p. 298–305.

Ver Straeten, C.A. 2007a, The Fate of Airfall Volcanic Ash in Large and Small Lacustrine Systems: Ash Stratinomy of the Eocene Green River and Florissant Formations: Geological Society of America Abstracts with Programs, Vol. 39, p. .

Ver Straeten, C.A. 2007b, Basinwide stratigraphic synthesis and sequence stratigraphy, Upper Pragian, Emsian and Eifelian Stages (Lower to Middle Devonian), Appalachian Basin, *in* Becker, R. T., and Kirchgasser, W. T., Devonian events and correlations: Geological Society of London, Special Publication 278, p. 39–81.

Ver Straeten, C.A. 2008, Volcanic ash bed formation and condensation processes: A review and examination from Devonian stratigraphic sequences: The Journal of Geology, v. 116, p. 545–557.

Ver Straeten, C. A. 2009. Devonian T-R cycle IB: the 'Lumping' of Emsian Sea Level History: Palaeontographica Americana, v. 63, p. 33-48.

Ver Straeten, C.A. 2010, Lessons from the foreland basin: Northern Appalachian basin perspectives on the Acadian orogeny, *in* Tollo, R.P., Bartholomew, M.J., Hibbard, J.P., and Karabinos, P.M., From Rodinia to Pangea: The Lithotectonic Record of the Appalachian Region: Geological Society of America Memoir 206, p. 251–282.

Ver Straeten, C.A., and Brett, C.A., 1995, Lower and Middle Devonian foreland basin fill in the Catskill Front: Stratigraphic synthesis, sequence stratigraphy, and the Acadian Orogeny: *in* Garver,

J.I., and Smith J.A., eds., New York State Geological Association, 67th Annual Meeting Guidebook, p. 313-356.
Ver Straeten, C.A., Griffing, D.H., and Brett, C.E., 1994, The lower part of the Middle Devonian Marcellus "Shale," central to western New York State: Stratigraphy and depositional History: *in* Brett, C.E., and Scatterday J., eds., New York State Geological Association, 66th Annual Meeting Guidebook, p. 270-321 (includes field trip log).
Ver Straeten, C. A., Ebert, J. R., Bartholomew, A., Benedict, L. J., Matteson, D. K., and Shaw, G. H. 2005, Devonian stratigraphy and K-bentonites in the Cherry Valley–Schoharie Valley region, *in* Rodbell, D. T., ed. Field trip guidebook, Northeast Section meeting. Geological Society of America, p. D1–D57.
Ver Straeten, C.A., Over, D.J., and Baird, G.C. 2007, Devonian K-bentonites and tuffs: A record of Caledonian magmatism from the Appalachian foreland basin (eastern U.S.): Geological Society of America, Abstracts with Programs, v. 39, no. 1, p. 53.
Way, J.H., Smith, R.C., and Roden, M., 1986, Detailed correlations across 175 miles of the Valley and Ridge of Pennsylvania using 7 ash beds in the Tioga Zone; *in* Sevon, W.D., Selected Geology of Bedford And Huntington Counties: 51st Annual Field Conference Of Pennsylvania. Geologists, Huntington, Pa., p. 55-72.
Wiesner, M.G., Wang, Y., and Zheng, L., 1995, Fallout of volcanic ash to the deep South China Sea induced by the 1991 eruption of Mount Pinatubo (Philippines): Geology, v. 23, p. 885-888.
Wilcott, M.J., and Over, D.J., 2005, Comparison of two Devonian ashes: Kashong-Windom boundary and lower Rhinestreet Shale, western New York State: Geological Society of America, Abstracts with Programs, v. 37, no. 1, p. 73.
Williams, E. A., Friend, P. F., and Williams, B. P. J., 2000, A review of Devonian time scales: databases, construction and new data, in Friend, P. F., and Williams, B. P. J., New Perspectives on the Old Red Sandstone: London, Geological Society, Special Publications, v. 180, p. 1-21.
Wilson, R.A. 2004, Geology of the Campbellton area, northern New Brunswick: Atlantic Geoscience Society, Colloquium & Annual General Meeting: Moncton, New Brunswick, Atlantic Geoscience Society, Abstracts volume, p. 31.
Zagorevski, A., van Staal, C. R., McNicoll, V. J., and Rogers, N. 2007, Upper Cambrian to Upper Ordovician peri-Gondwanan island arc activity in the Victoria lake Supergroup, central Newfoundland; Tectonic development of the northern Ganderian margin: American Journal of Science, v. 307, p. 339-370.
Zambito, J.J. IV, & Baird, G.C. 2006, Timing of compression and hydrothermal movement in the Mohawk Valley region of eastern New York, determined by slickenside surfaces in K-bentonites: American Association of Petroleum Geologists, Eastern Section Meeting, Buffalo, New York, p. 33.
Zambito, J.J.IV, Baird, G.C., & Blood, D.R. 2005, Slickenside surfaces within K-Bentonite beds: A potentially sensitive tool for assessing the timing of far-field tectonic compression, volcanic ash illitization, and diagenetic ash cementation: Geological Society of America, Abstracts with Program, v. 37, p. 210.

FIELD TRIP ROAD LOG

Begin trip at intersection of U.S. Rte. 20 and Otsego Co. Rte. 80 (42.837851°, -74.869873°), approximately 5.5 miles east of Richfield Springs, Otsego Co., NY.

Miles from last point	Cumulative mileage	Route description
0.0	0.0	If traveling from the west, turn left (north) onto Otsego Co. Rte. 80, and proceed ahead
1.5	1.7	Summit Lake to right
1.1	8.1	Enter Starkville
1.5	9.6	Otsego-Montgomery county line
0.9	10.5	Upper strata of Ordovician Utica Fm. on left.
1.1	12.1	Enter Hallsville

0.3	12.4	Brookman Corners; Przewtrzelski family, owners of Stop 1 (Pretzel Farm) at 121 Brookman Road
0.1	12.5-.7	Utica Shale on left, and both sides ahead.
0.2	13.0	Pullover for Stop 1 on right, before bridge

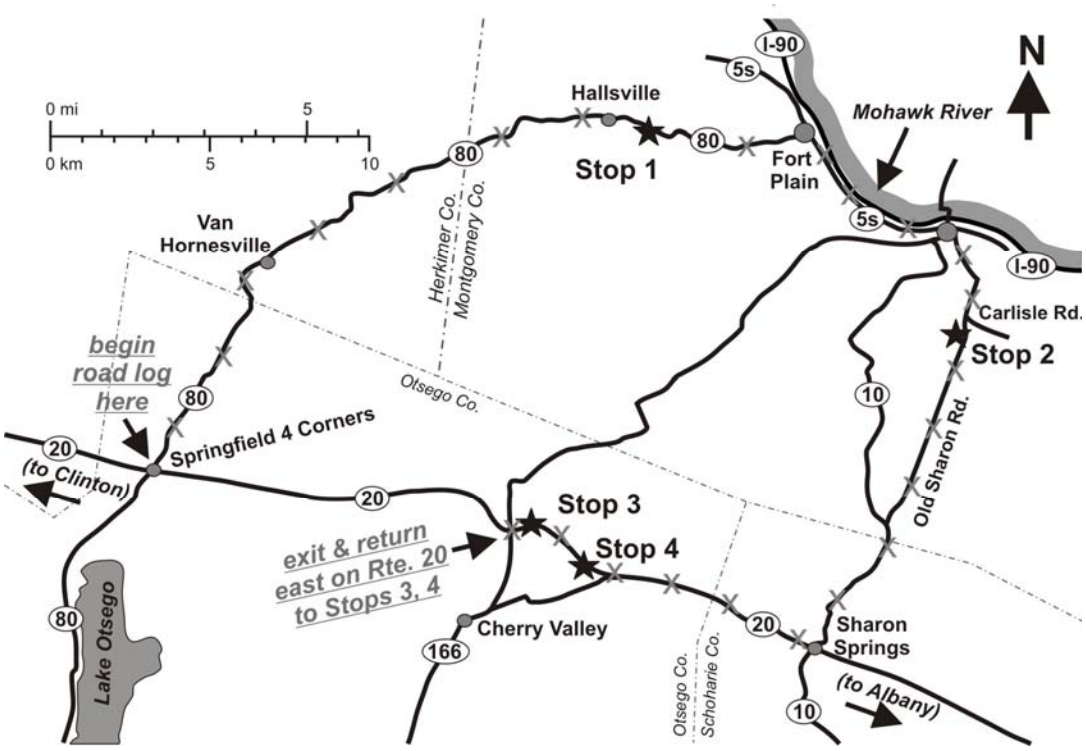

Figure 12. Map of fieldtrip route and stops. Trip begins ca. 40 miles from the Hamilton College campus.

Stop #1. Airfall volcanic tephras in Upper Ordovician Utica Shale, at Pretzel Farm, Hallsville (42.935179°, -74.692454°)

An expanse of gently westward-dipping, Upper Ordovician, black Utica Shale floors Otsquago Creek at Stop 1 (See Figure 5). This exposure displays a portion of the lower part of the Indian Castle Member that is exceptional for the abundance of classic Utica fossils such as exuviae and carcasses of the trilobite *Triarthrus*, as well as abundant orthoconic cephalopods and graptolites belonging to the *Climacograptus spiniferus* biozone (see Goldman et al. 1994; Figure 5). Several important tephra beds are present in this outcrop; these will be examined in ascending order from the downstream (east) end of this section. We will examine a thin, calcareous tephra bed near the base of this section that contains abundant volcanogenic phenocrysts and sand-size pumice clasts preserved in partial 3-D relief along the base of the layer. A higher, partially cemented tephra bed will also be a focus of examination and questions (See Figures 5, 6c,d).

---	13.0	Leave parking area, continue east on Otsego Co. Rte. 80
1.0	14.0	Contact of Ordovician-age Indian Castle Member (Utica Formation) and Dolgeville Formation in creek near red footbridge on right.

0.9	14.9	Road on right to type section of Valley Brook Shale Member, Flat Creek Formation, below Dolgeville Formation
0.2	15.9	Enter village of Fort Plain
0.6	16.8	Turn right onto NY Rte. 5S, toward Canajoharie
2.7	19.5	Enter Canajoharie
0.5	20.0	Fork to right, continue on Rte. 5S
0.2	20.2	Proceed through intersection with Rte. 10
0.1	20.3	Left onto Montgomery Street, then quick jog to left and right, onto Moyer Street (toward Wintergreen Park). Proceed uphill.
0.4	20.7	Floral Avenue on right; access to lower Canajoharie Gorge. Beekmantown Group carbonates, with large potholes, are succeeded upstream by Black River and Trenton Group carbonates.
0.4	21.1	Right onto Carlisle Road. Note flattening of road uphill, marking bedrock shift from carbonates to shales.
0.8	21.9	At fork, continue straight ahead onto Old Sharon Road.
0.1	22.0	Turn right into Wintergreen Park
0.2	22.2	Descend into valley. At stop sign, proceed ahead, then descend steep, narrow road with sharp bends.
0.2	22.4	Stop and park to right at base of slope. Follow trail to Canajoharie Creek at north end of parking area.

Stop #2. Airfall volcanic tephras in Upper Ordovician Flat Creek Shale, at Wintergreen Park, Canajoharie (at and downstream of 42.886244°, -74.564323°)

This section lies in the upper part of the gorge of Canajoharie Creek, upstream from the village of Canajoharie (see Figure 4). This is a classic Utica Shale section that exposes the entire Flat Creek Shale Member succession as well as higher strata of the Dolgeville Formation, which are visible high in the gorge face across from our entrance point. Vertical joint sets in the hard, calcareous shale are spectacularly displayed in the bank walls and creek floor along our route.

We will focus on a tephra-rich interval downstream from our point of ingress (Figure 4). Strata examined here contain graptolites belonging to the *Orthograptus americanus* biozone (Goldman et al. 1994). We will first examine several tephras exposed a short distance downstream from the path entrance that can be easily identified from the rusty stain of sulfides weathered from these layers (Figures 4, 6). Most notable among these beds is a coarse tephra layer, informally designated the "sand band" (Baird et al. 1994), that may record an episode of submarine erosion or sedimentary condensation (Figure 6a,b). This bed underlies an interval of calcareous shale and impure limestone layers containing numerous fossils, including the distinctive hemispherical bryozoan *Prasopora* and the large trilobite *Isotelus.*

Proceeding downstream, the creek canyon makes two scenic bends. On a high, east-facing wall, a cluster of orange-weathering tephra bands is conspicuously displayed. We will proceed to a minimally-weathered part of this face to look at the apparent record of countless thin laminae that record possible, "average" or "small-scale" volcanogenic events that constitute Ordovician background volcanic activity.

Return to cars, and continue south through parking area.

---	22.4	Leave parking area, proceed ahead through parking area
0.1	22.5	Left turn onto exit road, proceed uphill
0.3	22.8	Exit Wintergreen Park. Turn right and proceed south again on Old Sharon Road.
3.9	26.7	Make a very short jog to left and right at Latimer Hill Road, and continue south on Old Sharon Road
0.8	27.5	Left onto NY Rte. 10, and continue south
0.3	27.8	Enter Schoharie County
1.5	29.3	Enter village of Sharon Springs, and old spa resort town based on spring waters that surface here.
0.2	30.5	Junction with U.S. Rte. 20. Turn right/west and proceed.
0.5	32.7	Enter Otsego County
2.4	35.1	Classic Lower and Middle Devonian outcrops along Rte. 20 near Cherry Valley for next 0.6 miles. Strata include (east to west, and stratigraphically high to low) the Oatka Creek and Union Springs (="Marcellus subgroup"), Onondaga, Schoharie, Esopus, Oriskany and Kalkberg formations.
0.5	36.6	Bridge above highway
0.2	36.8	Fork right and take exit ramp for Cherry Valley/NY Rte. 166
0.1	36.9	Turn left onto Rte. 166.
0.4	37.3	Turn right onto entrance ramp for Rte. 20 east
0.2	37.5	Outcrops of Kalkberg Formation begin on right
0.1	37.6	Pull over to right and park near railroad overpass

Stop #3. Lower to Middle Devonian airfall tephra beds, U.S. Rte. 20 cuts, near Cherry Valley, NY. (between ca. 42.821797°, -74.731025° to ca. 42.822202°, -74.723747°)

Roadcuts on the south side of Rte. 20 east of Rte. 166 expose a long, nearly continuous section of the Lower Devonian Kalkberg, Oriskany, Esopus and Schoharie formations, and the Middle Devonian Onondaga Formation. Additional outcrops to the east expose the Union Springs and Oatka Creek formations (Marcellus subgroup of Ver Straeten 2007b). See Figure 13 for more details.

The Lower Devonian Kalkberg Formation, lowest in this section, features up to 15 thin volcanic airfall tuffs assigned to the Bald Hill K-bentonites (Smith et al. 1988; Shaw et al. 1991).. Rickard (1962) reported the first tephra in this interval, visible just east of the overpass as a prominent crevice, filled with light gray to tan, soapy-feeling, sticky clay about one to two meters above ground level (Figure 9a,b). Additional K-bentonitic tephras occur in the Kalkberg Formation here.

The Bald Hill Tephra Cluster is reported from New York to Virginia and West Virginia Rickard's original bed from Cherry Valley was dated by Tucker et al. (1998) at 417.6±1.0 Ma ($^{207}Pb/^{206}Pb$, zircons). Silicic volcanic and plutonic rocks with overlapping age dates and biostratigraphy are found in Maine and maritime Canada Up the road, lower strata of the Esopus Formation here consist of 4.4 m of interbedded cherts, K-bentonites, shales and minor thin sandstones (Spawn Hollow Member). Fifteen <1 to 14 cm-thick clay to claystone layers with zircons, apatites, and other phenocrysts indicative of a volcanogenic origin

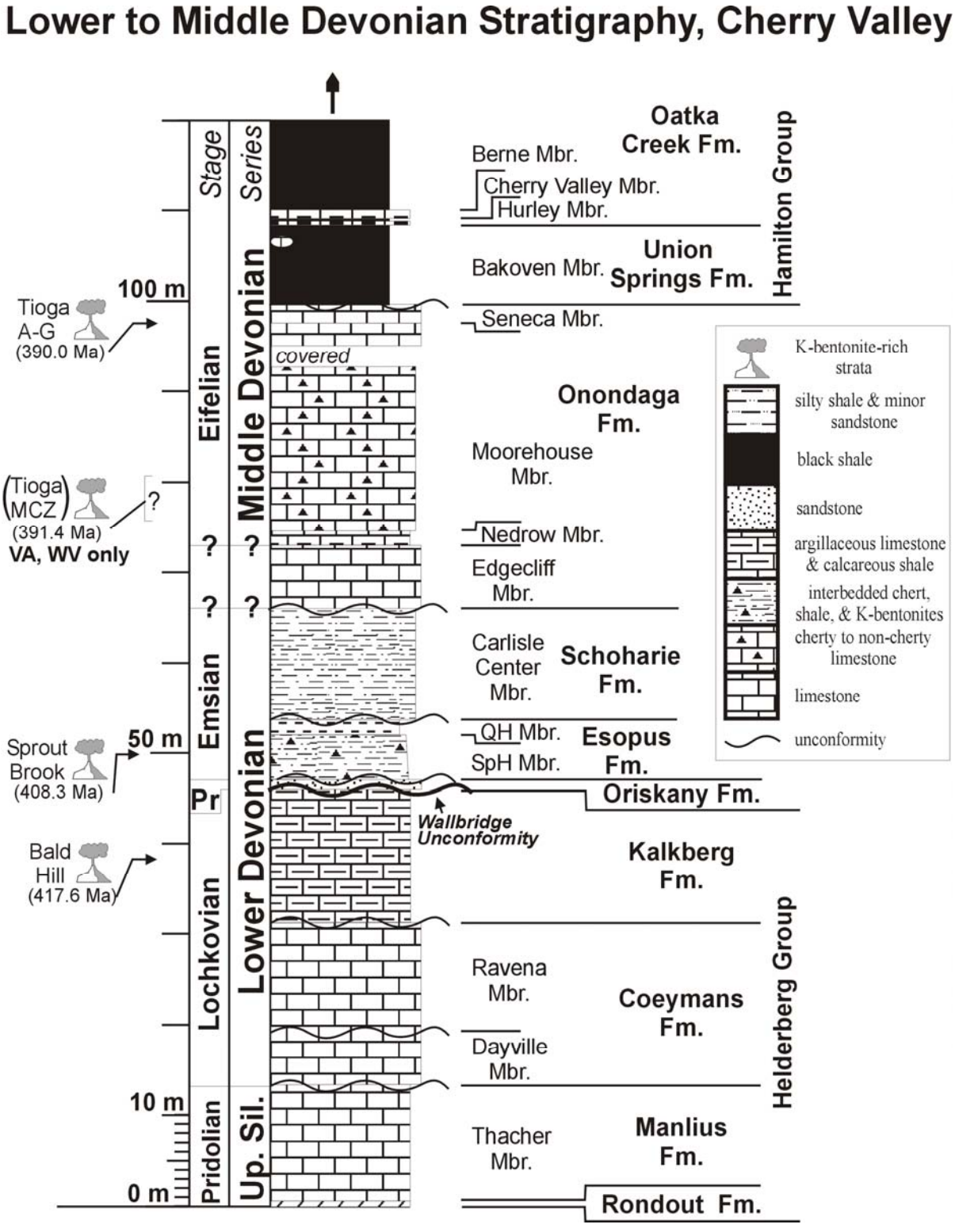

Figure 13. Upper Silurian to Middle Devonian stratigraphy near Cherry Valley, New York (Stops 3 and 4). Stop 3 examines strata of the Kalkberg through mid Onondaga formations. Stop 4 examines the topmost Onondaga Formation. Tioga Middle Coarse Zone tephra cluster is apparently found only in the southern part of the Appalachian Basin, in part of the Virginia-West Virginia outcrop belt. Abbreviations: Pr = Pragian; QH Mbr. = Quarry Hill Mbr., Esopus Fm.; SpH Mbr. = Spawn Hollow Mbr., Esopus Fm.; Up.Sil. = Upper Silurian.

(Sprout Brook K-bentonites) occur within the lower 3.6 m of the outcrop (Ver Straeten 2004b; Figure 9c). The site, now largely covered, is the type section of the Sprout Brook K-bentonites. Tephras of the Sprout Brook cluster are known only from eastern New York (Figure 9c-f). Two Sprout Brook beds from Cherry Valley were dated by Tucker et al. (1998) at 408.3±1.9 Ma ($^{207}Pb/^{206}Pb$). A number of silicic plutonic and volcanic rocks with dates that overlap that of the Sprout Brook K-bentonites are found in the northern Appalachians (e.g., the co-magmatic Katahdin Granite and Traveler Rhyolite, north-central Maine; Ver Straeten 2010; Figure 11).

Hanson (1995) reported a thin, discontinuous K-bentonite at the erosional base of the overlying sand-rich Schoharie Formation here (Carlisle Center Member). Another glauconite- and phosphate-rich clay bed marks the base of the Onondaga Limestone at Cherry Valley (Figure 10c). Best seen when dug out on the north side of Rte. 20 west of Rte. 166, the bed features a mix of detrital, authigenic, and volcanic grains (Ver Straeten 2004a).

Additional clay-dominated tephra beds occur through the lower three members of the Onondaga and equivalent units around the Appalachian basin. Most of these are difficult to find in relative shallower water facies in eastern New York, including at Cherry Valley.

Return to cars and proceed ahead (east) on Rte. 20

---	37.6	Pull onto Rte. 20 and proceed ahead
1.1	38.7	Elongate outcrop of Seneca Member on right. Black shales of Bakoven Member (Union Springs Formation, Marcellus subgroup) in covered slope above, capped at break in slope by Hurley and Cherry Valley members of the overlying Oatka Creek Formation (Marcellus subgroup).
0.4	39.1	Pull over to right and park at outcrop of Seneca Member limestone. Moorehouse Member visible in low ledges on north side of Rte. 20.

Stop #4. Airfall tephra beds of the Middle Devonian Tioga A-G cluster, U.S. Rte. 20 cut near Cherry Valley, NY.

Upper limestones of the Onondaga Formation (Figure 13) are found in this and nearby roadcuts. Topmost Moorehouse Member strata are visible on the north side of Rte 20. Two meters of the overlying Seneca Member represent the full thickness of the member locally.

The Tioga B Tephra, at the base of the Seneca Member, occurs in a deep reentrant near the base of this outcrop (Figure 10a,b). The Tioga B (anomalously thin at 12 cm here) is correlatable throughout most of the Appalachian Basin, except near Albany, and in central Ohio (Ver Straeten 2004a, 2007b).

A second thin K-bentonite, found in a crevice 0.73 m above the Tioga B is also found widely around the Appalachian Basin. A third K-bentonite was dug out 2.0 m above base of the Tioga B, at the Onondaga-Union Springs (Marcellus) contact 0.3 miles east of Stop 4.

The Tioga A-G K-bentonites occur throughout the Appalachian Basin; one of the beds has been reported from as far west as Illinois (Collinson 1968). The Middle Devonian Tioga-B K-bentonite was dated by Roden et al. (1990) at 390.0+0.5 Ma.

Kimberlitic rocks of New York State: The Dewitt "kimberlite"

David G. Bailey,
Hamilton College, Clinton, NY 13323
dbailey@hamilton.edu

Marian V. Lupulescu
New York State Museum, Albany, NY 12230
mlupules@mail.nysed.gov

INTRODUCTION

One of the very first scientific descriptions of a kimberlite was published in 1839 by Lardner Vanuxem in his third annual report on the geology of central New York State (Vanuxem 1839). The locality and samples he described were from the city of Syracuse, and were provided by the Principal of the Syracuse Academy, Oren Root (Williams 1887a, b). These early samples all came from a cluster of complexly related small intrusions in the northern portion of the city (Figure 1). Vanuxem (1842) described these rocks as part of "a great mass" of "well characterized serpentine" containing "particles of a yellow or golden color" (phlogopite) and "others of the red color of blood-stone" (pyrope). These intrusions received moderate scientific interest over the next thirty years as geologists struggled to understand the presence of these unusual rocks in the middle of the flat-lying Paleozoic sedimentary sequence of upstate New York (Dana 1878; Geddes 1860; Hunt 1858). Following the breakthrough work of Lewis (1887), who was the first to recognize that serpentinized, mica-bearing peridotites were the source rocks of gem diamonds in South Africa, the interest in the kimberlitic rocks of central NY increased dramatically. Over the next twenty years, numerous scientific reports (Clark 1908; Clarke 1899; Darton and Kemp 1895; Kraus 1904; Schneider 1902, 1903; Williams 1887b) and stories in local newspapers ("Gems here at home" 1906; "Syracuse has diamond hunt" 1905; "Would advance cash to probe stratums" 1902) were published on the Syracuse kimberlites.

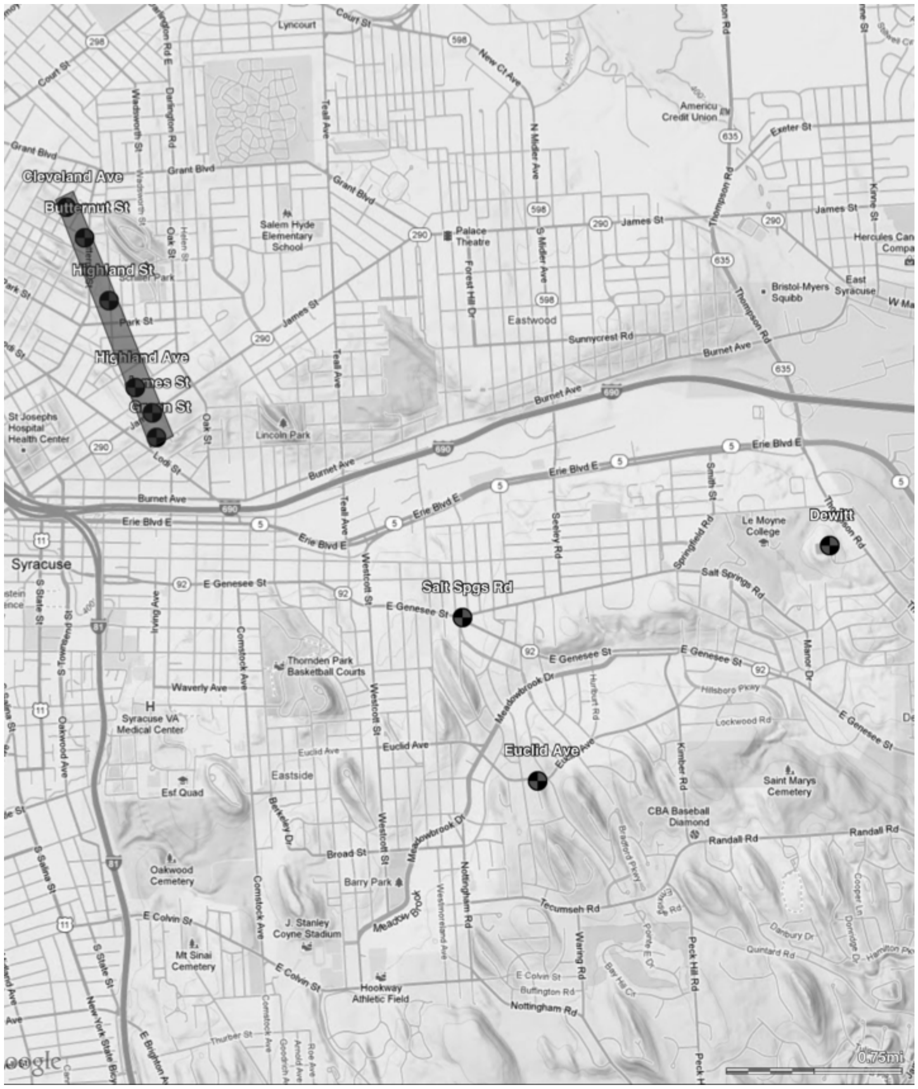

Figure 1. Map showing the reported locations of the Dewitt and other kimberlitic rocks in the vicinity of Syracuse, NY.

BACKGROUND & HISTORY

The Dewitt kimberlite was discovered in 1894 during the construction of a new water reservoir on the top of a small hill in east Syracuse (Figure 1) (Darton and Kemp 1895; Hopkins 1914). The dike was discovered by Philip Schneider, a teacher at Syracuse High School, who sent samples to J. F. Kemp at Columbia University for analysis (Darton and Kemp 1895). According to Darton, the reservoir was already filled with water by the time Schneider discovered the kimberlite, so few details about the size, shape, or number of

intrusions are known. The following information was passed on from the contractor to Schneider, and recorded by Darton:

"The dike was exposed by excavations for the reservoir and does not appear to reach the natural surface. It was buried under a mantle of glacial drift, and in part, at least, was covered by shales and limestones of the Salina formation. .... According to the statements of the contractor, the rock occurred in masses imbedded in a greenish-yellow earth which underlaid the entire area of the excavation, which was about 200 by 250 feet." (Darton and Kemp 1895), p.456.

Samples were sent to the United States Geological Survey for whole-rock analyses (Clarke and Hillebrand 1897), but following that, no significant scientific studies were done on the Dewitt kimberlite for more than 80 years.

AGE OF INTRUSION

Obtaining precise and accurate intrusion ages on kimberlites is difficult because they are complex and often highly altered rocks. In addition, many of the mineral phases are either xenocrystic, or of secondary (non-magmatic) origin. Researchers have tried to obtain ages on the NY kimberlites using the following methods: Rb-Sr and/or K-Ar on phlogopite macrocrysts (Watson 1979; Zartman 1967), fission track on apatite (Miller and Duddy 1989), K-Ar total fusion on whole rock samples (Basu et al. 1984), and most recently, U-Pb on perovskite separates (Heaman and Kjarsgaard 2000). Most of the analyses yielded Mesozoic ages of 180 to 110 Ma, with most between 120 and 150 Ma. The one date on the Dewitt kimberlite (K-Ar whole-rock) yielded an age of 130 +/-13 Ma (Basu et al. 1984). How closely this approximates the actual intrusion age is not clear because of the presence of xenocrystic material and the extensive alteration of many of the primary igneous phases. We attempted to extract groundmass perovskites for U/Pb dating because this technique yields the most precise estimates of the timing of intrusion and crystallization, but we have not yet been successful because the perovskites are very small (< 30 μm) and are commonly altered.

PETROGRAPHY & MINERALOGY

Like all kimberlitic rocks, the Dewitt intrusion is petrographically complex and highly variable. Every hand sample is texturally and mineralogically different. Phases identified to date in samples from the Dewitt reservoir include the following:

Macrocrysts

Most samples of the Dewitt kimberlite contain abundant, large (up to 1 cm), olivine macrocrysts. Most are anhedral, rounded, highly fractured, and partly to completely replaced by serpentine, magnetite, and/or calcite (Figure 2). Some samples contain a surprising amount of fresh olivine ($Fo_{89\text{-}91}$); no other New York kimberlite contains as much unaltered olivine. Some of the smaller olivine grains are sub- to euhedral, and are apparently microphenocrysts (Figure 3).

Much less common are macrocrysts of clinopyroxene ($\sim Di_{50.5}\ En_{45.5}\ Fs_{4.0}$) and pyrope garnet ($\sim Py_{73}\ Alm_{14}\ Gr_{13}$). The clinopyroxene grains are all anhedral and rounded like the olivine macrocrysts, but they are unaltered and often are very faint green under plane-polarized light. Garnet macrocrysts up to 5 mm in diameter are uncommon; they are all rounded, fractured, and have large opaque reaction rims (Figure 4). The garnets are homogeneous, Cr-bearing pyropes that classify as "G9" garnets, typical of garnets derived from lherzolitic mantle (Grutter et al. 2004).

Phlogopite macrocrysts, which are common in many New York kimberlites, are surprisingly uncommon in the Dewitt kimberlite. Those that exist are relatively small (< 1mm), and often highly altered and replaced by clouds of fine-grained opaques. Phlogopite macrocrysts, when found, are often deformed, indicating a xenocrystic origin (Figure 5).

Spinel and ilmenite macrocrysts are uncommon, always anhedral, and relatively small (< 0.5 mm). The spinels vary widely in color (from deep green to red-brown to opaque) and

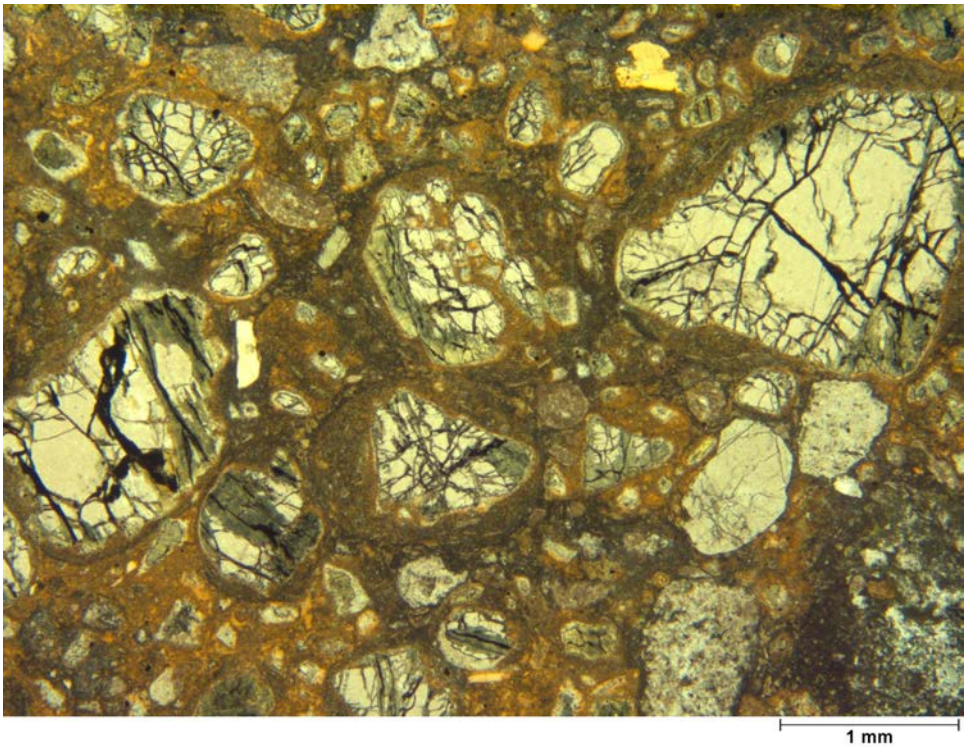

Figure 2. Sample of relatively unaltered kimberlite from Dewitt with abundant, anhedral, partly serpentinized olivine macrocrysts (Sample DT-2; PPL).

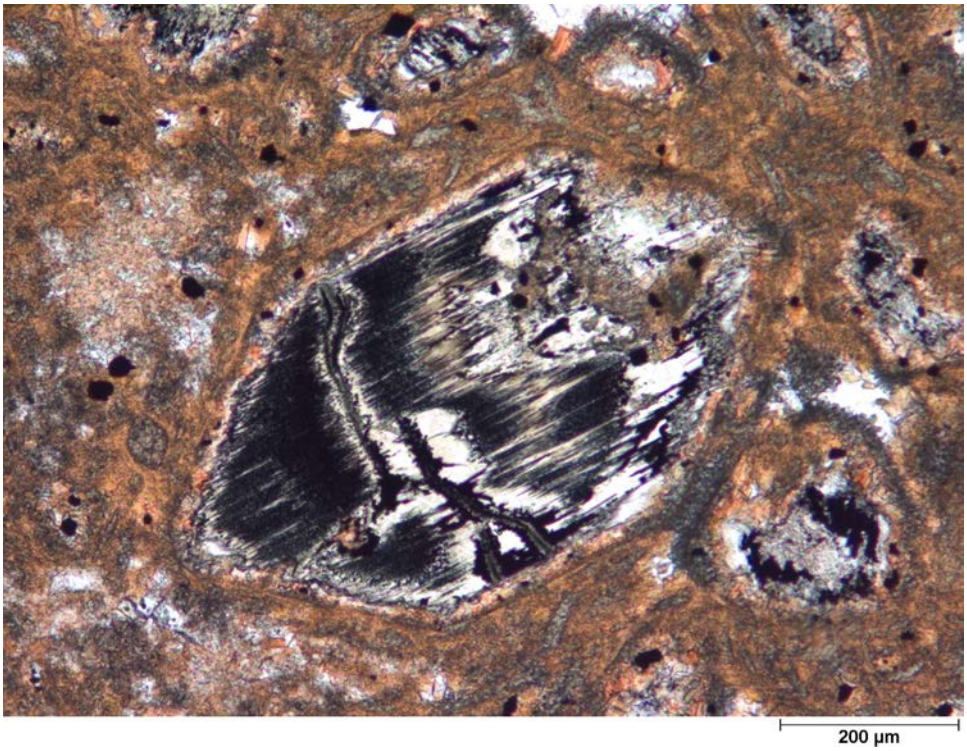

Figure 3. Small microphenocryst of olivine; replaced by serpentine and magnetite (Sample-DT-2a; PPL).

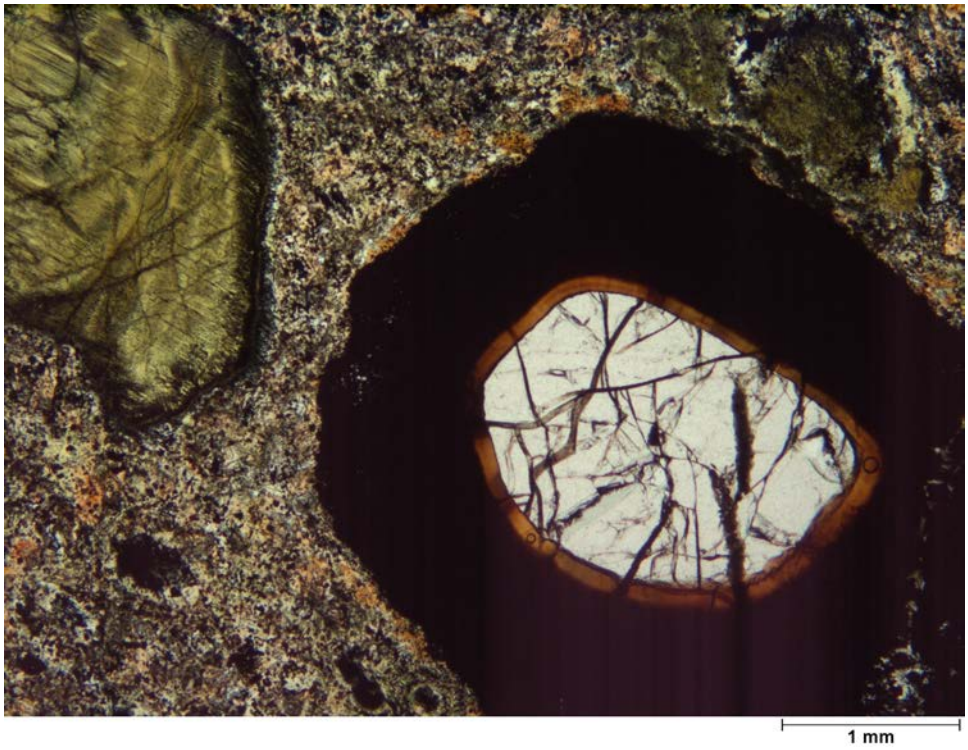

Figure 4. Garnet xenocryst with thick reaction rim (Sample DT-1a; PPL).

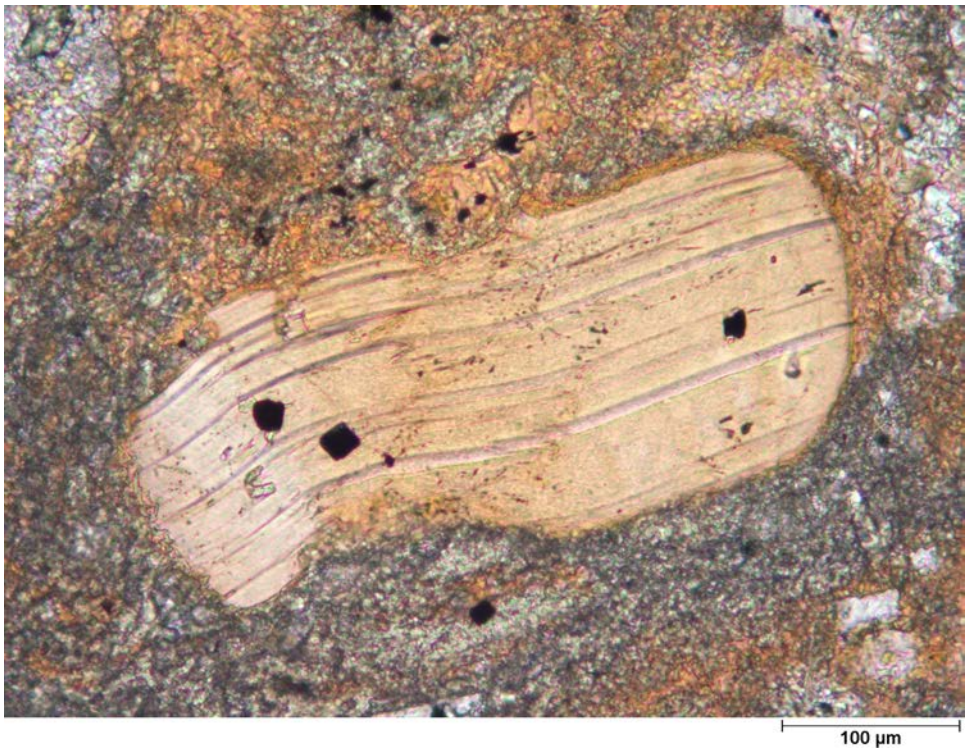

Figure 5. Small, deformed, xenocrystic phlogopite with chromite inclusions (Sample DT-2a; PPL).

composition (from true spinel to chromite to magnetite). They also vary in mode of origin, although a comprehensive and systematic study of the spinels in these rocks has not yet been done. The ilmenite macrocrysts are always rounded and surrounded by a zone enriched in dark orange phlogopite. The only other NY kimberlites with ilmenite macrocrysts are from the Green Street dike cluster in Syracuse, and the dikes in East Canada Creek in Montgomery County.

Groundmass phases

The groundmass of the Dewitt kimberlite is highly variable in texture and mineralogy. Serpentine, calcite, phlogopite, diopside, apatite, perovskite, and opaques are visible in most thin sections. Many additional phases have been identified by energy-dispersive X-ray spectrometry on a scanning electron microscope (e.g. magnetite, ilmenite, chromite, baddelyite, melilite, sodalite, Ni-pyrite, pyrrhotite, galena, sphalerite, and barite). With the exception of the opaque oxides, all of these phases are generally very small (<100 um). The sulfides tend to occur as small anhedral grains distributed throughout the groundmass; the sulfates tend to occur as small fracture fillings, and the melilite and sodalite are most common in the reaction zones surrounding crustal xenoliths. A number of complex, and as yet unidentified, Ti-silicates also have been found replacing perovskite and /or rutile. Undoubtedly, many more phases are present in the fine-grained groundmass of this intrusion.

WHOLE-ROCK CHEMISTRY

Kimberlites are, by nature, hybrid rocks containing complex mixtures of mantle and crustal derived materials, and almost all have experienced extensive post-emplacement hydrothermal alteration and/or surficial weathering. Because of these complications, whole-rock compositions almost certainly do not represent, or even approximate, magmatic liquid compositions. This limits our ability to understand the mineralogical and chemical nature of the mantle source of kimberlitic magmas, and their subsequent evolution. Nevertheless, whole-rock chemistry does provide important information that allows us to categorize and classify these unusual rocks, and to constrain the geological processes involved in their

formation. Forty-three whole-rock samples were analyzed by WD-XRF and ICP-MS at the Geoanalytical Laboratory at Washington State University; representative analyses are provided in Bailey & Lupulescu (2007).

Despite the extensive alteration and contamination, the whole-rock data allow us to identify individual dikes and/or clusters of dikes that have distinct geochemical signatures, particularly in terms of the ratios of relatively immobile, high field strength (HFS) minor and trace elements. All of the intrusions in the Syracuse area are chemically similar, and can be identified by their low Ti and Nb concentrations relative to the other kimberlitic rocks in New York (Figure 6).

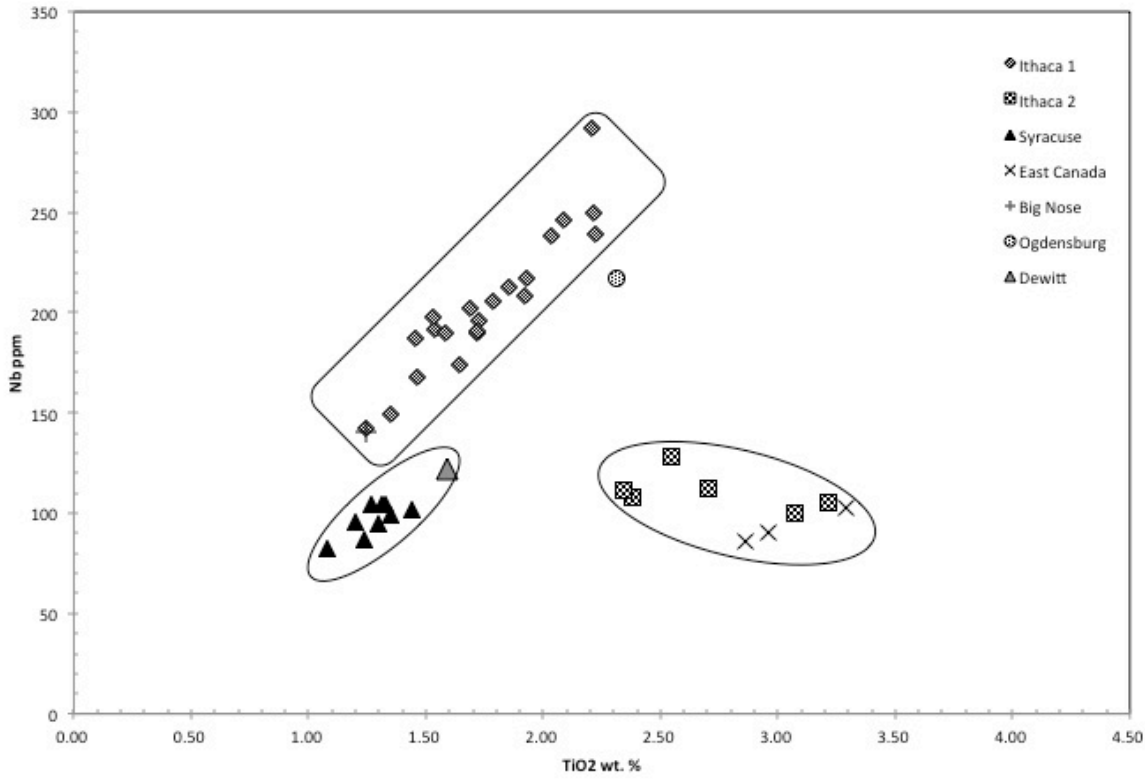

Figure 6. Scatter plot of Nb and TiO_2 concentrations in New York State kimberlites.

The average trace element contents of the Syracuse kimberlites are illustrated in Figure 7, along with the average compositions of the Lac de Gras and Kirkland Lake kimberlites in Canada. The Syracuse and Canadian kimberlites have broadly similar trace element

signatures, although the Syracuse kimberlites exhibit significantly higher K/Ba and K/Nb ratios.

Figure 7. Primitive-mantle normalized spider diagram of trace element concentrations in the Syracuse kimberlites compared to the Lac de Gras (LDG) and Kirkland Lake (KL) kimberlites in Canada (average of six analyses of each). Data sources: Syracuse (Bailey, unpublished), Lac de Gras and Kirkland Lake (MacBride 2005) Normalizing factors from (McDonough and Sun 1995)

CLASSIFICATION

Are these unusal rocks really kimberlites? Over the years they have been referred to as "serpentine bodies" (Vanuxem 1842), peridotites (Williams 1887b), alnoites (Smyth 1893), and kimberlites (Matson 1905). For most igneous rocks, classification is now straightforward, based primarily on modal mineralogy, rock texture, and/or rock chemistry (Le Maitre et al.

2002). Unfortunately, due to the mineralogical complexity of kimberlites, a simple definition does not exist; they are, in fact, a clan of complexly related rocks. The situation is nicely summarized by Winter (2001) who states: "The confusion (in classification) is most evident in the highly potassic lamprophyre-lamproite-kimberlite group, a diverse array of mafic to ultramafic rocks with high volatile contents. The numerous intertwined petrographic and genetic similarities and differences in this broad group present a classification nightmare." (p.362)

Kimberlites are currently divided into two groups (Le Maitre et al. 2002; Skinner 1989; Smith et al. 1985). Group I kimberlites are the analogue of the rocks originally found and described at Kimberley, South Africa (the "basaltic kimberlites" of Wagner, 1914). Group II kimberlites are the equivalent of the micaceous kimberlites of the Orange Free State, South Africa, and are also called orangeites (or "lamprophyric kimberlites" after Wagner (1914)). The two groups of kimberlites display subtle differences in their mineralogical composition (Mitchell 1995; Skinner 1989; Smith et al. 1985; Tainton and Browning 1991). According to Mitchell (1995), kimberlites are "characterized by the presence of macrocrysts and subhedral microphenocrysts of olivine set in a groundmass consisting of spinel, perovskite, monticellite, phlogopite, apatite, serpentine, and calcite" (p.74), whereas orangeites are composed principally of macrocrystal and "microphenocrystal phlogopite set in a fine-grained groundmass consisting essentially of phlogopite-tetriferriphlogopite and minor apatite, chromite, Mn-ilmenite, and perovskite with a mesostasis of calcite and/or dolomite together with serpentine" (p.61). Unfortunately, there is no one single defining mineralogical, or chemical characteristic of either group: for example, kimberlites can contain phologopite macrocrysts, and orangeites can contain olivine macrocrysts. Compositional trends of the groundmass spinels are one of the best criteria for distinguishing Group 1 kimberlites from orangeites (Mitchell 1995; Tappe et al. 2005).

Petrographically, the Dewitt intrusion exhibits features of both groups: the abundant olivine macrocrysts and quench texture apatite in the groundmass are features common in Group 1 kimberlites, whereas the abundant phlogopite and diopside in the groundmass are features more commonly seen in Group 2 kimberlites (orangeites) (Mitchell 1995). Presently, we do not have enough compositional data on the groundmass spinels to identify clear evolutionary trends.

Chemically, the two groups can usually be discriminated on the basis of whole-rock TiO_2 and K_2O concentrations (Figure 8). The Syracuse intrusions do not clearly lie within one field or the other; they appear to straddle the boundary between the two categories of kimberlitic rocks. Thus, both the chemical and petrographic features of these rocks indicate that, while the Syracuse intrusions clearly belong to the broad family of kimberlitic rocks, they are not archetypical Group 1 or Group 2 kimberlites. Overall, they tend to have stronger affinities with Group 2 kimberlites (orangeites).

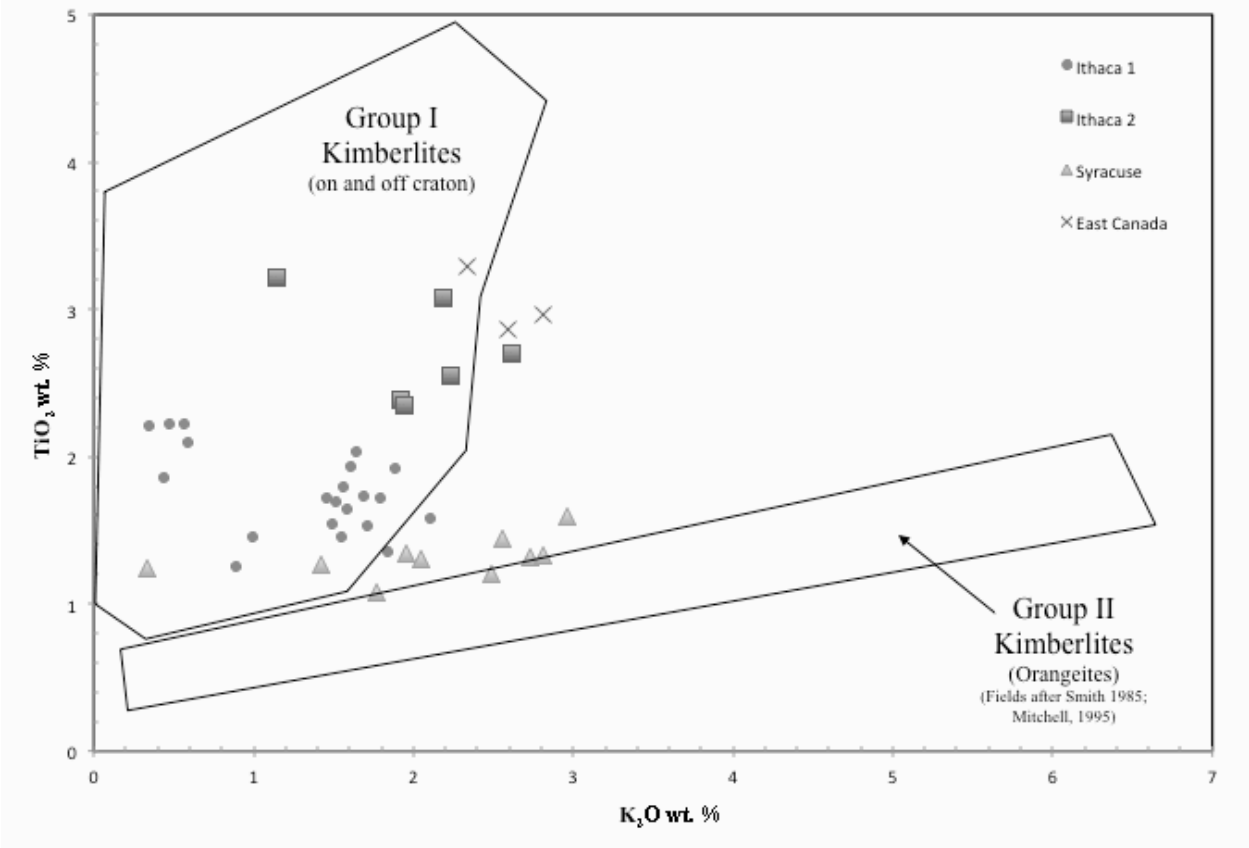

Figure 8. TiO_2 vs. K_2O concentrations for New York State kimberlites. Broad compositional fields for Group 1 and Group 2 kimberlites drawn based upon data in Smith et al. (1985) and Mitchell (1995).

ORIGIN

Currently, there are two theories that have been put forth to explain the origin of the Mesozoic kimberlitic rocks in New York state (Figure 9): 1) They are part of a chain of small, alkaline intrusions in eastern North America related to passage of the North American plate over the Great Meteor hot spot (Heaman and Kjarsgaard 2000); or 2) they are part of a belt of kimberlitic intrusions along the western flanks of the Appalachian Mountains that were intruded along old structures that were reactivated by crustal extension related to rifting and opening of the Atlantic Basin (Parrish and Lavin 1982). We believe the spatial and temporal distribution of the kimberlitic rocks in eastern North America is most consistent with the second hypothesis, although the lack of unequivocal and precise intrusion ages on most of the eastern North American kimberlites makes this, at present, a relatively speculative interpretation.

SUMMARY

The Dewitt intrusion is one of the largest kimberlitic intrusions in New York State; it is also one of the least altered, with some samples containing up to 30% fresh olivine. The material available today is mineralogically and texturally variable, but the abundance of phlogopite and clinopyroxene in the groundmass of many samples suggest that the intrusion has stronger affinities with orangeites than with Group 1 kimberlites.

The Dewitt intrusion is early Cretaceous in age, and is probably the result of small degrees of partial melting in the underlying asthenospheric mantle in response to lithospheric extension along the newly developed eastern margin of the North American plate. The kimberlitic magmas moved toward the surface along major crustal structures on the western flanks of the Appalachian Mountains that were reactivated during Mesozoic rifting.

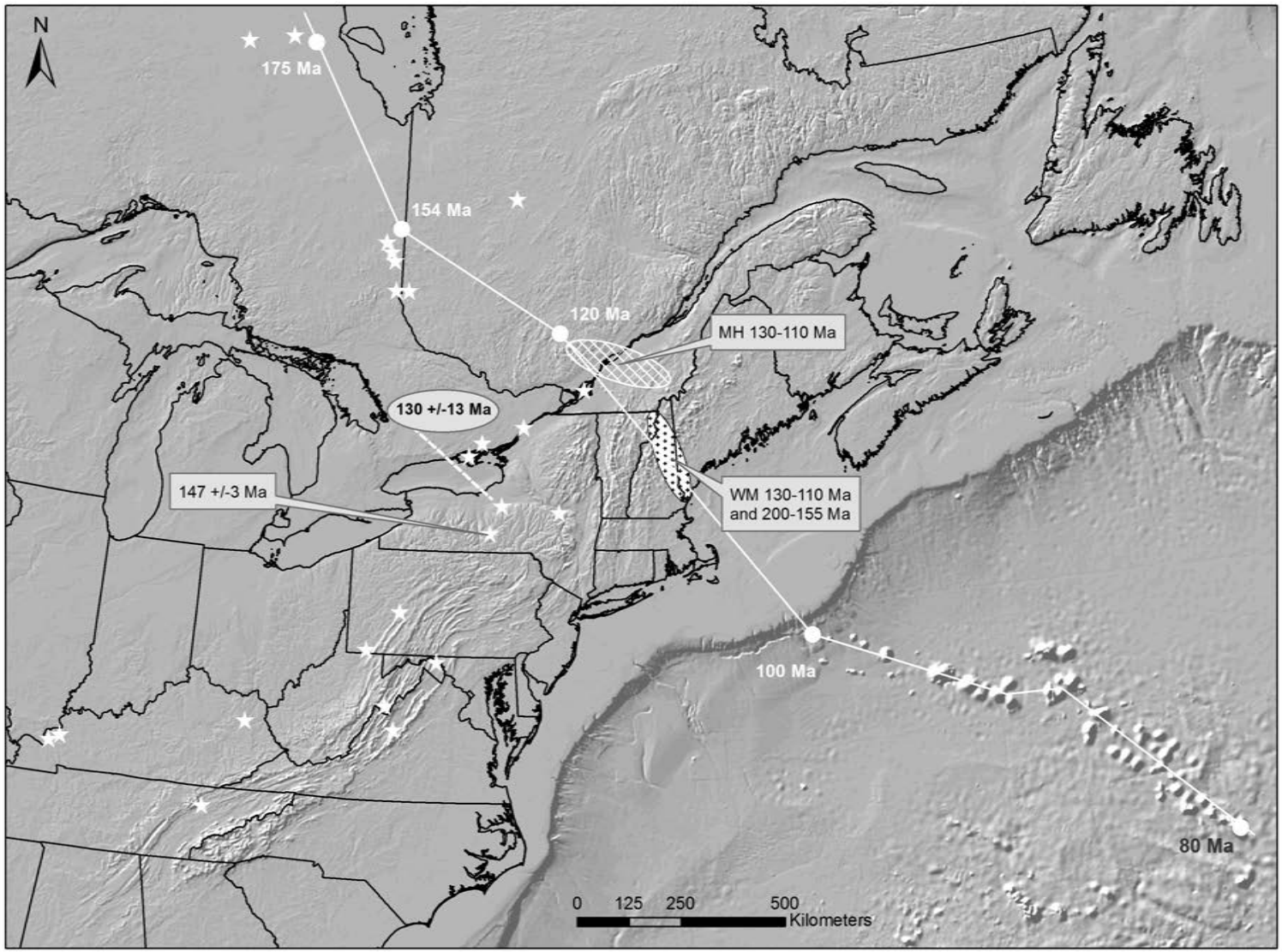

Figure 9. Locations of select Mesozoic age igneous rocks in eastern North America shown in relation to the Appalachian Mountains and the Great Meteor Hot Spot track (shown by line and solid white circles). White stars = kimberlitic rocks; MH = Monteregian Hills Alkaline Province; WM = White Mountains Magmatic Complex. Compiled from (Basu et al. 1984; Creasy 1989; Heaman and Kjarsgaard 2000; Meyer 1976; Parrish and Lavin 1982).

REFERENCES CITED

Bailey, D. G., and Lupulescu, M. V., 2007, Kimberlitic rocks of central New York: New York State Geological Association, Field Trip Guidebook, v. 79, p. 53-81.

Basu, A. R., Rubury, E., Mehnert, H. H., and Tatsumoto, M., 1984, Sm-Nd, K-Ar and petrologic study of some kimberlites from eastern United States and their implication for mantle evolution: Contributions to Mineralogy and Petrology, v. 86, no. 1, p. 35-44.

Clark, B. W., 1908, The peridotites of Onondaga County, New York [M.Sc.]: Syracuse University

Clarke, F. W., and Hillebrand, W. F., 1897, Analyses of Rocks: Bulletin - United States Gelogical Survey, v. 148, p. 79.

Clarke, J. M., 1899, The peridotite on Green Street hill: New York State Museum Handbook, v. 15, p. 81.

Creasy, J. W., 1989, Geology and geochemistry of the Rattlesnake Mountain igneous complex, Raymond and Casco, Maine Studies in Maine geology; papers to commemorate the 150th anniversary of C. T. Jackson's reports on the geology of Maine, Volume 4: United States, Maine Geol. Surv. : Augusta, ME, United States, p. 63-78.

Dana, J. D., 1878, Manual of Mineralogy, New York, 474 p.

Darton, N. H., and Kemp, J. F., 1895, A newly discovered dike at DeWitt, near Syracuse, New York: American Journal of Science, v. 49, p. 456-462.

Geddes, G., 1860, Geology of Onondaga County, New York: Transactions, New York State Agricultural Society, v. 19, p. 243-256.

Gems here at home, July 16, 1906, Syracuse Herald, Syracuse, NY, p. 9

Grutter, H. S., Gurney, J. J., Menzies, A. H., and Winter, F., 2004, An updated classification scheme for mantle-derived garnet, for use by diamond explorers: Lithos, v. 77, p. 841-857.

Heaman, L. M., and Kjarsgaard, B. A., 2000, Timing of eastern North American kimberlite magmatism; continental extension of the Great Meteor Hotspot track?: Earth and Planetary Science Letters, v. 178, no. 3-4, p. 253-268.

Hopkins, T. C., 1914, The geology of the Syracuse Quadrangle [New York]: Bulletin - New York State Museum, v. 171, 80 p.

Hunt, T. S., 1858, Contributions to the History of Ophiolites. Part II.: American Journal of Science, v. 26, p. 234-240.

Kraus, E. H., 1904, A new exposure of serpentine at Syracuse, New York: American Geologist, v. 33, p. 330-332.

Le Maitre, R. W., Streckeisen, A., Zanettin, B., Le Bas, M. J., Bonin, B., Bateman, P., Bellieni, G., Dudek, A., Efremova, S., Keller, J., Lameyre, J., Sabine, P. A., Schmid, R., Sorensen, H., and Woolley, A. R., 2002, Igneous rocks; a classification and glossary of terms; recommendations of the International Union of Geological Sciences Subcommission on the Systematics of Igneous Rocks Edition: 2, Cambridge, Cambridge University Press, 236 p.

Lewis, H. C., 1887, On diamantiferous peridotite and the genesis of diamond: Geological Magazine, v. 4, p. 22-24.

MacBride, L. M., 2005, A comparative study of the petrology, mineralogy, and geochemistry of kimberlite-like and carbonatitic rocks from Kontozero (Kola Peninsula, Russia) and bona fide kimberlites [M.Sc.]: University of Manitoba, 364 p.

Matson, G. C., 1905, Peridotite dikes near Ithaca, New York: Journal of Geology, v. 13, p. 264-275.

McDonough, W. F., and Sun, S. S., 1995, The composition of the Earth: Chemical Geology, v. 120, no. 3-4, p. 223-253.

Meyer, H. O. A., 1976, Kimberlites of the continental United States: A review: Journal of Geology, v. 84, no. 4, p. 377-402.

Miller, D. S., and Duddy, I. R., 1989, Early Cretaceous uplift and erosion of the northern Appalachian Basin, New York, based on apatite fission track analysis: Earth and Planetary Science Letters, v. 93, no. 1, p. 35-49.

Mitchell, R. H., 1995, Kimberlites, Orangeites, and Related Tocks, New York, Plenum Press, 410 p.

Parrish, J. B., and Lavin, P. M., 1982, Tectonic model for kimberlite emplacement in the Appalachian Plateau of Pennsylvania: Geology [Boulder], v. 10, no. 7, p. 344-347.

Schneider, P. F., 1902, New exposures of eruptive dikes in Syracuse, N Y: American Journal of Science, v. 14, no. 79, p. 24-25.
-, 1903, The geology of the serpentines of central New York: Proceedings of the Onondaga Academy of Science, v. 1, p. 110-117.
Skinner, E. M. W., Contrasting group I and group II kimberlite petrology; towards a genetic model for kimberlites, *in* Proceedings Fourth international kimberlite conference, Perth, Australia, Aug. 11-15, 1986 1989, Geological Society of Australia, Sydney, N.S.W., Australia, p. 528-544.
Smith, C. B., Gurney, J. J., Skinner, E. M. W., Clement, C. R., and Ebrahim, N., 1985, Geochemical character of southern African kimberlites: a new approach based upon isotopic constraints: Transactions Geological Society of South Africa, v. 88, p. 267-280.
Smyth, C. H., 1893, Alnoite containing an uncommon variety of melilite: American Journal of Science, v. 46, no. 272, p. 104-107.
Syracuse has diamond hunt, November 28, 1905, Syracuse Post Standard, Syracuse, NY, p. 14
Tainton, K., and Browning, P., 1991, The relationship between Group-2 kimberlites and lamproites; an example from the northern Cape Province, South Africa: European Union of Geosciences Terra Abstracts, v. 3, no. 1, p. 17-18.
Tappe, S., Foley, S. F., Jenner, G. A., and Kjarsgaard, B. A., 2005, Integrating ultramafic lamprophyres into the IUGS classification of igneous rocks: rationale and implications: Journal of Petrology, v. 46, no. 9, p. 1893-1900.
Vanuxem, L., 1839, Third annual report of the geological survey of the third district, New York, Annual Report of the New York Geological Survey, 3rd District, 283 p.
-, 1842, Geology of New York; Part III, Comprising the survey of the third geological district, Albany, NY, W. and A. White and J. Visscher, Natural History of New York, 306 p.
Wagner, P. A., 1914, The diamond fields of South Africa, Johannesburg,
Watson, K. D., 1979, Kimberlites of eastern North America, *in* Wyllie, P. J., ed., Ultramafic and related rocks, Robert E. Krieger Publ. Co., Huntington, NY, p. 312-323.
Williams, G. H., 1887a, On the serpentine (peridotite) occurring in the Onondaga salt group at Syracuse, New York: American Journal of Science, v. 34, no. 200, p. 137-145.
-, 1887b, On the serpentine of Syracuse, N.Y.: Science, v. 9, no. 214, p. 232-233.
Winter, J. D., 2001, An Introduction to Igneous and Metamorphic Petrology, Upper Saddle River, NJ, Prentice Hall, 697 p.
Would advance cash to probe stratums, November 3, 1902, Syracuse Post Standard, Syracuse, NY, p. 6
Zartman, R. E., Brock, M. R., Heyl, A. V., Thomas, H. H., 1967, K-Ar and Rb-Sr ages of some alkalic intrusive rocks from central and eastern United States: American Journal of Science, v. 265, p. 848-870.

ROAD LOG

****Note:** The Dewitt kimberlite locality is on property currently owned by LeMoyne College. This is private property, and permission must be obtained from the college administration prior to parking, hiking to the locality, and collection of any samples. Because specimens are limited, please only collect specimens for scientific research or for educational uses.****

Stop #1. The Dewitt "Kimberlite" (Lat: 43.049223, Long: -76.080701)
Park near the LeMoyne College Physical Plant, and follow the well-maintained trails to the slopes of the reservoir. Centimeter to meter-scale blocks can be found in the woods along the slopes of the reservoir. Please do not dig or excavate large blocks from the slopes!

We will examine a number of specimens and discuss the mineralogy and petrology of the intrusion.

Hydrogeology of a sand and peat aquifer, Rome Sand Plains, New York

Todd W. Rayne
Hamilton College, Clinton, NY 13323
trayne@hamilton.edu

INTRODUCTION

The Rome Sand Plains is a mosaic of sand dunes, bogs, pine barrens, meadows, and deciduous forest that covers 16,000 acres in Oneida County, New York (Russell 1996). The area is one of the few remaining inland pitch pine barrens in the northeastern United States and is partly protected by a consortium of government agencies and conservation groups. The field site for this trip is located approximately 4 miles west of the city of Rome, New York, on Hogsback Road (Figure 1).

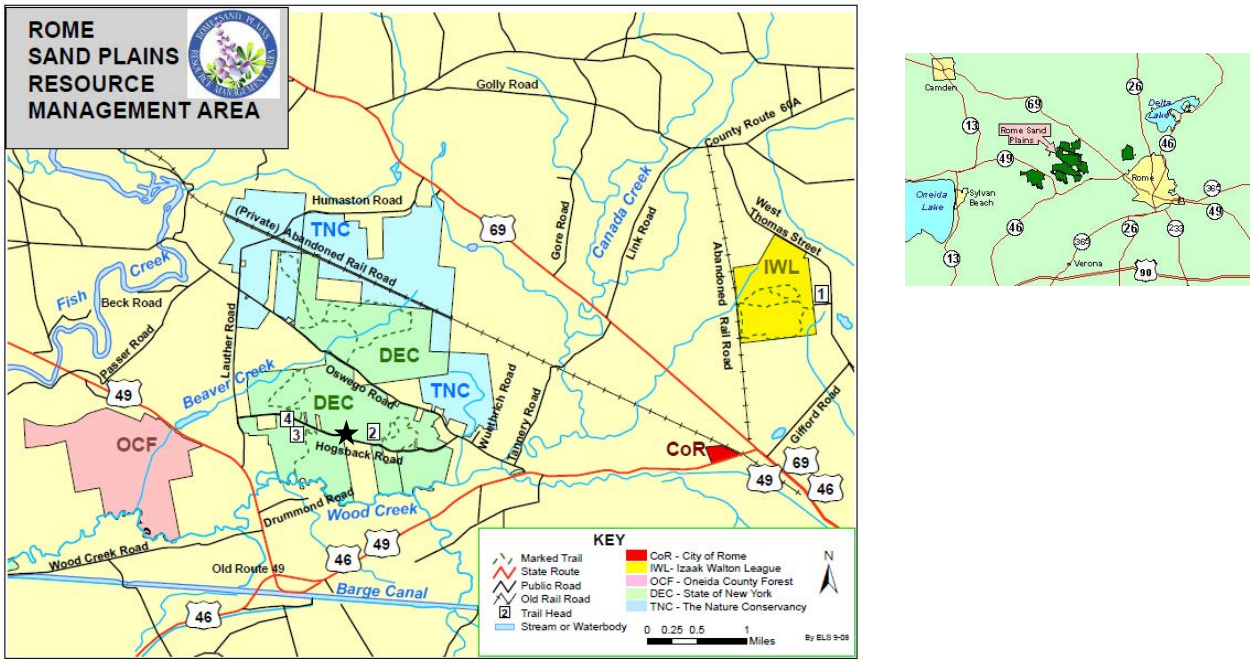

Figure 1. General location map of the Rome Sand Plains with approximate location of field site shown by the star along Hogsback Road (New York State Department of Environmental Conservation).

The field site is an area of parabolic dunes with an adjacent peat bog (Figure 2). There is approximately 50 feet of relief between the dune crests to the flat bog surfaces. The dunes were formed on what was probably a kame terrace that was about 50 feet above the surrounding lower area to the north (Eugene Domack, oral communication, 2012). When the ice melted, sand on the terrace surface was reworked by prevailing westerly winds into a

series of parabolic dunes (Figures 2 and 3). The dunes are composed of fine to medium sand with a Fe hydoxide coating that gives it a yellowish color. The low areas between the dunes became bogs, partly because of a high water table that inhibited the growth of larger plants. The bogs are dominated by S*phagnum* moss and a variety of distinctive plants such as bog rosemary and leatherleaf (Russell 1996). There are also sundew and pitcher plants in some bogs, but we probably won't see any on our trip. Peat thickness ranges from less than 1 m in bogs that were mined for peat to ~8 m in undisturbed bogs. Water in the peat is acidic, with a pH of 4 to 5.

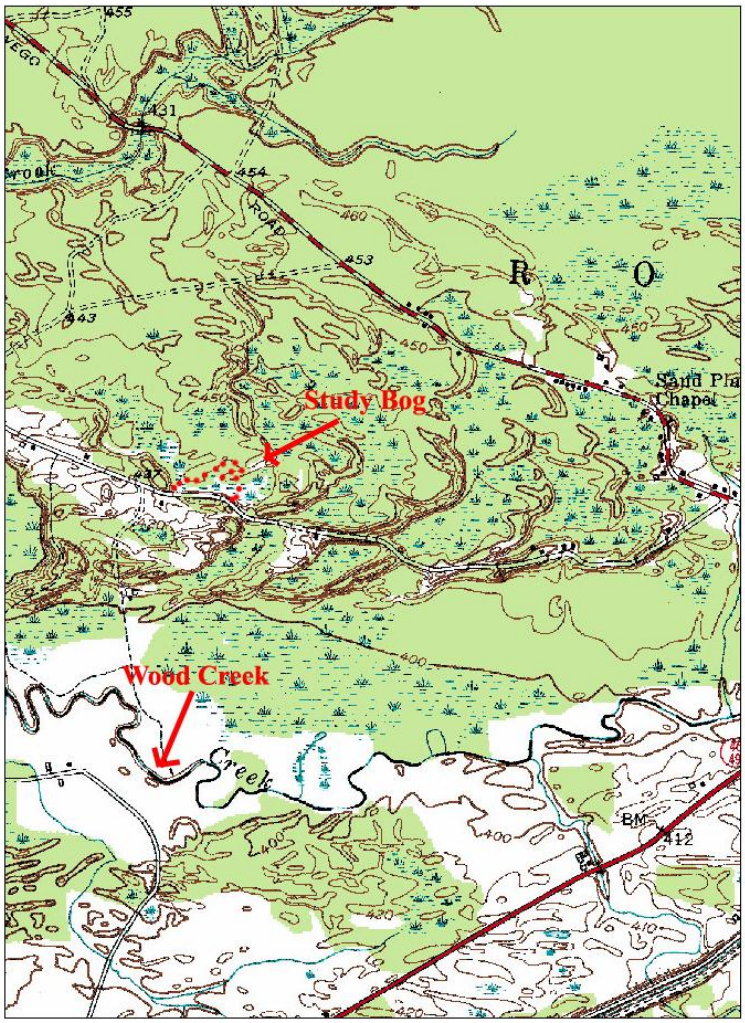

Figure 2. Part of the 1:24,000 Verona Quadrangle showing the parabolic dune area of the Rome Sand Plains.

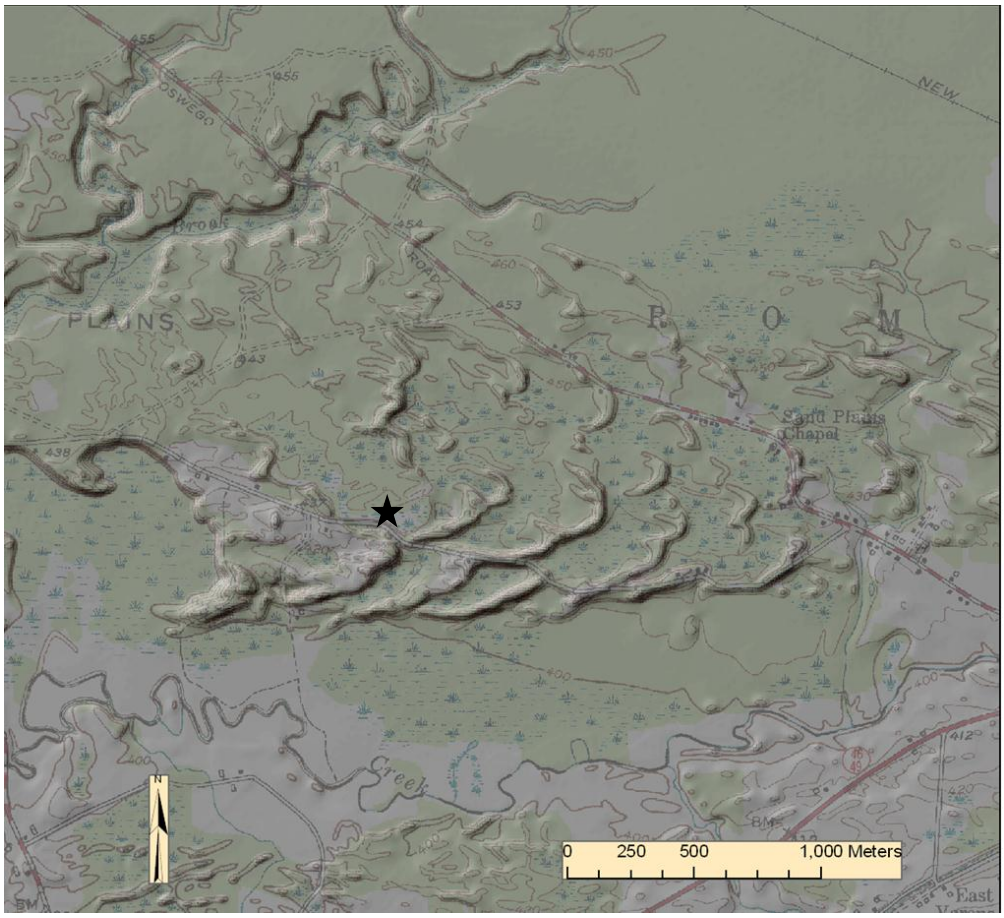

Figure 3. Composite LIDAR and topographic map showing the parabolic dunes and bogs. Study area is marked with a star.

STRATIGRAPHY

Based on dozens of hand auger borings and several outcrops and excavations, the dunes consist of uniform fine to medium grained yellowish brown sand (Brewer 2009). The soil orders in the sand areas are mostly entisols or inceptisols (young soils with little horizon development). In lower-lying areas where there is more available water and white pines grow, well-developed spodosols with prominent E horizons occur. There appears to be little or no soil development below about 1 m in the sand areas and on dune crests, which are drier, soils are even thinner.

The stratigraphy of the bogs and the sand immediately below the peat is more interesting. According to the former owner, peat in the study site bog was excavated during the 1960s for peat moss. The resulted in a relatively thin peat layer in this bog, ranging from less than 1 to

about 2 m. The peat consists mostly of partially decomposed *Sphagnum* moss with the occasional branch or log. The peat is usually saturated, with the water table at or just below the bog surface. The groundwater in the peat "aquifer" is acidic, with a pH of 4 to 5. While it's very difficult to measure field Eh values, it seems that groundwater in the peat is reducing.

Immediately below the peat is a light to medium gray sand layer that is distinctly lighter in color than the unaltered sand in the dunes. I believe this represents a leached layer in which the Fe hydroxide coatings of the sand grains have been dissolved by downward moving water that contains organic acids from the partially decayed peat. This layer ranges from 5 to 30 cm in thickness.

In most borings in the bog, a discontinuous, semi-cemented, dark reddish brown sand layer that is probably an ortstein (a weakly cemented spodic horizon) lies below the gray sand layer. The cement is Fe oxide or hydroxide that is precipitated from a change in Eh conditions from reducing to oxidizing, possibly by moving into a new geochemical environment as it moves below the peat and interacts with groundwater in the sand aquifer. The sand gradually changes to the yellowish brown sand of the sand dunes below the Fe-enriched layer (Brewer 2009).

HYDROGEOLOGY

Conceptual model

My conceptual model of the sand-peat aquifer system is based on shallow wells in and near the bog from several student theses and one deeper well that was drilled as a class demonstration 50 m south of the bog. In addition, a deep excavation on the south side of Hogsback Road appears to be an outcrop of the water table in the sand aquifer.

The bog is an area of downward groundwater flow during most or all of the year when heads in the peat are as much as 25 cm higher than heads in the sand aquifer that underlies the bog. Although the peat bogs are in topographic lows, the hydraulic conductivity of the peat is very low (~1E-6 cm/s) and makes the peat behave like a slowly leaking bathtub relative to the highly permeable sand. Vertical movement of recharge from direct precipitation and the relatively small amount of runoff into the bog is inhibited in the peat

and a groundwater mound forms in the peat as the water slowly moves downward. This area gets sufficient average annual precipitation (1.1 m/y) to keep the peat saturated (i.e. a groundwater mound) most of the year. The peat bogs are recharge areas, but the amount of recharge they contribute to the sand aquifer is relatively small because most recharge occurs in the sand areas where there is little runoff and the hydraulic conductivity is high. While it is possible that there are times when the head in the sand aquifer is higher than the head in the peat (making the bog a discharge area), I have never observed this.

Groundwater movement

Based on regional topography (Figure 4), head measurements in a limited number of wells and 'outcrops' of the water table, groundwater in the sand aquifer moves from north to south toward Wood Creek, the regional discharge area. However, the relationship between the sand and peat can complicate this generalization. Groundwater in the peat bogs flows radially away from the bogs and also moves downward (Figures 4 and 6). As it enters the sand aquifer, regional flow to the south is dominant.

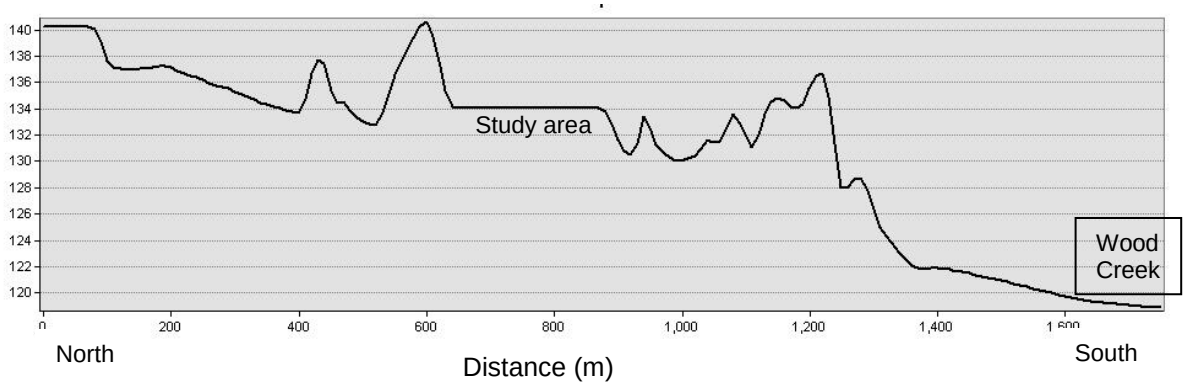

Figure 4. North – south topographic cross section through the study area to Wood Creek. Vertical scale in m.

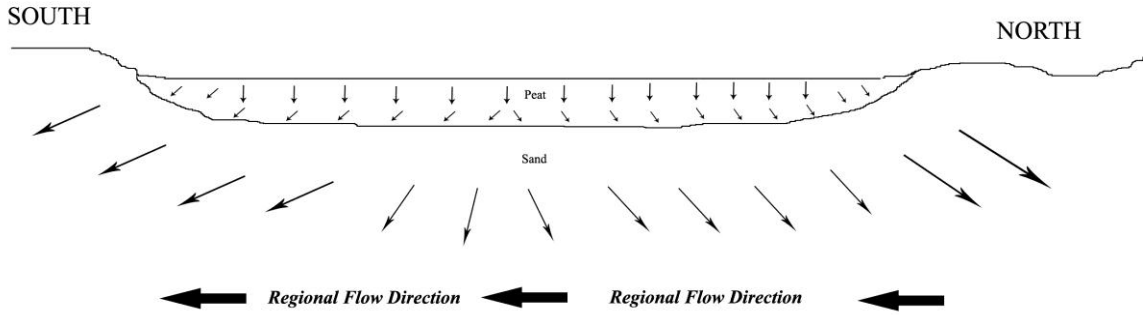

Figure 5. Schematic cross section showing downward movement of groundwater in the peat bog and southward movement of groundwater in the sand aquifer.

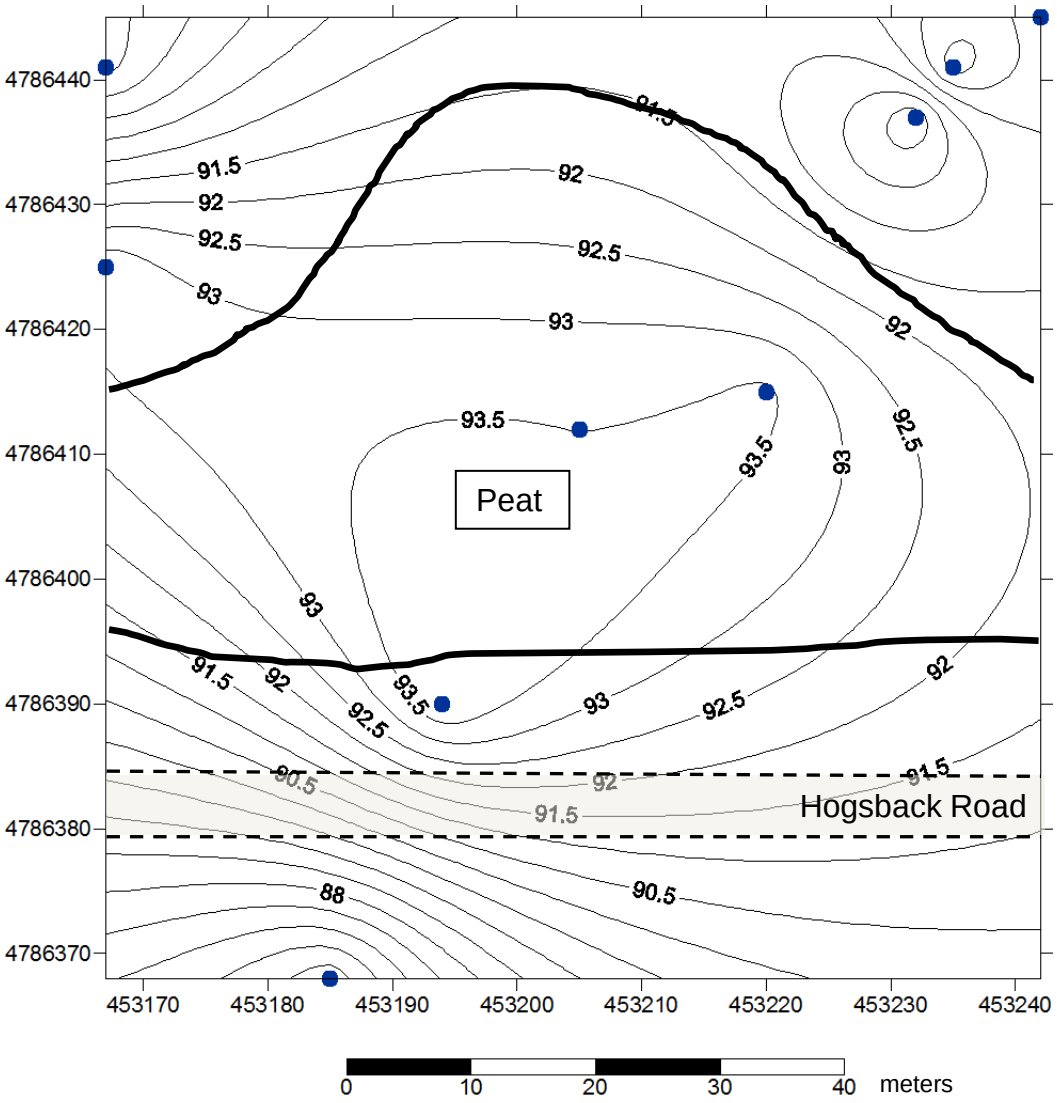

Figure 5. Surfer plot of peat and sand head values in the study area from March 2009. Dots show the location of wells. Thick solid lines show approximate boundary of the bog. Head values in m relative to a local datum on Hogsback Road of 100 m.

Shallow horizontal head gradients in the sand aquifer between Hogsback Rd and the adjacent peat bog appear to reverse depending on recharge conditions (Von Metzsch 2009). During rain events or snow melt, water entering the sand from the road makes a temporary mound adjacent to the road that produces groundwater flow toward the peat (opposite the 'regional' gradient). During dry weather, the mound disappears and the direction of groundwater flow is from the peat bog into the sand aquifer.

REFERENCES CITED

Brewer, R.S., 2009, Hydrologic interaction between peat and sand in the Rome Sand Plains, Rome, New York. Unpublished B.A. thesis, Hamilton College, Clinton, NY, 19 p.

Russell, E. W. B. 1996. Six thousand years of forest and fire history in the Rome Sand Plains. Report. The Central New York Chapter of The Nature Conservancy, Rochester, New York.

Von Metzsch, G.A., 2009, Groundwater movement and road salt migration in a sand aquifer, Rome Sand Plains, Rome, NY. Unpublished B.A. thesis, Hamilton College, Clinton, NY, 38 p.

Workshop B3a: Teaching Geologic Map Interpretation Using Google Earth

Barbara Tewksbury
Dept. of Geosciences, Hamilton College, Clinton, NY 13323 btewksbu@hamilton.edu

The interactive 3D terrain viewing capability of Google Earth makes it a terrific resource for teaching geologic map interpretation for both structural geology and introductory geology students. This workshop provided college/university-level faculty and researchers with hands-on experience in learning how to use Google Earth to help students visualize geologic structures in three dimensions and make their own geologic maps and cross sections so that they are better prepared to interpret traditional geologic maps.This approach is described in detail at http://serc.carleton.edu/NAGTWorkshops/structure/approach.html

Workshop B3b: Working with LiDAR (.las) Data in ArcGIS

David Tewksbury
Dept. of Geosciences, Hamilton College, Clinton, NY 13323 dtewksbu@hamilton.edu

Workshop participants learned to process LiDAR (.las) data using ArcGIS 10.1 to produce digital surface models (DSM), digital terrain models (DTM) and intensity images from data covering the local area. LiDAR sources were discussed as well.

Using raw (.las) LiDAR data from the Oneida County Planning Office in conjunction with ESRIs ArcGIS 10.1 software participants processed the data using the LiDAR first returns to create a Digital Surface Model (DSM) and corresponding hillshade of the Hamilton College campus area. Using the classified "bare earth" returns a Digital Terrain Model (DTM) and corresponding hillshade of the same area was also created. Using the Intensity attribute an intensity image, which resembles a B&W orthophoto, was also created. Intensity images can be very useful in land cover classification.

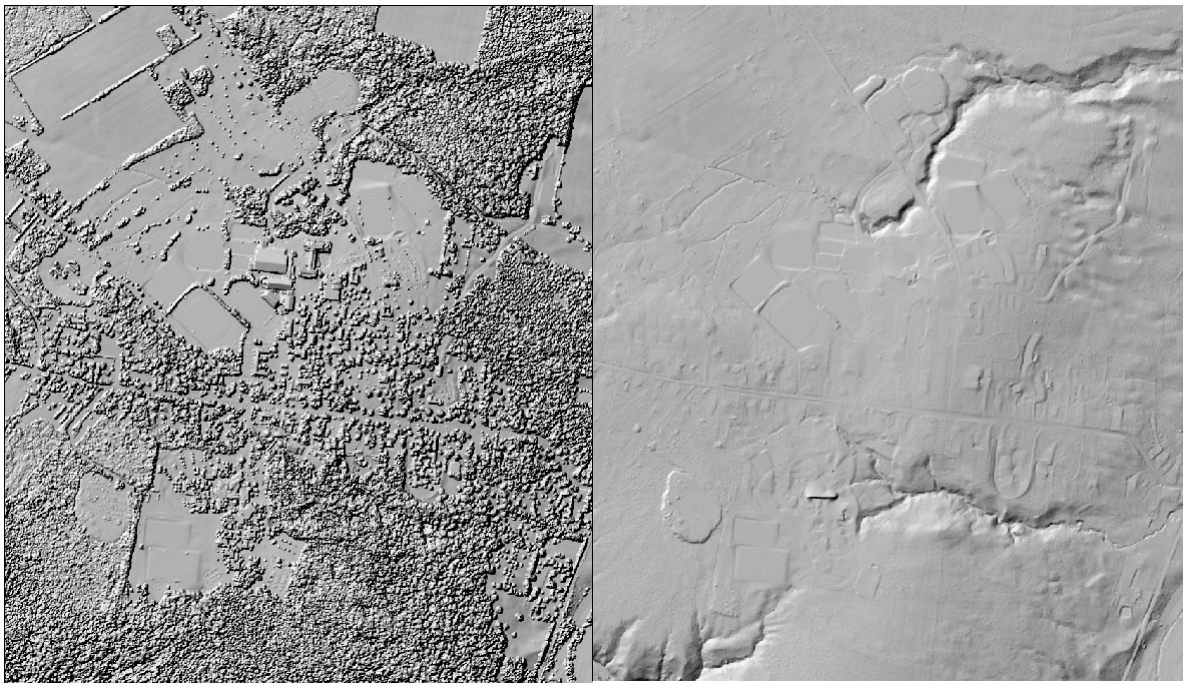

Hillshades derived from LiDAR first returns (left) and "bare earth" returns (right) of the Hamilton College campus area.

Intensity image derived from first return LiDAR data. Cell size is 2 meters and the intensity values are the mean of values in the BLOB intensity attribute recorded in the multipoint file. Raster created using point to raster tool from the multi-point file.

Geomicrobiology of a meromictic lake, Green Lake, Fayetteville, New York

Michael L. McCormick
Hamilton College, Clinton, NY 13323
mmccormi@hamilton.edu

INTRODUCTION

Meromictic lakes are composed of stratified non-mixing and geochemically distinct water bodies. The lack of annual turnover (*meromixis*) normally results in the depletion of oxygen in the bottom waters (*monimolimnion*) and a complementary limitation in nutrient return from sediments to surface waters (*mixolimnion*). Green Lake, located close to Fayetteville, New York, was the first meromictic lake described in North America (Eggleton, 1931). The earliest report of Green Lake (then named Lake Sodom) dates to 1839 in which the white marl that lines the shores and coats fallen trees was well described (Vanuxem, 1839). A decade later, the first qualitative geochemical assays of Green Lake confirmed the presence of hydrogen sulfide in the lake's bottom water (Clark, 1849). An excellent review of the early Green Lake literature, which spans 150 years, is provided by Thompson et al. (1990). This long record led Thompson to speculate that Green Lake may be the most well studied meromictic lake in the world. While this may be true with regard to the geology and limnology of Green Lake, much remains unknown about the lake's microbial ecology and biogeochemistry. Here I provide an overview of historic and recent work that addresses the relationship between Green Lake's microbial communities and its remarkable geochemical features. I also describe a low cost method developed for acquiring aseptic samples at high spatial resolution and present partial results from a survey of microbial community composition and geochemistry throughout the water column of Green Lake using this technique.

GEOLOGY AND LIMNOLOGY OF GREEN LAKE

Although the precise origins of Green Lake and its close neighbor Round Lake are debated, they are most commonly reported to have formed as waterfall plunge basins during the last glacial retreat (~13,000 years ago) (reviewed in Hilfinger and Mullins, 1997). The

basins of both lakes penetrate the Syracuse and Vernon formations and lie in an east-west oriented glacial melt water channel (Sissons, 1960). The lakes were privately owned until 1927, when the surrounding land was purchased by New York State to create Green Lakes State Park (New York State Office of Parks, 2004). Green Lake itself is shaped something like a comma, the central basin being nearly circular with a drainage channel to the northeast forming the comma's tail (Figure 1). The lake is 55 m at its deepest point, has a small surface area (0.26 km^2) and is surrounded by steeply rising hills to the northwest and southeast. These features (depth, small surface area and wind shelter) all contribute to the lake's meromixis. The lake's present elevation is 127 m, approximately equal to the Erie Canal, which lies just north of the park. The majority of recharge to Green Lake is comprised of ground water that enters the monimolimnion after percolating through the Syracuse

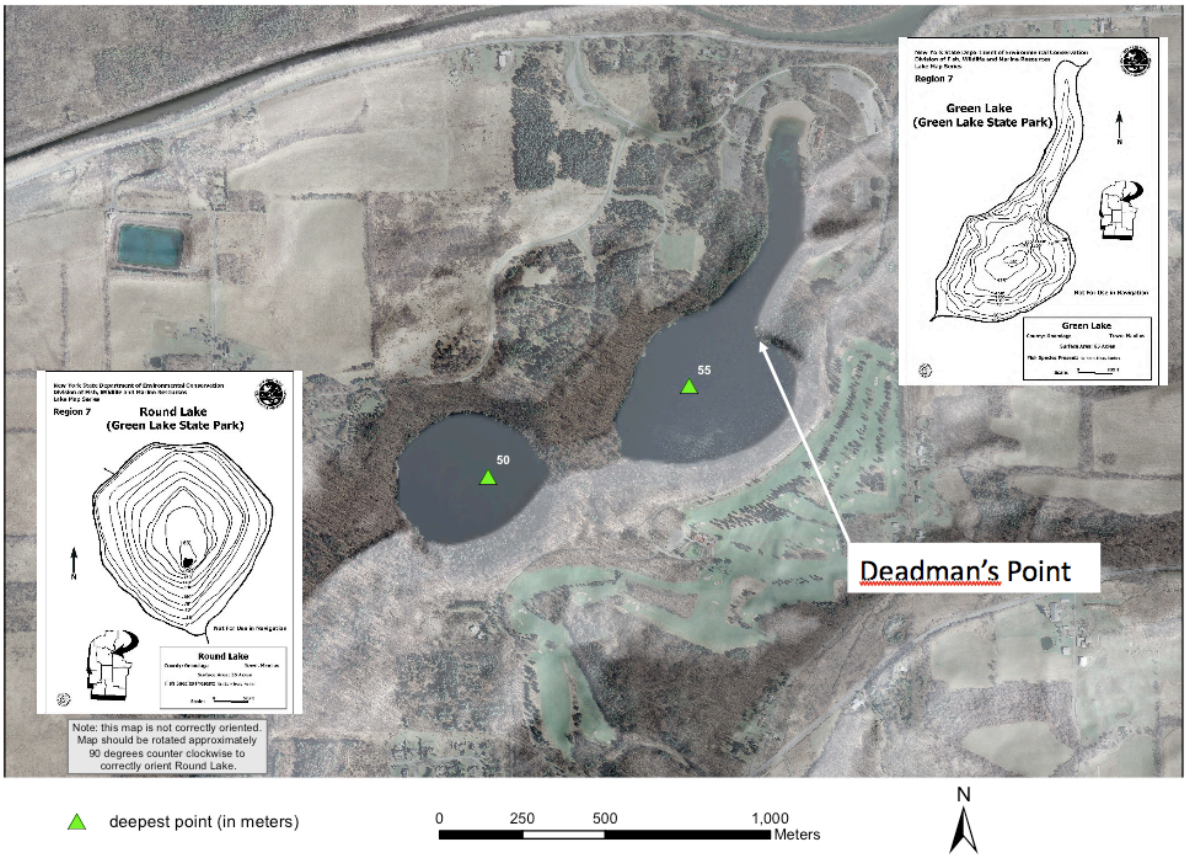

Figure 1: Satellite image of Green Lakes State Park showing Round Lake to the left and Green Lake on the right with the locations of the thrombolite at Deadman's Point and deepest water indicated. Inset bathymetric maps from the New York State Department of Environmental Conservation. Figure courtesy of Dave Tewksbury.

Formation and Vernon Shale. The ground water is saline and contains high concentrations of Ca^{2+}, Mg^{2+} and SO_4^{2-} attributed to the dissolution of dolomite ($CaMg(CO_3)_2$), gypsum ($CaSO_4$•H2O) and halite (NaCl) deposits (Thompson et al., 1990; Torgersen et al., 1981). This saline input sufficiently increases the density of the monimolimnion relative to the mixolimnion to establish stratification, thus Green Lake is a classic example of *crenogenic* meromixis (Bradley, 1929; Eggleton, 1956; Takahashi et al., 1968). To close hydrologic, isotopic and chemical balances on the lake, Takahashi et al. (1968) argued that a separate less saline ground water input must also enter the mixolimnion. A model of two ground water inputs was supported by the stratigraphic and sedimentological studies of Thompson et al. (1990) who suggested a shallow seep enters the mixolimnion along the Syracuse-Vernon contact (~10 m depth) and a deeper more saline input enters along the contact between the green and red units of the Vernon Shale (~18 m). This lower seep occurs at approximately the same depth as the *chemocline*, the transition zone lying between the mixolimnion and monimolimnion, marked by dramatic gradients in oxidized and reduced chemical species and a notable dense population of purple sulfur bacteria (Figure 2).

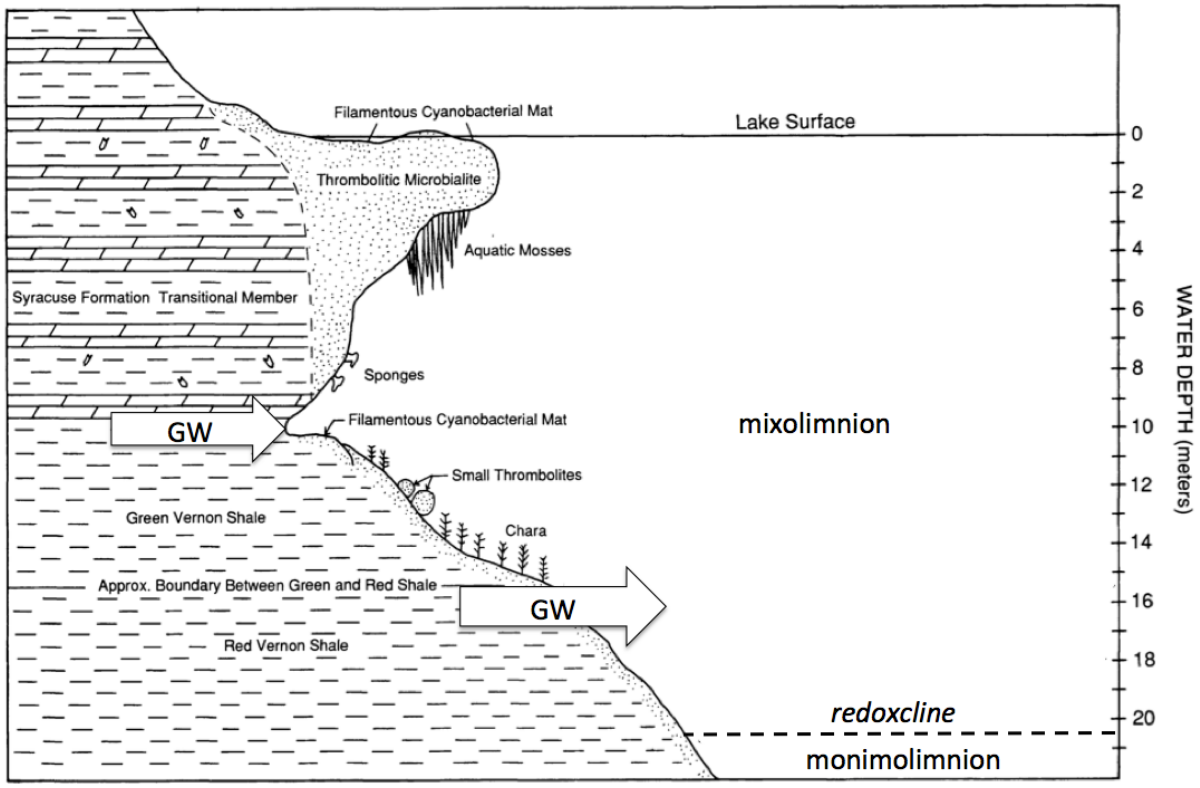

Figure 2: Profile of Green Lake at Deadman's Point illustrating local stratigraphy, points of suspected ground water entry and the present day position of the redoxcline. Figure modified from Thompson et al. 1990.

GEOMICROBIOLOGY OF GREEN LAKE

Early microbiological investigations of Green Lake relied on microscopic observations or culture based approaches (Bradley, 1929; Culver and Brunskill, 1969; Eggleton, 1956; Thompson et al., 1990). These studies established that a dense population of sulfur oxidizing phototrophs occurs at the chemocline (both purple- and green-sulfur bacteria) and that the cyanobacteria *Synechococcus* orchestrates an annual massive precipitation of calcite in the mixolimnion (termed the *whiting event*). They also showed that *Synechococcus* (and other cyanobacteria) are the dominant microbial constituents in Green Lake's calcareous bioherms (*thromobolites*).

One limitation of these prior studies was the use of culture dependent methods, which we now know miss the vast majority of microbial diversity in most natural environments (Amann et al., 1995). Recent studies have applied culture independent methods (largely DNA based) (Meyer, 2008; Meyer et al., 2011; Wilhelm and Hewson, 2012), but have been limited in spatial resolution (3-5 depths). Acquisition of aseptic samples at high spatial resolution is desirable as it permits detection of subtle changes in community composition, particularly across the chemocline where geochemical conditions change dramatically over short distances (<1 m). Given the time required to collect any single water sample, execution of a multi-level survey by repeated sampling raises the concern that the samples will not be truly contemporaneous. This could give rise to artifacts where diurnal cycles are coupled to shifts in microbial assemblage composition. To address this need we developed a low cost mulit-level sampling device to acquire synchronous aseptic samples for microbial and geochemical analysis at 0.25 m to 1.0 m resolution throughout the water column (up to 72 depths collected in one sample event). Below I describe this sampling method then discuss past and present studies of the major geomicrobial features of Green Lake adding results from our own work where relevant.

A low cost multi-level sampling device for aseptic synchronous sampling

The multi-level sampler is comprised of an anchored sampling tube held vertically in the water column to which sterile 60 ml disposable syringes are affixed (Figure 3). Windows are cut in the side of the tube at desired intervals. In Green Lake, we use 1.0 m intervals throughout the water column with additional 0.25 m intervals across the chemocline (16 to

24 m). The plunger of each syringe is predrilled to hold a pin that allows it to be locked while drawn under vacuum. The tip of each syringe is fitted with a short length of silicone tubing connected to a glass Pasture pipette that has been heat sealed at the tip and bent to create an elbow (Figure 3c). Prior to deployment, the syringes, tubes and tips are assembled and autoclaved, then carefully transported to the lake. As the sampling tube is deployed, the plunger of each syringe is pulled and locked under vacuum, a numbered float is then slipped over the pipette tip and the syringe is carefully attached to the sampling tube with the pipette tip passing through the window (Figures 3b and 3c). Once all syringes are deployed and the sampling tube is vertical (and at the correct depth), a messenger is dropped through the center of the tube. As the messenger drops it breaks each pipette tip at the elbow drawing water into the syringe. The elbow is positioned a few centimeters away from the hose to avoid contamination from the sampling hose. Once broken, the floats return the tips to the lake surface where we recover them (Figure 3d). As each float is uniquely coded we know precisely which depths have been acquired.

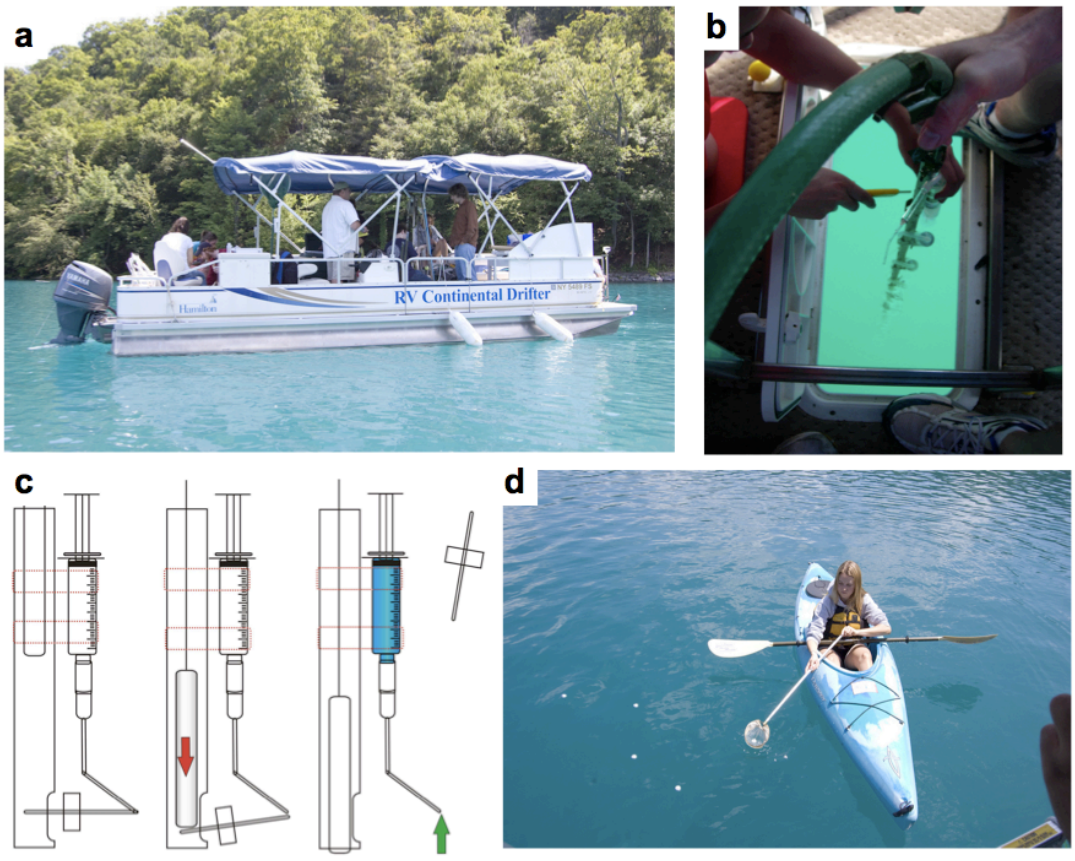

Figure 3: (a,b) Deployment and operation of the multilevel sampler. (c) Mechanism of sample collection. Sterile syringes are fitted with bent flame sealed glass Pasteur pipettes and deployed under vacuum. Each syringe is fitted with a numbered float. (d) Upon triggering, floats are collected to confirm water was collected at the target depth.

Green Lake's trophic structure

The first studies of the trophic structure of Green Lake reported an unusual absence of phytoplankton (other than the purple sulfur bacteria) (reviewed in Thompson et al., 1990). The zooplankton population exceeded phytoplankton 50,000 fold and skewed toward the chemocline, suggesting the use of purple sulfur bacteria as the primary food source (Culver and Brunskill, 1969; Jackson and Dence, 1958). However, the gut contents of lake copepods often show little evidence of purple sulfur bacteria and many instances of calcite ingestion (Brunskill, 1969; Fields, 1974). These perplexing observations were reconciled by the discovery of abundant small cyanobacteria belonging to the genus *Synechococcus* throughout the mixolimnion (Thompson et al., 1990; Thompson et al., 1997). The small size of the *Synechococcus* cells (0.5 μm) explained their omission in earlier phytoplankton surveys that expected to find algae, which are much larger. Furthermore, the nucleation and growth of calcite on the surface of *Synechococcus* cells explained the presence of high numbers of calcite crystals in the guts of copepods (see below) (Thompson et al. 1997).

Primary productivity in Green Lake was estimated at 290 g C/m^2 per year by Culver and Brunskill (1969) with 83% of this occurring in the chemocline mediated by purple sulfur bacteria (photolithoautotrophs that require sulfide for CO_2 fixation) (Thompson et al. 1990). Integrating over the entire lake, Pfennig (1978) estimated this accounts for 60 tons of carbon assimilation and 84 tons of hydrogen sulfide photoxidation per year! However, this is an underestimate of total sulfide oxidation as abiotic chemical oxidation of sulfide also occurs. Based on the distribution of major and minor sulfur isotopes at the chemocline, Zerkle et al. (2010) suggest a seasonal variation in dominance of biotic and abiotic sulfide oxidation processes. In the spring, prior to the annual whiting event when light penetration is greatest, the activity of anoxygenic phototrophs (purple and green sulfur bacteria) is at a maximum and sulfide oxidation is primarily biological. During and after the whiting event, when light is less abundant at the chemocline, abiotic oxidation of sulfide by molecular oxygen becomes dominant.

Calcite precipitation and the cyanobacteria *Synechecoccus*

The input of calcium ions from ground water into Green Lake results in supersaturation with respect to calcite throughout the water column (Takahashi et al., 1968; Brunskill, 1969).

This leads to two notable phenonmena, both of which involve calicite precipitation induced by cyanobacterial photosynthesis; an annual whiting event, in which *Synechococcus* cells induce the massive precipitation and export of calcite from the upper waters of the mixoliminum, and the formation of extraordinary thrombolytic reefs at select points along the shoreline.

Whiting events

Though Green Lake is supersaturated with respect to calcite at all depths (Brunskill, 1969), there appears to be insufficient driving force to permit precipitation by homogeneous nucleation. When precipitation does occur, it happens via heterogeneous nucleation on *Synechococcus* surfaces, catalyzed by calcium adsorption and epitaxial growth of calcite around each cell (Thompson et al., 1990; Thompson et al., 1997). The cell is not passive in this process. Indeed photosynthetic activity appears necessary to drive precipitation evidenced by two observations; 1) the majority of annual calcite precipitation forms in the mixolimnion (Figure 4a)(Brunskill, 1969) where *Synechococcus* populations are abundant, and 2) precipitation peaks during the summer months when photosynthetic activity is at a maximum (driven by longer daily light exposure and elevated epilimnion temperature) (Thompson et al., 1990; Thompson et al., 1997). The mechanism of calcite biomineralization, termed *photosynthetic alkalization*, involves a shift in the chemical equilibrium in the vicinity of the cell. As cells remove bicarbonate from solution they increase the local pH, which, in turn, shifts DIC speciation to favor CO_3^{2-} (Figure 4b). The co-localization of carbonate and Ca^{2+} (by adsorption) results in sufficient supersaturation to form calcite on the cell surface. This mechanism is supported by $^{13}\delta C$ measurements made by Takahashi et al (1968) of sediment calcite (-4 per mil) and mixolimnion DIC (-7 per mil). The difference in $^{13}\delta C$ is attributed to preferential uptake of ^{12}C during photoautotrophy, leaving ^{13}C enriched carbonate on the cell exterior (Thompson et al., 1990; Thompson et al., 1997).

Brunskill (1969) quantified the vertical distribution of calcite and total sedimentation rates during the annual whiting event. The highest suspended concentrations occurred at 5 m in June and July with the total suspended calcite load reaching 35 g/m^2. Annual sedimentation of calcite following each summer whiting event forms well preserved varves, with each calcite layer separated by darker organic detrital material. Sedimentation rates have

averaged 1 mm/year for the last 200 years (Hubeny et al., 2011). The thicknesses and chemical/isotopic composition of these calcite layers have been used, among other things, to establish a record of recent anthropogenic impacts on the Green Lake watershed and to assess regional trends in precipitation and drought during the late Holocene (Hilfinger et al., 2001; Hubeny et al., 2011).

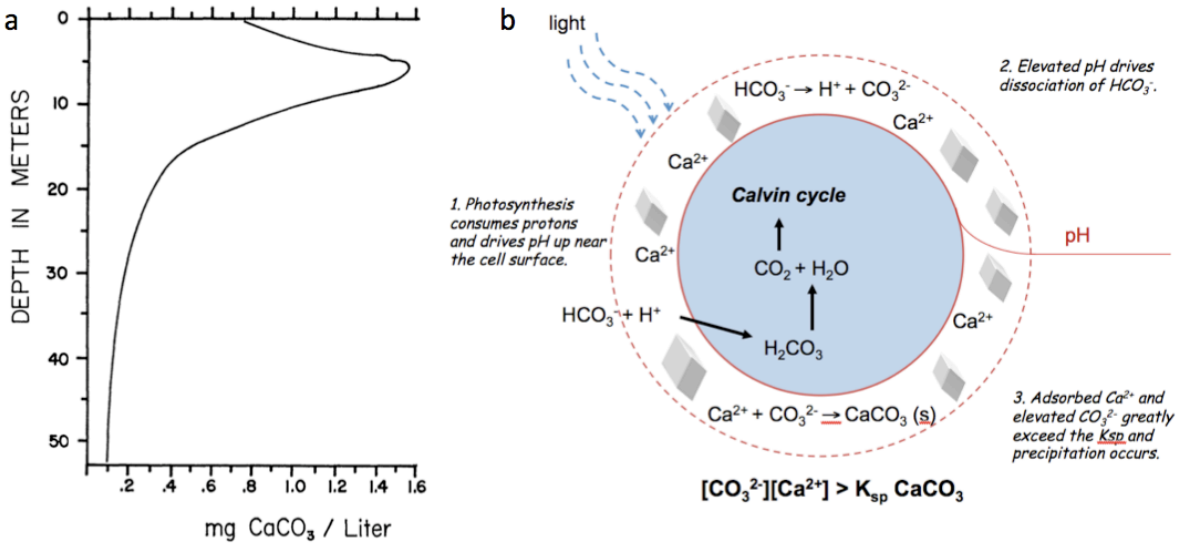

Figure 4: (a) Profile of suspended calcite concentration in late May, 1966 from Brunskill (1969). (b) Mechanism of calcite precipitation by photosynthetic alkalization. Figure modified from Thompson et al. (1997).

Green Lake thrombolites

Similar to stromatolites, thrombolites are a type of microbialite, organosedimentary deposits that grow through particle trapping or in-situ precipitation induced by cellular metabolism and nucleation on cell surfaces (Riding, 2011). Unlike stromatolites, thrombolites lack lamination and are "characterized by a macroscopic clotted fabric" (Aitken, 1967). As microbialites provide some of our earliest fossils dating to ~3.5 billion years ago (Allwood et al., 2009), examples of living microbialite systems are of great interest as they provide contemporary analogs for ancient ecosystems (Wilhelm and Hewson, 2012).

Although a few thrombolites grow along the north shore of Green Lake's central basin, the most impressive is that known as "Deadman's Point" located at intersection of the eastern shore of the central basin and the southern edge of the drainage channel (Figure 1). Extending approximately 10 m from the shore and reaching a depth of 10 m below the surface, this thromolite is significantly larger than any other in the park (Figure 2). The surface is now routinely exposed to air, the result of a 1 to 2 m drop in lake level in the early

1800's coincident with the opening of the local section of the Erie Canal (Thompson et al., 1990). Visual inspection of Deadman's Point while scuba diving shows the structure to be undercut by alcoves that lie at the contact between the lower dolostone bed of the Syracuse Formation and the green Vernon Shale (Thompson et al., 1990). Based on sedimentologic and stratigraphic evidence, Thompson et al. (1990) concluded that ground water enters the lake through these alcoves.

Recently, Wilhelm and Hewson (2012) examined the diversity of cyanobacteria in thrombolite surface samples collected at multiple water depths along north, west and south facing aspects of Deadman's Point. They observed high taxonomic richness, identifying 123 operationally defined taxanomic units (OTUs) based on automated ribosomal intergenic spacer analysis (ARISA). This is approximately four times the richness observed for cyanobacteria in Bahamian stromatolites (Foster et al., 2009). A general trend of increasing taxonomic richness and diversity was observed with depth, yet the highest similarity between communities on all faces of the thrombolite occurred at the greatest depth sampled (2 m). Likely drivers of diversity include variation in solar irradiation, temperature and habitat stability. Dissimilarities between assemblages at shallow depths were attributed to more frequent habitat disturbance and allochtonous inputs (e.g., rainfall, runoff and ice).

Interestingly, none of the dominant internally transcribed spacer lengths (the ARISA molecular fingerprints used to define each OTU) matched those expected for *Synechococcus* species, which clearly comprise the dominant cyanobacterial population in the mixolimnion (Wilhelm and Hewson 2012). This suggests that other, as yet unidentified, cyanobacterial populations contribute to thrombolite formation at Green Lake.

Green Lake chemocline and monimolimnion

A review of the Green Lake literature reveals some variation in the chemocline depth. This is attributable, in part, to inconsistent definitions. Eggleton (1956) did not use the term *chemocline* but he did describe the lake's characteristic chemical gradients. He reported that oxygen "dropped rapidly in concentration between the 15- and 20-meter depths and was never present in any demonstrable amount below 22 m" (Eggleton 1956, pp. 366). This description remains accurate today (Figure 5a). Takahashi et al. (1968) appears to be the first to use the term chemocline with regard to Green Lake, defining it (at 18 m) simply as the

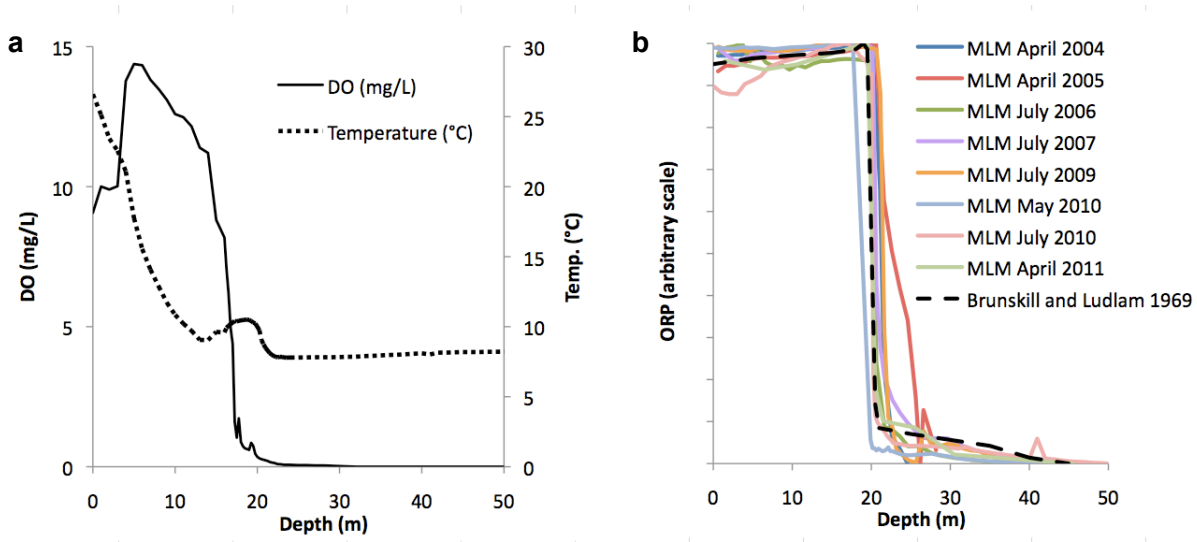

Figure 5: (a) Dissolved oxygen and temperature profiles in Green Lake for July 2008. The redoxcline was located at 20.5 meters. (b) Compilation of oxidation reduction potential measurements made between 2004 and 2011 compared to the measurement of Brunskill and Ludlam (1969).

depth that separates the mixolimnion from the monimolimnion. Using the same definition, Culver and Brunskill (1969) reported that the chemocline extended from 17.5 m to 20 m. However, geochemical profiles from 1974 and 1975 clearly show the chemocline at shallower depths with measurable methane at 15 m and elevated concentrations of methane and sulfide at 17 m (Torgersen et al., 1981). A slightly lower chemocline is indicated between 1985 and 1988 by reports of the purple sulfur bacterial plate (a layer of dense growth) between 16-18 m (Thompson et al., 1990). Recent studies from 2007 and 2008 used oxidation-reduction potential (ORP) to locate the chemocline at 20.5 m (Meyer et al., 2011; Zerkle et al., 2010), although this may more precisely be called the *redoxcline*. Comparing these reports with our surveys of ORP from 2004-2010 and that of Brunskill and Ludlum (1969) we see the redoxcline of Green Lake appears remarkably consistent (Figure 5b). Although Torgerssen et al. (1981) did not report ORP, the sulfide levels they measured assure the redoxcline must also have risen in the 1974-75 period. The cause of this apparent decades long rise and fall of the chemocline/redoxcline is not known. Although seasonal variations in the elevation of the lake occur (differences of ~20 cm have been observed by the author), these are insufficient to account for the relatively large shifts in the chemocline depth observed over the last 40 years.

The most impressive feature of the chemocline is the purple color caused by the high density of purple sulfur bacteria (less obvious are the green sulfur bacteria that live slightly

lower in the water column). The concentration of cells in the plate is so great (10^6 to 10^7 cells/ml) that virtually no light penetrates below the chemocline and solar absorption creates a thermal "bump" in the temperature profile (Culver and Brunskill, 1969) (Figure 5a).

The characteristics of the chemocline that make it an ideal habitat for purple sulfur and green sulfur bacteria are the abundance of light from above and the continuous provision of hydrogen sulfide from below. These nutritional requirements reflect the metabolic peculiarities of these bacteria, which are examples of anoxygenic photoautotrophs (organisms that use light to generate energy but do not produce oxygen). This process relies on photo-excitation and transport of electrons in closed circuits within photosynthetic reactive centers that ultimately drive production of adenosine triphosphate (ATP), the principal energy currency of life (Madigan et al., 2011). In addition to light, all autotrophs also require a source of electrons to assimilate inorganic carbon. This need arises from the fact that carbon, as it is found in CO_2, is fully oxidized (+IV oxidation state) and in order to form the carbon-carbon bonds comprising biological macromolecules a lower average oxidation state must be achieved. In oxygenic photosynthesis (the type of photosynthesis used by cyanobacteria and algae), the organism derives electrons for carbon fixation from the photo-driven oxidation of water (producing diatomic oxygen as a byproduct). As the electrons used for energy generation during anoxygenic photosynthesis remain in a closed circuit, they are not available for carbon fixation and an external source of reducing power is needed. This need is fulfilled by the oxidation of sulfide, producing zero-valent sulfur (S^0), which accumulates intracellularly or extracellularly depending on the species (Madigan et al., 2011).

The most notable features of the monimolimnion are the stable temperature and pH profiles, lack of light and the presence of reduced chemical species, particularly sulfide, which makes itself immediately apparent during sampling. In a recent study of sulfur isotope geochemistry in the monimolimnion, Zerkel et al. (2010) found evidence of sulfur disproportionation (SD) at and just below the chemocline. Thiosulfate, sulfite and zero valent sulfur (including polysulfides) are common substrates for bacterial sulfur disproportionation and are present in the chemocline and monimolimnion of Green Lake (Zerkle et al., 2010). Interestingly, gene sequences for *Desulfocapsa*, a bacteria capable of SD have been recovered from Green Lake (Meyer, 2008). In the case of zero valent sulfur

disproportionation, low ambient sulfide concentrations are required. Thus this mechanism may only be significant near the upper portion of the chemocline although the authors suggest syntrophic associations with sulfide consuming partners may make disproportionation favorable at greater depths (Zerkle et al. 2010). Such syntrophic associations have been speculated between *Desulfocapsa* sp. and the sulfide oxidizing phototroph *Lamprocystis* in lake Cadagno, Switzerland (Peduzzi et al., 2003; Tonolla et al., 2003).

Molecular approaches to characterizing Green Lake's microbial diversity

The earliest taxonomic identifications of bacteria in Green Lake relied on microscopy. Eggleton (1956) reported discovering the purple sulfur bacteria in 1935, identifying them as *Lamprocystis roseopersicina*. Subsequent studies identified *Chromatium*- and *Thiocystis*-like purple sulfur bacteria and the green sulfur bacteria *Chlorobium phaeobacteroides* (Culver and Brunskill, 1969). In a recent study of carotenoid biomarkers in Green Lake, Meyer et al. (2011) used clone library construction and 16s rRNA gene sequencing to characterize the bacterial community in two water samples (one in the chemocline and one in the monimolimnion). They found the purple sulfur bacteria and green sulfur bacteria respectively comprised 25% and 15% of the sequences recovered from the chemocline (20.5 m). Four phylotypes of purple sulfur bacteria were identified including some closely related to *Chromatium okenii* and *Thiocystis*. The green sulfur clones were related to *Chlorobium phaeobacteroides*, affirming the findings of the early microscopy studies. In contrast, the mixolimnion sequences from 25.0 m were dominated by bacteroidetes (27%), followed by sulfate reducing δ-proteobacteria (22%), and ε-proteobacteria (14%) (Meyer et al., 2011). These groups are common members of anoxic communities, representing a wide diversity of metabolic capabilities including substrate hydrolysis, fermentation and anaerobic respiration (Madigan et al., 2011). The ε-proteobacteria are particularly known for their versatility in mediating redox reactions with sulfur compounds (Campbell et al., 2006).

Small ribosomal subunit gene sequencing is a powerful tool for microbial diversity analysis, however, the time and cost of clone library construction made this an impractical choice for analyzing large numbers of samples in the recent past. Next generation high-

throughput sequencing methods such as the Illumina platforms have overcome this limitation (Logares et al., 2012). For our high-resolution surveys we used an alternative gene-based technique known as terminal restriction fragment length polymorphism (TRFLP). This approach involves the amplification of 16s rRNA genes from environmental samples via the polymerase chain reaction (PCR) using fluorescently tagged primers. The PCR products are then digested with restriction enzymes that cleave the sequences at specific sites. Finally the size and abundance of the terminal fragments (easily identified by their fluorescent tag) are quantified. In closely related organisms the 16S rRNA sequences are similar, therefore the restriction sites will occur at many of the same locations and similar terminal fragments will result. In distant relatives the terminal fragment sizes will differ. Thus the diversity of TRFLP peaks in a given sample reflects genetic diversity in the microbial community. The usefulness of combining of high-resolution sampling with low cost molecular finger printing is illustrated in Figure 6, which presents TRFLP results for 29 samples collected using the multi-level sampler in July of 2008. Note the stark contrast in community composition above and below the redoxcline (20.5 m). When TRFLP results are combined with clone library analysis, it is possible to assign putative identities to specific fragments at least at the class or order level (as shown in Figure 6). The magnitude of each peak provides a semi-quantitative measure of abundance, allowing us to visualize the distribution of specific groups such as the *Synechecoccus* population, which skews toward the chemocline before abruptly disappearing at the redoxcline. This pattern is similar to the skewed distribution of copepods reported by Culver and Brunskill (1969), suggesting that cyanobacterial harvesting may offer an additional explanation for the copepod distribution other than the grazing of purple-sulfur bacteria.

Final remarks

After 170 years of study, Green Lake continues to fascinate us. Most of this past work addressed the geologic and limnologic characteristics of the lake. With the advent of low-cost high-throughput sequencing, we are now able to interrogate the composition of microbial communities in ways that were impractical just a decade ago. Because it is an ideal natural laboratory, we are likely to see several new and exciting studies from Green Lake in the

decades ahead addressing complex links between biogeochemical dynamics, community composition and metabolic function that will have impact far beyond the bounds of the park.

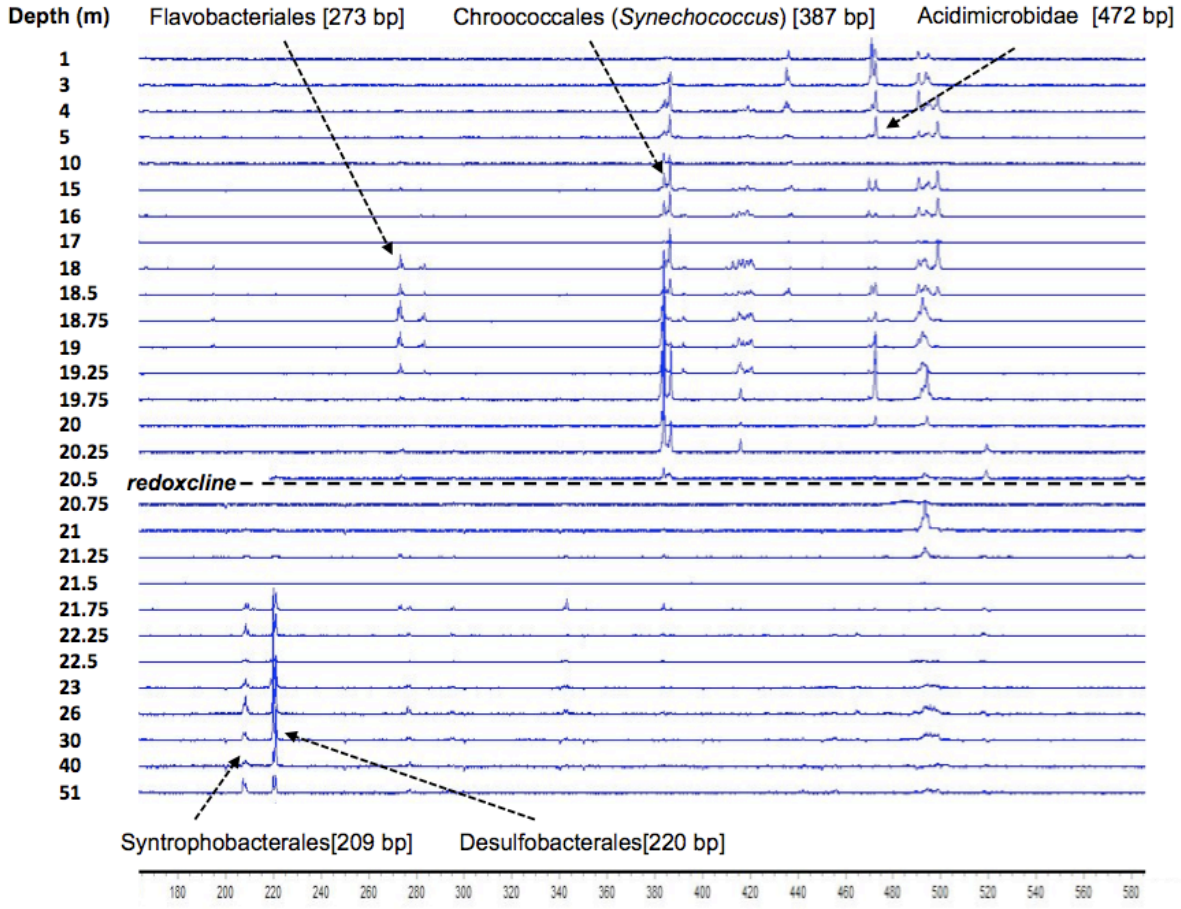

Figure 6: Example distribution of TRFLP identified taxonomic groups through the Green Lake water column. (6FAM labeled forward fragments from the Rsa1 digest of bacteria amplicons). Taxanomic assignments based on matching virtual digests of clone library sequences prepared at 13 depths (data not shown).

Acknowledgements

My thanks to the many students and collaborators who have worked with me on Green Lake: Nikola Baniski, Dr. Eric Boyd (Montanta State University), Falon Chipidza, Professor Eugene Domack (Hamilton College), Professor Jinnie Garrett (Hamilton College), Meghan Greisbach, Sean Linehan, Professor Lorraine Olendzenski (St. Lawrence University), Libby Penderey, Sarah Powell, Greg Ray, Amy Rumack, Valerie Valant, and Bruce Wegter. I am particularly thankful to the Green Lake State Park Manager Jim Semar and staff for providing access to the lake and for kindly permitting us to use park boats in support of our

work. Thanks also to David Tewksbury for preparing Figure 1 in this manuscript. Funding for this work was provided, in part, by NSF SGER grant ANT-0624020.

REFERENCES

Aitken, J.D., 1967, Classification and environmental significance of cryptalgal limestones and dolomites with illustrations from the Cambrian and Ordovician of southwestern Alberta: Journal of Sedimentary Petrology, v. 37, p. 1163-1178.

Allwood, A.C., Grotzinger, J.P., Knoll, A.H., Burch, I.W., Anderson, M.S., Coleman, M.L., and Kanik, I., 2009, Controls on development and diversity of Early Archean stromatolites: Proceedings of the National Academy of Sciences of the United States of America, v. 106, p. 9548-9555.

Amann, R.I., Ludwig, W., and Schleifer, K.H., 1995, Phylogenetic identification and in situ detection of individual microbial cells without cultivation: Microbiological Reviews, v. 59, p. 143-169.

Bradley, W.H., 1929, Algae reefs and oolites of the Green River Formation, *in* Survey, U.S.G., ed.: U. S. Geological Survey Professional Paper, p. 203-223.

Brunskill, G.J., 1969, Fayetteville Green Lake, New York ; [Part] 2, Precipitation and sedimentation of calcite in a meromictic lake with laminated sediments: Limnology and Oceanography, v. 14, p. 830-847.

Brunskill, G.J., and Ludlam, S.D., 1969, Fayetteville Green Lake, New York ; [Part] 1, Physical and chemical limnology: Limnology and Oceanography, v. 14, p. 817-829.

Campbell, B.J., Engel, A.S., Porter, M.L., and Takai, K., 2006, The versatile epsilon-proteobacteria: key players in sulphidic habitats: Nature Reviews Microbiology, v. 4, p. 458-468.

Clark, J.V.H., 1849, Onandaga; or reminisences of earlier and later times: Syracuse, New York, Stoddard and Babcock.

Culver, D.A., and Brunskill, G.J., 1969, Fayetteville Green Lake, New York. V. Studies of primary production and zooplankton in a meromictic marl lake: Limnology and Oceanography, v. 14, p. 862-873.

Eggleton, F.E., 1931, A limnological study of the frofundal bottom fauna of certain fresh-water lakes: Ecological Monographs, v. 1, p. 231-331.

—, 1956, Limnology of a meromictic, interglacial, plunge-basin lake: Transactions American Microscopical Society, v. 75, p. 334-378.

Fields, T.C., 1974, Vertical migration of Diaptomus sicilis Forbes in Fayetteville Green Lake: Syracuse, State University of New York.

Foster, J.S., Green, S.J., Ahrendt, S.R., Golubic, S., Reid, R.P., Hetherington, K.L., and Bebout, L., 2009, Molecular and morphological characterization of cyanobacterial diversity in the stromatolites of Highborne Cay, Bahamas: Isme Journal, v. 3, p. 573-587.

Hilfinger, M.F., and Mullins, H.T., 1997, Geology, Limnology and Paleoclimatology of Green Lakes State park, New York, *in* Rayne, T.W., Bailey, D.G., and Tewksbury, B.J., eds., Field Trip Guid for the 69th Annual Meeting of the New York State Geological Association, New York State Geological Association.

Hilfinger, M.F., Mullins, H.T., Burnett, A., and Kirby, M.E., 2001, A 2500 year sediment record from Fayetteville Green Lake, New York: evidence for anthropogenic impacts and historic isotope shift: Journal of Paleolimnology, v. 26, p. 293-305.

Hubeny, J.B., King, J.W., and Reddin, M., 2011, Northeast US precipitation variability and North American climate teleconnections interpreted from late Holocene varved sediments: Proceedings of the National Academy of Sciences of the United States of America, v. 108, p. 17895-17900.

Jackson, D.F., and Dence, W.A., 1958, Primary productivity in a dichothermic lake: The American Midland Naturalist, v. 59, p. 511-517.

Logares, R., Haverkamp, T.H.A., Kumar, S., Lanzen, A., Nederbragt, J., Quince, C., and Kauserud, H., 2012, Environmental microbiology thorugh the lens of high-throughput DNA sequencing: Synopsis of current platforms and bioinformatic approaches: Journal of Microbiological Methods, v. 91, p. 106-113.

Madigan, M.T., Martinko, J.M., Stahl, D.A., and Clark, D.P., 2011, Brock Biology of Microorganisms, Benjamin Cummings.

Meyer, K.M., 2008, Biogeochemistry of Oceanic Euxinia in Earth History: Numerical modeling and evaluation of biomarkers using modern analogs, The Pennsylvania State University.

Meyer, K.M., Macalady, J.L., Fulton, J.M., Kump, L.R., Schaperdoth, I., and Freeman, K.H., 2011, Carotenoid biomarkers as an imperfect reflection of the anoxygenic phototrophic community in meromictic Fayetteville Green Lake: Geobiology, v. 9, p. 321-329.
New York State Office of Parks, R., and Historic Preservation, 2004, New York's Heartland: The development of the state parks program in central New York 1925-1950, The Preservationist, Volume 8, p. 14-19.
Peduzzi, S., Tonolla, M., and Hahn, D., 2003, Isolation and characterization of aggregate-forming sulfate-reducing and purple sulfur bacteria from the chemocline of meromictic Lake Cadagno, Switzerland: Fems Microbiology Ecology, v. 45, p. 29-37.
Pfennig, N., 1978, General physiology and ecology of photosynthetic bacteria: New York, Plenum Press.
Riding, R., 2011, Microbialites, stromatolites, and thrombolites, *in* Reitner, J., and Theil, V., eds., Encyclopedia of Geobiology: Encyclopedia of Earth Sciences Series, Springer, p. 635-654.
Sissons, J.B., 1960, Submarginal, marginal and other glacial drainage in the Syracuse-Oneida area, New York: Geological Society of America Bulletin, v. 71, p. 1575-1588.
Takahashi, T., Broecker, W., Li, Y.H., and Thurber, D., 1968, Chemical and isotopic balances for a meromictic lake: Limnology and Oceanography, v. 13, p. 272-292.
Thompson, J.B., Ferris, F.G., and Smith, D.A., 1990, Geomicrobiology and sedimentology of the mixolimnion and chemocline in Fayetteville Green Lake, New York: Palaios, v. 5, p. 52-75.
Thompson, J.B., SchultzeLam, S., Beveridge, T.J., and DesMarais, D.J., 1997, Whiting events: Biogenic origin due to the photosynthetic activity of cyanobacterial picoplankton: Limnology and Oceanography, v. 42, p. 133-141.
Tonolla, M., Peduzzi, S., Hahn, D., and Peduzzi, R., 2003, Spatio-temporal distribution of phototrophic sulfur bacteria in the chemocline of meromictic Lake Cadagno (Switzerland): Fems Microbiology Ecology, v. 43, p. 89-98.
Torgersen, T., Hammond, D.E., Clarke, W.B., and Peng, T.H., 1981, Fayetteville, Green Lake, New York; (super 3) H- (super 3) He water mass ages and secondary chemical structure: Limnology and Oceanography, v. 26, p. 110-122.
Vanuxem, L., 1839, Third annual report of the geological survey of the Thrid District: Documents of the Assembly of the State of New York, Sixty-second Session, v. 5, p. 241-285.
Wilhelm, M.B., and Hewson, I., 2012, Characterization of Thrombolitic Bioherm Cyanobacterial Assemblages in a Meromictic Marl Lake (Fayetteville Green Lake, New York): Geomicrobiology Journal, v. 29, p. 727-732.
Zerkle, A.L., Kamyshny, A., Kump, L.R., Farquhar, J., Oduro, H., and Arthur, M.A., 2010, Sulfur cycling in a stratified euxinic lake with moderately high sulfate: Constraints from quadruple S isotopes: Geochimica Et Cosmochimica Acta, v. 74, p. 4953-4970.

Ironstones, condensed beds, and sequence stratigraphy of the Clinton Group (Lower Silurian) in its type area, central New York

Nicholas Sullivan
[nsullivan742@gmail.com]
Department of Geology, University of Cincinnati, Cincinnati, OH 45221-0013

Carlton E. Brett
[brettce@ucmail.uc.edu]
Department of Geology, University of Cincinnati, Cincinnati, OH 45221-0013

Patrick McLaughlin
[pimclaughlin@wisc.edu]
Wisconsin Geological and Natural History Survey, 3817 Mineral Point Rd., Madison, WI 53705

ABSTRACT

The fossiliferous and oolitic ironstones of the Clinton Group (Silurian, late Llandovery to early Wenlock) in central New York have inspired considerable interest since the early surveys of Eaton in the 1820s. Although these ores have never been mined on industrial scales, they were processed extensively up to the mid 1900s for oxides used in red paints. Three of these horizons, Westmoreland, "basal Dawes" or Salmon Creek, and Kirkland, will be examined and discussed on this excursion, with emphasis placed on their sedimentology, taphonomy, correlation, and regional significance in the context of depositional cycles.

Recent work has recast these classic deposits in the context of sequence stratigraphy, wherein ironstones and related phosphatic and shelly deposits are viewed as condensed facies: the product of siliciclastic sediment starvation during periods of rapid transgression at the bases of small- and large -scale depositional sequences. These strata and the environmental conditions they represent will also be considered in the context of recently collected geochemical and geophysical data, which have implications for the correlation of these sections and their importance with regard to regional and global environmental changes and bioevents.

1. INTRODUCTION

Although iron rich horizons in the sedimentary record are the subject of numerous studies, many critical questions remain concerning the processes of their formation (see Van Houten and Bhattacharyya, 1982; Kimberley, 1994 and references therein). Ferruginous strata of the lower Silurian (Aeronian-Sheinwoodian) Clinton Group in east central New York State feature prominently in this debate, owing to many excellent exposures and a rich history of study (e. g. Eaton, 1824; Vanuxem, 1839, James Hall, 1852, Smyth, 1918). These ores, commonly referred to as the "Clinton Ironstones", have never been mined on industrial scales, but they were processed extensively up to the mid 1900s as a source of red paint pigment (for a more comprehensive history see also Van Houten, 1991; Williams, 1998). Eight named ironstones are recognized within the Clinton Group; although these strata are of little economic importance today, they hold considerable stratigraphic, paleoecological, taphonomic, and sedimentological interest (e. g. Smyth, 1918; Gillette, 1947; Schoen, 1964; Brett et al., 1998; see Van Houten, 1991 for a detailed review). Three of the aforementioned eight ironstones will be featured in this field excursion through the classic type area of the Clinton Group, with considerations given to their history, stratigraphic significance, depositional conditions, and sedimentological features.

2. GEOLOGIC SETTING

2.1 Regional Structure

The regional architecture of Paleozoic sedimentary rock in the eastern United States is the product of several orogenic events occurring along the eastern margin of the Laurentian plate throughout the Phanerozoic (Root and Onasch, 1999; Ettensohn, 2008). Much of this bedrock is contained within the Appalachian Foreland Basin, a large structural and depositional province bounded by the Cincinnati, Findlay, and Algonquin Arches to the west and the Appalachian Highlands to the east (Figure 1a; Colton, 1970). In central and western New York, Silurian strata are exposed along a roughly east-west trending outcrop belt, running between Niagara and Schoharie Counties (Figure 1b), which marks the northern margin of the Appalachian Foreland Basin.

2.2 Early Silurian Tectonics and Paleogeography

Accretion of one or more island arcs onto the eastern margin of the paleocontinent Laurentia produced several episodes of mountain building during the Late Ordovician into the Early Silurian (Rodgers, 1970; Waldron and van Staal., 2001; Ettensohn and Brett, 2002; van Staal et al., 2007). These episodes of uplift, referred to collectively as the Taconic Orogeny, resulted in structural loading and subsidence in the Appalachian Basin, which was rapidly filled with clastics flushed off the newly formed mountain ranges (Beaumont et al., 1988; Ettensohn and Brett, 1998; Ettensohn, 2008). However, toward the end of the Rhuddanian, local orogenic activity had begun to taper off, commencing a period of relative tectonic quiescence that lasted until the end of the Telychian.

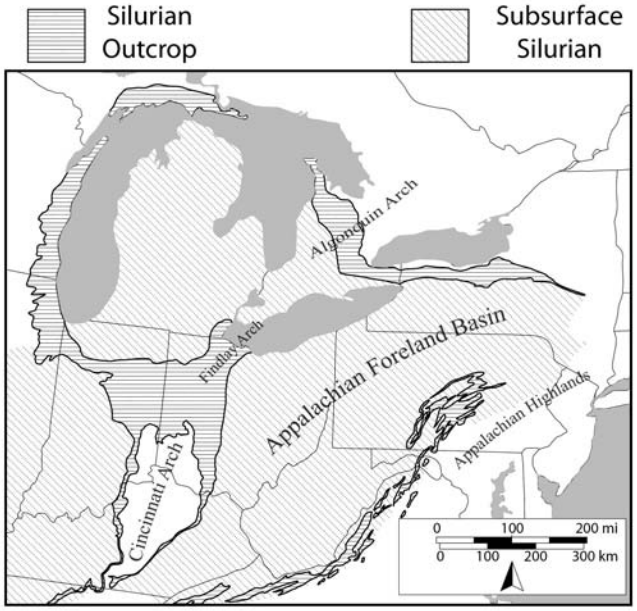

Figure 1a – Regional geographic map of the northeastern United States. Major structural features are labeled. Silurian outcrop is highlighted with horizontal lines; subsurface distribution of Silurian strata is highlighted in diagonal lines. Modified from Berry and Boucot, 1970.

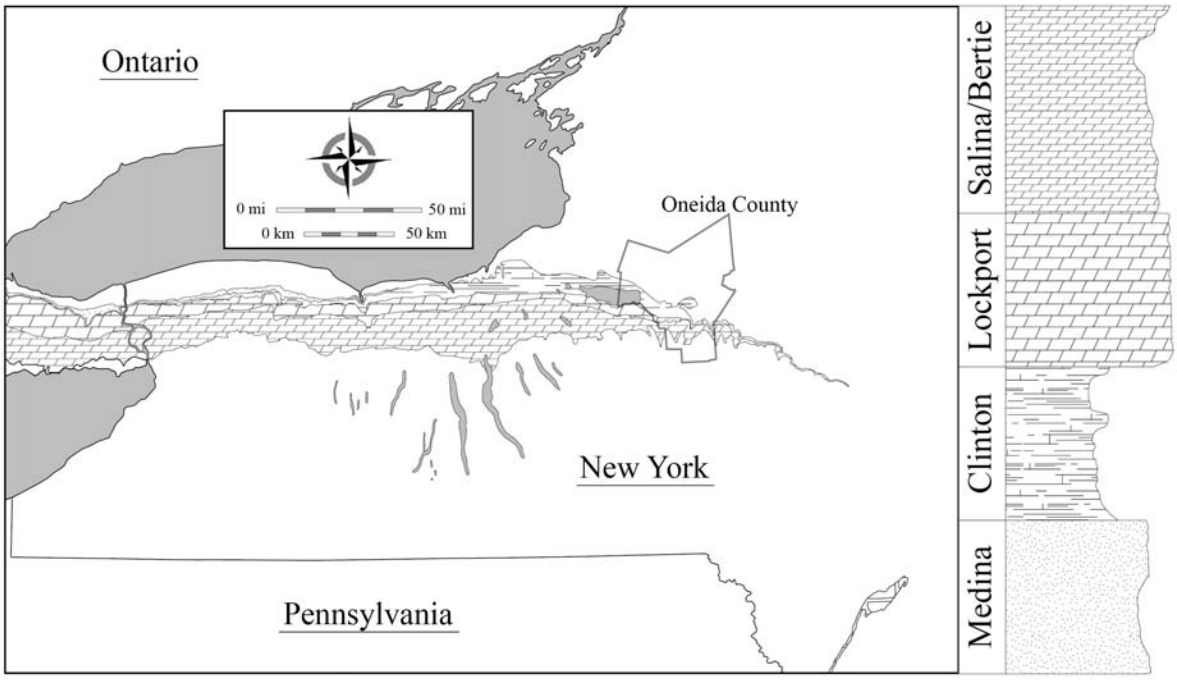

Figure 1b – Geologic map of upstate New York with Medina, Clinton, Lockport, and Salina/Bertie Groups highlighted (modified from Fisher et al., 1970). The outcrops featured in this excursion are located in Oneida County, which is outlined in black on this map.

At this time renewed tectonic loading caused the basin axis to migrate and form a new forebulge in the Appalachian Basin (Goodman and Brett, 1994; Ettensohn and Brett, 1998). This minor episode of uplift and erosion, termed the Salinic Disturbance, is recorded by the thick siliciclastic successions of the Upper Clinton Group in New York and the Shawangunk Conglomerate of southeast New York (Goodman and Brett, 1994; Ettensohn and Brett, 1998; Brett et al., 1998). These recurrent pulses of tectonic activity, followed by episodes of quiescence occurred lock-step with a lateral migration of the basin depocenter, a phenomenon that reflected the repeated flexure and relaxation of the crust (Goodman and Brett, 1994; Ettensohn and Brett, 1998).

The Clinton Ironstones were deposited in the Appalachian Foreland Basin starting in the Early Silurian following the end of the Taconic Orogeny; they were deposited sporadically at discrete time intervals up to, and during, the time of the Salinic Disturbance (see Brett et al., 1998). During this time, the Appalachian Foreland Basin was a topographic low within an epicratonic sea that covered the paleocontinent of Laurentia (Figure 2; Scotese and McKerrow, 1990; Cocks and Scotese, 1991). This depositional basin was bounded to the northwest by a carbonate bank and to the southeast by the much beveled Taconic Highlands (Figure 2; Scotese and McKerrow, 1990; Brett and Ray, 2005); strata now exposed in upstate New York were deposited in this region at approximately 20-30° south latitude (Cocks and Scotese, 1991). The internal architecture of the Appalachian Basin is inferred on the basis of widely traceable facies belts that show coarse siliciclastic dominated successions to the east, which grade westward into depositional environments dominated progressively by fine grained sediments and carbonates (Hunter, 1970; Brett et al., 1990; 1998).

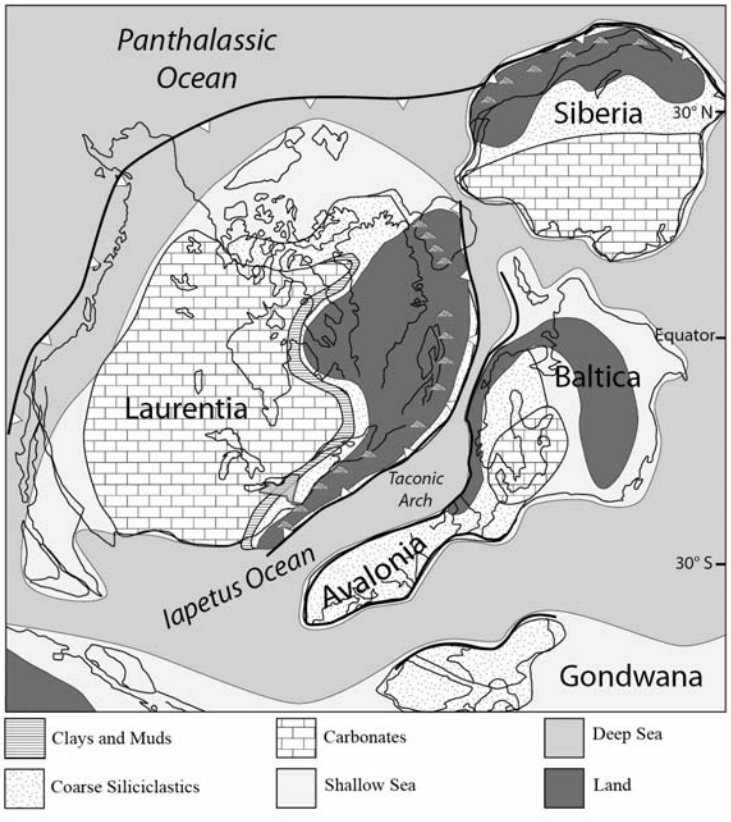

Figure 2 – Paleogeographic map of Laurentia during the Silurian with New York State highlighted. Modified from Scotese (1990), Cocks and Scotese (1991), and Brett and Ray (2005).

2.3 Climate and Oceanographic Conditions

The Early Silurian has traditionally been characterized as a period of climatic stability marked by high sea levels, extensive reef buildups, and widespread greenhouse climates (Copper and Brunton, 1991; Brenchley et al., 1994; Brunton et al., 1998; Veizer et al., 2000; Copper, 2002; Miller et al., 2005). However, a recent and ongoing resurgence of interest and study in the Silurian has characterized the time period as one of exceptional and unusual climatic, oceanic, and biotic trends (e. g. Jeppsson, 1990; 1997; Munnecke et al., 2003; McLaughlin et al., 2008; Cramer et al., 2011; McLaughlin et al., in review). Several short-lived episodes of cooling and glaciations have been documented through this interval on the basis of oxygen isotopes (Lehnert et al., 2010) and regional mapping of diamictites in South America (Caputo, 1998). Related to these climatic changes are widely documented oscillations in relative sea-level, which appear to reflect eustatic fluctuations (Johnson et al., 1998; Loydell, 1998; Brett et al., 2009). These sea level changes, together with tectonic uplift and subsidence, have produced widespread depositional sequences, which form a major theme of this trip.

Over the past few decades, high-resolution biostratigraphic studies of the Silurian have revealed widespread and severe biotic crises affecting a broad range of taxa around the world (Jeppsson et al., 1995; Jeppsson, 1997; Gelsthorpe, 2004; Eriksson, 2006; Manda et al., 2011). Many of these biotic events are closely coupled with strong shifts in the ratios of stable carbon isotopes (i. e. $\delta^{13}C$) recorded in marine carbonate rocks, which is thought to reflect dramatic and widespread fluctuations in marine circulation patterns, rates of primary productivity, and the efficiency of nutrient recycling (see Cramer and Saltzman, 2007 for a more detailed review). During this time, New York State was situated in the subtropics, where the shallow seas would likely have been subjected to consistently warm weather, with sharp annual variation in precipitation and powerful tropical storms. These warm, shallow waters were home to a rich and diverse fauna of epibenthic suspension feeders such as brachiopods, favositid and rugosan corals, bryozoans and echinoderms, which are present in great abundance throughout lower Silurian strata (e. g. Hall, 1852; Foerste, 1931; Gillette, 1947).

3. STRATIGRAPHY OF THE CLINTON GROUP

3.1 Overview

The Lower Silurian Clinton Group in east central New York is bounded at its base by the coarse siliciclastic successions of the Medina Group and at its upper contact by the carbonate

dominated Lockport Group (Fisher et al., 1970; Rickard, 1975). The name Clinton Group was proposed by Lardner Vanuxem in 1842, though Amos Eaton, working in 1824 made reference to "ferriferous slates" distributed throughout east central and western New York. The Clinton Group received numerous revisions and refinements from several authors working in the early twentieth century, notably Hartnagel (1907), Chadwick (1918), Goldring (1931), and Sanford (1935). Working primarily in Maryland, Ulrich and Bassler (1923) developed a detailed ostracod biozonation for lower Silurian strata of the Appalachian Basin. Given the relative paucity of zonally significant conodonts and graptolites in these successions, Ulrich and Bassler's zonation remains a primary standard for interregional correlation of Clinton Group strata to this day.

The lithostratigraphic nomenclature proposed by workers in New York and the ostracod biozonation of Ulrich and Bassler (1923) was integrated by Tracy Gillette in his 1947 publication *The Clinton of Western and Central New York*, a work of considerable scope. Gillette (1947) subdivided the Clinton Group into Lower, Middle and Upper subdivisions on the basis of lithology and ostracod faunas (Figure 3). He argued that an unconformity beneath the Upper Clinton

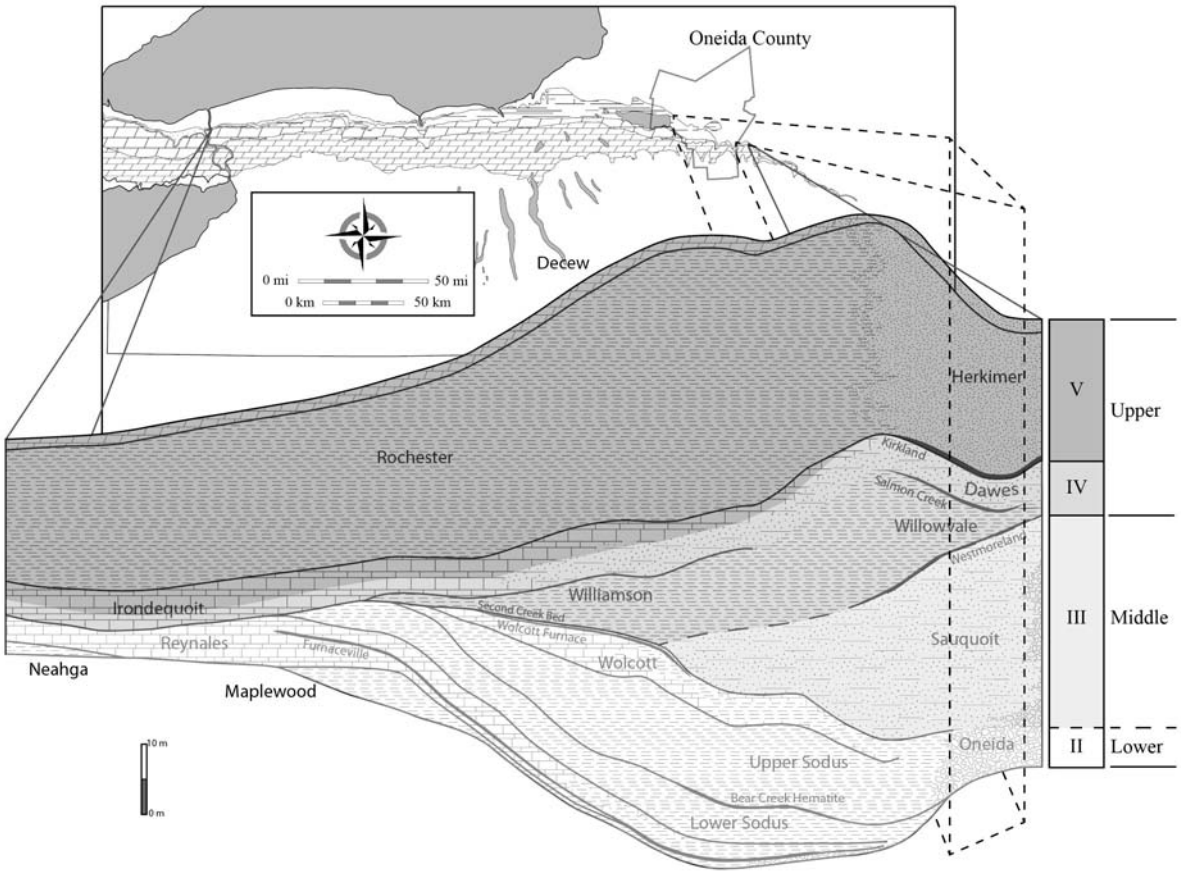

Figure 3 – Regional cross section, showing litho– and sequence stratigraphic relationships of the Clinton Group. Cross section modified from Gillette (1947) and Brett and others (1998). Map modified from Fisher and others (1970).

progressively truncates strata to the west; in the vicinity of Niagara Falls, much of the Lower Clinton and all of the Middle Clinton are missing (Gillette, 1947). Hunter (1970) further refined this stratigraphy, correlated strata to this reference standard along the Appalachian Basin as far as eastern Kentucky and Virginia, and emphasized the importance of ironstones as regional markers.

A sequence stratigraphic framework was erected for the Clinton Group by Brett and others (1990, 1998) who divided the unit into four unconformity-bound packages of genetically linked strata (Figure 3). They argued that many the ironstones distributed throughout the Clinton Group represent transgressive units overlying regionally angular unconformities (Brett et al., 1990). As such, they would represent deposition during times of sea-level transgression, when landward migration of depocenters, and sequestration of siliciclastic sediments in coastal area, caused a decrease in the amount of sediment reaching the basin and offshore sediment starvation. Brett and others (1990, 1998) subdivided the Silurian strata of New York State into seven or eight major, third -order sequences, termed S-I to S-VIII. Sequences S-III (the Sauquoit Formation of the Middle Clinton), S-IV (the Willowvale and Dawes Formations of the Upper Clinton), and S-V (the Kirkland Iron Ore and Herkimer Formations of the Upper Clinton) will be the focus of this trip.

3.2. Overview of Stratigraphic Units Exposed in the Type Clinton Area

Eight named rock units will be observed and discussed during this excursion. These units collectively comprise the Clinton Group as it is expressed in Oneida County; an idealized representation of this succession is shown in Figure 4. Each named unit is described briefly herein.

Oneida Conglomerate

Definition and Type Area - Defined by Vanuxem (1842) as the conglomeratic unit exposed in Oneida County

Thickness and Extent - The Oneida Conglomerate has been traced as far west as the Oswego River; to the east, it grades into thick undifferentiated siliciclastic successions. In the vicinity of Oneida County, it attains a maximum thickness of approximately 10 meters (30 feet)

Age - Late Aeronian to Middle Telychian (Brett et al., 1990)

Sequence Stratigraphy - S-II to lower S-III lowstand and transgressive systems tract (Brett et al., 1998)

Facies and Deposition Environment - Massive quartz pebble conglomerates are typical of the Oneida, but these are commonly interbedded with light grey sandstones and dark, clay shales. The coarser beds are generally cemented with silica.

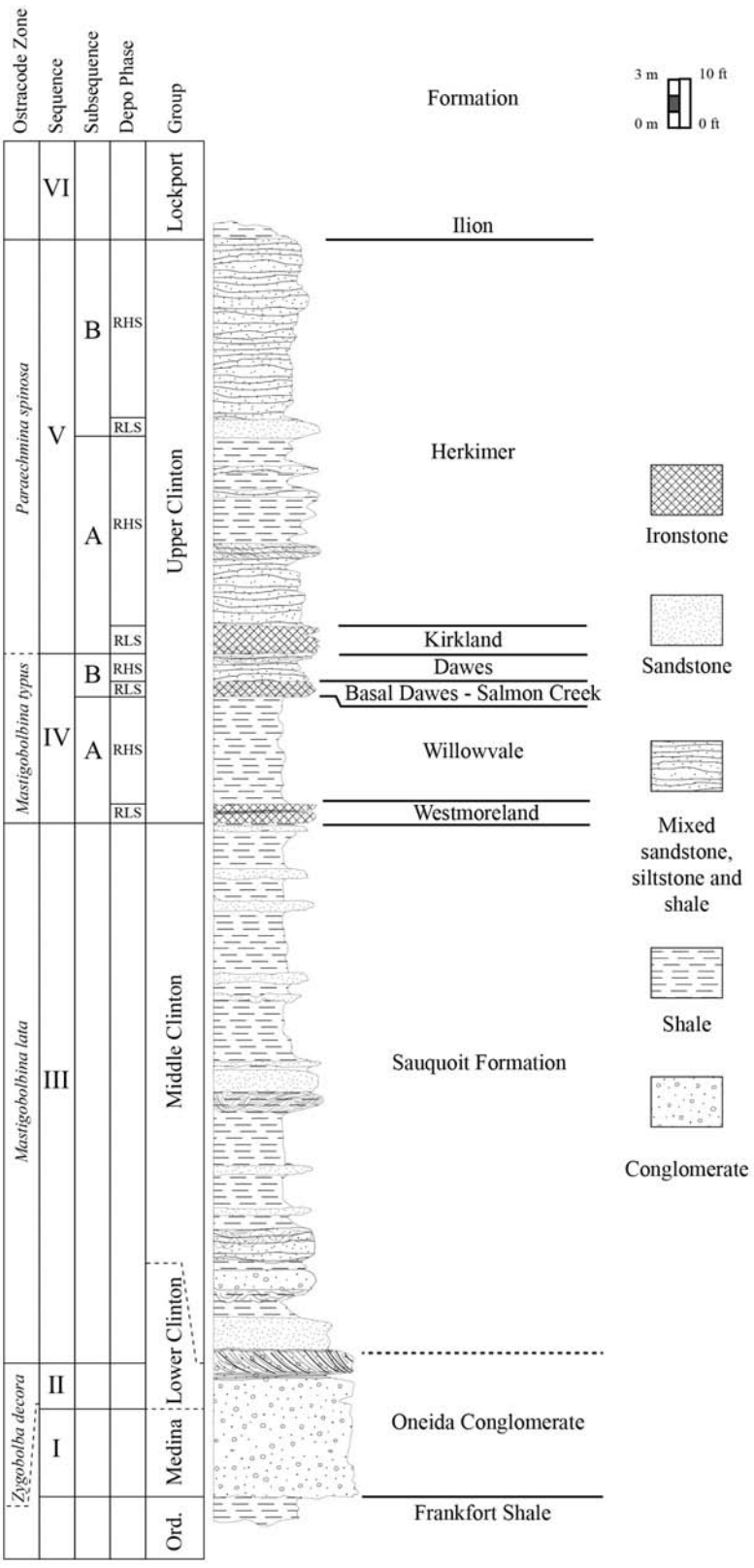

Figure 4 – Generalized stratigraphic column for the Clinton Group in east central New York with biozonations plotted (modified from Muskatt, 1972; Brett and Goodman, 1996).

Biostratigraphy -

Mastigobolbina lata Zone (Gillette, 1947)

Paleoecology - The Oneida Conglomerate is typically unfossiliferous. However, several shale and sandstone beds occurring near the top of the formation in the Clinton Area may yield a typical normal marine fossil assemblage that includes bivalves, brachiopods, and ostracodes.

Correlations

Thorold Sandstone of western New York (in part; Gillette, 1947)

Shawangunk Formation of southeastern New York (Willard, 1928)

Possibly much of the Lower Clinton Group in western New York (Brett et al., 1990)

Sauquoit (Shale) Formation

Definition and Type Area – Defined as all sandstone and shale beds between the Oneida conglomerate and the Westmoreland Hematite at Swift Creek, the type section, which is just north of the hamlet of Sauquoit (Chadwick, 1918)

Thickness and Extent – The Sauquoit attains its maximum thickness of approximately 27 m (90 feet) near Verona Station; the Sauquoit thins dramatically to the west and pinches out somewhere between the towns of Fulton and Wolcott, NY (Gillette, 1947)

Age – middle Telychian (C-5 of Berry and Boucot, 1970; see Brett et al., 1998)

Sequence Stratigraphy - Sequence III highstand (Brett et al., 1998)

Facies and Depositional Environment – The Sauquoit Formation is predominantly greenish to bluish gray shales with interbedded sandy limestones, calcareous sandstones, and conglomeratic horizons.

Biostratigraphy –

Eocoelia sulcata brachiopod Zone (Gillette, 1947; Brett et al., 1998)

Mastigobolbina lata ostracod Zone (Gillette, 1947)

Pterospathodus amorphognathoides conodont Zone (Rexroad and Richard, 1965)

Pterospathodus celloni Zone (Kleffner, pers. comm. in Brett et al., 1998)

Pterospathodus amorphognathoides Zone conodonts were reported by Kleffner (pers. comm. in Brett et al., 1998) from dolomitic sandstones at the base the Westmoreland Formation.

Paleoecology – The fossil assemblages of the Sauquoit formation are distinct from those of over- and underlying units (Gillette, 1947). Bivalves are the dominant macrofossils, though brachiopods and gastropods are also common. Ostracodes are also present in

great abundance and many of them are biostratigraphically useful, at least within the Appalachian Basin. The lower Sauquoit contains fine- to medium- grained interbedded sandstones and conglomerates that display hummocky cross stratification, well defined sole marks, and hummocky to symmetrical ripples (Muskatt, 1972). These indicate deposition within shallow storm wave base, at perhaps 10 to 30 m depths; sands and well rounded quartz pebbles were transported offshore from proximal sources, perhaps Taconic terranes re-uplifted in early phases of the Salinic Orogeny. The mixture of quartz pebbles with phosphatic nodules including fossil steinkerns at three or more levels within the Sauquoit indicates that some of these pebbly beds reflect remaining sediments associated with prolonged periods of sediment starvation. Abundant phosphates may reflect inputs from fluvial sources or possibly upwelling in the narrow Sauquoit foreland basin. The Sauquoit passes eastward gradationally with red sandstones and conglomerates of the Otsquago Formation within about 60-70 km of the study area; the latter reflect near-shore, possibly tidal deltas to non-marine sediments. The presence of abundant *Eocoelia* brachiopods in some beds of the Sauquoit suggests a BA-2 (*Eocoelia* community of Ziegler, Cocks and Bambach (1968). However, some portions of the Sauquoit contain more typical offshore biotas, including dalmanitid trilobites, suggesting possibly deeper water conditions.

Correlations –

Otsquago Sandstone of central New York (Gillette, 1947; Brett et al., 1998)

Center Member of the Rose Hill Formation of Pennsylvania (Brett et al., 1998)

Westmoreland Iron Ore

Definition and Type Area – The dark red, oolitic, hematitic iron ore exposed at Roaring Brook, which is the informal name given to a small tributary of Oriskany Creek approximately half a mile east of Lairdsville in the town of Westmoreland, Oneida County (Gillette, 1947).

Thickness and Extent – The Westmoreland Iron Ore is approximately 70 centimeters thick at its type section, it reaches its maximum thickness in the vicinity of Clinton, where it may reach up to 80 centimeters in thickness. Exposures of this unit are scarce outside of Oneida County though a thin phosphatic and glauconitic zone containing some hematite has been recognized at the top of the Sauquoit Formation in drill cores taken east of Oneida Lake (Gillette, 1947).

Age – Late Telychian (Rickard, 1975; Brett et al., 1998); Early Sheinwoodian (McLaughlin et

al., in review)

Sequence Stratigraphy - Relative lowstand (=lowstand to early transgressive systems tract) of subsequence IV-A (Brett et al., 1998)

Facies and Depositional Environment – The Westmoreland Iron Ore is a dark red ironstone composed primarily of rounded, sand sized grains that display concentric laminae, textures that have been characterized as oolitic (Smyth, 1918; Gillette, 1947). The lower contact of the Westmoreland is sharp, and the upper contact contains large, symmetrical ripple marks. The unit may also contain rip-up clasts, apparently derived from underlying strata. At some sections, the Westmoreland Iron Ore contains a thin tongue of dark gray shale. The latter contains fossils, including brachiopods and graptolites. This juxtaposition of evidently high energy and low energy, dysoxic facies is difficult to reconcile. Baird and Brett (1986) reported similar ripple-like features interbedded with black shale in the Leicester Pyrite, another transgressive lag deposit but in that case conditions were evidently dysoxic to anoxic. In the case of the Westmoreland, the presence of hematitic ooids indicates well oxygnated conditions at least episodically on the seafloor. It is possible that the ooids were originally chamosite and thus represent mildly reducing conditions in the sediment. However, the presence of large ripple forms in red hematite indicates that these ooids were subsequently reworked and concentrated under fully oxic and intermittently high-energy conditions, possibly forming submarine shoals or bars. The interbedded dark shale could record preservation of dysoxic lagoonal or intershoal muds. However, the fauna, including monograptid graptolites, suggests an offshore setting (BA 3 to 4). It is possible that the dark shale represents a remnant of highstand muds associated with a small scale (high frequency) depositional sequence; in this case true deepening to muddy out shelf conditions occurred following the initiation of the larger scale (3rd order) transgression. A second lowering of base level may have removed much of the shale and stacked a younger, transgressive oolitic hematite onto the erosion surface.

Biostratigraphy –

Stimulograptus clintonensis (formerly assigned to *Monograptus clintonensis*) was reported by Gillette (1947); however, this report has not been confirmed. All specimens studied by Loydell et al. (2007) from the overlying Willowvale Shale turned out to be the long-ranging *Monograptus priodon.*

Retiolites geinitzianus venosus, a graptolite typical of the Williamson Shale and characteristic of late Llandovery faunas, was reported by Gillette (1947) from the

Westmoreland shale tongue.

Palaeocyclus rotuloides (Gillette, 1947)

Mastigobolbina typus Zone (Gillette, 1947)

Paleoecology – In contrast to the other ironstones in the region, the Westmoreland Iron Ore is sparsely fossiliferous. Nearly all fossils reported from the unit are found within the black shale interbed described above. This fossil assemblage is noted for its similarity to that of the overlying Willowvale (Gillette, 1947).

Correlations –

Second Creek Phosphate Bed of west-central New York State on the basis of similar faunas and seemingly transitional phosphatic nodule beds underlying the Williamson in drill cores recovered from near Syracuse (Gillette, 1947; Lin and Brett, 1988; Eckert and Brett, 1989; Brett et al., 1998). However, this correlation has not been substantiated by subsequent biostratigraphic work (see Kleffner, pers. comm. in Brett et al., 1998; Loydell et al., 2007).

Merritton Limestone of Ontario (Brett et al., 1998). However, this unit underlies the Second Creek Phosphate Bed, making this correlation unlikely for the reasons described above.

Ferruginous limestones bearing *Palaeocyclus* at the base of the Upper Shaly Member of the Rose Hill Shale in Pennsylvania (Brett et al., 1998).

Willowvale Shale

Definition and Type Area – The term Willowvale was introduced by Gillette (1947) to include the blue grey shales between the Westmoreland and the Kirkland Iron ores, or the base of the Dawes Sandstone where it is present. As a type locality he designated a small, east-flowing tributary of Sauquoit Creek, informally referred to as "The Glen" or "Willowvale Creek" in the town of Willowvale, New York (Gillette, 1947).

Thickness and Extent – The Willowvale Shale is approximately 6.7 m (22 feet) thick at its type section, a value that remains consistent where typical Willowvale is exposed (Gillette, 1947). The unit is not found west of Oneida County, though its proposed lateral equivalent, the Williamson Formation, has been traced as far as Niagara County (Gillette, 1947; Brett et al., 1990). The Willowvale grades eastward into large, undifferentiated sections of coarse clastics (Gillette, 1947).

Age – Late Telychian (Brett et al., 1998), Early Sheinwoodian (McLaughlin et al., in review)

Sequence Stratigraphy – Relative highstand of subsequence IV-A (Brett et al., 1998)

Facies and Depositional Environment – The Willowvale Formation is predominantly dark gray to purple, thin bedded shales with calcareous sandstone and argillaceous, shelly limestone interbeds. The unit is interpreted as the product of proximal deposition in relatively shallow and well oxygenated environments (Eckert and Brett, 1989). The presence of siltstones and silty carbonates with small scale hummocky cross lamination and tool marks suggests at position near storm wave base.

Biostratigraphy –

Ancyrochitina gutinica (Loydell et al., 2007)

Conochitina proboscifera (Loydell et al., 2007)

Mastigobolbina typus Zone (Gillette, 1947)

Monograptus priodon (Loydell et al., 2007), reported as *Monograptus clintonensis* (Gillette, 1947)

Palaeocyclus rotuloides (Gillette, 1947)

Pterospathodus amorphognathoides Zone (Kleffner, pers. comm. reported in Brett et al., 1998)

Paleoecology – The Willowvale Shale has a rich and varied fossil fauna that is noted for its unusual co-occurrence of disparate taxa not known to inhabit similar depositional environments; graptolites, cephalopods, bryozoans, corals, and brachiopods are all commonly found (Gillette, 1947). Eckert and Brett (1989) characterized the Willowvale fauna in easternmost outcrops as a near-shore benthic assemblage (BA-2 to 3 of their terminology) dominated by *Eocoelia.* However, in the Clinton area, the occurrence of a diverse fauna with *Dicoelosia, Skenidioides, Eoplectodonta* and rare *Costisticklandia* indicate a BA 4-5 position (Eckert and Brett, 1989). This fauna shows affinities with that of the Williamson Formation to the west, a relationship also noted by Gillette (1947). The lower part of this unit and the underlying Westmoreland Iron Ore contain abundant specimens of the solitary coral *Palaeocyclus rotuloides,* an unusual, button-shaped coral found in coeval sections worldwide (Duncan, 1867; Gillette, 1947; Ehlers, 1973; Munnecke et al., 2003). The widespread, but stratigraphically narrow occurrence constitutes a useful marker, representing a global epibole of this unusual organism. Rare *Palaeocyclus* have been found in what appear to be transitional facies the lower Williamson-Westmoreland as far west as Syracuse, NY. The near-simultaneous invasion of what may have been a deep-water coral into shallow seas on several continents may reflect a response to elevated sea level and incursion of cool and perhaps dysoxic water masses onto the craton during the strong and rapid late Telychian

transgression (locally Sequence IV TST).

Correlations –

Williamson Formation of west-central New York has been correlated with the lower Willowvale Shale and both units have yielded diagnostic *Mastigobolbina typus* Zone ostracodes (Gillette, 1947; Lin and Brett, 1988; Eckert and Brett, 1989; Brett et al., 1990; 1998). However, graptolite and conodont work suggests that the basal Williamson may actually be older than the lower Willowvale, belonging to the *Pt. amorphognathoides angulatus* Zone (Rexroad and Richard, 1965; Loydell et al., 2007).

Upper Shaly Member of the Rose Hill Formation of Pennsylvania, which contains the diagnostic ostracod *Mastigobolbina typus* (Brett et al., 1998)

Salmon Creek ("Basal Dawes") Bed

Definition and Type Area – The term "Salmon Creek Bed" was proposed by Lin and Brett (1988), who established the type section at Salmon Creek West, approximately 50 meters south of NY route 104 in the town of Williamson, Wayne County, New York. In its type area, the Salmon Creek Bed is a phosphatic, quartz bearing conglomeratic bed that separates the Irondequoit Formation from the underlying Williamson (Lin and Brett, 1988). However, this unit was correlated eastward to a cross-bedded, impure hematitic sandy carbonate referred to in some publications as the "basal Dawes bed" (Lin and Brett, 1988; Eckert and Brett, 1989; Brett et al., 1998).

Thickness and Extent **–** The Salmon Creek Bed has been traced from Tryon Park in Rochester New York, to the Clinton Type Area (Lin and Brett, 1988). Although this unit is only a few centimeters thick at its type locality in northern Wayne County, it reaches a thickness of 80 centimeters in Oneida County. The Salmon Creek Bed has been traced eastward at least to Ohisa Creek in Herkimer County (Zenger, 1971; Brett, pers. observation)

Age **–** Late Telychian (Brett et al., 1998); Late Llandovery to early Wenlock (Lin and Brett, 1988); Early Sheinwoodian (McLaughlin et al., in review)

Sequence Stratigraphy **–** Relative lowstand (LST to early TST) of subsequence IV-B (Brett et al., 1998).

Facies and Depositional Environment – The Salmon Creek Bed in the Clinton type area is characterized as a crossbedded, sandy dolostone with locally abundant stringers of hematite and phosphate nodules (Brett and Goodman, 1996). The unit has a sharp base, which is interpreted as an erosive contact.

Biostratigraphy –

Upper *Mastigobolbina typus* Zone (Gillette, 1947)

Pterospathodus amorphognathoides amorphognathoides Zone (Loydell et al., 2007)

Paleoecology – Stalked echinoderm fragments are the dominant component of the Salmon Creek Bed. This, coupled with observations of sedimentary structures such as cross stratification, suggest the bed was deposited in a relatively high energy, well oxygenated environment similar to the Kirkland Formation (see below).

Correlations –

Basal bed of the Keefer Sandstone in Pennsylvania, Maryland, Virginia, and Tennessee (Brett et al., 1998)

Salmon Creek Phosphate Bed of central-western New York (Lin and Brett, 1988)

Dawes Formation

Definition and Type Area – The Dawes Formation is defined as the dolomitic sandstones, siltstones, and shales found between the top of the Willowvale Shale and the base of the Kirkland Iron Ore; the designated type locality is Dawes Quarry creek, a westward flowing stream in the village of Clinton (Gillette, 1947).

Thickness and Extent – In his original description of the Dawes Sandstone, Gillette (1947) suggested that it was restricted to the area between College Hill Creek in Clinton and the unit's type locality at Dawes Quarry Creek, where it is approximately 2.5 meters thick. At localities further to the east, the overlying Kirkland Iron Ore rests directly on mudstones that have been referred to as the upper Willowvale Shale (Gillette, 1947). However, at localities to the west, other authors have recognized the position of the Dawes-Rockway interval based on the presence of a basal hematitic, pyritic and phosphatic carbonate bed, the Salmon Creek equivalent (Lin and Brett, 1988).

Age – Late Telychian (Brett et al., 1998); Late Telychian to Early Sheinwoodian (Brett and Goodman, 1996); Early Wenlock (Lin and Brett, 1988), Early Sheinwoodian (McLaughlin et al., in review)

Sequence Stratigraphy – Relative highstand of subsequence IV-B (Brett et al., 1998); late highstand to falling stage of third-order Sequence IV.

Facies and Depositional Environment – The Dawes Sandstone is predominantly light gray, slightly calcareous sandstones. Gillette (1947) describes the bed as irregularly bedded, and very cross-bedded, though finely laminated siltstones and sandstones characterize the unit at some localities (e. g., Theime Gulf). On the basis of these sedimentary

structures, the rarity of normal marine fossil assemblages, and the limited extent of this unit, Gillette (1947) hypothesized that this unit may represent a small delta deposit. Several sections of the Dawes Sandstone contain a zone of deformed calcareous sandstones and shales just below the overlying hematitic unit. These beds are interpreted as the product of soft sediment deformation, possibly formed by seismic activity.

Biostratigraphy –

Mastigobolbina typus Zone (inferred by Brett et al., 1998; though no ostracodes have been reported directly from this unit)

Pterospathodus amorphognathoides Zone (inferred by Brett et al., 1998; though no conodonts have been reported directly from this unit)

Paleoecology – In contrast to the hematitic beds that bracket this unit, the Dawes Sandstone contains very few fossils, though occasional, fragmentary remains of brachiopods, gastropods, and cephalopods have been reported (Brett and Goodman, 1996). Like the Sauquoit, the Dawes Sandstone shows evidence of deposition in shallow, storm influenced waters. Fossils, other than burrows are generally scarce but some bedding planes are covered with *Strophochonetes cornutus*, which is viewed as an opportunistic shallow water species. The lenticular fine sandstones of the Dawes may represent offshore sandbars. Their rapid accumulation on mud may have produced substrate instability that, in the presence of seismic shocks may have resulted in extensive foundering of ball and pillow masses (seismites). The presence of abundant small brachiopod *Clorinda*, together with *Skenidioides* and *Dicoelosia* suggests BA-4 to 5 positions. However, the occurrence of small ischaditid algae within these beds at Second Creek and bedding planes covered with these algal thalli near Verona suggest that water depths were still relatively shallow and well within the photic zone.

Correlations –

Rockway Dolostone (or Rockway Member of the Irondequoit Formation) of west-central New York (Eckert and Brett, 1989; Brett et al., 1998)

Lower Keefer Sandstone of Pennsylvania, Virginia, and Maryland (Brett et al., 1998; McLaughlin et al., in review)

Kirkland Iron Ore

Definition and Type Area – The Kirkland Iron Ore was defined by Chadwick (1918) as the fossiliferous hematitic bed well exposed in the vicinity of Kirkland in Oneida County, New York. Also referred to as the upper iron ore of Vanuxem (1842) and the red-flux

ore of Smyth (1895), the Kirkland sharply overlies the Willowvale Shale or the Dawes Sandstone where it is present. Its upper contact with the Herkimer Sandstone is gradational (Gillette, 1947).

Thickness and Extent – The Kirkland Iron Ore is highly variable in thickness, reaching up to two meters at sections near Lairdsville, New York. Within the Clinton Type area, the Kirkland serves as an important stratigraphic marker. However, like many of the other Clinton Ironstones, the Kirkland cannot be easily traced in surface exposures outside of Oneida County (Gillette, 1947).

Age – Sheinwoodian (Brett and Goodman, 1996; Brett et al., 1998; McLaughlin et al., in review)

Sequence Stratigraphy – Relative lowstand (LST to early TST) of subsequence V-A (Brett et al., 1998)

Facies and Depositional Environment – The Kirkland is a fossiliferous, hematitic grainstone with highly variable concentrations of iron and several cross-stratified horizons. The beds also have high concentrations of carbonate which made this unit it a valuable target for miners and smelters as a self-fluxing ore (Van Houten, 1991). It is composed primarily of crinoid-dominated packstones and grainstones, indicative of relatively shallow water and moderate- to high energy transgressive shoal conditions.

Biostratigraphy –

Kockelella ranuliformis Zone (Kleffner pers. comm. reported in Brett et al., 1998)

Paraechmina spinosa Zone (Gillette, 1947)

Paleoecology – Like the Salmon Creek Bed, the Kirkland contains abundant remains of rather large pelmatozoans (stalked echinoderms), though bryozoans and brachiopods are also common. The preservational state of these organisms is highly variable, and a taphonomic gradient of ferruginization has been noted by previous workers (Gillette, 1947) suggesting strong reworking and time-averaging the Kirkland with preferential preservation of more robust skeletal elements. The presence of moderately large brachiopods including *Meristina* (=*Cryptothyrella*) *cylindrica*, *Coolinia* and *Leptaena* suggests a BA-3 open shelf, shoal position.

Correlations –

Upper Irondequoit Formation of west-central New York and Ontario (Lin and Brett, 1988; Brett et al., 1998)

Upper Keefer Of Pennsylvania, Maryland, and Virginia (Brett et al., 1998)

Lower Keefer of Pennsylvania (McLaughlin et al., in review)

Herkimer Sandstone

Definition and Type Area – The Herkimer Sandstone was defined by Chadwick (1918) as the upper sandstones of the Clinton Group as they are exposed in southern Herkimer County.

Thickness and Extent – In the Clinton Type Area, the Herkimer Formation is approximately 22 meters in thickness. The unit expands to the west; in the vicinity of Verona, New York, the unit is up to 28 meters in thickness. The unit is widely traceable, but to the west of Oneida Lake it becomes increasingly shaly and interfingers with the Rochester Shale (Gillette, 1947).

Age – Sheinwoodian (Brett and Goodman, 1996), Middle to Late Wenlock (Berry and Boucot, 1970)

Sequence Stratigraphy – Relative highstand of subsequence V-A and subsequence V-B (Brett et al., 1998)

Facies and Depositional Environment – The lower part of the western or Joslin Hill facies of the Herkimer Sandstone (Zenger, 1971) is composed of interbedded dark gray fossiliferous shales and coarse, calcareous sandstones, many of which display ripple marks. The unit becomes increasingly sandy toward its upper contact with several prominent reddish hematitic, sandy horizons (Gillette, 1947). Trace fossils, including excellent *Rusophycus* (trilobite resting traces) are present as hypichnia on the bases of some sandstone beds. The depositional setting of the Herkimer in central New York State is thought to be similar to that of the Willowvale and Dawes and the unit shows four major o coarsening- upward cycles of, dark gray mudstone and shale to fine hummocky bedded sandstone and quartz granule to fine pebble conglomerates with some open marine brachiopod faunas. These beds are abruptly overlain by calcareous, pebbly sandstones and sandy, hematitic crinoidal pack- and grainstones, resembling the Kirkland Formation, with relatively diverse fossil assemblages (possibly BA-3) of rhynchonellid and strophomenid brachiopods. These beds have been interpreted as the relatively siliciclastic starved transgressive deposits. The Joslin Hill passes westward into dark gray mudstones and thin dolomitic siltstones of the Rochester formation and eastward into the unfossiliferous massive, cross bedded quartz arenites of the Jordanville facies. The latter record offshore muddy shelf settings with BA 4 faunas while the Jordanville represents near-shore high-energy sand bar and shoal complexes. The absence of body fossils and presence of *Skolithos* traces suggests strong reworking of sands in high energy very shallow subtidal to intertidal conditions. Overall, the

increased input of siliciclastic sediments into the foreland basin during Rochester-Herkimer depositions suggests an increased pulse of uplift and erosion associated with a second Salinic tectophase.

Biostratigraphy –

Paraechmina spinosa Zone (Gillette, 1947)

Paleoecology – Fossil assemblage reported in the Herkimer Sandstone are indicative of normal marine deposition. The sandstone beds of the lower Herkimer Sandstone are sparsely fossiliferous. However the shales yield fairly common brachiopods, bivalves, and ostracodes.

Correlations –

Rochester Shale of west-central New York (Gillette, 1947; Berry and Boucot, 1970; Brett et al., 1998).

Upper Rochester Shale of west-central New York (McLaughlin et al., in review)

Upper Keefer of Pennsylvania (McLaughlin et al., in review)

4. THE NATURE OF IRONSTONES

4.1 Mineralogy and Sedimentology

Phanerozoic ironstones are a heterogeneous mixture of various iron-bearing and non-ferruginous minerals. The predominant iron oxide mineral found within the Clinton Ironstones is hematite, which gives the horizons their characteristic dark red color (Schoen, 1962). Although the predominance of these oxides within the Clinton Ironstones suggests an oxic depositional environment, the presence of reduced iron minerals such as chamosite and berthierine indicates a complex history of redox conditions. Small, but ubiquitous crystals of pyrite are also present, and in nearly all cases show a late-stage mineral replacement history. Other common minerals within the Clinton Ironstones are illite, calcite, and quartz.

Iron bearing minerals in the Clinton Ironstones are commonly manifested as intergranular cements, cavity fillings, or concentric laminae accreted around a nucleus (Cotter and Link, 1993). Beds composed primarily of sand-sized quartz grains surrounded by concentric, ferruginous laminae have been characterized as having an "oolitic" texture (Smyth, 1892; 1919), though in contrast to carbonate ooids, these grains typically have an elliptical flax-seed shape (Chowns, 1996). Fossiliferous ironstones are similar to oolitic ironstones in many ways, though bioclasts commonly form the nucleus for accreted rinds of iron minerals in these beds. Fossils in ironstone horizons may

be tinted bright red where carbonate minerals have been impregnated or replaced by iron oxides.

4.2 Genetic Models

The ubiquity of ferric iron bearing minerals in many types of ironstones suggests that they were deposited in environments that experienced oxidizing conditions at least sporadically, yet it is widely acknowledged that iron is highly immobile in oxic environments (Kimberley, 1989, Boggs, 2001). This apparent contradiction is referred to as the "ironstone paradox" or the "oxidation-reduction paradox", which has been the subject of numerous studies (Maynard, 1986; Cotter, 1992; Kimberley, 1994; McLaughlin et al., in review).

Ironstones occur non-randomly within the Phanerozoic, and are particularly common within the Ordovician through Devonian and Jurassic through Early Cenozoic (Van Houten and Bhattacharrya, 1982; Van Houten and Arthur, 1989). These intervals of earth's history are traditionally associated with greenhouse climates and subdued tectonism, leading to the conclusion that deep weathering of continental bedrock would provide a ready source of iron, favoring the deposition of ironstones (Van Houten and Bhattacharrya, 1982). However, Van Houten and Arthur (1989), citing a close temporal relationship between ironstones and black shales, suggested a common cause in poorly circulated anoxic water masses, which have the capacity to transport large quantities of dissolved iron in its reduced, ferrous state. Cotter and Link (1993) expanded on this idea suggesting that ironstones could form along the pycnocline, where dysoxic deeper waters came into contact with more oxygenated shallow waters. Under these mildly reducing conditions, ferrous iron dissolved in the dysoxic water mass could have precipitated near the sediment water interface as iron rich clays such as chamosite and berthierine, which may occur as intergranular cements, oolitic coatings, or cavity fillings, possibly mediated by microbial activity (Cotter and Link, 1993; Chowns, 1996). They argue that these minerals could then be altered to ferric oxide during later diagenesis (Cotter and Link, 1993).

However, Silurian ironstones are commonly associated with diverse open marine fossil assemblages (Gillette, 1947) and *in situ* bioturbating organisms (Chowns, 1996) indicating oxic conditions at the site of deposition. Regional stratigraphic studies traced many of these ironstones laterally into thin, pyrite and phosphate rich conglomeratic horizons, suggesting a genetic link between them (Lin and Brett, 1988). The position of some ironstones and coeval phosphatic horizons upon unconformities, created during global lowstands of sea level, indicate that deposition occurred during times of sea level rise (transgression) and siliciclastic sediment starvation. As such, ironstones were interpreted to represent highly condensed beds that represent much more time per

unit thickness than the shales and sandstones that bracket them (Brett et al., 1990; 1998; McLaughlin, Brett, and Wilson 2008). However, because the iron transported into the Appalachian Basin was in the form of grain coatings on clay particles and silt and sand grains under background conditions, siliciclastic sediment starvation would stop the influx of iron into the basin during transgression, thus requiring mobilization of iron from out of the preexisting basin sediments or from a source outside the basin.

Recent carbon isotope analysis across the Appalachian Basin indicates synchrony between the timing of globally recognized positive carbon isotope excursions and the occurrence of ironstones (Figure 5; McLaughlin and others, in review). The large positive shifts in carbon isotopes reflect burial of massive amounts of light organic carbon globally. The incredible increase in primary productivity and burial required to drive such enormous fractionation (up to 10 per mil in the late Ludlow) required oceanic anoxia. The presence of widespread anoxic conditions is supported by proxy data from geochemical studies and the shift to black, laminated shales in basin-center deposits during these events around the world. Within the Appalachian Basin a shift from red and green shales to olive, gray and black shales records this change in organic carbon burial. Ironstones and phosphorites are coincident with this shift in sediment color. Where ironstones are traced down-ramp into phosphorites, the position of this facies transition reflects the original position of a redox interface within the basin. Geochemical analysis of tens of meters of strata below the ironstones shows an iron concentration typical of marine rocks (several orders of magnitude lower than the ironstones) and no significant stratigraphic variation in iron concentration. Thus, there is no evidence that the iron that makes up the ironstones was leached from the underlying strata. Thus, without a sufficient source of iron from riverine input (as predicted during transgressive siliciclastic sediment starvation) or from the underlying sediments, it follows that the primary source of iron was extra-basinal. It is likely therefore that advance of an anoxic water mass into the Appalachian during global organic carbon burial events provided the medium for delivery of massive amounts of dissolved iron. The ironstones and iron-rich carbonates were deposited at a water mass boundary as indicated by their "bath tub ring" distribution around the margins of the basin. The composition and distribution of the ironstones indicates that this water mass boundary was somewhat diffuse and fluctuated between oxic conditions prevalent above and the anoxic conditions present below.

No clear consensus has emerged among the scientific community regarding the origin of ironstones; it may well be that several models or a combination thereof may be responsible for their genesis. Several of the classic "Clinton Ironstones" will be examined through the course of this excursion in the context of these models.

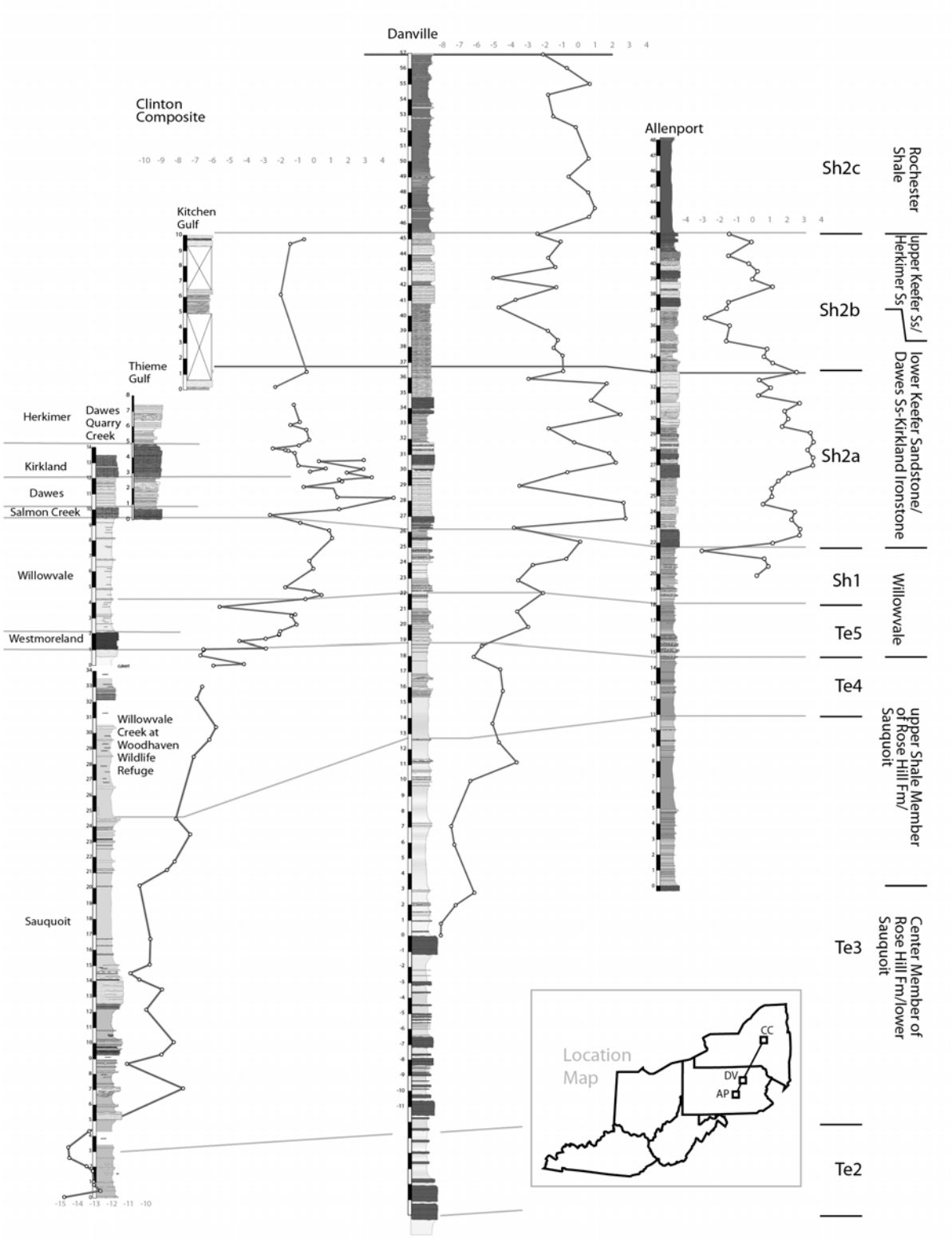

Figure 5 - A regional cross section of Lower Silurian strata in the eastern Appalachian Basin showing regional correlations and the interrelationships between $\delta^{13}C$ values and the stratigraphic distribution of ironstones, which are shaded dark grey in this figure. Modified from McLaughlin and others (in review).

4. CONCLUSIONS

Dramatic and dynamic global patterns of climatic, biotic, and oceanographic change in the Silurian are now thoroughly documented and the equally vivid record of these patterns are well represented in the ironstone bearing stratigraphic successions of Oneida County. Considerable progress has been made in constraining the depositional setting of Phanerozoic sedimentary ironstones such as these, though much remains to be done. For example, ironstones appear to be preferentially associated with basal lowstand to early transgressive lag deposits of depositional sequence; sediment starvation appears to have allowed buildup of early diagenetic minerals without dilution. However, ironstones are also restricted to particular time intervals (McLaughlin et al., in press) and the source of the iron, whether intra- or extrabasinal, and the process of concentration remain a source of discussion. As this debate and others evolve, the Silurian successions of east central New York will continue to play an important role in our understanding in this pivotal episode of earth's history.

6. REFERENCES CITED

Baird, G. C., and Brett, C. E., 1986, Erosion on an Anaerobic Seafloor: Significance of Reworked Pyrite Deposits from the Devonian of New York State: Palaeogeography, Palaeoclimatology, Palaeoecology, v. 57, p. 157-193.

Beaumont, C., Quinlan, G., and Hamilton, J., 1988, Orogeny and Stratigraphy: Numerical Models of the Paleozoic in Eastern North America: Tectonics, v. 7, no. 3, p. 389-416.

Berry, W. B. N., and Boucot, A. J., 1970, Correlation of the North American Silurian Rocks, Geological Society of America Special Paper 102, 289 p.:

Bolton, T. E., 1957, Silurian Stratigraphy and Paleontology of the Niagara Escarpment in Ontario: Geological Society of Canada, Memoir 289.

Boucot, A. J., 1975, Evolution and Extinction Rate Controls, Amsterdam, NY, Elsevier, 427 p.:

Brenchley, P. J., Marshall, J. D., Carden, G. A. F., Robertson, D. B. R., Long, D. G. F., Meidla, T., Hints, L., and Anderson, T. F., 1994, Bathymetric and isotopic evidence for a short-lived Late Ordovician glaciation in a greenhouse period: Geology, v. 22, p. 295-298.

Brett, C. E., Baarli, B. G., Chowns, T., Cotter, E., Driese, S. G., Goodman, W., M., and Johnson, M. E., 1998, Early Silurian Condensed Intervals, Ironstones, and Sequence Stratigraphy in the Appalachian Foreland Basin, *in* Landing, E., and Johnson, M. E., eds., Silurian Cycles: Linkages of Dynamic Stratigraphy with Atmospheric, Oceanic and Tectonic Changes. New York State Museum Bulletin, Volume 491: Albany, NY, New York State Museum, p. 89-143.

Brett, C. E., Ferretti, A., Histon, K., and Schöenlaub, H. P., 2009, Silurian sequence stratigraphy of the Carnic Alps, Austria: Palaeogeography, Palaeoclimatology, Palaeoecology, v. 279, p. 1-28.

Brett, C. E., and Goodman, W., M., 1996, Silurian Stratigraphy of the Type Clinton Area of Central New York, *in* Broadhead, T. W., ed., Sedimentary Environments of Silurian Taconia: Fieldtrips to the Appalachians and Southern Craton of Eastern North America, Volume 26.

Brett, C. E., Goodman, W., M., and LoDuca, S. T., 1990, Sequences, cycles, and basin dynamics in the Silurian of the Appalachian Foreland Basin: Sedimentary Geology, v. 69, p. 191-244.

Brett, C. E., and Ray, D., C., 2005, Sequence and Event Stratigraphy of the Silurian Strata of the Cincinnati Arch Region: Correlations with New York-Ontario Successions: Proceedings of the Royal Society of Victoria, v. 117, no. 2, p. 175-198.

Boggs, S., 2001, Principles of Sedimentology and Stratigraphy (Third Edition), Upper Saddle River, New Jersey, Prentice Hall, 726 p.:

Brunton, F. R., Smith, L., Dixon, O. A., Copper, P., Nestor, H., and Kershaw, S., 1998, Silurian Reef Episodes, Changing Seascapes, and Paleobiolgeography, *in* Landing, E., and Johnson, M. E., eds., Silurian Cycles: Linkages of Dynamic Stratigraphy with Atmospheric, Oceanic and Tectonic Changes. New York State Museum Bulletin, Volume 491: Albany, NY, New York State Museum, p. 265-282.

Caputo, M. V., 1998, Ordovician-Silurian Glaciations and Global Sea-Level Changes, *in* Landing, E., and Johnson, M. E., eds., Silurian Cycles: Linkages of Dynamic Stratigraphy with Atmospheric, Oceanic and Tectonic Changes. New York State Museum Bulletin, Volume 491: Albany, NY, New York State Museum, p. 15-25.

Chadwick, G. H., 1918, Stratigraphy of the New York Clinton: Geological Society of America Bulletin, v. 29, p. 327-368.

Chowns, T. M., 1996, Sequence Stratigraphy of the Silurian Red Mountain Formation in Alabama and Georgia, *in* Broadhead, T. W., ed., Sedimentary Environments of Silurian Taconia: Field Trips to the Appalachians and Southern Craton of Eastern North America. University of Tennessee, Department of Geological Science, Studies in Geology 26, p. 31-42.

Cocks, L. R. M., and Scotese, C. R., 1991, Global Biogeography of the Silurian Period: Special Papers in Paleontology, v. 44, p. 109-112.

Colton, G. W., 1970, The Appalachian Basin - Its depositional sequences and their geologic relationships, *in* Fisher, G. W., Pettijohn, F. J., Reed, J. C., and Weaver, K. N., eds., Studies of Appalachian Geology Central and Southern: New York, NY, John Wiley.

Copper, P., 2002, Silurian and Devonian Reefs: 80 Myr of global greenhouse between two ice ages, *in* Flugel, E., and Kiessling, W., eds., Society of Economic Paleontologists and Mineralogists Special Publication, Volume 72, p. 181 -238.

Copper, P., and Brunton, F. R., 1991, A Global Review of Silurian Reefs: Special Papers in Paleontology, v. 44, p. 225-259.

Cotter, E., 1992, Diagenetic alteration of chamositic clay minerals to ferric oxide in oolitic ironstone: Journal of Sedimentary Petrology, v. 62, p. 54-60.

Cotter, E., and Link, J. E., 1993, Deposition and diagenesis of Clinton ironstones (Silurian) in the Appalachian Foreland Basin of Pennsylvania: Geological Society of America Bulletin, v. 105, no. 7, p. 911-922.

Cramer, B. D., Brett, C. E., Melchin, M. J., Männik, P., Kleffner, M. A., McLaughlin, P. I., Loydell, D. K., Munnecke, A., Jeppsson, L., Corradini, C., Brunton, F. R., and Saltzman, M. R., 2011, Revised correlation of Silurian Provincial Series of North America with global and regional chronostratigraphic units and δ13Ccarb chemostratigraphy: Lethaia, v. 44, no. 2, p. 185-202.

Cramer, B. D., and Saltzman, M. R., 2007, Fluctuations in epeiric sea carbonate production during Silurian positive carbon isotope excursions: A review of proposed paleoceanographic models: Palaeogeography, Palaeoclimatology, Palaeoecology, v. 245, no. 1-2, p. 37-45.

Duncan, P. M., 1867, On the Genera *Heterophyllia*, *Battersbyia*, *Palaeocyclus*, and *Asterosmilia*; The Anatomy of Their Species, and Their Position in the Classification of the Sclerodermic Zoantharia: Philosophical Transactions of the Royal Society of London, v. 157, p. 643-656.

Eaton, A., 1824, A Geological and Agricultural Survey of the District Adjoining the Erie Canal, in the State of New York, Albany, NY, Packard and Van Benthuysen.

Eckert, B.-Y., and Brett, C. E., 1989, Bathymetry and paleoecology of Silurian benthic assemblages, late Llandoverian, New York State: Palaeogeography, Palaeoclimatology, Palaeoecology, v. 74, p. 297-326.

Ehlers, G. M., 1973, Stratigraphy of the Niagaran Series of the Northern Peninsula of Michigan, University of Michigan Museum of Paleontology Papers on Paleontology, v. 3, 200 p.:

Eriksson, M. E., 2006, The Silurian Ireviken Event and vagile benthic faunal turnovers (Polychaeta; Eunicida) on Gotland, Sweden: GFF, v. 128, p. 91-95.

Ettensohn, F. R., 2008, Chapter 4: The Appalachian Foreland Basin in Eastern United States: Sedimentary Basins of the World, v. 5, p. 105-179.

Ettensohn, F. R., and Brett, C. E., 1998, Tectonic components in Third-Order Silurian Cycles: Examples from the Appalachian Basin and Global Implications, *in* Landing, E., and Johnson, M. E., eds., Silurian Cycles: Linkages of Dynamic Stratigraphy with Atmospheric, Oceanic and Tectonic Changes. New York State Museum Bulletin, Volume 491: Albany, NY, New York State Museum, p. 89-143.

Ettensohn, F. R., and Brett, C. E., 2002, Stratigraphic evidence from the Appalachian Basin for continuation of the Taconian Orogeny into Early Silurian time: Physics and Chemistry of the Earth, v. 27, p. 279-288.

Fisher, D. W., Isachsen, Y. W., Rickard, L. V., 1970. Geologic Map of New York State. 1:250,000, New York State Museum Map and Chart Series No. 15.

Foerste, A. F., 1931, The Silurian Fauna of Kentucky, *in* Jillson, W. R., ed., The Paleontology of Kentucky: Frankfort Kentucky, The Kentucky Geological Survey, p. 170-193.

Gelsthorpe, D. N., 2004, Microplankton changes through the early Silurian Ireviken extinction event on Gotland, Sweden: Review of Palaeobotany and Palynology, v. 130, p. 89-103.

Gillette, T., 1947, The Clinton of Western and Central New York: New York State Museum Bulletin, v. 41, p. 1-191.

Goldring, W., 1931, Handbook of paleontology for beginners and amateurs, Part II: The Formations: New York State Museum Handbook, v. 10, p. 488.

Goodman, W., M., and Brett, C. E., 1994, Roles of Eustasy and Tectonics in Development of Silurian Stratigraphic Architecture of the Appalachian Foreland Basin: Tectonic and Eustatic Controls on Sedimentary Cycles, SEPM Concepts in Sedimentology and Paleontology #4, p. 147-169.

Hall, J., 1852, Palaeontology of New York. Volume II. Containing Descriptions of the Organic Remains of the Lower Middle Division of the Silurian System (Equivalent in Part to the Middle Silurian Rocks of Europe), Albany, New

York, C. Van Benthuysen.
Hartnagel, C. A., 1907, Geologic Map of the Rochester and Ontario Beach quadrangles: New York State Museum Bulletin, v. 114, p. 1-35.
Hunter, R. E., 1970, Facies of iron sedimentation in the Clinton group, *in* Fisher, G. W., ed., Studies of Appalachian geology, central and southern: New York City, New York, John Wiley and Sons, p. 101-121.
Jeppsson, L., 1990, An oceanic model for lithological and faunal changes tested on the Silurian record: Journal of the Geological Society, v. 147, p. 663-674.
Jeppsson, L., 1997, The anatomy of the mid-Early Silurian Ireviken Event, *in* Brett, C. E., and Baird, G. C., eds., Paleontological Event Horizons - Ecological and Evolutionary Implications, Columbia University Press, p. 451-492.
Jeppsson, L., Aldridge, R. J., and Dorning, K. J., 1995, Wenlock (Silurian) oceanic episodes and events: Journal the Geological Society, London, v. 152, p. 487-498.
Johnson, M. E., Rong, J.-y., and Kershaw, S., 1998, Calibrating Silurian eustasy against the erosion and burial of coastal paleotopography, *in* Landing, E., and Johnson, M. E., eds., Silurian Cycles: Linkages of Dynamic Stratigraphy with Atmospheric Ocean and Tectonic Changes. New York State Museum Bullettin, Volume 491: Albany, NY, New York State Museum, p. 3-13.
Kimberley, M. M., 1989, Exhalative Origins of Iron Formations: Ore Geology Reviews, v. 5, p. 13-145.
Kimberley, M. M., 1994, Debate about ironstone: has solute supply been surficial weathering, hydrothermal convection, or exhalation of deep fluids: Terra Nova, v. 6, no. 116-132.
Lehnert, O., Männik, P., Joachimski, M. M., Calner, M., and Frýda, J., 2010, Palaeoclimate perturbations before the Sheinwoodian glaciation: A trigger for extinctions during the 'Ireviken Event': Palaeogeography, Palaeoclimatology, Palaeoecology, v. 296, no. 3-4, p. 320-331.
Lin, B.-Y., and Brett, C. E., 1988, Stratigraphy and disconformable contacts of the Williamson-Willowvale interval: revised correlations of the late Llandoverian (Silurian) in New York State: Northeastern Geology, v. 10, p. 241-253.
Loydell, D. K., 1998, Early Silurian sea-level changes: Geological Magazine, v. 135, no. 4, p. 447-471.
Loydell, D. K., Kleffner, M. A., Mullins, G. L., Butcher, A., Matteson, D. K., and Ebert, J. R., 2007, The lower Williamson Shale (Silurian) of New York: a biostratigraphical enigma: Geological Magazine, v. 144, no. 02, p. 225.
Manda, Š., Štorch, P., Slavík, L., Frýda, J., Kříž, J., and Tasáryová, Z., 2011, The graptolite, conodont and sedimentary record through the late Ludlow Kozlowskii Event (Silurian) in the shale-dominated succession of Bohemia: Geological Magazine, p. 1-25.
Maynard, J. B., 1986, Geochemistry of oolitic iron ores, an electron microprobe study: Economic Geology, v. 81, p. 1473-1483.
McLaughlin, P.I., Brett, C. E., and Emsbo, P., in review. Beyond black shales: the sedimentary and stable isotope records of oceanic anoxic events in a dominantly oxic basin (Silurian; Appalachian Basin, USA). Palaeogeography, Palaeoclimatology, Palaeoecology.
McLaughlin, P. I., Brett, C. E., and Wilson, M. A., 2008, Heirarchy of Sedimentary Discontinuity Surfaces and Condensed Beds from the Middle Paleozoic of Eastern North America: Implications for Cratonic Sequence Stratigraphy, *in* Pratt, B. R., and Holmden, C., eds., Geological Association of Canada Special Paper 48: Dynamics of Epeiric Seas, p. 175-200.
McLaughlin, P. I., Cramer, B. D., Brett, C. E., and Kleffner, M. A., 2008, Silurian high-resolution stratigraphy of the Cincinnati Arch: Progress in recalibrating the layer-cake, *in* Maria, A. H., and Counts, R. C., eds., From the Cincinnati Arch to the Illinois Basin. Geological Field Excursions along the Ohio River Valley: Geological Society of America Field Guide 12, p. 119-180.
Miller, K. G., Kominz, M. A., Browning, J. V., Wright, J. D., Mountain, G. S., Katz, M. E., Sugarman, P. J., Cramer, B. S., Christie-Blick, N., and Pekar, S. F., 2005, The Phanerozoic Record of Global Sea-Level Change: Science, v. 310, p. 1293-1298.
Munnecke, A., Samtleben, C., and Bickert, T., 2003, The Ireviken Event in the lower Silurian of Gotland, Sweden – relation to similar Palaeozoic and Proterozoic events: Palaeogeography, Palaeoclimatology, Palaeoecology, v. 195, no. 1-2, p. 99-124.
Muskatt, H. S., 1972, The Clinton Group of east-central New York: New York State Geological Association 44th Annual Meeting Guidebook, p. A1-A37.
Rexroad, C. B., and Richard, L. V., 1965, Zonal Conodonts from the Silurian Strata of the Niagara Gorge: Journal of Paleontology, v. 39, no. 6, p. 1217-1220.
Rickard, L. V., 1975, Correlation of the Silurian and Devonian Rocks of New York State: New York state Museum, Map and Chart Series, v. 24.
Rodgers, J., 1970, The Tectonics of the Appalachians, New York, NY, Wiley/Interscience, 271 p.:
Root, S., and Onasch, C., M., 1999, Structure and tectonic evolution of the transitional region between the central Appalachian foreland and interior cratonic basins: Tectonophysics, v. 305, p. 205-223.
Sanford, J. T., 1935, The "Clinton" in Western New York: The Journal of Geology, v. 43, no. 2, p. 169-183.
Schoen, R., 1962, Petrology of Iron-Bearing Rocks of the Clinton Group in New York State, Unpublished Doctoral Thesis, p. 151.
Schoen, R., 1964, Clay Minerals of the Silurian Clinton Ironstones, New York State: Journal of Sedimentary Petrology, v.

34, no. 4, p. 855-863.
Scotese, C. R., and McKerrow, W. S., 1990, Revised World maps and introduction: Geological Society, London, Memoirs, v. 12, no. 1, p. 1-21.
Smyth, C. H., 1892, On the Clinton iron ore: American Journal of Science, Third Series, v. 43.
Smyth, C. H., 1918, On the genetic significance of ferrous silicate associated with the Clinton iron ores: New York State Museum Bulletin, v. 208, p. 178-198.
Ulrich, E. O., and Bassler, R. S., 1923, Paleozoic Ostracoda; Their Morphology, Classification, and Occurrence: Maryland Geological Survey Publication.
Van Diver, B., 1985, Roadside Geology of New York, New York, NY, Mountain Press Publishing Company, 411 p.:
Van Houten, F. B., 1991, Interpreting Silurian Clinton Oolitic Ironstones: Journal of Geological Education, v. 39, p. 19-22.
Van Houten, F. B., and Arthur, M. A., 1989, Temporal patterns among Phanerozoic oolitic ironstones and oceanic anoxia, *in* Young, T. P., and Taylor, W. E. G., eds., *Phanerozoic Ironstones* Geological Society Special Publication No. 46, p. 33-49.
Van Houten, F. B., and Bhattacharyya, D. P., 1982, Phanerozoic Oolitic Ironstones - Geologic Record and Facies Model: Annual Review of Earth and Planetary Sciences, v. 10, p. 441-457.
van Staal, C. R., Whalen, J. B., McNicoll, V. J., Pehrsson, S., Lissenberg, C. J., Zagorevski, A., van Breeman, O., and Jenner, G. A., 2007, The Notre Dame arc and the Taconic Orogeny in Newfoundland: Geological Society of America Memoirs, v. 200, p. 511-552.
Vanuxem, L., 1839, Third Annual Report of the Geological Survey of the Third District: New York State Geological Survey Annual Report, v. 3, p. 241-285.
Vanuxem, L., 1842, Geology of New York, Part III. Comprising the Survey of the Third Geologic District, Albany, NY, C. Van Benthuysen, 306 p.:
Veizer, J., Godderis, Y., and Francois, L. M., 2000, Evidence for decoupling of atmospheric CO_2 and global climate during the Phanerozoic eon: Nature, v. 408, p. 698-701.
Waldron, J. W. F., and van Staal, C. R., 2001, Taconian Orogeny and the accretion of the Dashwoods block: A peri-Laurentian microcontinent in the Iapetus Ocean: Geology, v. 29, p. 811-814.
Willard, B., 1928, The Age and Origin of the Shawangunk Formation: Journal of Paleontology, v. 1, no. 4, p. 255-258.
Williams, R. L., 1998, Iron Ore Mining and Manufacturing in the Town of Kirkland. Lecture Presented at the Clinton Historical Society Meeting on 16 April, 1998. Retrieved from [http://www.clintonhistory.org/A019.html]
Zenger, D. H., 1971, Stratigraphy of the Lockport Formation (Middle Silurian) in New York State: New York State Museum Bulletin, v. 404.
Ziegler, A. M., Cocks, L. R. M., and Bambach, R. K., 1968, The Composition and Structure of Lower Silurian Marine Communities: Lethaia, v. 1, p. 1-27.

STOP DESCRIPTIONS

This field excursion features three well-known exposures of the Clinton Group: Roaring Brook at Lairdsville (Type Westmoreland), Theime Gulf, and the Woodhaven Wildlife Refuge (also called Willowvale Creek, or the Glen). All three sections are exposed in the beds of small streams and glens running through Oneida County in the Vicinity of the town of Clinton (Figure 6). A fourth locality, the Forever Wild Nature Preserve, is also included here as an optional stop. This is the first published description of the strata exposed at this last section.

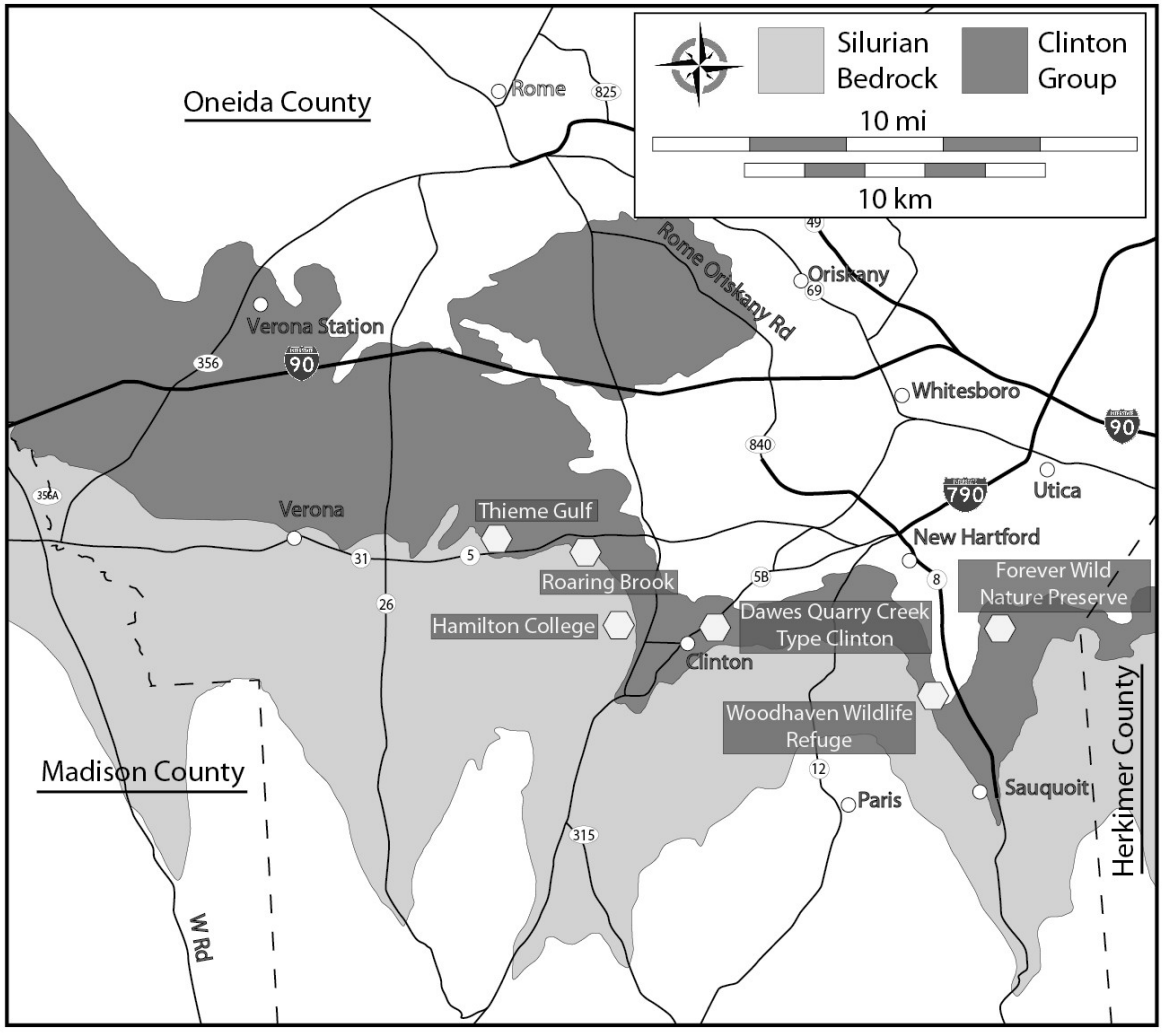

Figure 6 – Map of the Clinton Type Area with all sections mentioned in this write up plotted. Modified from Fisher and others (1970).

Route Description	Number of Miles	Cumulative mileage
Starting Point **Taylor Science Center,** Hamilton College, Clinton, NY 13323	Depart	
Head **north** toward **Campus Rd/County Rd 77**	0.08	0.08
Turn left onto **Campus Rd/County Rd 77**	1.1	1.2
Turn left onto **County Rd 15A/Norton Ave**	1.1	2.3
Turn right onto **NY-5 E/Seneca Turnpike**	0.6	2.9
Stop 1 **Roaring Brook - Type Section of the Westmoreland** 7041 NY Rte. 5 (Seneca Turnpike), Clinton, NY 13323	Arrive	

Stop #1. Roaring Brook - Type Section of the Westmoreland Iron Ore

Coordinates: N 43° 04' 48.30", W 75° 25' 16.79"

Roaring Brook is the informal name given to a small, south flowing tributary of Oriskany Creek found in Lairdsville, a small Hamlet of Clinton, New York, in Oneida County. This locality was designated by Gillette (1947; p. 91-93) as the type section for the Westmoreland Hematite, though no detailed description of the outcrop was given. This section is located on private property and those wishing to view it must first obtain permission from the residents of 7012 NY Rte. 5 (Seneca Turnpike), in Lairdsville, NY. The most straightforward way of accessing the stream bed is by walking down the western slope of the valley cut by the stream where several paths provide relatively easy access to the section. A large (3-4 meter) waterfall, capped by the Westmoreland Iron Ore is a notable feature of this locality. A smaller falls, upstream and closer to the road, is capped by the Salmon Creek Bed.

This section has been featured previously as stop 13 of Brett and Goodman (1996). Five named rock units are exposed here; they are described and illustrated in ascending order herein (Figure 7).

Unit 1 - Sauquoit Formation

All strata exposed below the large waterfall at this locality are assigned to the Sauquoit Formation of the Middle Clinton Group (Sequence S-III of Brett et al, 1990). The Sauquoit Formation is reported to be approximately 30 meters thick in this area; the upper 6-7 meters of the unit is relatively well exposed along an approximately 0.25 kilometer stretch of creek bed extending

downstream from the large waterfall.

Here, the Sauquoit Formation is dominantly greenish grey clay shale with thin interbeds of varying lithology that include planar to cross laminated, fine- to medium-grained calcareous quartzose sandstone and phosphatic, quartz pebble conglomerates. Many of these interbeds display numerous sedimentary structures, including sole marks, gutter casts, and asymmetrical, symmetrical,

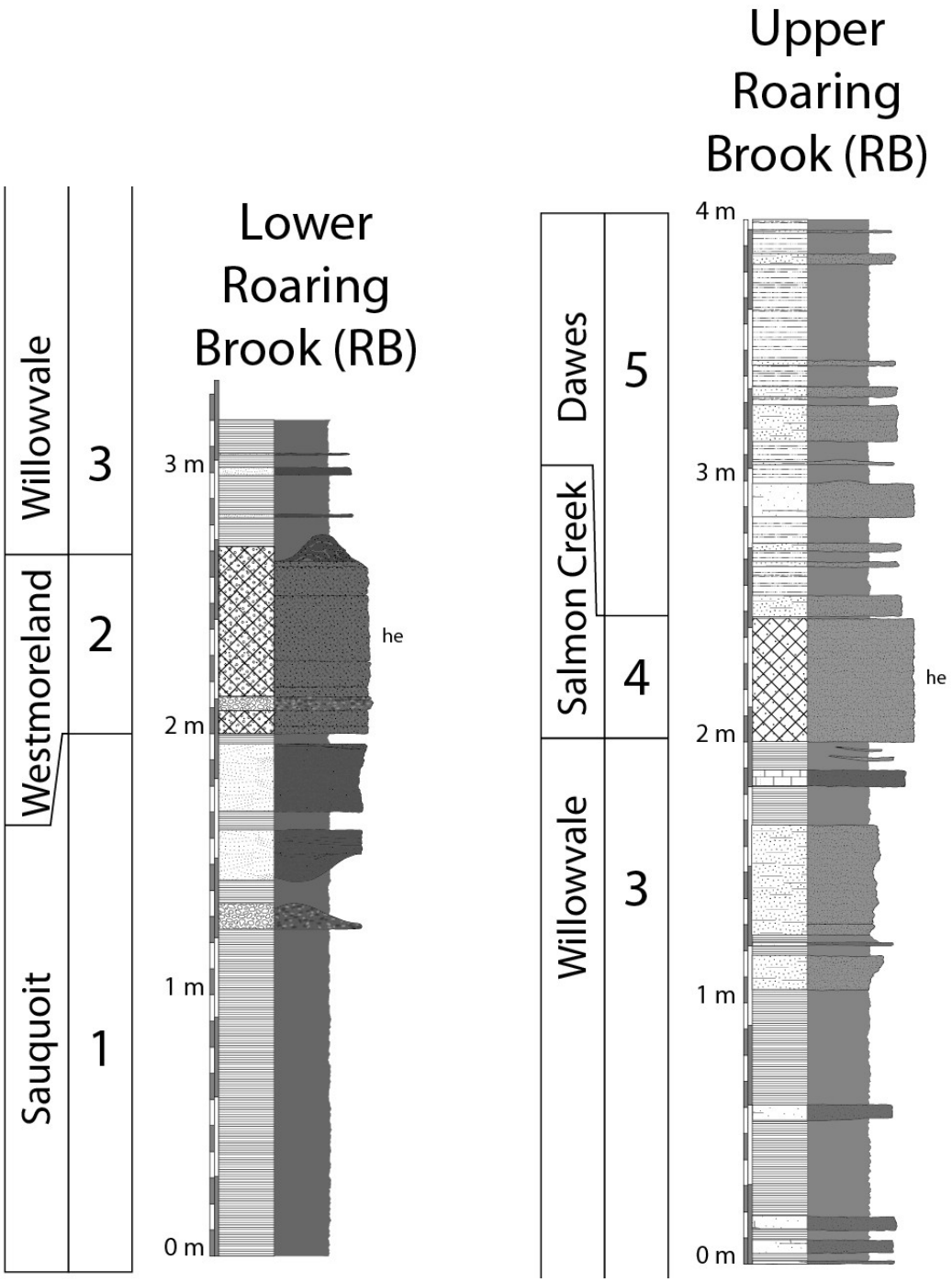

Figure 7 - Stratigraphic columns for outcrops at Roaring Brook, in Lairdsville New York.

and interference ripple marks. Several thick, cross bedded sandstone interbeds occur near the top of the Sauquoit Formation at this locality, which contain abundant phosphatic shell fragments tentatively interpreted as lingulid remains. Below these upper sandstone beds is a locally present, rippled quartz phosphate pebble conglomerate.

Macrofossils are relatively sparse, though bedding planes may contain abundant bivalves and brachiopods. The brachiopods *Strophochonetes* (?) *cornutus, Leptaena rhomboidalis,* and *Eocoelia sulcata* are all relatively common, suggesting assignment to Boucot's (1975) benthic assemblage 2. Bivalves are also quite common on some bedding planes, and very rare large trilobites have been found here as well. The presence of Ostracodes belonging to the *Mastigobolbina typus* Zone suggest a mid Telychian (C-5) age for these beds.

Unit 2 - Westmoreland Iron Ore

The large waterfall at Roaring Brook is capped by a 70-80 centimeter thick interval of bright red hematitic beds assigned to the Westmoreland Iron Ore. This horizon has been mined extensively here, and large portions of this unit are removed.

The bed is composed primarily of small, sand sized "oolitic" sediments composed of concentric laminae of hematite, chamosite, and berthierine surrounding a nucleus that is usually composed of a rounded quartz grain (Schoen, 1962). Several conglomeratic horizons are also found in the Westmoreland Iron Ore at this locality, composed primarily of quartz and phosphatic pebbles surrounded by a matrix of oolitic, hematitic grains. Brett and Goodman (1996) reported centimeter wide rectilinear cracks infilled with quartz and phosphate grains underlying the Westmoreland, which they interpreted as sedimentation within emergent mudcracks forming in the underlying Sauquoit. The upper surface of the unit displays large (~10 cm high) symmetrical ripple marks.

The Westmoreland is sparsely fossiliferous here, though conodonts of the *Pterospathodus celloni* to *Pterospathodus amorphognathoides* Zones have been reported from the unit here (M. Kleffner, pers. comm. 1990 *in* Brett and Goodman, 1996). Brett and Goodman (1996) also report *Eocoelia sulcata*, *Eospirifer radiatus,* and *Eoplectodonta transversalis,* suggesting a late Telychian age for this unit. The thin, fossiliferous black shale bed reported in the Westmoreland Iron Ore at other sections by Gillette (1947) is not present here.

Unit 3 - Willowvale Shale

Sharply overlying the Westmoreland Iron Ore is the Willowvale Shale, which is approximately 6.1-7.6 meters thick in this area. At Roaring Brook, the unit is primarily gray to olive grey shaly mudstone with minor interbeds of light colored, sandy fossiliferous dolostones.

The Willowvale Shale yields a diverse marine fossil assemblage interpreted as the remnants of a relatively deepwater fauna (Eckert and Brett, 1989). The lower 0.3 to 0.75 meters of the Willowvale Shale contains several dolostone interbeds, which contain abundant specimens of a small discoidal rugose coral identified as *Palaeocyclus rotuloides* a fossil that appears in equivalent late Telychian strata throughout the world.

Unit 4 - Salmon Creek - Basal Dawes Bed

Upstream from the Willowvale bank exposures, the stream takes a sharp bend that leads up to a second, small falls just below the culvert under NY Route 5. This small falls is capped by a 40-50 centimeter thick, pinkish, blocky, sandy dolostone, which contains numerous small stringers of hematite; in the past this unit has been misidentified as Kirkland iron ore at some sections. This bed is interpreted as the basal bed of the Dawes, also referred to as the Salmon Creek Bed. The dominant fossils found in this unit are fragments of stalked echinoderms, primarily crinoids which are highly disarticulated and often impregnated with hematite.

Unit 5 - Dawes Sandstone

Above Unit 4 are a few meters of interbedded siltstones, sandstones and shales assigned to the Dawes Sandstone, which is the highest stratigraphic unit observed in Roaring Brook on the south side of NY Route 5. The unit is not fossiliferous and it is poorly exposed, being largely covered by soil and rip-rap sitting below the culvert under the road. Better exposures of this unit and some of the underlying beds can be viewed at the next stop.

Route Description	**Number of Miles**	**Cumulative mileage**
Stop 1 **Roaring Brook - Type Section of the Westmoreland** 7012 NY Rte. 5 (Seneca Turnpike), Clinton, NY 13323	Depart	
Head **west** on **NY-5 W/Seneca Turnpike** toward **County Rd 15A/ Norton Ave**	0.8	3.7
Take the 1st right onto **Theime Gulf Rd**	0.2	3.9
Stop 2 **Theime Gulf** 4486 Theime Gulf Rd, Clinton NY 13323	Arrive	

Stop #2. Theime Gulf

Coordinates: N 43° 04' 48.17", W 75° 26' 10.80"

The outcrops exposed at Theime Gulf are found in the banks of a small, northwest flowing tributary of Oriskany Creek. Five named stratigraphic units are featured at this stop, which partially overlap the section exposed in Roaring Brook at Stop # 2 (See Figure 8). These outcrops are located on a private residence at 4486 Theime Gulf Road, in Clinton New York; visitors must obtain permission before entering. This section has been featured previously as Stop 14 of Brett and Goodman (1996).

Unit 1 - Willowvale Shale

The lowest exposed strata at Theime Gulf are assigned to the upper part of the Willowvale Shale. Here the unit is primarily a dark grey shaly mudstone with very few interbeds. Only the upper few meters of the Willowvale Formation are exposed here, and these can only be accessed with some excavation. A single interbed was observed, approximately 15 centimeters below the base of Unit 2. This bed was a dark grey, orange-brown weathering dolomitic carbonate containing abundant fossils, particularly the high spired gastropod *Murchisonia*, which is commonly infilled by a black mineral interpreted as phosphate.

Unit 2 - Salmon Creek - Basal Dawes

Overlying the Unit 1 is an 80-90 centimeter, reddish pink sandy carbonate grainstone horizon interpreted as the Salmon Creek, or Basal Dawes Bed which supports a small falls near the bottom of this section. This horizon appears to be much more ferruginous at this locality than at Roaring Brook (Stop 2). The unit is blocky and heavily cross stratified. Its upper and lower contacts are sharp, and small rip-up clasts are observed at several horizons. In contrast to the overlying beds, the Salmon Creek Bed is fairly fossiliferous. Stalked echinoderm columnals are the primary constituent of this assemblage, many of which are stained dark red with hematite.

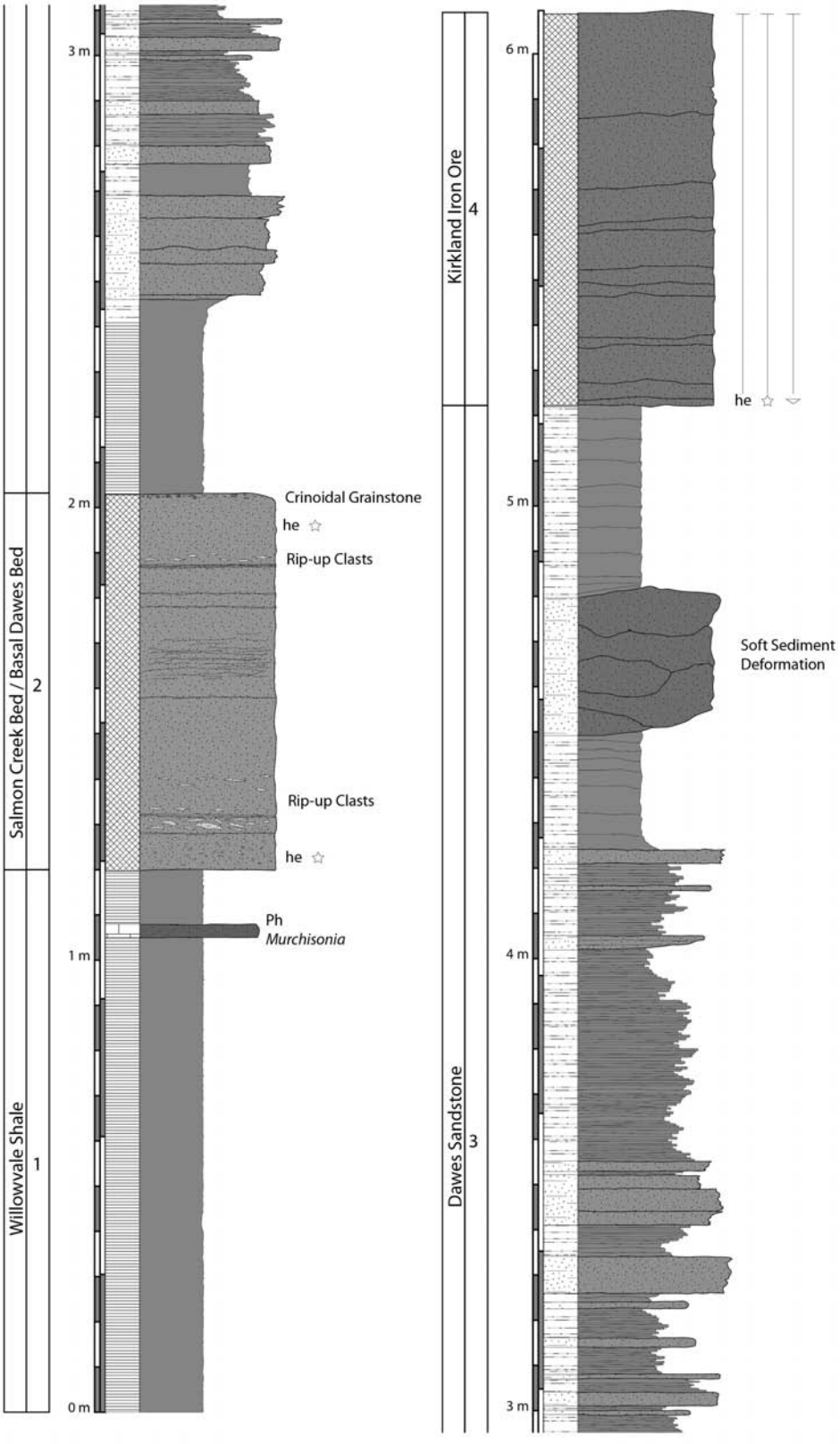

Figure 8 - Stratigraphic column showing the units exposed at Theime Gulf.

Unit 3 - Dawes Sandstone

Overlying Unit 2 are approximately 3.2 meters of dark grey shales, siltstones and sandstones assigned to the Dawes. Fine grained shales and siltstones are the predominant lithology this interval, in contrast to the coarser beds observed at Dawes Quarry Creek. These units are generally finely laminated, though the numerous 5-25 centimeter sandstone interbeds are often massive, with ripples on their upper surfaces. Near the top of this unit is an approximately half meter interval of sandstone and shale showing extensive deformation and ball and pillow structures, which are interpreted as post depositional soft-sediment deformation.

Unit 4- Kirkland Iron Ore

Approximately two meters of massive, dark red dolomitic carbonates overlie Unit 3; these beds are assigned to the Kirkland Iron Ore. The unit is a highly fossiliferous crinoidal, pack- to grainstone with hematitic cement. Although crinoids are the dominant component of the Kirkland's fossil assemblage, bryozoans such as *Acanthoclema* and *Eridotrypa* are also important components. Several beds of the Kirkland are display prominent cross stratification. The basal contact of the unit is sharp, but its upper boundary with the overlying unit is gradational.

Route Description	**Number of Miles**	**Cumulative mileage**
Stop 2 **Theime Gulf** 4486 Theime Gulf Rd, Clinton NY 13323	Depart	
Head **south** on **Theime Gulf Rd** toward **NY-5 W/Seneca Turnpike**	0.2	4.1
Turn left onto **NY-5 E/Seneca Turnpike** Continue to follow NY-5 E	6.8	10.9
Continue onto **NY-12 N**	0.6	11.5
Take the exit toward **NY-8 S/New Hartford**	0.2	11.7
Merge onto **Campion Rd**	0.4	12.1
Continue onto **Oxford Rd**	2.6	14.7
Turn right onto **Oneida St**	0.6	15.3
Stop 3. **Willowvale Creek at Woodhaven Wildlife Refuge** Woodhaven Lane and Oneida Street, Chadwicks, NY, 13319	Arrive	

Stop #3. Willowvale Creek at Woodhaven Wildlife Refuge

Coordinates: N 43° 01' 50.02, W 75° 16' 44.42"

The Woodhaven Wildlife Refuge is a privately owned nature preserve occupying the site of a former picnic area in Chadwicks, New York. At this locality several tens of meters of section can be observed in the bed of Willowvale Creek, a small east-flowing stream which eventually passes under Oneida Street in Chadwicks. This section was described in detail by Gillette (1947; Section 34), and it represents perhaps the most complete, and best exposed outcrop of the Clinton Group in its Type Area. However, only thin, ironstone bearing excerpts of this entire section have been drafted here. Those interested in a more detailed and comprehensive descriptions of the outcrop are referred to Gillette (1947).

The creek was dammed in three places, forming small artificial ponds along the creek. At least two ironstone horizons are located some distance upstream; they may be accessed by a short walk through the scenic preserve. All outcrops described herein are on private land, visitors must first obtain permission from the administrators of the Woodhaven Wildlife Refuge.

Unit 1 – Sauquoit Formation

Unit 1, assigned to the Sauquoit Formation, is at least 35 meters thick at this locality, consisting primarily of blue grey to green gray shales and mudstones with many interbeds composed of calcareous sandstone, siltstone, and quartz-phosphate pebble conglomerates. The unit is abundantly fossiliferous; bivalves, ostracodes, and brachiopods predominate though some trilobites have been reported here as well. Intervals containing ball-and-pillow structures have been observed in shales at several intervals of the Sauquoit at this locality, which are interpreted as the post depositional soft sediment deformation of units, possibly due to seismic activity. The upper few meters of the Sauquoit Formation at this locality are difficult to access, though a relatively complete reconstruction can be compiled through a comparison of creek bed and gully wall outcrops.

Unit 2 – The Westmoreland Hematite

Numerous fragments of oolitic ironstone litter the creek bed, where their bright red color makes them easy to pick out. Many of these fragments are believed to originate from Unit 2, which is assigned to the Westmoreland Hematite. The only outcrop of this bed is located at N 43° 01' 47.39", W 75° 16' 49.25", this is within a very steep gully above the lake formed behind the lowest of the three Willowvale dams (Figure 9). Accessing the outcrop is quite difficult.

The unit is composed primarily of sand sized, iron coated grains which are deeply weathered

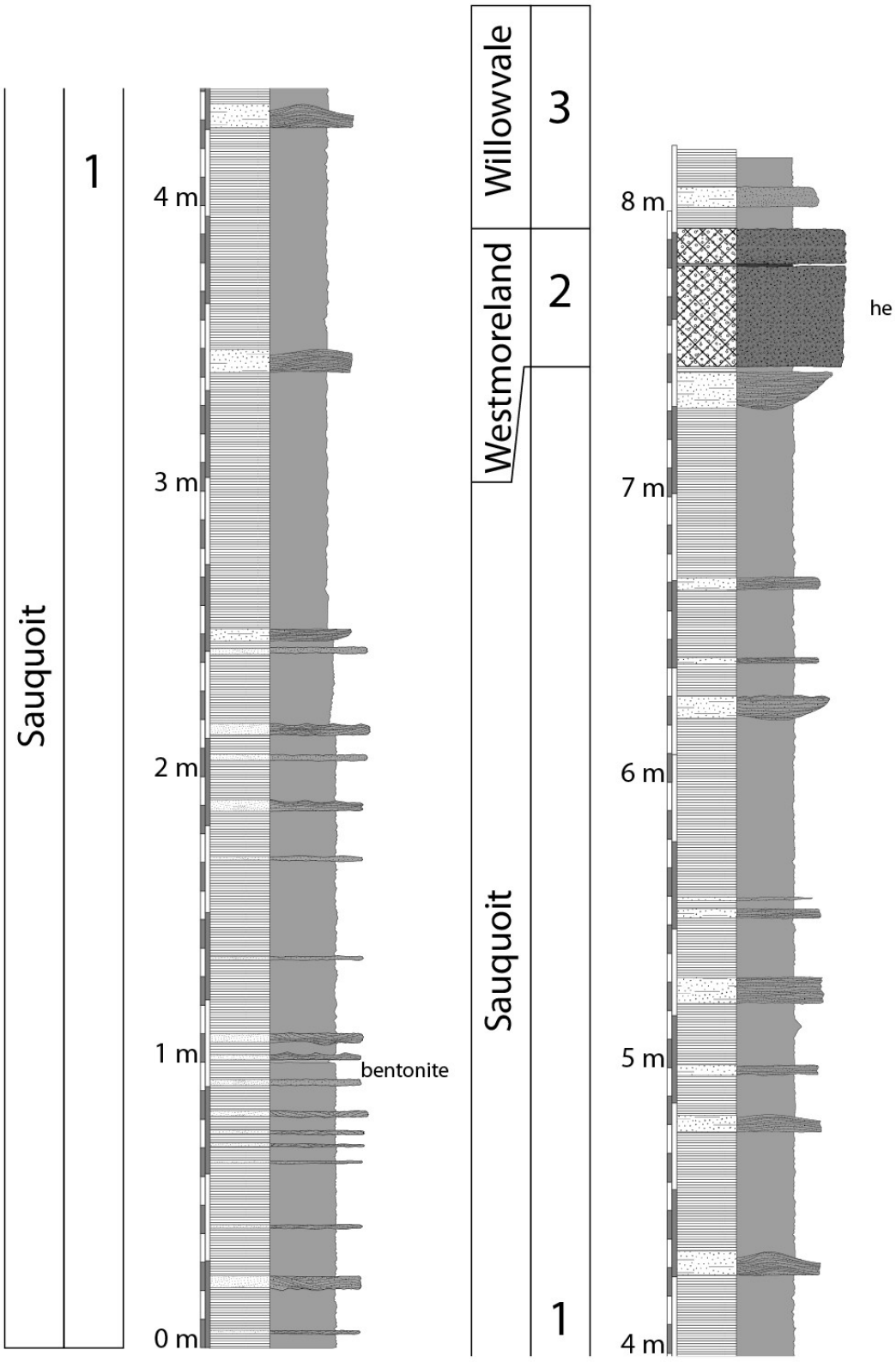

Figure 9 – Stratigraphic column of the upper Sauquoit Formation, Westmoreland Hematite, and Willowvale Shale exposed within the steep gully above the lake formed by the lowest dam on Willowvale Creek.

in the outcrop. These are bright red in color, and unfossiliferous. A black shale lens within the hematite was observed here, similar to the ones described by Gillette (1947), but no fossils were observed in this horizon either.

Unit 3 – Willowvale Shale

Unit 3 constitutes the predominantly shaly unit between the ironstones represented by Units 2 and 4.This interval is interpreted as the Willowvale Shale which, like the Sauquoit Formation, consists of dark grey shales with occasional interbedded, fossiliferous calcareous sandstones. Unlike the Sauquoit, the shales of the Willowvale are dark to olive grey in color, and there are no conglomeratic horizons. The coral *Palaeocyclus* is abundant in the beds of the lower part of this horizon, though these can only be accessed with difficulty here. Other common fossils are brachiopods, bivalves, ostracodes, and graptolites.

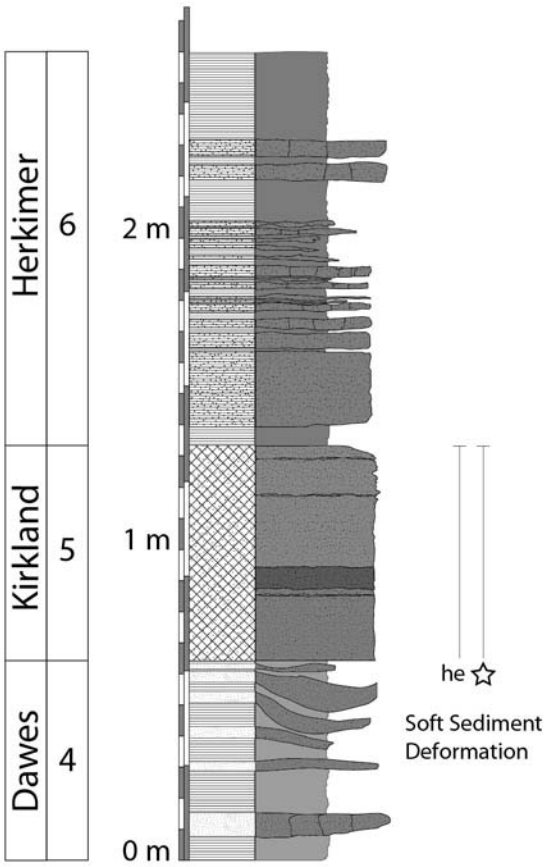

Figure 10– Stratigraphic column of the upper Willowvale Shale, Kirkland Hematite, and lower Herkimer Sandstone exposed at the waterfall just upstream from the lake formed by the middle Willowvale Creek dam.

Unit 4 - Dawes Sandstone

Unit 4 is a succession of relatively unfossiliferous blue grey shales with sandstone and siltstone interbeds. Although these beds were interpreted previously by Gillette, 1947, as the Willowvale Formation, we submit that this is a manifestation of the Dawes Sandstone. Although the Dawes is more shaly here than at Roaring Brook and Theime Gulf the zone of ball-and-pillow structures is similar to that of those and other successions of the Dawes.

Unit 5 - Kirkland Hematite

Unit 5 is a ferruginous limestone that forms the caprock of a small waterfall at approximately N 43° 01' 44.40", W 75°16' 57.31", just upstream from the lake formed by the middle Willowvale Dam. This bed is interpreted as the Kirkland hematite (or flux ore), a calcareous, fossiliferous hematitic ore overlying a zone of soft sediment deformation in the upper Dawes Formation (Figure

10). The unit contains abundant crinoids and stalked echinoderms, which are often stained dark red by hematite.

Unit 6 – Herkimer Sandstone

The Herkimer sandstone consists of orange brown sandstone horizons interbedded with very dark grey silty shales. Abundant ripple marks and cross beds indicate the unit was likely deposited in a relatively shallow environment close to normal wave base. The unit is fairly unfossiliferous, though large brachiopods and cephalopods have been found occasionally. Trace fossils, such as *Palaeophycus* and *Rusophycus* are relatively common.

Route Description	**Number of Miles**	**Cumulative mileage**
Stop 3. **Willowvale Creek at Woodhaven Wildlife Refuge** Woodhaven Lane and Oneida Street, Chadwicks, NY, 13319	Depart	
Head **northwest** on **Oneida St** toward **Bleachery Pl**	1.7	17.0
Turn right onto **Chapman Rd**	1.1	18.1
Take the 1st right onto **Meadowbrook Dr**	0.2	18.3
Take the 2nd right onto **Brookside Terrace**	0.05	18.3
Stop 4 (Optional) **Forever Wild Nature Preserve** Brookside Terrace, New Hartford, NY 13413	Arrive	

Stop #4. (Optional) Forever Wild Nature Preserve

Coordinates: N 43° 03' 07.54", W 75° 15' 05.28"

The Forever Wild Nature Preserve is a heavily forested area east of Washington Mills. The property is a privately owned and permission must be obtained before entering the property. Several excellent exposures of Lower Silurian strata may readily accessed from Brookside Terrace, a small, dead-end lane connected to Meadowbrook Drive in New Hartford New York. A well exposed section is exposed in the creek just south this road. These outcrops are described and illustrated herein (Figure 11), to our knowledge, for the first time in publication.

Unit 1 - Oneida Conglomerate

Strata exposed in the lower part of this creek section are predominantly unfossiliferous interbedded dark grey sandstones and quartz-phosphate pebble conglomerates assigned herein to the

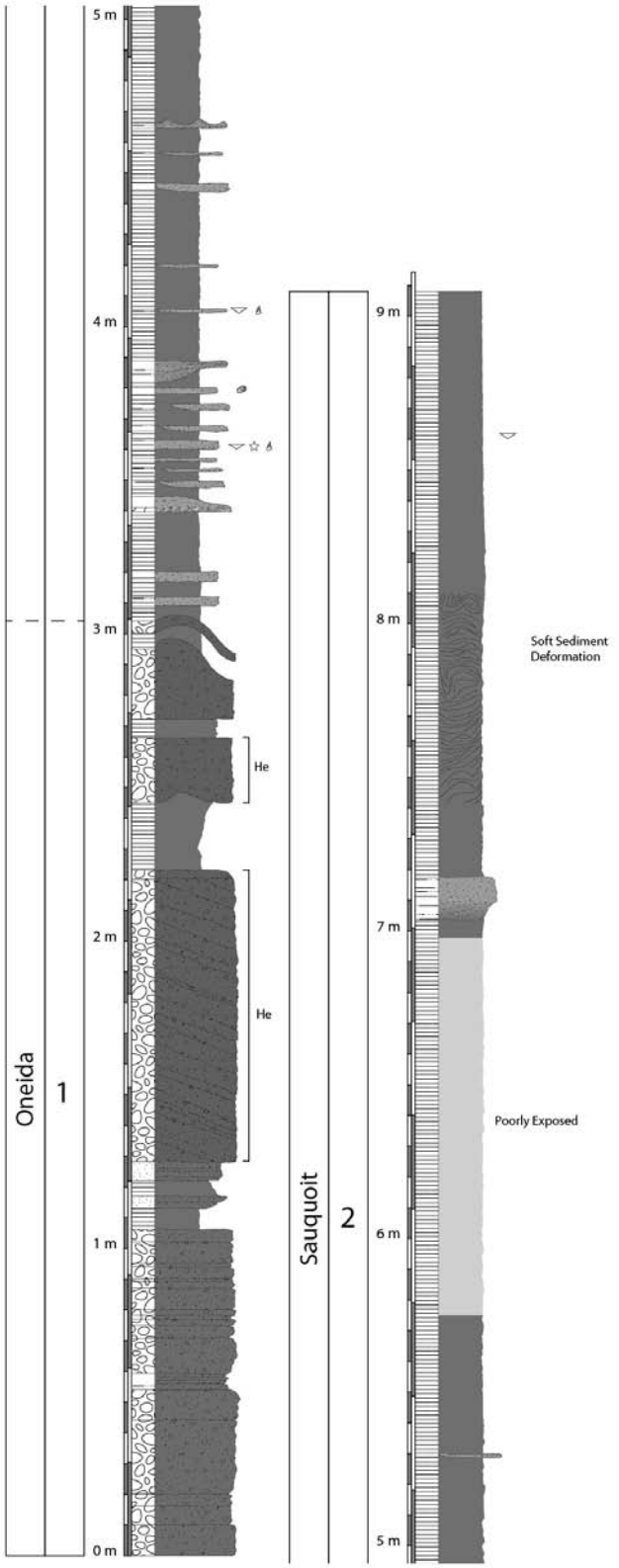

Figure 11 - Strata exposed in the small northwest flowing stream on the Forever Wild Nature Preserve, just south of Brookside Terrace.

Oneida Conglomerate. Several of the sandstone beds have rippled upper surfaces. A meter thick zone of cross bedded conglomerate occurs near the top of the unit; these beds are composed primarily gravel sized, rounded clasts of phosphate and quartz set within a matrix of dark red, hematitic sandstone. This zone is overlain by a 25 centimeter interval of blue grey shale, which is in turn overlain by a pair of hematitic, conglomeratic units with lithologies similar to the beds found in the cross bedded zone. The upper of these two beds contains very large, symmetrical ripple marks that have amplitudes up to 15 centimeters. The Oneida-Sauquoit contact is tentatively placed at the top of this unit.

Unit 2 - Sauquoit Formation

Overlying unit 1 is a succession of blue to greenish grey shales with interbedded calcareous sandstones assigned herein to the Sauquoit Formation. These calcareous sandstone interbeds often have ripple marks on their upper surfaces, and many display hummocky cross stratification. Several of these beds are fossiliferous, containing abundant gastropods, bivalves, brachiopods, and ostracodes. Near the top of the section illustrated in Figure 11, there is a zone of

irregularly bedded shales interpreted as the product of post depositional, soft-sediment deformation, possibly as a result of seismicity.

Route Description	**Number of Miles**	**Cumulative mileage**
Stop 4 (Optional) **Forever Wild Nature Preserve** Brookside Terrace, New Hartford, NY 13413	Depart	
Head **northeast** on **Brookside Terrace** toward **Meadowbrook Dr**	0.05	18.4
Turn left onto **Meadowbrook Dr**	0.2	18.6
Take the 2nd left onto **Chapman Rd**	1.2	19.8
Turn right onto the **NY-8** ramp	0.3	20.1
Merge onto **New York 8 N**	1.8	21.9
Continue onto **NY-840 W**	0.2	22.1
Take the exit onto **NY-12 S/NY-5 W** toward **Syracuse/ Binghamton**	1.1	23.2
Turn left onto **New York 12B S/Clinton Rd**	4.1	27.3
Slight left onto **E Park Row**	0.1	27.4
Take the 2nd right onto **S Park Row**	0.05	27.4
Continue onto **College St**	0.9	28.3
Continue onto **College Hill Rd/County Rd 13**	0.5	28.8
Turn right onto **Campus Rd/County Rd 77**	0.3	29.1
Turn left	0.05	29.2
Ending Point **Taylor Science Center,** Hamilton College, Clinton, NY 13323	Arrive	